Optimising the Energy Performance of the Residential Stock of the Kingdom of Saudi Arabia by Retrofit Measures

Author:
Azzam ALOSAIMI

Supervisor:
Dr. Benjamin JONES

A thesis submitted in fulfillment of the requirements for the degree of Doctor of Philosophy

in the

Buildings, Energy and Environment
Department Architecture and Built Environment

July 13, 2023

Declaration of Authorship

I, Azzam ALOSAIMI, declare that this thesis titled, "Optimising the Energy Performance of the Residential Stock of the Kingdom of Saudi Arabia by Retrofit Measures" and the work presented in it are my own. I confirm that:

- This work was done wholly or mainly while in candidature for a research degree at this University.
- Where any part of this thesis has previously been submitted for a degree or any other qualification at this University or any other institution, this has been clearly stated.
- Where I have consulted the published work of others, this is always clearly attributed.
- I sought the support of Scribendi company who proof read this thesis and they provided scintific insight and all conclusions are my own.
- Where I have quoted from the work of others, the source is always given. With the exception of such quotations, this thesis is entirely my own work.
- I have acknowledged all main sources of help.
- Where the thesis is based on work done by myself jointly with others, I have made clear exactly what was done by others and what I have contributed myself.

Signed:

Azzam Hamed Alosaimi

Date:

31-03-2023

Abstract

Building energy demands and green house gases are raising and a variety of energy efficiency frameworks, legislation, and housing approvals have evolved worldwide. The KSA is one of the largest energy producers and consumers internationally, with the residential sector using 52% of total energy generation. The KSA government has begun energy efficiency initiatives and policies that intend to reduce the residential energy demands via a series of regulations including *Vision 2030* and the KSA building code. The regulations aim to assess the energy performance of residential buildings in order to lower the energy demands and greenhouse gas emissions to meet international carbon emissions requirements. The KSA targets to generate 9.5 GW from renewable energy by 2023, and 58.7 GW by 2030, which accounts for about 30% of the total energy generation capacity. Research has shown that in order to effectively reduce the energy demands and achieve worldwide carbon emissions targets, large-scale implementation interventions are required.

The KSA housing stock consists of 3.6 million wide and varied residences due to various terrain. The diversity of the KSA dwellings encompasses housing type, age, amounts of rooms and bedrooms and flooring areas while common characteristics comprise construction materials and energy and cooking fuels. Therefore, this thesis develops housing archetypes that are representative of the KSA housing stock to be assessed and evaluated for the aim of reducing there energy demands and associated carbon emissions along with monthly running costs. The housing archetypes are used to quantify the housing energy performance and define the major sources of heat loss or gain. Two major reason for the high energy demands are solar radiation and heat gain due to infiltration. The infiltration occurs due to pressure differential across the thermal envelope. This is responsible for 40 TWh of lost energy from the housing stock, which accounts for 9.9 million $MtCO_2e$.

The research methodology applied an engineering bottom-up approach to quantify the energy performance of the KSA's housing stock using EnergyPlus dynamic tool. EnergyPlus is a new generation modelling tool that incorporates the best features of two prior modelling tools: Building Load Analysis and System Thermodynamics (BLAST) and the Department of Energy (DOE–2). EnergyPlus is a free available tool and so allows data comparisons with international housing stocks. EnergyPlus was used to create the KSA's housing energy baselines to predict the existing housing energy performance and to simulate various scenarios to reduce the total energy demands.

The KSA housing energy demands can be optimised through a large-scale implementation of energy efficiency retrofitting schemes comprising 25 exterior thermal insulation types, eight exterior shading systems, and LED lighting systems and equipment, and the application of PV systems. This resulted in reducing the total KSA housing energy demands by 12.95 TWh/month, equivalent to 40% of the monthly housing energy use, and lowered associated carbon emissions by a total of 5.61 million $MtCO_2e$/month, equivalent to 40% of monthly housing carbon emissions, and decreased the total housing stock cost about 72.39 million USD/month, equivalent to 50% of the total monthly cost.

Acknowledgements

This PhD journey has been a great deal of learning for me, and I believe the encouragement and support I have received from the start has contributed significantly. I would like to convey my deepest gratitude to my supervisor Dr Benjamin Jones for invaluable patience and feedback for the past four years during supervision meetings, and his dedication and diligence for the natural world and scientific research have pushed me beyond my capabilities to produce my finest work. I would like to express my sincere appreciation to Dr Christopher Wood for generously sharing his knowledge and expertise and for consistently assisting me to achieve my best work. I would like to extend my thanks to Dr Constanza Molina for her early assistance by sharing her thoughtful insights and knowledge exchange.

This research would not have been feasible without the full support I have received from my mother, father, sisters, and my uncle Eid Aljuaid, my dearest friend March Anas Mahjoub, and my mentor Dr Alaa Nassif for the continuous motivation and inspiration. Their confidence in me has maintained my spirits throughout this endeavour.

Contents

List of Figures

List of Tables

Nomenclature

$\bar{\rho}$	Mean air density between indoors and outdoors (kg/m^3)
$\bar{N}_I$	Mean infiltration rate (h^{-1})
χ^2	Chi-square test
ΔP	Pressure difference (Pa)
ΔT	Temperature Difference (°C)
$\dot{Q}$	Airflow rate (m/h)
$\dot{V}$	Airflow rate (m^3/h)
λ/k	Thermal conductivity (W/k)
μ	Mean
σ	Standard deviation
θ	Wind direction (°)
$\tilde{Q}$	Party wall relative permeability
C_P	Wind pressure coefficient
C_v	Coefficient of variation
H/Q	Heat
H_I	Heat loss due to exfiltration (MWh)
N_{50}	Air change per hour at 50 Pa (h^{-1})
Q_{50}	Air permeability at 50 Pa (m^3/h/m^2)
CO_2	Carbon dioxide

A Area (m^2)

a flow coefficient ($m^3/h/Pa^b$)

ACH Air change rate per hour (h^{-1})

AGR annual growth rate

ALP Air leakage path

ALR Air leakage rate (m^3/h)

ARAMCO Arabian American Oil Company

ASHRAE American Society of Heating, Refrigerating, and Air–Conditioning Engineers

b Flow exponent

BLAST Building Load Analysis and System Thermodynamics

BREDEM Building Research Establishment Domestic Energy Model

C Flow coefficient

CG Cellular Glass

CI Confidence interval

CVS Comma Separated Values

d Housing surface depth (m)

DOE–2 Department of Energy

EER Energy Efficiency Rates

EERM Energy Efficiency Retrofitting Measures

EUI Energy use intensity (W/m^2)

FG Fiber Glass

FYDPs Five Year Development Plans

GAH General Authority for Housing

GAS General Authority for Statistics

GCC Gulf Cooperation Council

GDP Gross Domestic Product

GHG Greenhouse Gas Emissions

GHP Guarded Hot Plat

GT Ground Temperature (°C)

GWP Global Warming Potential

H Heat loss (kWh)

h Altitude (m)

HES Household Energy Survey

IAQ Indoor Air Quality

IAT Indoor air temperature (°C)

IEA International Energy Agency

INE National Institute of Statistics

ISFT Inside surface face temperatures (°C)

KAPSARC King Abdullah Petroleum Studies and Research Center

KEM King Abdullah Petroleum Studies and Research Center Energy Model

KPM Key performance metric

KSA Kingdom of Saudi Arabia

KSABC KSA Building Code

KSABC The Kingdom of Saudi Arabia Building Code

L leakage infiltration ratio

LCA Life Cycle Assessment

LPD Equipment power density (W/m^2)

LPD Lighting power density (W/m^2)

MAT mean air temperature (°C)

ME Middle East

MENA Middle East and North African

MMRAH Ministry of Municipal and Rural Affairs and Housing

MoH Ministry of Housing

MoP Ministry of Planning

MPWH Ministry of Public Works and Housing

MRT Mean radiant temperature (°C)

$MtCO_2e$ Metric tons of carbon dioxide equivalent

N Sample size

n Flow exponent

NDP Ninth Development Plan

NG Natural gas

NHST Null hypothesis significance testing

NL Normalised leakage

OAT Outdoor air temperature (°C)

OPT Operative Temperature (°C)

OSFT Outside surface face temperatures (°C)

Pa Pascal

PE Primary Energy

PO Polystyrene

REDF The Real Estate Development Fund

SAMA Saudi Arabian Monetary Authority

SAP Standardized Assessment Procedure

SBS Sick Building Syndrome

SE Standard error or standard deviation of the mean

SEC Saudi Electricity Company

SEEC Saudi Energy Efficiency Centre

SGBC Saudi Green Building Council

SHGC Solar Heat Gain Coefficients

SRC Saudi Real Estate Refinance Company

STC Standard test conditions

TH Traditional house

TMY Typical Meteorological Year

TWh Terawatt-hour

u Dwelling height (m)

u_0 Weather station wind speed (m/s)

USEPA United States Environmental Protection Agency

w Housing surface width (m)

WHO World Health Organization

z_max Top surface height above ground (m)

z_min Bottom surface height above ground (m)

z_s Housing surface height (m)

z_u Dwelling height (m)

Chapter 1

Introduction

The Kingdom of Saudi Arabia (KSA) is a Middle Eastern country that encompasses 80% of the Arabian Peninsula (Nyrop, 1984). It has a population of 34.2 million people and is growing at a rate of 1.7% per annum (GAS, 2019). The KSA's economy is the most developed in the Middle East (ME), with a *per capita* gross domestic product (GDP) of US $23,139 in 2019 (Mujeebu and Alshamrani, 2016). Its economy depends on oil, which represents more than 90% of its export revenues and 40% of its GDP. The oil crisis of 1973 dramatically altered the economy when financial restrictions were lifted because of a substantial increase in petroleum earnings due to high international oil demands. The KSA's government has continued to generate significant revenues from the sale of oil and has used it to achieve long-term growth through targeted advancements in power generation, telecommunications, trade, social development and infrastructure projects (Alkhathlan, 2013).

The KSA's cumulative carbon dioxide (CO_2) emissions are around 14.9 billion tonnes (Roser et al., 2013), a figure that is accelerating. Iran is the only country in the Middle East that has emitted more CO_2 than the KSA. For instance, Saudi greenhouse gas (GHG) emissions have doubled more than three times, from 172 million tonnes in 1985 to 582 million tonnes in 2019 (Roser et al., 2013). This high level of GHG emissions is typical of Middle Eastern nations. Gulf Cooperation Council (GCC) countries are all significant oil and natural gas exporters and are among the top 25 nations with the highest CO_2 emissions *per capita*. Accordingly, they will play a key role in helping the global community to meet future international climate change targets (Mujeebu and Alshamrani, 2016).

In December 2014, the United Nations Framework Convention on Climate

Change (UNFCCC) presented strategies for implementing the Paris Agreement to reduce GHG emissions. Signatories committed to reducing their annual GHG emissions after 2020 (Scott et al., 2016), and the KSA committed to reducing its CO_2 emissions by 130 million tonnes by 2030 (Averchenkova and Bassi, 2016). However, the KSA faces a dilemma because its economy and entire energy sector centre on fossil fuels (Alkhathlan, 2013). Oil prices were high between 2004 and 2008, and the Kingdom took the opportunity to expand its economy (Stevens and Lahn, 2011). However, household energy costs have decreased, while domestic fossil fuel usage has grown. Consequently, this hampered investments in renewable energy sources and low-energy public transport (Alyousef and Stevens, 2011). There is anecdotal evidence that low energy prices encourage households to use their air-conditioning throughout the day.

In 2020, the government commissioned new renewable energy projects, revised their building codes and made a public commitment to reduce their national energy demand (Amran et al., 2020). The government initiated various energy-efficiency programmes; perhaps the most important is the Vision 2030 road map, which was announced in 2016. Vision 2030 presents new strategies that aim to achieve a more diverse and sustainable economy. The Vision addresses a wide number of sectors, including industrial, governmental, building, manufacturing, tourism and leisure, mining and energy. In addition, the National Renewable Energy Programme of the Vision and the National Transformation Programme have already taken measures to substantially raise the production share of renewable energy to 3.45 GW by 2020 and to 9.50 GW by 2023. These percentages represent about 4% and 10%, respectively, of the overall energy production in the KSA (Amran et al., 2020).

Effective, safe procedures and policies designed to decrease national energy demands were applied to reduce GHG emissions, starting with the building stock, especially the housing sector, because its energy demands and carbon emissions are the most significant. The building sector is responsible for 75% of the total electrical energy demands of the KSA (AlGhamdi et al., 2020). The housing stock accounts for about 52% of the building sector's energy demands, followed by the industrial and commercial sectors with 18% and 12%, respectively (Alaidroos and Krarti, 2015). It is estimated that a large-scale retrofitting programme for the housing stock could reduce the demand for electrical energy by more than 10^4 GWh/year while lowering peak electrical energy demand by 25^3 MW (Al-Homoud and Krarti, 2021). The International Energy Agency (IEA) argues that building energy codes and standards are important for increasing energy performance and occupants' comfort (statistics and analysis, 2019). However, compliance is currently only assessed at the initial design phase; it is not in use. To assess the energy efficacy of existing codes, a comprehensive description of housing's energy behaviour is required, which can be extended to include a housing stock (Sousa et al., 2017). Preferably, information for current houses should be collected from large-scale housing surveys. Nonetheless, due to time and expense constraints, a modelling method is needed.

Kavgic et al. (2010) demonstrate that energy models are generally categorised as *top-down* (Edmonds et al., 1994; Wiesmann et al., 2011) or *bottom-up* (Edmonds et al., 1994; Krarti et al., 2020; Swan and Ugursal, 2009; Oladokun and Odesola, 2015) and work at aggregated and disaggregated levels, respectively. *Bottom-up* models apply empirical data to describe each element of a dwelling using a physical model that can then be used to assess the impacts of an intervention on those elements. There are many existing analyses of the energy demand of individual dwellings in the KSA (Alaidroos and Krarti, 2015; Algarni and Nutter, 2013a). Consequently, they do not represent the wider stock. Others have modelled housing types by considering their age, type and location (Bagneid, 2007; Krarti et al., 2020; Aldubyan et al., 2021). Nonetheless, they have not used statistical techniques, such as clustering, to identify common physical factors, and they have not assessed their housing representation statistically.

A vast amount of data inputs are needed to accurately predict heat loss and mass transfer. Molina et al. (2020) noted that this data might not be available or only appear in aggregate formats, which prohibit data comparisons. The acquisition and processing of information can be time consuming and prone to systemic errors, such as translation and typing faults, if they are not monitored. However, when the information is available, it can be used to understand the existing stock and to consider the effects of changes made to that stock. Modelling every dwelling of a stock is computationally expensive, and it is unnecessary if dwellings share similar properties. Subsequently, similar dwellings can be clustered and classified by unique details into *archetypes* to simplify the database so the programming process can become more comprehensible.

Previous research about buildings energy performance in the KSA have extensively explored the effects of reducing the housings energy demands, with consistent evidence supporting its high negative impact on energy usage, carbon emissions and costs. However, most of these studies have focused on one building or a few buildings approaches, neglecting a crucial segment of the housing population: housing that comply with the building code. Despite the moderate prevalence of buildings' energy analysis in the KSA, there is a surprising lack of research in two major areas; Firs, investigating the potential benefits of implementing the minimum requirements of the KSA building code on the energy model baselines for bench-marking, which allows the building code's evaluation to elaborate areas for future improvements. Second, predicting air infiltration rate of the KSA's housing stock because there is no study predicts air infiltration rate in the KSA, which shows a clear data shortage. The infiltration rate of housings is critical to understand since the majority of existing energy simulation tools employ thermal loads modelling techniques to assess heat transfer in buildings and not computational fluid dynamics. Thus, energy simulation tools assume deterministically constant air infiltration rates all over the year. Predicting the housing infiltration rates allows future research by coupling the predicted infiltration rate values with the energy simulation tools, which provides more accurate outputs. Therefore, the present study aims to fill this critical gaps by developing a set of housing archetypes for examining the effects of applying alternative energy efficiency retrofitting measures on the KSABC's compliant housings and to predict the air infiltration rate and associated heat loss of the KSA housing stock. By addressing this research gaps, we aim to contribute novel insights into the existing knowledge of the potential housing energy conservation role of the KSA. This assesses the Kingdom's energy policy and improve the decision making process by informing and listing recommendations for new housing constructions, which enhances the quality of future research.

1.1 Research questions

The research questions were crafted by conducting a thorough review of existing literature about buildings energy demands in the KSA, which identified research gaps, inconsistencies, and unanswered questions in the current knowledge base. This project addresses these key research questions to quantify the energy performance and air infiltration rate of the KSA's housing stock to reduce the the energy demands and heat loss:

1. What are the archetypal housing units of the KSA's housing stock?

2. What are the indoor environmental conditions of the archetypal homes in the KSA?

3. How can the energy performance of the KSA's housing stock be predicted?

4. What is the infiltration rate of the KSA's housing stock?

5. To what extent can energy demands, associated CO_2 emissions and cost be reduced from the KSA's housing stock?

1.2 Aim and objectives

The aim of this research is to establish a tool suitable for assessing the consequences of reducing peak energy demands, CO_2 emissions and cost of the KSA's housing stock via thermal envelope adjustments, and to predict the housing infiltration rates. This research develops archetypal energy model baselines for the KSA's housing stock for benchmarking and assessment purposes. The energy baselines can predict the current energy performance of the KSA's housing stock to reduce energy demand. It will predict how a Saudi dwelling will perform and how its performance changes when its fabric and services are optimised. The research is conducted using computational modelling approaches rather than field studies due to COVID-19, time and cost restrictions.

To achieve the aim of this study, several objectives must be defined:

1. Archetypal housing units and their typical components, including an envelope, lighting, equipment power densities and materials.

2. Analyses of the internal environment of the housing and energy performance in various locations.

3. Establishing an accurate predictive model would enable the measurement of energy performance at any given location according to the building code's minimum requirements.

4. Developing an infiltration model that concisely predicts the airflow rate of the KSA's housing stock.

5. Assessing the energy performance of the KSA's housing stock in various locations and implementing alternative energy-efficiency measures to reduce the stock's energy demand, CO_2 emissions and cost.

1.3 Thesis structure

The thesis's structure highlights several phases intended to attain the aims and objectives in Section 1.2. See Figure 1.1. The structure and content of this thesis is as follows:

Chapter 1 Introduction: Presents the background information, context and significance of this research. It states the research problem, objectives and final aim.

Chapter 2 The development of the KSA's housing stock: Gives historical information about total energy and gas usage in the KSA. It also clarifies historic housing developments by reviewing all responsible governmental agencies since their establishments. This work concludes by defining barriers to expanding sustainability across the KSA.

Chapter 3 Literature review: Describes existing academic knowledge and is split into five major sections. The first section addresses building energy demand. The second section examines indoor environmental quality and indoor pollutants. The third section highlights reviews buildings' air infiltration rates. The fourth section defines research gaps. The fifth section provides a summary the chapter.

Chapter 4 Data analysis and housing representation in the KSA Defines current KSA housing data sources' availability and accessibility and classifies data according to relevant key parameters weighted by kind and quantity. It describes the method of employing data systematically to develop representative housing archetypes for the KSA's housing stock. It also highlights the methods results, limitation and discussion. It emphasises data scarcity in several sectors and calls for further data collection and research.

Chapter 5 Methodology: Details the measures performed using probabilistic modelling techniques for data processing to identify the factors with the greatest impact on the model's predictions. The methodology is divided into two key methods. The first method highlights the process of developing the KSA's housing energy models. The second method demonstrates the procedure to predict the infiltration rates of the KSA's housing stock.

Chapter 6 Results: Summarises the findings obtained from a sensitivity analysis and from simulations. It presents descriptive statistics for the energy performance of the KSA's housing stock, associated heat loss and air infiltration rates. It applies energy-efficiency retrofitting measures (EERMs) to test their sensitivity under identical circumstances.

Chapter 7 Discussion: Discusses the KSA's information sources and housing archetypes and clarifies where and why different datasets or surveys overlap or do not compare. It discusses housing archetypes' energy baselines and the EERMs applied to reduce energy demands. It compares the KSA's housing infiltration rates. It also identifies strengths, knowledge gaps, data availability, data utilisation and future work possibilities.

Chapter 8 Conclusion: Concludes this research by summarising crucial facts and research findings. It illustrates future research opportunities and knowledge gaps.

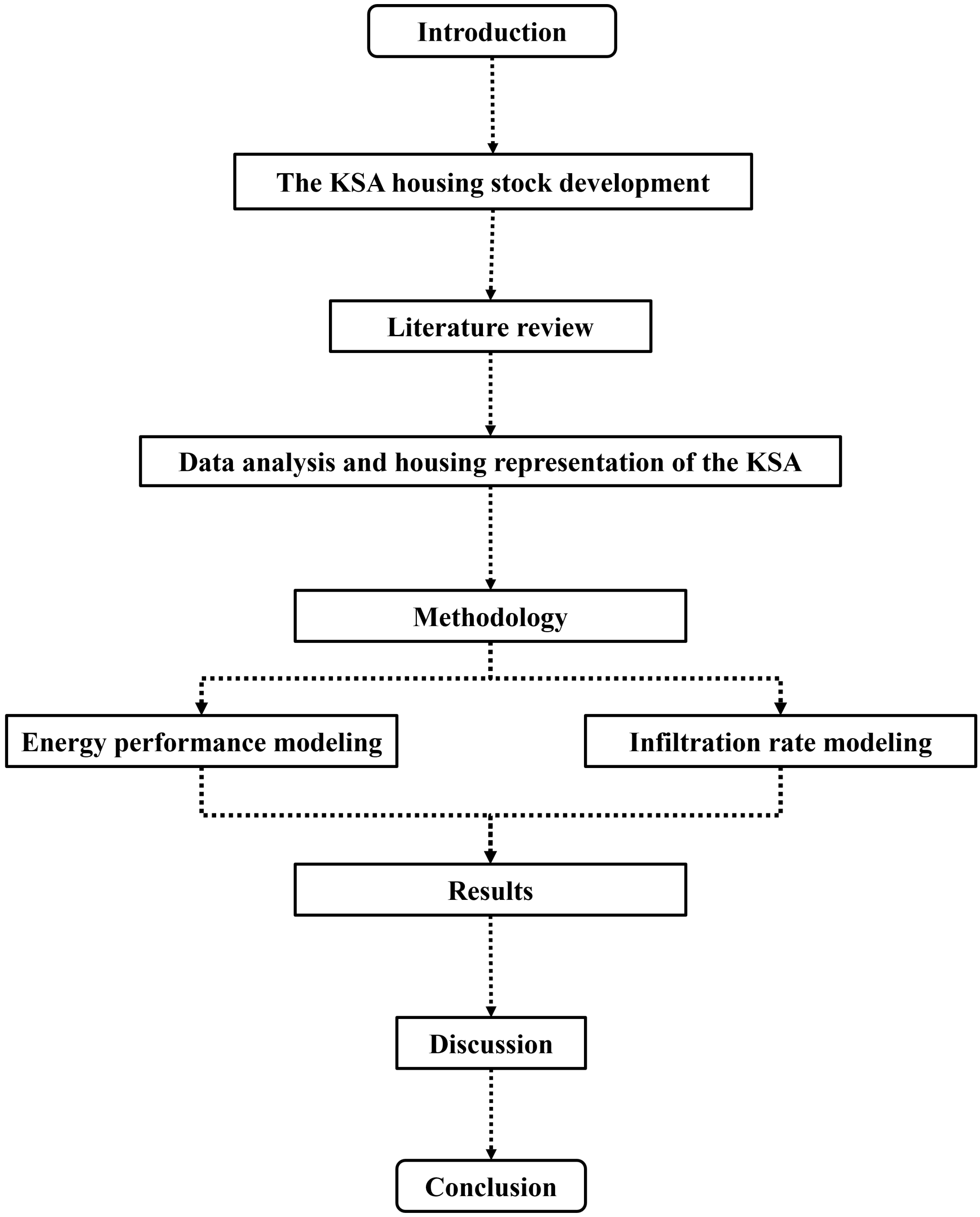

FIGURE 1.1: Thesis structure.

Chapter 2

The development of the KSA's housing stock

Chapter 1 highlights the need for a more complete analysis of the housing stock's energy demands and their variance across stock classifications. The KSA's domestic housing energy use is excessive and presents a threat to the environment due to its burning fossil fuels for energy. The burning of fossil fuels from coal, oil and gas emits vast volumes of GHG involving carbon dioxide and nitrous oxide. This causes concerns about trapping heat in the Earth's atmosphere, which could increase the world's average air temperature and eventually raise the sea level (Desai, 2018). This may be due to several factors, including population growth, increases in housing permits, low energy tariffs and extreme weather conditions. This concern, which scientific data strongly support, should be prioritised so efforts may be undertaken to better educate and safeguard the public. This is fundamental to the potential for climate change; its resolution is indispensable.

Figure 2.1 summarises this chapter's structure. This chapter is divided into three major sections. Early housing types and a chronological description of the KSA's housing stock's development are presented in sections 2.1 to 2.9. These sections review the KSA's housing stock development and the governmental agencies responsible for supplying dwellings to the public, including each agency's housing contribution through the years. Section 2.10 identifies the government's efforts to reduce energy demands and CO_2 emissions using public or private agencies. Section 2.11 reveals the current challenges facing the KSA's government to reduce domestic energy demands and to meet international carbon emission requirements.

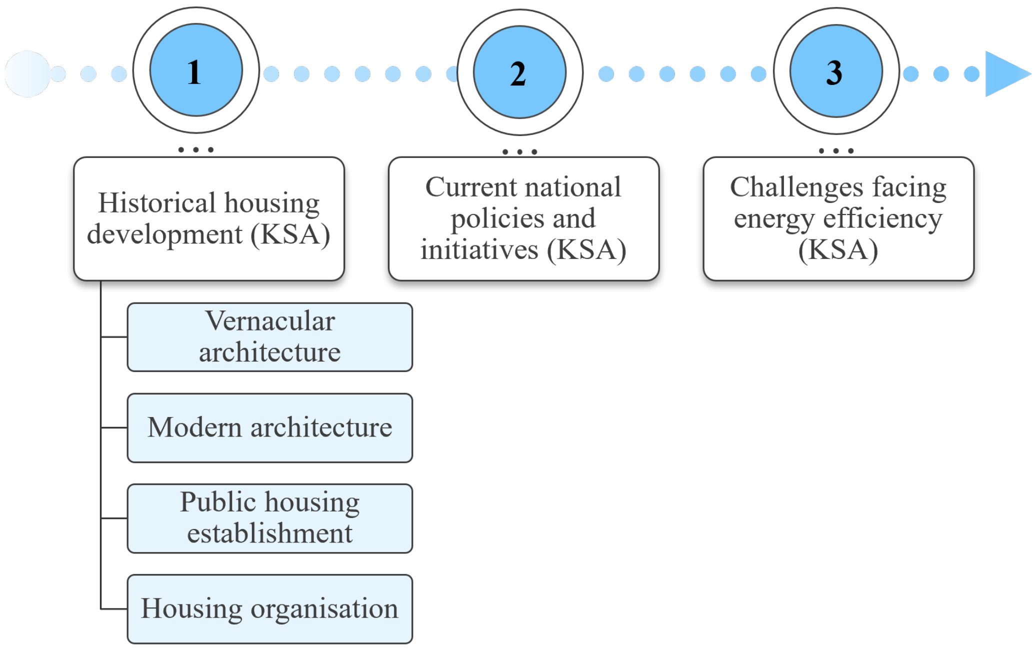

FIGURE 2.1: Chapter structure.

2.1 Vernacular architecture

It is useful to review the development of the KSA's housing stock since it informs the progression of each housing agency and its overall contribution to the housing stock. Multiple terms have referred to dwellings throughout the history of the KSA. The term *shelter* is used in the central region regarding traditional and climatic requirements. There are two sorts of shelters based on the characteristics of residents, as mentioned by Almehrej (2015) referring to Talib (1984a). Urban settlements are constructed using mud, stone and wood, while desert shelters consist of tents to be more convenient for the nomadic Bedouins, who relocate in their search for water and food. In the 1930s, modernisation invaded desert life with three main types of shelter: the tent, the courtyard and the villa. In addition, some nomadic herdsmen moved to villages and raised livestock on modest farms Talib (1984a). Wight (1953, cited in Talib (1984a) presented the design of the tent, which is rectangular with two or three sections separated by goat-hair curtains.

The second housing type is the courtyard, a space open to the sky that circulates sunlight and air to the entire dwelling. It is considered an open patio and living space where families spend much of their time. It has two common forms:

underground and above ground. Eid and Yousef (2000) claimed that the courtyard's style reflects the impact of the weather, as it is more convenient for a hot climate. In addition, it is acceptable for a wide range of socio-cultural and religious factors. Additional courtyards surround a house's service areas. Courtyards commonly have square or rectangular shapes. Another investigation recognised thermal comfort and privacy in Tripoli's traditional houses. The courtyard constituted a physical and cultural symbol due to its suitability for Islamic teachings on gender separation and outdoor activities (Sharif et al., 2010). It regulates the climate in hot and arid locations by storing heat during the day and releasing it at night, when the temperature drops. See Figure 2.4 (Almehrej, 2015).

Moustapha et al. (1985) introduced the common design of traditional houses grouped into four types related to the location of the courtyard: the central patio surrounded by living space, a U-shaped courtyard with space on only three sides, an L-shaped courtyard occupying one corner of the building and the two-part courtyard with segregated private and public entrances, as represented in Figure 2.2. The courtyard house is a massive, thick-walled mud structure constructed over one or more square courtyards. There are small orifices on the exterior walls while there are large openings on the interior walls around the courtyard. The openings and the internal walls are covered with white plaster for decoration and cleanliness. In addition, the household and a master builder supervise the construction of the traditional house form (Bahammam, 1998). Figure 2.3 depicts traditional houses in the KSA.

FIGURE 2.2: Courtyards types and shapes (Almehrej, 2015).

FIGURE 2.3: Traditional houses in the KSA (Baik, 2017).

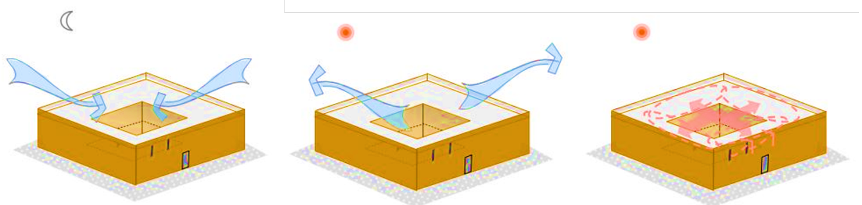

FIGURE 2.4: Courtyard environmental circle during day and night (Almehrej, 2015).

2.2 Modern architecture

Data from several sources have identified the increased number of a new housing style, the villa, associated with the grid pattern street plan (Al-Hathloul, 1981; Talib, 1984b; Bahammam, 1998; Alnowaiser, 1996a; Saleh, 1998; Saleh, 2001a; Mubarak, 2004). This modern style of housing proliferated with the first two housing projects in the country. A few governmental regulations were also applied to these projects for the first time, aiming to control the buildings' height, ratio to the site area and setbacks. Alnowaiser (1996b) discussed the regulations for the required distances on all sides to centre the home on the property and expose windows and outdoor spaces to neighbours. Although the villa accesses natural light, air and views, it

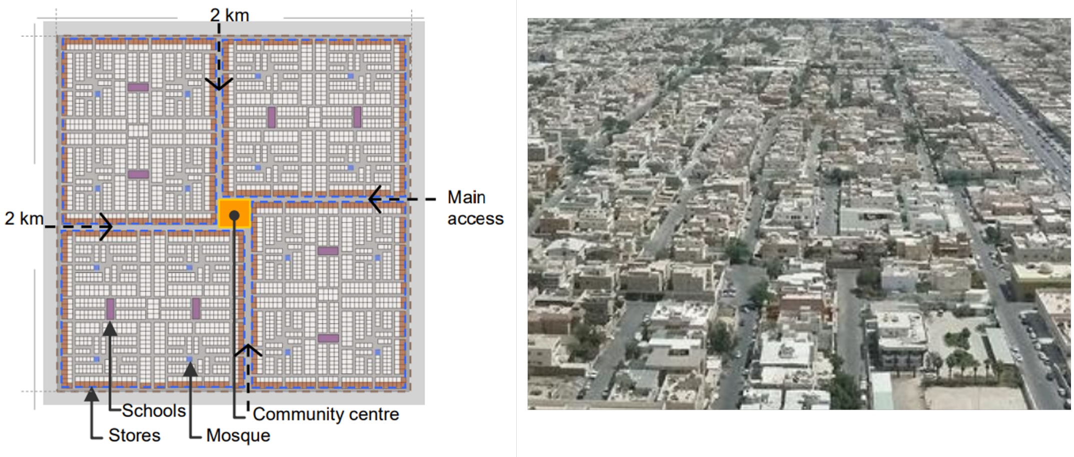

FIGURE 2.5: Typical residential neighbourhood layout located in Riyadh city (Saleh, 2001b; Almehrej, 2015).

eliminates the private space of the household. Thus, most residents reject regulations that inhibit their normal lifestyle (Almehrej, 2015).

Furthermore, Saleh (2001a) demonstrates that a projected contemporary neighbourhood would encompass a perimeter road and be separated into sub-neighbourhoods by major roads that cross in the centre of a net grid. There are community amenities, shops, schools, police and a post office in the crossroads area. Each subdivision contains detached homes, public schools, a Jami Mosque and public gardens connected to the Mosque. See Figure 2.5. The villa's orientation reverses the typical courtyard home's layout since the courtyard house's windows face in while the villa's windows face out. In 2007, Riyadh Municipality established technical specifications for four types of villas: detached, attached on one side and two varieties of attached on two sides (Municipality, 2018). See Figure 2.6.

2.3 Establishment of Public Housing Projects

The first stage of the housing sector's development lasted more than 40 years. Two major factors influenced the government's interventions: demographic changes or urbanisation and the Kingdom's economic growth since the discovery of oil in 1938 (Nurunnabi, 2017). After 1974, here was a disparity between housing supply and demand due to the rapidly increasing population (Public Works and Ministry, 1990). Heightened national income from the oil industry and the goal of urbanisation helped the government construct the first two housing projects in the

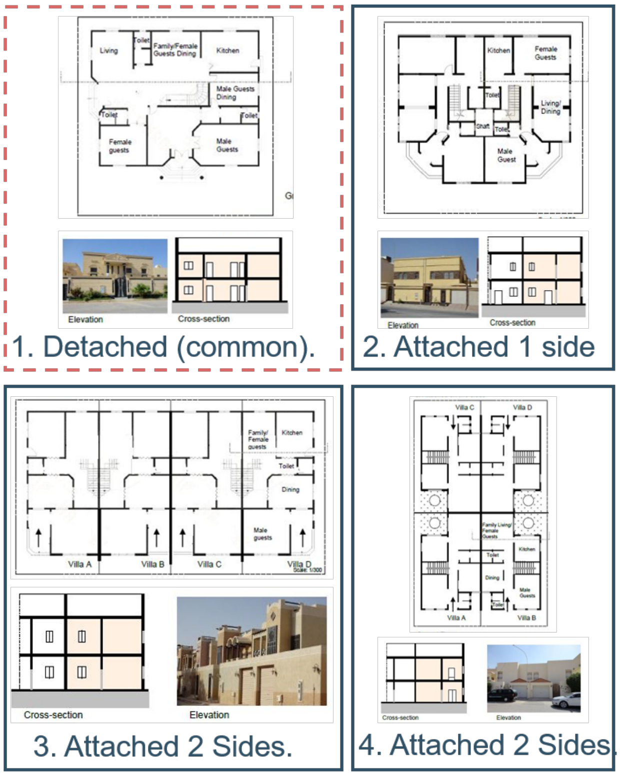

FIGURE 2.6: The villa types in the KSA (Almehrej, 2015).

central and eastern regions of the nation (Al-Mayouf and Al-Khayyal, 2011). The housing projects motivated citizens to gain governmental settlements supplied with technology that was advanced for the time. This encouraged more urbanisation, and citizens started moving to major cities to gain more access to utilities and services, including jobs.

A considerable reason for housing demands' increment is population growth. Ideally, population growth and housing demand increase simultaneously. In 1932, only 20% of the KSA's total population inhabited urban areas, which led to earlier regulations. These regulations included new standards for political and socio-economic groundwork started at the beginning of the 20th century. Regarding Mubarak (1999), in the early 1950s, the government started its development through two primary housing programmes spearheaded by ARAMCO (Arabian American Oil Company) and Al-Malaz. See Figure 2.7.

2.3.1 ARAMCO housing project

Since the development of the oil industry, the human workforce of ARAMCO has expanded, leading to the need for more international and national experts. Therefore, housing units with certain facilities and designs were permitted. The Saudi workers of ARAMCO had two types of temporary shelter, either basic houses adjacent to their job locations or existing settlements in the Eastern Province near the oil fields. This led to the urgent need to increase the existing housing stock (Fadan, 1983).

Consequently, ARAMCO prepared a plan for modern accommodations for its growing workforce. In 1953, the company established the first housing programme in the country, the Home Ownership Programme, for its employees with the help of the Saudi government, which supplied land plots for free. Correspondingly, the company introduced the Housing Loan Plan for Saudi employees to guarantee the required funds for building or purchasing family housing in their local communities, as urbanisation was one of the goals of the government. Al-Hathloul (1981) claimed that the proposal included a variety of municipal structures and public amenities, such as a public library, municipal halls, city park, racetrack, sports field, zoo, health centre, schools and educational buildings.

2.3.2 Al-Malaz housing Project

According to Al-Hathloul (1981), government offices were transferred to the capital city, Riyadh, to ease and accelerate communications starting in 1953. This required more housing units for employees, especially in 1957, due to the non-existence of a governmental housing agency. Therefore, the government employed foreign expertise to design a complete housing project for their employees in the Al-Malaz neighbourhood, 4.5 km northeast of Riyadh's city centre, with the assistance of the Ministry of Finance and National Economy in cooperation with the Municipality of Riyadh. The project sought to provide 754 independent residences (villas) and 180 apartments in three apartment complexes on 500 hectares of land. This was the first time that villas were introduced to the Saudi public. These villas were admired, because the government had granted them the latest technologies of the time,

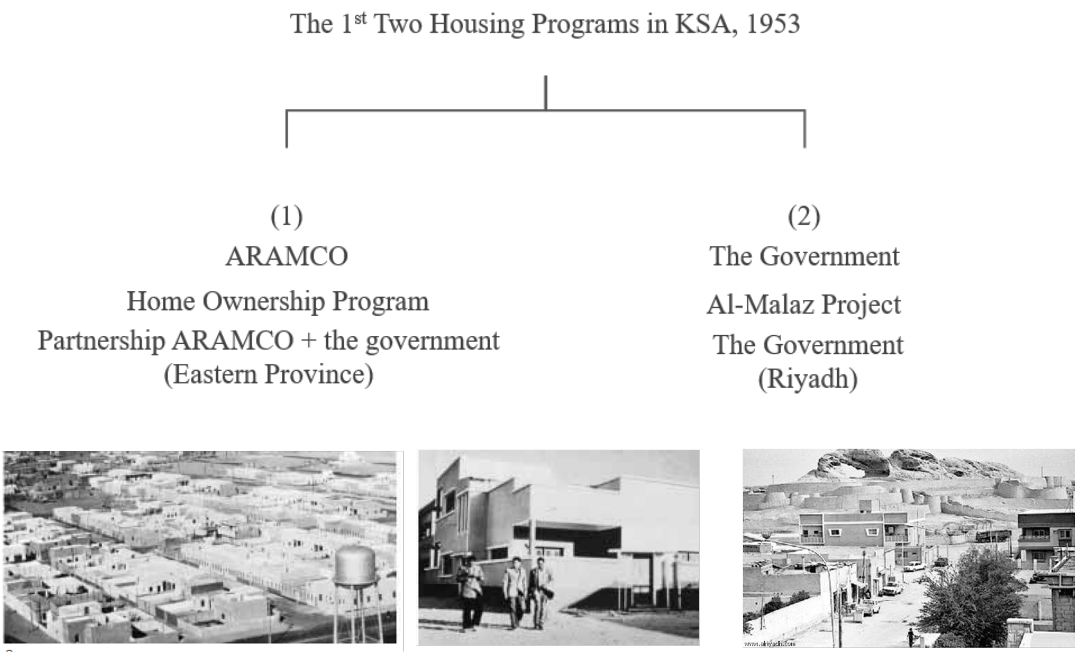

FIGURE 2.7: First housing projects in the KSA in 1953 (Al-Mayouf and Al-Khayyal, 2011)

though these villas did not adhere to climatic and cultural principles (Al-Hathloul, 1981). Conversely, Kayyal (2004) mentioned that the Al-Malaz project provided new standards of good living, introducing pre-planned and innovative designs to new neighbourhoods.

2.4 Formulation of Public Housing (1970-1990)

During this period, government entities attempted to construct public housing with the support of the mid-1970s' oil economic boom. This boom helped build major cities due to the rapid development of the economy and the population. Although the establishment of the first planning organisation in the Kingdom launched in 1958, the actual planning was minor in the 1960s due to pressure from financial restraints. Additionally, the government's direct attention was on developing the transportation and infrastructure systems. In 1965, the planning sector was institutionalised and grew more successful, and by 1975, the Central Planning Organization changed its name to the Ministry of Planning (MoP).

According to Public Works and Housing Ministry (1990), the MoP introduced five-year development plans (FYDPs) that aimed at three dimensions: the economy, the infrastructure and social aspects. FYDPs' intentions aimed to meet the desires and aspirations of citizens, supply housing services and encourage the role of the private sector. The housing services, on the one hand, included more appropriate housing to fit the average household income and satisfy health and safety standards. On the other hand, the private sector's engagement was to guarantee funding for the housing sector's development and a low-cost housing delivery process (Al-Mayouf and Al-Khayyal, 2011).

2.5 The Ministry of Public Works and Housing (MPWH; from 1975)

In 1975, the government established MPWH plus six new ministries added to the Council of Ministers to cope with accelerated government development. The MPWH supplied technical and engineering services, conducted surveys and statistics, and prepared studies and research on the housing sector. The Ministry particularly succeeded in managing two major forms of national projects, rush housing, including high-rise residential buildings in three major cities with a total of 4,752 apartments, and detached units on generous plots of land in various districts were sold to residents with long-term mortgage plans (Mubarak, 2004).

MPWH established 13 projects in nine cities resulting in 14,686 apartment units, 9,854 villa units and 3,793 land plots. The plots were supplied with full services and connected to the government's public networks. Moreover, governmental organisations and military parties collaborated and established housing projects in different areas for the employees. Housing departments were incorporated for establishing, delivering and maintaining housing projects. The projects were characterised as self-sufficient because they accommodated all services, such as leisure, shopping, religious and educational facilities. A total of 221,600 units, 9% of the total residential sector in 1990, were granted to employees either for free or for annual fees. Because of this essential contribution to the housing stock, the housing supply significantly increased (Al-Mayouf and Al-Khayyal, 2011).

2.6 The Real Estate Development Fund (REDF)

The REDF was established in 1974 and started operations in 1975. It is a financial lending agency under the supervision of the Ministry of Finance and National Economy. The REDF has a significant goal, as it arranges long-term loans for Saudi residents, with zero-interest and two types of loans, private and investment. Private loans primarily address low- and middle-income plot owners to support the construction of their homes, up to $ 80,000 USD, while *investment loans* target landowners to construct multi-unit investment housing projects, up to $ 3.75 million USD. Granted to the public, the loans are due in 25 years, with no interest fees. This eased the process for the residents, themselves, building housing units. Regarding Fadaak (1984), lending operations included only families, after which operations expanded to include real estate investors. Consequently, rental units gradually increased from 11% to 39% to 42.2% of the total housing stock from 1974 to 1986 to 1996, respectively. REDF contributed 20%, or 446,700 units, of the total residential construction (Fadaak, 1984),

A total of 712,870 homes were built for public housing projects and REDF, occupying 29% of the entire residential sector (Al-Mayouf and Al-Khayyal, 2011). Interest-free loans and land plot grants substantially contributed to housing developments. The policies granted Saudi citizens free residential land plots in cities with residences in developed neighbourhoods. Correspondingly, the total number of land plots reached 375,972 by the end of 1990 (Fadaak, 1984).

2.7 Public Housing decline (1990-2005)

By the early 1990s, greater pressure on the Kingdom's economy occurred due to the Gulf War, exacerbating the national budget deficit. Therefore, the national development plans cribbed, especially those regarding the housing sector throughout the 1990s. Housing demand reached its peak due to two main factors: the absence of financial allowances from housing agencies because of economic deficits and a rapid spike in the population. Over 5.7 million Saudis were added to the population within 12 years, from 16.9 million in 1992 to 22.6 million in 2004, representing 25% population growth. In contrast, housing units slightly increased compared to the population. Housing increased from 2.7 million dwellings in 1993 to only 3.9 million dwellings in 2004. By 2005, only 6.2% of all homes contributed to the total housing sector, which maximised the gap between the population and housing ownership growth rates (Al-Maghlouth, 2007).

2.8 General Authority for Housing (GAH; 2005-2001)

During this stage, there were fundamental achievements in the housing sector. The reformation of the sector included a new housing authority supplied with suitable funds to meet citizens' requirements, such as quality housing units. Another shift was reassigning the power and regulations from the MPWH to the GAH, which was approved by the Saudi Council of Ministers in 2007. It received all housing-related projects from entities to facilitate and to provide better solutions (Arabia, 2020).

In 2005, about 45% of Saudis lived in rented apartments, while 55% lived in homes they owned. The National Strategy to Combat Poverty stated that 30%, or 695,000 families, lived in unsuitable dwellings due to income and socio-cultural characteristics. This motivated the government to create another housing authority to clarify the critical reasons for the housing deficit and the small ownership rates of housing (Al-Mayouf and Al-Khayyal, 2011).

Subsequently, the government arranged two sorts of subsidies; a budget of $ 2.6 billion USD for the public housing and the acquisition of land through the GAH. This occurred to develop housing projects with the help of the Ministry of Municipal and Rural Affairs and Housing (MMRAH) (Swecon and Abha, 2020).

2.9 Ministry of Municipal & Rural Affairs & Housing (2011-2021)

King Abdullah bin Abdul-Aziz made a royal decision in 2011 to establish the Ministry of Housing (MoH), which became the MMRAH in 2020. The MMRAH aims to coordinate and deliver sustainable environments, including homes of multiple types, villas and apartments. Its mission is to incorporate the governmental and the private sectors to facilitate sustainable environmental housing projects for the public. The mission included managing, monitoring and organising housing projects for segments of Saudis at reasonable cost. Reinforced by research, it was established to fulfil housing supply and demand. By December 2019, the Ministry had established 111 projects with 138,622 housing units. A total of 41 projects accounted for 13,832 units, which were villas with an identical design. Even though the Ministry attempts to enhance the sustainability of housing, that was not evident in these granted units (Housing, 2020).

In 2020, the Ministry conducted a detailed evaluation of the entire housing market to define the risks confronting the housing sector considering the major transformations occurring in the Kingdom. A large portion of the transformations fall under the framework of housing programmes. Recently, the Ministry published a report illustrating citizens' process of gaining land, home or financial aid. The process differs depending on the grant type for which the citizen is eligible. Although the process depicts the participation of the private sector, the homes delivered are not sufficiently suitable in terms of sustainability. Another aim of this latest initiative is to narrow the disparity between housing supply and demand. According to the Ministry, the cumulative housing demand reached 1.4 million, while about 60% of the demand fell in 10 major cities. Most housing demands are in the three most populated cities: Dammam, Makkah and Riyadh with 242,000; 281,000 and 325,000 units, respectively (Housing, 2020). Table 2.1 and Figure 2.8 summarise housing projects in the country from 1970 to the present, indicating the contribution of each governmental housing agency to the total housing stock and to the population.

2.10 Current national policies and initiatives

Even though the KSA is the highest primary energy (PE) producer worldwide, its international PE exports have decreased due to high domestic energy demands, especially in the building sector. These high internal energy demands encouraged the government to introduce an essential priority, supporting energy efficiency in levels by establishing agencies that consider sustainability. These interventions

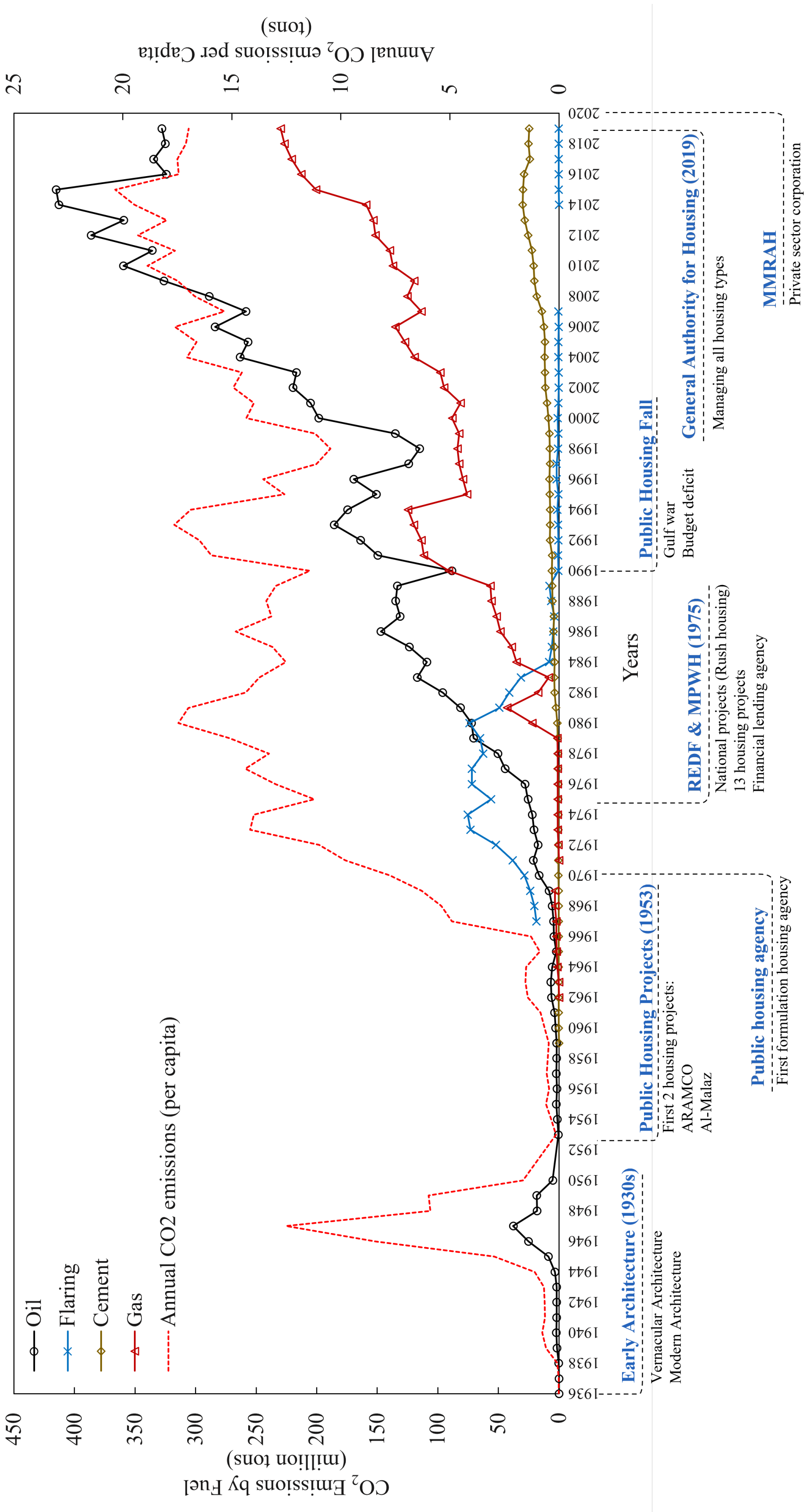

FIGURE 2.8: Summary timeline of the residential stock development of the KSA.

TABLE 2.1: Housing projects developments timeline of The KSA (Al-Mayouf and Al-Khayyal, 2011).

Provider	1970-1990	1990-2005	2006-2010	2011-2018	Total	Growth	Observation
MPWH	24,570	-	-	-	24,570	0.6%	Housing financial restraints pressure to improve infrastructure resulted in low housing contribution.
Public housing fall	221,600	-	-	-	221,600	5.6%	National economic pressure due to Gulf War, and rapid growth of population resulted in early housing increase.
REDF	466,700	143,300	-	-	610,000	15.3%	Governmental long-term loans for housings with zero-interest fees resulted in major contribution.
GAH	-	-	7,291	-	7,291	1.1%	Reformation of the housing sector process lowered housing ownership rates and resulted in a budget deficit of 2.6 billion USD.
MoH	-	-	-	145,739	145,739	9%	Governmental housing programs for citizens (loans or land acquisition), and the private sector participation resulted in housing rates increase.
Self financed	1,749,120	1,384,710	641,429	1,598,731	4,820,017	68.4%	Unsupervised projects built by home owners or investors resulted in housing rates contribution.
Total housing growth	2,461,990	1,528,010	1,392,001	1,744,470	5,829,217	100%	The majority of housing rate is self financed projects
Total Population growth	16,233,785	23,816,183	27,421,461	33,699,947	-	-	Dramatic population increases (doubled)
Housing growth rate (%)	15.1	6.4	2.3	5.2	-	-	Low housing growth rate compare to population growth rate
Population growth rate (%)	106	42	14	21	-	-	This increases the demands for housing and natural resources

MPWH: The Ministry of Public Works and Housing; REDF: The Real Estate Development Fund; GAH: General Authority for Housing; MoH: Ministry of Housing; MMRAH: Ministry of Municipal & Rural Affairs & Housing.

reflect excessive domestic energy consumption and GHG emissions. Another role of such interventions is to shift the reliance on oil as a fundamental source of income to involve alternative energy resources (Matar et al., 2016).

The KSA's government planned to review and increase energy, water and electricity prices gradually for five years (Salam and Khan, 2018). Thus, the government introduced development plans to achieve sustainable economic development. The Ninth Development Plan (NDP) clearly emphasised sustainability in sectors that included buildings (Al-Tamimi, 2017). The NDP targets six ambitions, including enhancing living standards, diversifying the economy and encouraging competitiveness and human resources for both genders. The long-term strategy is to attain a thriving, developed economy by 2024, protecting the environment by conserving natural resources.

Due to unexpected increases in local electricity demands in the Kingdom, more than a 6% increase will be required in power generation capacity from 77 to 120 GW by 2032. The government believes that renewable energy projects can overcome the energy dilemma. A crucial plan aims to generate about 9.5 GW in renewable energy by 2023, the first stage of Vision 2030, and about 58.7 GW directly connected to the public electric grid by 2032 (GAS, 2019). Vision 2030 was introduced to the public in 2016 as the new development plan for a robust economy. Established renewable energy projects involve the King Abdullah City for atomic and renewable energy (Abdmouleh et al., 2015), the King Abdulaziz City for Science and Technology, the Ministry of Higher Education, 2 MW photo-voltaic cells, a solar parking project (Almasoud and Gandayh, 2015) and private sector participation in renewable energy projects to enhance competitiveness (Al-Tamimi, 2017). Table 2.2 summarises the relevant solar power projects of the KSA in sequential order.

In 2007, a non-profit organisation was funded by groups involving engineers and academics, the Saudi Green Building Council (SGBC). The World Green Building Council has approved it to promote awareness, especially in the construction sector. Its accomplishments encompass public alertness, green building requirements, sustainable building materials, green labelling promotions and a rating system for buildings (Aboneama, 2018).

Efforts have been made to propagate an awareness of sustainable living and

TABLE 2.2: Summary of current and future solar power projects in the KSA (Ball, 2015; Mahdi and Roca, 2012; Matar and Elshurafa, 2018; Öst and Paldanius, 2017; Amran et al., 2020).

Year	Project	Capacity	Application
1981-87	PV systems	350;kW	DC/AC electricity generation
1986-91	Solar hydrogen	2 kW	Testing materials
1987-93	Production plant	350 kW	Solar hydrogen testing
1993-95	Cell development	1000 kW	Hydrogen practice
2012	PV solar project	10 GW	PV generation
2013	PV solar project	1,100 MW	Thermal power
2016	PV project capacity	1,800 MW	power converter and Fiber optic application
2017	PV solar project	3,200 MW	electricity generation
2018	PV solar project	200 GW	Connected to grid
2020	PV solar project	24 GW	PV generation
2023	Smart solar power	9500 MW	Advanced technologies
2030	PV system testing	58.7 GW	Connected to grid
2032	PV solar project	54 GW	Electricity generation

energy conservation to promote overall energy efficiency. Awareness programmes include personal and commercial activities. Personal activities are delivered by radio, newspapers and television, while commercial activities include conferences and research centres. Currently, the KSA has 14 universities in various regions to expand sustainable concepts. The universities offer architecture courses for undergraduate and graduate students, and they are available to Saudi citizens for free. Conversely, sustainability is neither applied efficiently in university courses nor in real buildings (Hamdan, 2015).

In 2010, the government made an alternative attempt to raise awareness among the public by establishing the Saudi Energy-Efficiency Centre (SEEC). This centre aims to increase energy efficiency and involve the government and private sectors. The SEEC conserves natural resources and wealth, and it targets the lowest energy consumption in the building, transportation and industrial sectors. The SEEC's achievements have been documented by the Saudi Electricity Company (SEC) as involving air-conditioning standards, thermal insulation regulations, the KSA Building Code (KSABC) update, appliance specifications and monitoring and energy-efficiency labels (Aboneama, 2018).

The KSABC was available for the public in 2007; it was based on the International Energy Conservation Code. The KSABC aims to decrease building-sector energy use because it is a huge energy consumer among all sectors. The building code became mandatory in 2018 and included electrical, architectural and engineering requirements that minimise energy performance in the construction field. It also introduces envelope, air-conditioning, materials and appliance requirements.

The MMRAH intends to enhance the supply of homes through the governmental ministry and the private sector. In 2020, the Ministry published *The Housing Programme Delivery Plan*, which indicated the efforts made to bridge the gap between housing supply and demand. The most important programmes included Etmam, Mullak Union and Sakani. Etmam is a group of approved projects with a total area of 44 million m2. This enables contractors to administer projects more professionally to meet their financial obligations. Mullak Union consists of 540 residential and commercial associations that plan to motivate citizens to buy residences and to raise property market values. Finally, the new partnership model, Sakani, comprises 30 to 40 contractors supervised by MMRAH programmes. In 2017, Sakani provided 120 housing units and 75,000 plots. It provides budgets based on housing options for developments (Saudi Arabia, 2020).

2.11 Challenges facing Energy efficiency in the KSA

According to a survey conducted by Alrashed and Asif (2012), 2.5% of professionals admitted that sustainability is the most crucial factor for projects, while 34% agreed that cost is the most fundamental factor. The survey concluded that cost is more essential than sustainability, which makes sustainable buildings a more challenging task in the country. Even though most support cost over sustainability, the survey was conducted before the new development plan Vision 2030. Vision 2030 introduced the importance of energy efficiency and emphasised sustainable development. However, there are encouraging potential reasons for sustainability, such as manufacturing or energy generation (Nurunnabi, 2017).

The KSA is the largest oil exporter worldwide and consumes about one-third of its energy production for local uses: electricity, transportation and manufacturing. Even though petroleum consumption is too high domestically, different entities assume that the KSA will be a net oil importer by 2030. This reliance on petroleum for energy is making sustainable housing more challenging due to the cheap electrical tariff compared to the rest of the world (Krane, 2017).

Moreover, the growth of residential buildings prevents sustainable development due to the problems with existing buildings. According to the GAS (2019), 61% of buildings lack of thermal insulation. This maybe a major reason for the excessive use of electricity energy for cooling. Thus, the residential sector consumes about 52% of the energy demands of buildings in the country, primarily attributable to cooling. Even-though residential buildings consume a major portion of energy, researchers expect its growth to continue. This is due to the rapid growth of the population, 2.5% since 2014, yet despite that, only 25% of the Saudis own homes (Rehman, 2012).

Climate is another challenge. Extreme air temperatures exceed 50°C during summer and drop to less than 9°C in winter. The climate is hot and arid with low levels of rain. Regardless, climate studies do not agree with the climatic zoning of the KSABC (Al-Naimi, 1989a; Alrashed and Asif, 2015; Almehrej, 2015; Calaqutit et al., 2015; Saudi Arabia, 2020). Different studies define the climate to five climatic zones (Alrashed and Asif, 2015), while the KSABC classifies it as only three zones. Buildings energy demands is mostly dominated by cooling and exceeds 60% of the total building energy demand, and this is due to the reliance on air-conditioning units to deliver thermally comfortable indoor environments (Felimban et al., 2019).

Therefore, this chapter attempts to highlights some of these challenges and shows the necessities for developing a set of representative housing archetypes to be used for energy performance optimisation and air infiltration rate prediction. Optimising the housing energy performance would reduce the infiltration rate and increase the indoor environmental quality. This can be accomplished by sealing the envelope's openings like window and doors' frames and outlets, or by installing thermal insulation on the exterior surfaces which reduces thermal bridges, gaps and cracks found in the thermal envelope.

2.12 Summary

This chapter reviews the housing stock development of the KSA since the 1930s, and shows the disparity between population growth and housing ownership rate. Various governmental agencies held responsibility, see Section 2.1 to 2.9, to manage the housing stock and to supply dwellings to the citizens, but the housing ownership rate has remained low due to rapid population growth, see Table 2.1 and Figure 2.8 in Section 2.9. The government allowed the private sector to participate in the building construction to improve its quality and to meet the population growth demand, see Section 2.10. This collaborative effort to deliver sustainable dwellings has different challenges including extreme harsh weather conditions and issues in the existing building stock, see Section 2.11.

This chapter defined the KSA's government efforts to enhance the energy efficiency of the building stock, but this resulted in different challenges that may make energy efficiency a harder task to tackle. However, recognising this challenges provides deep understanding about the KSA housing context as it has unique climatic conditions, different cultural aspects, and strong religious impacts. The climatic challenges are in contradictory and explained in Section 4.1.4 of Chapter 4, the modern housing styles did not consider cultural aspect including gender segregation, while the religious impacts did not consider housing privacy where housing opening areas are exposed to the neighbors.

This resulted in using more of the KSA energy production domestically, mostly by the housing sector, and increased the total carbon emissions. This prevent meeting the international carbon emissions targets and increases energy wastes, cost and global warming potential. Therefore, its worth mentioning that the governmental effort highlighted in this chapter and the challenges facing sustainability should be considered in this research to assess in providing a set of recommendations for future housing constructions and the building code.

Chapter 3

Literature review

The literature review is the main chapter to assess defining research gaps using existing knowledge in buildings energy performance in the KSA. This chapter establishes the theoretical framework of this thesis according to the defined research gaps to contributes to knowledge using previous work, which explores the major theories and relevant research areas. This chapter informs the research methodology and illustrates the determined methodologies based on earlier methods and knowledge gaps using available data, and highlights research constraints. This provides methodological insights, identifies most useful research practice, addresses research gaps, refines research questions, supports data analysis, clarifies applied tests and data interpolation. This articulates identified research's hypothesis, questions, objectives and the major aim, and draws attention to unresolved questions and identifies areas that require further exploration that need more study.

This chapter considers relevant peer-reviewed literature and methodologies for quantifying the energy performance of an existing stock of homes that has influenced the research. A wide and growing body of literature has been investigated and fragmented into three key sections, see Figure 3.1. Section 3.1 reviews housing energy demands, assessment approaches, housing archetypes, and simulation methods. Section 3.2 investigates buildings indoor environmental quality with spacial attention to the KSA homes, and it reviews different treatment techniques. Section 3.3 reviews air infiltration studies and assessment techniques.

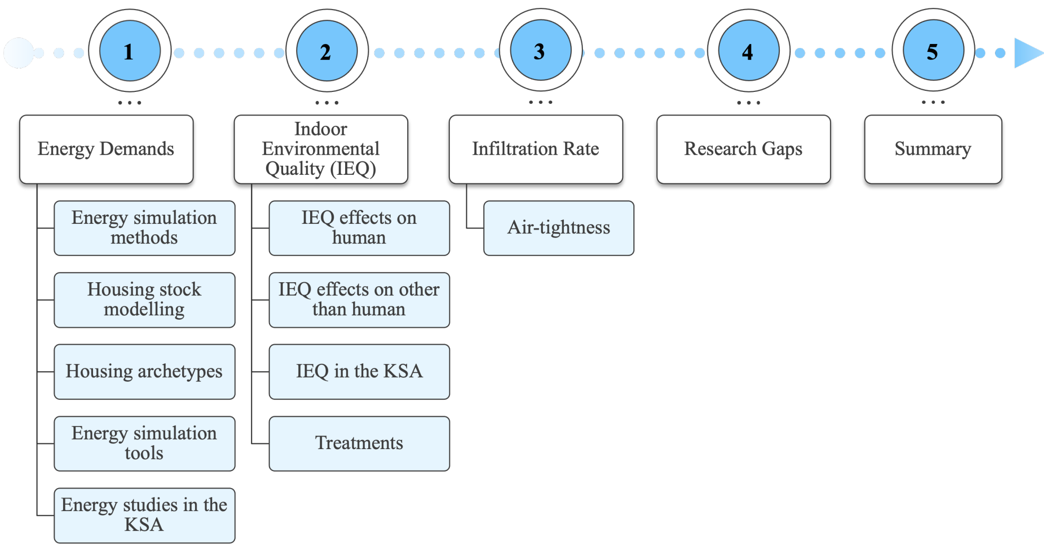

FIGURE 3.1: Literature review summary.

3.1 Energy demands

For many years, energy demands were surprisingly neglected by the KSA's government and homeowners. The KSA's energy demand is high and mostly attributable to residential stock at 52% (Alaidroos and Krarti, 2016). About 60% of this excessive energy use is due to cooling purposes. See 4.2 of Chapter 2. A potential reason for this high energy demand is the population; see Section 4.1.3 of Chapter 4. Population increases often lead to more energy use. Additionally, the low electrical energy prices of the KSA have encouraged citizens to rely on cooling systems to achieve indoor thermal comfort. The cost of the delivery of this electrical energy to Saudi buildings is much lower than for assorted countries because it is locally produced by burning fossil fuels. The KSA's electrical tariff is 0.048 $/kWh while it is 0.22, 0.12 and 0.35 $/kWh for the UK, USA and Germany, respectively (Company, 2018). Vision 2030 declared new energy prices, including raising the electrical tariff to reduce local energy demands and CO_2 emissions. See Section 4.2.2 of Chapter 4. The new tariff for the residential stock has two pricing strategies, including the marginal cost. The tariff remains at 0.048 $ per kWh for homes that consume less than less than 6 MWh per month, while it increased to 0.08 $ per kWh for homes that consume over 6 MWh per month (SEC, 2018). Even though this was previously proposed by Faruqui et al. (2011). Regardless of households' monthly electrical usage, it helps the Saudi public to become more conscious of high electrical energy demands and CO_2 emissions. This is critical because the KSA household is the third-highest energy consumer internationally (Council, 2017). See Figure 4.2 in Chapter 4. In fact, the first three highest household consumers are from the GCC.

Climates with extremely high temperature swings are another potential factor for these high energy demands, as described in Section 4.1.4 of Chapter 4. The population increase, low electrical tariff and harsh climatic conditions resulted in massive energy usage. An alternative intervention was proposed by Avci et al. (2013a) to adjust thermostat setpoints to reduce overall cooling costs. More recently, Algarni and Nutter (2013b) simulated the most common types of KSA housing units (villa, traditional house and apartment) and identified interventions that might reduce cooling loads. However, the study was limited to three regions and assumed that all dwellings have no thermal insulation. They claimed operating schedules for air-conditioning, lighting, equipment and occupancy were collected from questionnaires. In addition, the survey's sources were unavailable, and air conditioners were assumed to operate 100% of the time.

A relationship between electricity demand and scheduling assumptions was also identified by Algarni and Nutter (2013a). They concluded that energy costs and demand reductions can be achieved by optimising the schedule of services. In-depth discussions on the subject were presented by Matar (2015), Matar et al. (2016) and Matar (2017). They proposed an integrated model since there is a high correlation of the trade-off between thermal comfort and adjustments in cost. The integrated model combined a prototype residential model with the King Abdullah Petroleum Studies and Research Centre (KAPSARC) Energy Model (KEM) for the KSA. The KEM is a free online equilibrium energy model that allows the analysis of variable parameters and their impact on the Kingdom's energy sector. It investigates energy resources and performance to assess economic decision-making processes. The model was used to predict the correlations and the interference with the utilities and the wider economy.

The KEM model's developers utilised time-of-use pricing for homeowners to manage their energy consumption, excepting the households' reactions to energy price changes (Matar, 2017). They found that the demand for electricity can be lowered by adjusting thermostat setpoints, as mentioned by Avci et al. (2013b). Due to the homogeneity of people's behaviours, only four human reactions were analysed and related to energy price shifts. Finally, they calculated the effects of human behaviours to price changes and presented them, limiting the values between which reactions may lie. They concluded with 12 scenarios of household responses for each archetype (Matar, 2017). The study resulted in high afternoon energy peak reductions, even though the highest reduction was achieved regardless of occupants' thermal comfort. Indeed, indoor thermal comfort should be briefly considered for all housing energy analysis. However, this model is not resilient for the defined modifications in occupancy, post-occupancy evaluation, scheduling and systems' power densities. It has limited options for determining building systems, such as cooling systems. On the contrary, it is the only available model that considers buildings' orientations. The user can define a building's orientation before running the simulation, which may affect the model's energy predictions. Nonetheless, this is not determined by landowners and is usually fixed.

Typically, researchers calculate buildings' energy performance to assess the energy demands of a particular stock of buildings. They rely on previously developed approaches and may integrate building energy performance calculation methods and simulation techniques.

3.1.1 Building energy performance calculation

There are two approaches for calculating the energy performance of buildings: steady state and dynamic. The steady-state calculation approach is a simplified method governed by a set of basic functions. It has the benefit of straightforward and standard computation (UNI, 2008). Researchers have adopted this method, but more important are the building codes and international standards of the European Energy Performance of Buildings Directive (EPBD; (Union, 2002)). ISO 13790 defines a normalised method for calculating energy load requirements according to building thermal heat gain and loss. IOS 13790 considers buildings' energy dynamic impact by using empirically established coefficients to anticipate heat gains or losses. It determines buildings' energy demands by balancing infiltration heat losses versus indoor and solar gains. ISO 13790 also considers the conjunction with building mass, environmental variables and occupancy activities (Van Dijk et al., 2005). The benefits of using this approach are that this basic model requires a few inputs explicitly described by visual mathematical procedures and the intuitive and concise detection of relationships among data inputs and outputs. Nonetheless, its shortcomings involve the insufficient display of the dynamic performance of complicated building system controllers. Therefore, engineers must rely on advanced dynamic simulation tools to predict buildings' energy performance dynamics, such as EnergyPlus, which is described in Section 3.1.2.3.

The dynamic approach has a few additional advantages over the steady-state approach. The benefits involve dynamic simulations within time-varying variables, high-level modelling abilities to dynamically consider energy performance fluctuations and the embedded performance measurements of parameters such as thermal comfort, IEQ and daylight. It also allows the assessment of novel building designs and systems such as double-skin facades that are not addressed well by the steady state (Kim et al., 2013). This may be accomplished using diverse energy simulation analysis methods.

3.1.2 Energy simulation analyses methods

The literature classifies energy simulation analyses for buildings' energy demand assessments into six major techniques, which are proactive building simulations (PBS), holistic designs, optimisation, statistical methods (SM), CAD models and building performance simulations (BPS), including interoperability and knowledge-based input generation (Østergård et al., 2016). Figure 3.2 presents the methods utilised for building energy simulation analysis. These techniques can be used to simulate buildings' energy performance using the simulation tools described in Section 3.1.2.3 (Tian, 2013).

According to Østergård et al. (2016), only three of 392 tools used by the U.S. Department of Energy's approaches can be classified as pre-design informative. Pre-design informative refers to building simulations' attempts to express buildings' energy performance in early design stages. The simulations aim to answer **what if** questions for possible scenarios, such as: What if we allow external shading or increase the envelope area? Buildings' architects or engineers should respond to these questions and use them as references for alternative solutions for energy reduction targets. These responses are useful in modelling various base cases during early design phases, but they frequently require simulation expertise due to the complexity of the process.

A holistic design is another internationally employed simulation technique for buildings' energy evaluations. Each building design can be achieved by using contradictory requirements and objectives. These objectives can be evaluated by using certification schemes, such as the German Sustainable Building Council (DGNB), Leadership in Energy and Environmental Design (LEED) and the Building Research Establishment Environmental Assessment Method (BREEAM). A percentage of these objectives can be estimated using quantitative or qualitative computational simulations. In some circumstances, this technique has difficulty computing room acoustics, draughts and life cycle cost because altering one object alters others. This designer-focused solution must be used throughout the conceptual design stage for simultaneous design assessment, which requires the application of superior interoperability using common file exchange schemes or integrating many algorithms into one software platform (Østergård et al., 2016; Nagel, 2016).

Optimisation techniques are an automatic application of mathematical optimisation in conjunction with simulations of building performance. This term refers to a general description of patterns, advantages and obstacles based on assessments of buildings' design optimisation. A building optimisation analysis comprises two main processes derived from two reviews that might be repeated in the design process. The reviews require the selection of design factors and restrictions, the determination of a simulation tool and the development of a base-case model for benchmarking. The selections may comprise calculation functions, an optimisation algorithm, the execution of a simulation until optimisation convergence is attained and quantitative data reasoning and display. Building optimisation has become one of the most essential approaches of computer science breakthroughs due to the parallel applications of cloud computing, optimisation and genetic algorithms (Evins, 2013; Attia et al., 2013; Stevanović, 2013; Machairas et al., 2014; Nguyen et al., 2014).

Moreover, software developers and academics are concentrating more research on the data sharing and interoperability between CAD models and BPS (Attia et al., 2012). There are many varieties of interoperability, such as run-time interoperability, which requires a standard file exchange format to function. Through using an integrative and optimised procedure, a single type of analysis can be conducted continuously for early design support. However, more detailed analyses could be used in later stages, such as detailed simulation data using computational fluid dynamics (CFD) applications, such as CONTAM (Dols, Polidoro, et al., 2015).

SM is one of the most important simulation analyses for data processing, and it is related to the design process since the energy modeller performs extensive simulations using statistical techniques to obtain interpolated values. This approach assesses the building's energy model with the required data inputs and energy performance to determine the challenges related to the probabilistic nature of users' behaviours and weather conditions. SM includes four disciplines: uncertainty analysis, sensitivity analysis, meta-modelling and multivariate analysis. See Section 3.1.2.1. The workflow of the statistical analysis depends on using statistical software packages with building performance software. Regarding the importance of such workflows, the developers aim to establish more extensions related to building simulation environments to improve the quality of the parametric analysis (Tian, 2013).

Finally, knowledge-based input generation requires building a performance database that includes buildings' features, such as physical and operational characteristics derived from thousands of real buildings' information. Energy performance software requires a massive quantity of inputs, which may be provided directly by the user or by importing information from previously developed databases. Even though this is essential for modelling and data reliability, it may be time consuming (Nilashi et al., 2015).

In summary, researchers used all six types of simulation analysis to evaluate the energy efficiency of a single building or a whole housing stock. The techniques can be used independently or integrated with other techniques.

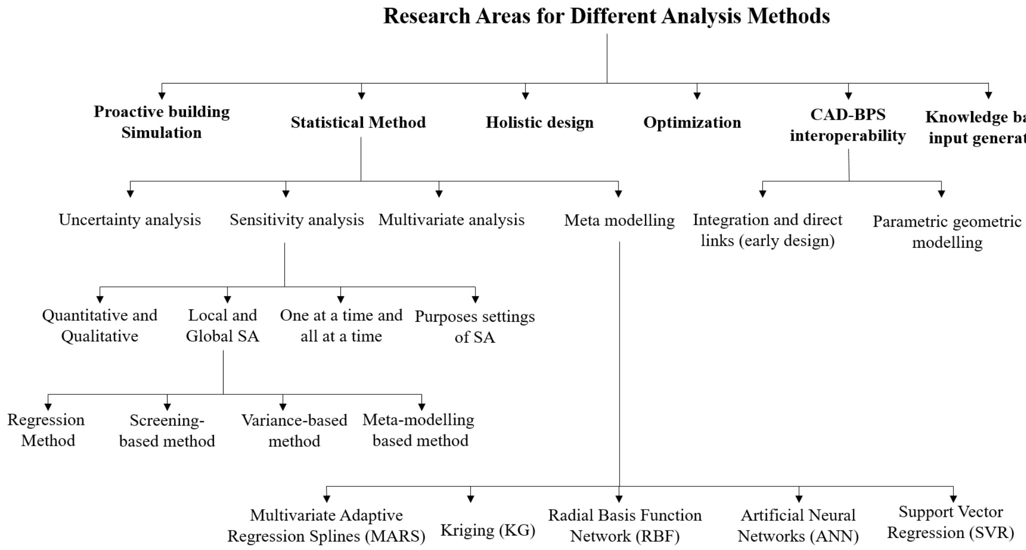

FIGURE 3.2: Various methods utilized for building energy simulation analyses (Tian, 2013; Østergård et al., 2016).

3.1.2.1 Statistical methods

Statistical approaches are a design process in which the modeller conducts vast groups of simulations in an organised manner and employs statistical techniques to obtain design support from simulated data. Four key types are included: uncertainty analysis (UA), sensitivity analysis (SA), multivariate analysis and meta-modelling. UA has been employed to investigate the influence of uncertainty on predictions obtained from a building simulation tool. UA aims to evaluate data separately from the decision-making process. The integration of uncertainties into building performance supplies decision-making support with the desired building solutions. The combination of UA and SA facilitates the quality assurance of the model, evaluates design variations, enhances the understanding of the design's resilience, offers plausible boundaries of performance indicators and provides limited values for factors including cost analysis (Hopfe, 2009).

Most authors recommend incorporating SA into early design phases because it determines input parameters' effectiveness and significantly influences energy performance (Hopfe, 2009; Østergård et al., 2016; Tian, 2013). This is crucial for answering **what-if** questions throughout calculations of regressional equations to interpret the size and direction of changes in performance (Saltelli and Annoni, 2010). Alternative SA methods are demonstrated in detail and cited in books such as Global Sensitivity Analysis: The Primer by Saltelli and Annoni (2010).

Furthermore, Tian (2013) discussed the utilisation of SA in building energy analyses and divides SM into local and global approaches. The local approach determines the impact of uncertain inputs and their effect on the initial design (or base-case model) by changing one parameter at a time (OPAT). Changing OPAT is less computationally complex, even though it is not suitable for non-linear systems (Saltelli, 1999). However, the global approach focuses on unpredictable inputs across the entire input space. They are more adoptable for non-linear, non-additive and non-monotone applications. They also are suitable for evaluating the impact of interactions between inputs and outputs and for calculating total energy usage.

The third key type of SM is multivariate analysis and filtering, which concentrates on stochastic approaches for creating simulations of the design space. After the identification of favourable areas in the design space, filtering methods are best for identifying a desired criterion. Multivariate analysis is most suitable for an extensive amount of data obtained from various simulation systems along with data visualisation using scatter plots or histograms (Østergård et al., 2016).

The SMs employ numerical values for planning, collecting and analysing data to interpret and to provide meaningful understanding of the results on a a systematic and a proven approach. This might be helpful to develop a data-set for the KSA housing stock for energy performance research. This can be used to identify the most relevant building elements that influence the energy performance. The SMs show the relationship between variables and how can they be improved or adjusted in the baseline environment.

3.1.2.2 Meta-modeling analyses

A massive number of variables should be considered when exploring a large area of interest to assist with decision-making procedures. This can be accomplished through the meta-modelling technique. Meta-modelling seeks to explore variables to present the best dataset for the decision-making process. Instead of spending a long time simulating all possible parameters for energy analysis purposes using an energy modelling tool like AutoCAD, the energy model can be converted to a

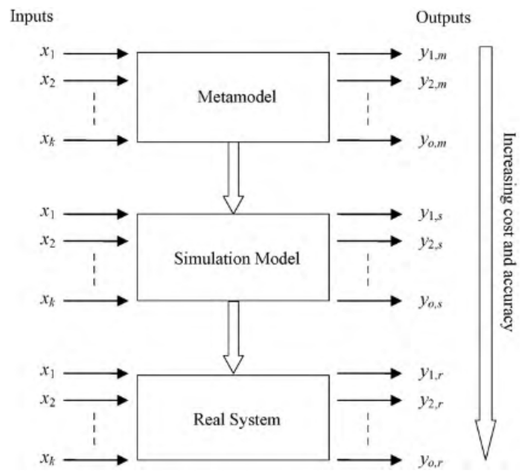

FIGURE 3.3: Accuracy comparisons of meta-modeling against the real system (Li et al., 2010).

mathematical or statistical model to hasten the running process. This alternative approach is a model of the model (Li et al., 2010), or a *meta-model*.

A *meta-model* searches for optimal decision variables in a faster and less costly manner. It is commonly constructed to approximate the input and output variables of a simulated energy model. The verification stage follows. It is conducted by implementing the results of the simulated energy model. Subsequently, an SA is applied to define the optimal solution. Even though accuracy is slowly increasing because meta-modeling is an iterative process, it is less accurate than the real system or the simulated model, as shown in Figure 3.3. Conversely, it consumes less time and cost due to the level of complexity, which is also less compared to the real or the simulated system (Li et al., 2010).

A meta-model is widely acknowledged as a much faster technique compared to direct inputs to the simulated energy model. Several frequently applied techniques of meta-modelling have been observed in the recent literature, including multivariate adaptive regression splines (MARS), Kriging (KG), the radial basis function network (RBF), artificial neural networks (ANN) and support vector regression (SVR). MARS and KG are the oldest and have been frequently employed for meta-modelling, while ANN, RBF and SVR are commonly employed for artificial intelligence techniques. Meta-modelling techniques have recently adopted them due to their flexibility and capability of approximation (Li et al., 2010).

3.1.2.3 Energy simulation tools

As described in Section 3.1.5, building archetypes are often developed using two types of large-scale modelling approaches, including top-down and bottom-up, as described in Section 3.4. The development of a stock of building archetypes allows a faster, more valuable energy performance assessment before decision making. The energy assessment is usually conducted using various energy modelling techniques, including building performance simulation (BPS) tools.

BPS tools are frequently used throughout the design process of new buildings to comply with regulations and lower buildings' energy demands. BPS is a powerful analytic approach for retrofitting buildings since it provides insights into individual buildings' energy demands in its existing state and predicts a variety of hypothetical scenarios involving changing climatic conditions or occupancy schedules. This enables scientists to investigate scenarios and apply improvement initiatives to forecast heat transfer and energy demands or savings, human thermal comfort, IEQ conditions and life cycle cost. The energy modelling technique is a robust approach known for analysing buildings' energy demands, including the ability to diversify data inputs to capture energy cases, including occupant profiles, schedules, climatic conditions and extreme weather variations (Carratt et al., 2020; Solmaz, 2019).

According to Carratt et al. (2020), 100% of studies that merely conducted a theoretical evaluation of retrofits employed building energy simulation tools. Numerous BPS tools were used in the literature, although more than half of the research used EnergyPlus, TRNSYS, IDA-ICE and DesignBuilder. See Table 3.1. EnergyPlus is free and is one of the most user interface energy simulation tools that enables the transfer or exchange of data with various simulation tools. This is important because it allows models' integration and coupling for different evaluation purposes, including energy demands, airflow using a computational fluid dynamics (CFD) tool known as CONTAM (Walton and Dols, 2006), which has a CFD component for evaluating indoor air contaminants and occupant thermal comfort.

TABLE 3.1: Energy simulation tools comparisons (modified from (Solmaz, 2019)).

Simulation tool	**Major capabilities**	**Required expertise**	**Users**	**License**	**Company/ Country**
EnergyPlus	Whole building energy simulations Lighting simulation Code compliance checking	Building physics and mechanical engineering background	Architects, Engineers (mechanical, energy, control), Building auditors and operators analysts	Free/Open source license	US-DOE National Renewable Energy Laboratory (NREL)/US
DesignBuilder	Whole building energy simulations Load calculations Parametric and optimization	Easy learning process	Architects, Engineers, Desingers, and researchers	Required	DesignBuilder software Ltd./UK
EDSL-TAS	Whole building energy simulations HVAC system design and sizing Parametrics and optimization Detailed cost analyses	Training courses are not necessary Includes comprehensive tutorials	Architects Building services engineers Consulting engineers	Free for non-commercial academic use, free to try	Environmental Design Solutions Limited (EDSL)/UK
eQUEST	Whole building energy simulations	Energy analyses experience Knowledge of building technology	Building designers, operators owners, and LEED consultants	Free/Open source license	James J. Hirsch & Associates/US
ESP-r	Whole building energy simulations Complex buildings and systems	Building physics, environmental and controls system knowledge	Building designers Engineers Energy consultants Researchers Multi-disciplinary design firms	Free/Open source license	University of Strathclyde Energy Systems Research Unit (ESRU)/UK
Green Building Studio (GBS)	Whole building energy simulations Parametric and optimization	Non, only CAD for geometry modeling	Architects, Engineers, Construction managers	Free for non-commercial, academic use,	Autodesk Inc./US

3.1.3 Buildings energy demands in the KSA

Previous studies in the KSA have explored the relationships between buildings' thermal envelope and energy demands and found that the transfer of heat through the envelope accounts for 40% – 45% of a building's thermal load. This is important because it conveys that accessible energy-efficiency measures in the KSA can reduce heat transfer through buildings' thermal envelope (Mujeebu and Alshamrani, 2016). Nevertheless, this optimisation requires more information regarding building details including envelope thermal properties, which highlights critical factors influenced formulating the research's questions and major aim. Building energy demand studies in the KSA are divided into four sections, as follows: Section 3.1.3.1 addresses the thermal conductivity of buildings' thermal envelope. Section 3.1.3.2 reviews thermal envelope studies to reduce energy demands. Section 3.1.3.3 highlights relevant energy optimisation studies and existing energy models. Section 3.1.3.4 discusses HVAC evaluation studies.

3.1.3.1 Thermal properties

The thermal properties of materials determine how much heat is transmitted between the interior conditioned and the exterior unconditioned spaces of buildings and are measured by W/m.K. It describes how much heat can be stored or absorbed in the building's envelope via heat conduction, convection and radiation. Conduction is the heat flow of molecules through solid materials or liquids. Convection is the travelling of the heat energy of a material through the bodily movement of fluids and gases' particles. Radiation is a cycle of heat waves released into the atmosphere and then absorbed, reflected or transmitted by a colder body (McMullan, 2017).

In harsh climatic zones, applying thermal insulation to a building's envelope can effectively reduce electrical energy usage, cost and GHG. The thermal insulation's performance is primarily dictated by its thermal conductivity (k), which is influenced by the density, porosity, moisture content and mean ΔT of the material (Abdou and Budaiwi, 2005). According to the Standard Terminology Relating to Thermal Insulation C168 (2014), the k-value is assessed in typical conditions at

24°C. However, the actual mean temperature and moisture content of a building's envelope vary according to the climate, which impacts thermal insulation materials and performance.

The thermal conductivity measurement of thermal insulation is usually classified into two categories: steady-state and transit methods. The most common steady-state technique is the guarded hot plate (GHP) to evaluate the insulation's k. The GHP operates by maintaining a constant temperature gradient across a specified thickness of a sample to control the heat flow at the sides. The GHP has a significant downside, as it requires a long time to create a considerable temperature gradient over a large sample size. Conversely, transient methods send a signal to generate heat in a sample to record it and to achieve the desired results in a short time. The laser flash is a common technique in the transit method, as it determines the thermal diffusivity of conducting solid materials (Al-Ajlan, 2006). The GHP was employed in the KSA to test the k of the most widely utilised construction materials and evaluated against data found in the literature (Abdelrahman et al., 1990). The findings showed that k-values fall in the higher range of the reported data, perhaps due to differences in materials' density, moisture content and temperature.

In 2008, a study evaluated the effectiveness of the k for insulation materials made of fibre across a temperature range of $300-973\,K$. It found a non-linear relationship between k and the mean temperature. This study highlighted the need to set minimum mandatory requirements for thermal insulation materials and k-values (Zhang et al., 2008). Although setting minimum requirements for k-values is essential, it should account for the location due to weather variations.

3.1.3.2 Building thermal envelope

The building's physical barrier that shields the air-conditioned indoor environment from unair-conditioned outdoor environment is known as the building envelope. The existing literature on the building envelope of the KSA is extensive and focuses on applying thermal insulation materials or fenestration. These divergent analysis studies started in 1987 and are chronologically summarised in Table 3.2.

An early study evaluated solar gains through fenestration that increases cooling systems' usage in buildings. The study proved that electrochromic glazing highly reduced heat gains compared to outdoor fixed shading (Tinker & Buijan, 1987, cited in Mujeebu and Alshamrani (2016)). Even though this was a smart solution to decrease energy demands, it is still an expensive, luxurious product. The first serious discussions and analyses of buildings' thermal envelope emerged in 1989, supported by the King Fahd University of Petroleum and Minerals (KFUPM). KFUPM's architectural engineering department constructed an actual residential building unit in Dhahran city for energy evaluation purposes (Grondzik et al., 1989). This study is significant because it establishes the foundation for future housing energy demand evaluations in the KSA. However, several articles have investigated the same residential unit without applying envelope thermal insulation, including Ahmad (2004), Alaidroos and Krarti (2016), Alaidroos and Krarti (2015), Krarti et al. (2020), and Aldubyan et al. (2021).

Al-Naimi (1989b) and Abdelrahman et al. (1993) examined the energy savings of residential units by modifying the envelope configuration. They claimed that a major reduction in energy usage by 40% is possible by selecting more efficient construction materials for the envelope. Ten years later, Ahmad (2004) evaluated envelope configurations for the KFUPM residential unit and reduced energy demands. Al-Hazmy (2006b) investigated the hollow bricks available on the Saudi market. This study analysed heat transference through hollow bricks and inserted polystyrene bars in the envelope, which reduced heat by 25%. Al-Mofeez (2007) evaluated a single-storey residential unit in Dhahran city and proved that 40% of cooling energy use can be acquired by using envelope modifications. Similarly, Al-Hadhrami and Ahmad (2009) optimised building envelope configurations, including various types of local bricks on the Saudi market for potential energy savings. This study was significant because it clarified the energy efficiency of local envelope construction materials. Building envelopes frequently feature gaps and cracks that may transfer unlimited amounts of heat indoors. This was addressed by numeric investigations by Antar and Baig (2009a) and Antar (2010a) who developed criteria for selecting energy-efficient building envelope materials.

Moreover, previous attention has focused on the provision of the thermal mass impact on energy performance. Budaiwi (2011) examined the effects of energy performance by modifying the envelope configuration of a mosque. Another study involved varying the amount and allocation of the thermal mass in the insulated walls of buildings. The study showed that 17% and 35% yearly maximum energy savings of cooling and heating loads are attainable, respectively (Al-Sanea et al., 2012a). However, the amount of cooling energy savings can be higher than 17% due to advancements in construction and insulation materials. More recent studies were conducted by Budaiwi (2011) and Aldawoud (2013) on double skin facades (DSF) and glazing types. Both studies claimed that more savings were achievable, but practising DSF appears complex because it necessitates more building area, construction materials and cost.

Most of the KSA research focuses on energy demands only for one building or a few buildings approaches due to insufficient information about the housing stock. Information about the housings' types, geometry, dimensions, thermal properties, human activities, and other are missing, see Section 3.1.5.3. It would have been more informative if building energy studies considered housing archetypes to assess the overall energy performance of the stock, similar to the work of Krarti et al. (2020), but Krarti et al. (2020) assumed infiltration rate and neglected ground temperature, which are sensitive factors that highly effect the energy performance (Papst et al., 1999), see Section 3.3.1. The housing archetypes can be used to analyse infiltration rate, IEQ, and thermal comfort. Key questions remain like what are the indoor environmental conditions of the archetypal homes in the KSA? What causes the high energy demands of the archetypes? How much energy can be saved? What are the optimal strategies for saving energy?

3.1.3.3 Energy optimization

Energy optimisation is using or avoiding using energy in buildings to reduce demand to mitigate GHGs and GWP. Studies on potential energy-efficiency improvements in the KSA can be grouped into two categories: 'early studies', published in the late 1980s and early 1990s, and more recent experimental or simulation studies. Early studies investigated the impact of the weather and presented it on data sheets for a few Saudi cities that can be used by building energy simulation tools. Simultaneously, experimental studies used the data and simulated buildings to predict energy performance. In an early attempt to collect weather data from 1970 to

TABLE 3.2: Relevant thermal envelope studies in the KSA (modified version from (Mujeebu and Alshamrani, 2016)).

Source (Year)	**Area of study**
Al-Naimi (1989b)	Socio-economics of cooling systems and traditional building materials
Eben Saleh (1990)	Insulation materials thermal performance
Abdelrahman and Ahmad (1991)	Insulation material type and thickness review
Said and Al-Hammad (1993)	Residential buildings energy retrofitting measures
Abdelrahman et al. (1993)	Different bricks types used in homes for energy analyses
Tinker and Buijan (1998)	Buildings external solar gains evaluation
Al-Sanea and Zedan (2001)	Allocation of insulation materials (inner or outer envelop surface)
Ahmad (2002)	Cost analyses of insulation and performance
Ahmad (2004)	Residential buildings insulation types
Al-Homoud (2005b)	Insulation materials review
Al-Hazmy (2006a)	heat transfer of hollow bricks
Al-Mofeez (2007)	Energy retrofitting measures for homes
Baig and Antar (2008)	Heat transfer assessment of local Hollow bricks
Al-Hadhrami and Ahmad (2009)	Local bricks energy performance analyses
Antar and Baig (2009b)	Heat transfer assessment of Hollow brick
Antar (2010b)	Heat transfer assessment of Hollow brick
Budaiwi (2011)	Parametric energy analyses of mosques envelope
Al-Sanea et al. (2012b)	Thermal mass impacts on energy performance
Budaiwi (2011)	Double skin facades analyses
Aldawoud (2013)	Electrochromic glazing energy performance impact
Mujeebu and Alshamrani (2016)	Review of building energy and management

1991 for the five regions of the KSA, the authors presented weather characteristics for 20 cities, including monthly ambient temperature, the degree-day base temperature and summer and winter outdoor temperatures (Said et al., 1996). These data are important, as researchers can use them to evaluate the quantities of solar radiation in the country.

The experimental and simulation investigations were conducted on a few selected housing units. This type of studies concentrated on the impact of buildings' envelope properties and total energy savings. According to Al-Homoud (2001), computer tools may be used to perform various building energy analyses, evaluate prospective energy-efficiency technical implementations and test a building's energy performance. It presented the impact of simulation tools in predicting energy demands in the residential sector of the KSA. This encouraged future developments in the KSA's energy conservation models and in using alternative energy resources. The simulation tools evaluated illustrate economic and environmental constraints on energy resources. This is valuable for making superior decisions in buildings' designs and operations to upgrade envelopes' thermal performance and to lower energy demands (Al-Homoud, 2001).

Ahmad (2004) performed an initial simulation study for a two-storey residential building in Dhahran using the DOE-2.1E tool. The outcomes verified that adding sufficient thermal insulation to walls and roof components led to a 42% savings of the total annual energy, which is greater than in Al-Sanea et al. (2012a), who saved a maximum of 17% cooling energy. Another study investigated the impact of various types of thermal insulation on a single residential house in Riyadh. It revealed that implementing an insulation layer led to 24% to 46% savings in annual energy use (Al-Homoud, 2004). An hourly building energy simulation analysis to reduce energy use was conducted by Al-Homoud (2005a). The simulation provided an optimisation model that helps to evaluate solutions and rank them to select the most appropriate energy-saving measures. This study is interesting because it enabled engineers to operate alternative measures to be examined in the design phase before the actual implementation of incorrect decisions. However, they did not consider other factors that highly influence buildings' energy performance, including infiltration rates and ground temperatures. Additionally, the study was performed in only cold weather and did not include other climate zones of the country.

The EnergyPlus's tool use in the building sector of the KSA was studied by Altan and Alshareef (2006, cited in Mujeebu & Alshamrani, 2016), who evaluated the energy use of a school building. A school's energy use can differ depending on a building's location and climate. However, additional factors may change the prediction of energy use involving occupants' scheduling or behaviour. Al-Mofeez (2010) employed DOE 2.1 software to evaluate energy performance and implement retrofitting measures for residential buildings. Most of the energy was saved in July due to the hot weather and the use of cooling systems. Taleb and Sharples (2011) investigated an apartment building's energy performance in Jeddah city and offered distinctive recommendations for buildings' energy reduction. They employed an energy simulation tool known as eQuest 3.64. The results enabled the authors to draw up guidelines for future buildings in the KSA with respect to climate. This study was notable because it was the first to research an apartment building rather than a villa.

More recently, a study in the KSA prepared an integrated method including an engineering-based residential electricity demand model to determine an economic equilibrium framework (Matar, 2015). This method can evaluate electrical energy

TABLE 3.3: Relevant energy optimization studies in the KSA (modified version from (Mujeebu and Alshamrani, 2016)).

Source (Year)	Area of study
Bahel et al. (1985)	Cooling loads of AC systems
Bahel et al. (1989)	Energy performance tools
Al-Homoud (1997a)	Energy performance for offices
Al-Homoud (1997b)	Energy performance for homes
Numan et al. (1999)	Typical residential building energy evaluation
Kinsara et al. (1996)	Techniques for building energy optimization
Monawar (2001)	Apartments energy performance
Al-Homoud (2004)	Energy Optimisation technique for building
Al-Homoud (2009)	Optimisation technique for building envelope
Al-Mofeez (2010)	Residential building energy savings
Al-Shaalan et al. (n.d.)	Energy saving strategies for mosques
Al-Shaalan et al. (2014)	Guidelines for Saudi Buildings designs
Aldossary et al. (2014a)	Residential buildings energy performance
Alaidroos and Krarti (2015)	Envelope optimization for a dwelling
Matar (2015)	Residential building modeling for economical developments

use throughout the day and record its impact. Recording this impact is important because it may identify major sources of heat gain or loss. This was the KSA's first step to construct a web-based residential building energy model for the public for free. The online model, known as KEM, is described in Section 3.1. KEM is a bottom-up economic model that evaluates six sectors in the KSA's energy economy: upstream production, oil refining, petrochemicals, power and water desalination and cement (Matar, 2015). The KEM model can be developed to include unique data inputs to estimate the KSA's power generation technologies, including conventional thermal plants, nuclear energy, photo-voltaic energy, concentrated solar power and wind. According to Matar et al. (2013) and Matar and Elshurafa (2018), the KEM model adopted a mathematical formula to estimate cost reduction using chronological load demand curves. The load demand curve illustrates the variation in the power plant load and supports the decision-making process. Relevant energy optimisation studies in the KSA are summarised in Table 3.3.

3.1.3.4 Heating, Ventilation, and Air Conditioning systems

The HVAC systems in buildings use the most electricity than any other appliance, especially in hot and humid climates. It is well known that traditional air-conditioning systems use more than 70% of the electricity used for the KSA's residential buildings (Mujeebu and Alshamrani, 2016). According to Vakiloroaya et al. (2014), employing the unique innovations of conventional cooling system components is a well-known method for enhancing the energy efficiency of HVAC

TABLE 3.4: Relevant HVAC systems studies in the KSA (Mujeebu and Alshamrani, 2016).

Author	Area of study
Bahel et al. (1985)	Four central AC systems performance
Bahel et al. (1989)	Residential cooling load simulations
Kinsara et al. (1996)	Proposal for energy efficient AC system
Budaiwi and Al-Homoud (2001)	Ventilation impacts on energy performance
Said et al. (2003)	Database about outdoor conditions
Budaiwi (2003)	HVAC impacts on energy performance and comfort
Iqbal and Al-Homoud (2007)	Parametric analyses of HVAC system and EEMs
Najid (2010)	HVAC system operation and applications of EEMs
Fasiuddin and Budaiwi (2011)	EEMs on HVAC system for commercial buildings
Al-Shaalan (2012)	EER enhancement for RACs
Budaiwi and Abdou (2013)	EEMs on HVAC system in commercials
Almutairi et al. (2015)	LCA of AC system applied in residential unit

systems. Researchers have investigated HVAC systems for different building types and provided impressive work, summarised in Table 3.4. For example, Bahel et al. (1985) found that an air-conditioning system consumed about 22,200 kWh of the total electrical energy used in a single residential unit in Dhahran, KSA. This was expanded to apply a strategy for conserving a latent fraction of AC cooling loads by storing water vapour using liquid desiccant Bahel et al. (1985). The liquid desiccant is useful because it eliminates moisture, as well as latent and sensible energy from the air. Similarly, Kinsara et al. (1996) applied the liquid desiccant technique to a typical cooling system and reduced energy demands. Another area of focus is a building's ventilation strategy. Budaiwi and Al-Homoud (2001) showed that a proper ventilation strategy can conserve 50% of ventilation energy requirements.

3.1.4 Housing stock modelling approaches

There has been an increasing amount of literature on energy modelling techniques for large-scale housing stock; it evaluates energy demands and carbon emissions for reduction purposes. It has been practised by researchers for the further comprehension of housing stock electrical energy demands. Beyond one single building or a few buildings' approach, modelling techniques contribute, enhance and support decision making process using evidence for an entire building stock and its energy retrofits (Molina et al., 2020).

According to a review on modelling approaches by Swan et al. (2008), modelling approaches are comprehensive due to their ability to investigate techno-economic, environmental and energy demand impacts. There are two approaches: top-down

TABLE 3.5: Modeling approaches comparison strengths (top) and weaknesses (bottom) (Swan and Ugursal, 2009).

Top-down	Bottom-up Statistical	Bottom-up Engineering
Long term predictions	occupants activity	Predicts new technologies
macro/socioeconomic impact	macro/socioeconomic impact	Bottom up estimations
easy data input	End-use representation	End-use Usages
comprises trends	Billing data	End-use qualities
Historical data required	Historical data required	Assumptions
No end-uses representations	Multiple correlation	Detailed data inputs
Coarse analyses	large samples	Simulation complexity
No new technologies	less data provided	no economic factors

and bottom-up. The top-down method perceives the housing stock as an energy sink and disregards the energy needs of specific end uses. It has two distinctive techniques, econometric and technological. However, the bottom-up modelling approach evaluates the total energy consumption of a set of houses compared to regional or national values. This approach includes statistical and engineering techniques. Figure 3.4 summarises modelling approaches and their corresponding techniques, while Table 3.5 compares the approaches' strengths and weaknesses.

In similar fashion, Kavgic et al. (2010) reviewed modelling approaches and incorporated their pros and cons. They introduced policies for energy demands and carbon emission reductions by applying holistic building stock model analyses. They evaluated the technical, economic and environmental impacts of the required energy for the existing building stock. They investigated various energy-efficiency strategies over time and their contribution to IEQ.

Grandjean et al. (2012) revealed a detailed analysis for modelling techniques to estimate the residential sector's energy demand. The top-down models used to determine the impact of socio-economic factors on the economy in aggregated forms, however, this approach does not provide the decomposition of energy use due to data aggregation. An end-use evaluation requires a data calibration regime, which necessitates historical information. Due to the unavailability of these data, the bottom-up approach can be employed. The bottom-up approach requires expensive devices and computational skills. It lacks socio-economic treatments, and it assumes the patterns of occupants' behaviour.

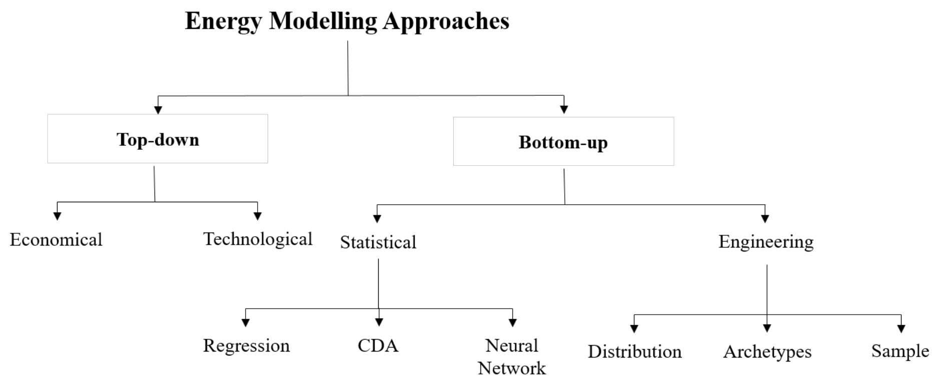

FIGURE 3.4: Energy modeling approaches (Swan and Ugursal, 2009).

3.1.4.1 Top-down approach

The *top-down* approach determines the effect of long-term transitions on total energy consumption. It sets out divergent factors, such as supply requirements and macroeconomic indicators, including GDP, employment rates and public expenditures. It collects data from the historical time series of aggregated national energy indicators or CO_2 emissions statistics. Consequently, it is used to interpret the inter-dependencies between the energy sector and the overall economy. This approach has two techniques: econometric and technological. Econometric models focus on the costs of energy and appliances' prices compared to income, while technological models highlight the energy consumption of the housing stock, such as appliance ownership trends (Swan and Ugursal, 2009). The two techniques depend only on the available data, so no estimation is employed. It aims to offer a real view of the total energy required in buildings compared to the collected historic data. Thus, it can be developed according to economic plans to deliver more energy-efficient homes (Kavgic et al., 2010).

In contrast, using historic data are a drawback since there is no inherent ability for the discontinuous technological advances model plus the shortage of detailed information about the energy consumption of individual end uses. Top-down models cannot explicitly account for end-use energy consumption. However, it was established to bring together energy use and economics to develop policy measures (Grandjean et al., 2012).

The econometric model focuses on energy use according to the surrounding variables – income, fuel prices, GDP and climate – using primary data incorporating income and prices. It cannot describe current or future technological exchanges and depends on historic information to estimate today's energy usage (Kavgic et al., 2010). It also cannot account for climate and socio-environmental changes and provides insufficient detail for development plans (Swan and Ugursal, 2009). On the contrary, technological models employ broad characteristics of the entire residential sector attributed to energy demands. It considers several factors that influence the total stock energy demand, such as appliances and equipment ownership, though the factors cannot be distinguished or detailed.

3.1.4.2 Bottom-up approach

According to Swan and Ugursal (2009), the bottom-up modelling approach compares the energy demands of sectors in disaggregated data forms supplied on a hierarchically restricted level. It assesses the energy use of single items of equipment, residences or even entire stocks. It may be used to calculate each individual's proportion of energy use and the impact on carbon emissions. It describes optimal solutions including cost, technologies and processes. The bottom-up approach can be carried out using the two independent techniques mentioned by Kavgic et al. (2010): SM, explained in Section 3.1.2.1, and the engineering method (EM). SM employs regression analysis to attribute the proportions of overall energy use to certain equipment in the dwelling, while the EM specifies equipment energy use depending on power ratings and system utilisation.

Common data inputs involve dwelling properties: geometry, envelope, equipment, appliances, location, occupancy, lighting and equipment, power and densities and operation schedules. The merits of the bottom-up approach include a high degree of detail, the capacity to model technological options, the ability to individually investigate various houses' equipment and the ability to draw up plans for improvement. Total energy demand estimations do not require historical data; however, it has limitations due to the detailed information. The limitations involve data input requirements, advanced computers and professional simulation capabilities, resulting in a complex approach. In other words, a vast database with highly competent software programs is necessary to describe the intricacies of each component. Assumptions of occupants' behaviour and scheduling have a substantial influence on energy demands, which may lead to inaccurate model prediction (Grandjean et al., 2012).

The massive amount of clients' energy billing data maintained by major energy suppliers offers an extraordinary data source for energy modelling and CO_2 emissions targets. Researchers have developed a range of SMs to extrapolate energy use as a factor of housing attributes; see Section 3.1.2.1. The SM incorporates dwellings' energy demand data, previously identified as a sample of houses or archetypes, using three techniques: regression (R), conditional demand analysis (CDA) and neural network (NN). SM techniques are employed to regress energy consumption and its relationships to each individual end use or equipment. It uses indicators, such as income, energy prices and macroeconomic and national data, which is more beneficial than the top-down approach (Swan and Ugursal, 2009).

The R technique regresses the aggregated energy use data to obtain a coefficient of the model, which corresponds to parameters based on data inputs. For simplicity, irrelevant energy use parameters are neglected, and physical importance is not always necessary (Swan and Ugursal, 2009). The CDA technique employs disaggregated data and applies multiple regression analysis based on the appliances' ownership. After regressing the total energy consumption of the dwelling, the coefficients can be determined and represent usage. The energy uses are explicitly determined and assigned to particular systems. This technique becomes concise if energy billing data are acquired. Nevertheless, the data must encompass thousands of residences (Kavgic et al., 2010). Furthermore, the NN technique is a biological structure constructed by a simplified mathematical model. All systems are interconnected and mutually influential similar to neurons, which have multiple coefficient arrays. As it minimises errors because it is a parallel model, it has no physical significance. Although the NN is often used in artificial intelligence, it is limited (Grandjean et al., 2012).

EM explicitly calculates energy usage and links it to the accurate appliance based on its ratings. It accounts for thermodynamic relationships and heat transfer. Even though EM models can be developed without relying on historical data, the degree of difficulty is high since a large database of residences is required. The required data include geometry, envelope configurations, climate information, IAT, occupancy, appliances and schedules. As is usually assumed, schedules can be difficult to distinguish, which highly impacts total energy use. The models of the EM can be transparent, simple or detailed, and can model new technologies. It requires representative houses or archetypes, as a sample of a national residential stock, to estimate energy demands. The EM also can facilitate new regulations for the housing stock. Researchers use EM for buildings energy performance evaluations and have utilised three techniques: distribution, sample and archetypes (Swan and Ugursal, 2009).

The distribution technique calculates the energy usage of each system by utilising appliances' ownership distribution and usage, including appliance ratings. The systems do not interact because each is calculated separately. The result of the combination of appliance ratings, ownership, usage and efficiency is total energy use (Swan and Ugursal, 2009). The sample technique utilises an actual sample of housing data to inform the energy model using direct data input. The sample must involve a wide range of houses from locations within the stock to capture housing heterogeneity and estimate total energy use (Grandjean et al., 2012). Finally, the archetype technique classifies a huge residential stock according to housing age, type, size and other details. Each major class can be identified and described with extremely detailed or simplified data. Houses from the same class share the same characteristics that are used as data input for the modelling process. The estimation of the total energy consumption of the stock can be calculated by multiplying the results by the total number of houses regionally or nationally (Kavgic et al., 2010). Section 3.1.5 describes and further investigates the archetypes.

3.1.4.3 Summary

Modelling approaches are defined by two techniques: top-down and bottom-up. The top-down modelling approach employs aggregated data and long-term forecasting to evaluate energy consumption from an economic perspective. It is simple and efficient to adjust, though it cannot clarify the exact reasons for electrical energy consumption, and it limits plans' developments. Meanwhile, the bottom-up modelling approach applies disaggregated data to calculate energy demands and to precisely indicate appliances' energy usage. It estimates energy consumption for a single unit or for the entirety of a housing stock. However, it is a complex process, as it requires detailed data input and uses assumptions for scheduling systems and equipment.

Bottom-up modelling approaches usually employ a set of housing archetypes that can represent a housing stock, as seen in Molina et al. (2020).

3.1.5 Housing archetypes

Housing archetypes, or typology, is a systematic technique that have been utilized for years because it is a valuable method for predicting the energy performance of a given building stock. It can be used to analyse the current housing stock of the KSA and to estimate future changes. It identifies potential energy efficiency resources, economic growth and assists the decision making process. Archetypes can be complex, however, if appropriate and educated assumptions were employed, it may save time, cost and effort (Swan and Ugursal, 2009).

3.1.5.1 Building stock models

Buildings' physics-based models are distinguished by the desire to describe representative buildings of a large-scale stock. Diverse properties should be included in representative buildings; hence, there is a variety of theories and models. Unfortunately, academics have not investigated representative buildings in sufficient depth to establish why and what constitutes a typical building that sufficiently represents a proportion of the stock. This may be due to the many definitions of archetypes, which make comparing models problematic. Researchers neglect the comprehensive details of buildings' representativeness to produce global or national stock models that can be compared to other models or even nations (Brøgger and Wittchen, 2018). One of the most critical measures for developing buildings' representativeness is to assess their energy performance. Housing archetypes have been extensively researched. Nonetheless, no single study considers realistic energy performance on the level of the individual building, perhaps due to a lack of data (Brøgger and Wittchen, 2018). This issue makes verifying the validity of the presented models problematic, as emphasised by Reinhart and Davila (2016) and Österbring et al. (2016). Optimistically, future building representativeness might include actual energy performance measurements for various types of homes to advance science.

3.1.5.2 International housing archetypes

Housing archetype models can be utilised to forecast international concerns, including energy demand, GHG emissions and global warming potential (GWP). To model the national energy demand of the total housing sector, two approaches are often utilised: top-down and bottom-up. See Section 3.1.4.

Archetypes are usually created using classification algorithms, which arrange houses so the buildings in each group share more common attributes than the buildings in other groups. This method is extensively accepted and was recently applied to English housing stock, for which more than 14,000 archetypes were used to represent a total of 22.3 million housing units, employing a cross-sectional study for clustering common features. Every housing archetype was weighted against the total number of archetypes in the stock, being the sum of all weights (Sousa et al., 2017). Seven distinct models have employed this method to examine relevant studies associated with energy. The same authors included eight more parameters relevant to housing. They lowered the total amount of the archetypes to around 10,000 units to reduce the housing stock's energy demands and carbon emissions (Sousa et al., 2018). Adding 10 variables to describe the residential stock model in the US resulted in over 200 housing archetypes, found to represent more than 80% of its stock (Persily et al., 2006). These archetypes were then utilised by Persily et al. (2010) to analyse the infiltration rates of the same housing stock. A total of 593 archetypes were constructed to analyse three European countries and the UK (Mata et al., 2014). Importantly, the availability, accessibility and accuracy of data for these countries is more advanced and easier than data available for the KSA.

Moreover, Geyer et al. (2017) described a feasible strategy for clustering buildings according to their sensitivity to various retrofit approaches, assisting in the development of large-scale building retrofit solutions in Switzerland. However, it was only applied to one defined case study, which requires manual interventions to extend stocks. Another research simulated the heating demands of Austrian housing stock, applying the bottom-up modelling approach. The model was employed to provide urban scale energy queries considering change and intervention scenarios incorporating buildings' physical and technological features. Nonetheless, the method's impact in terms of other energy elements, such as temporal distribution, merits more examination using well-resolved data (Ghiassi and Mahdavi, 2017).

The creation of archetypes can be determined by the common factors generated from the outputs of the model (top-down approach) or by their unique performance indicators (bottom-up approach). Due to the fluctuation of the composition and attributes of the building stock over time, archetypes must enable fast and simple modifications. Housing archetypes must be developed in the KSA to reduce energy demands, cost and CO_2 emissions, which meets the overall aim of this research.

3.1.5.3 The KSA housing archetypes

Only three studies have attempted to develop housing archetypes in the KSA to portray dwellings on a large scale for energy-evaluation purposes (Krarti et al., 2020; Aldubyan et al., 2021; Aldubyan and Krarti, 2021). The three studies utilised the same housing archetypes developed eventually by Krarti et al. (2020), but the villa archetype originates from an older study by Abdelrahman et al. (1993) and extended by Ahmad (2004). Although the studies relied on data provided by the GAS (2019) and the literature to evaluate the housing stock's energy performance, it assumed various parameters that have a significant degree of influence on energy demands, such as systems' power densities, scheduling, infiltration rate and cooling setpoints.

The engineering bottom-up modelling approach was adopted by Krarti et al. (2020) and Aldubyan et al. (2021) for developing a residential building stock model in the KSA. The model was qualified for investigating energy-efficiency retrofitting measures (EERMs), including energy performance and cost-effectiveness. The model used 54 housing prototypes to represent the total housing stock based on three fundamental building characteristics: building type, location and age. Although this study employed these three characteristics to generate housing archetypes, it neglected floor space. Flooring area is a fundamental factor for archetypal building generation, as it affects building size, air volume and heating or cooling loads. Another drawback is that the scheduling of internal systems was assumed. These archetypes, though, were modelled using a detailed hourly whole-building simulation tool, DOE-2, to predict the energy demand per hour (Hirsch, 2018). The results were verified using monthly reported data by sources including GAS (2019), SEC (2018) and the literature (Taleb and Sharples, 2011; Alaidroos and Krarti, 2015; Aldossary et al., 2014a; Aldossary et al., 2014a; Algarni and Nutter, 2013a). The results revealed that air conditioning is the dominant electrical energy consumer at approximately 66% of the total residential electrical energy use. This high cooling energy use is due to different factors – most importantly, the harsh local weather conditions (Krarti et al., 2020). Therefore, EERMs were applied and evaluated to reduce this excessive energy use, carbon emissions and cost. Nineteen measures were applied, including envelope thermal insulation, double pane low-e glazing, LED lighting and shading. The results showed that 50% of the annual electrical energy consumption of the housing stock can be reduced. The authors suggested that the KSA should reform energy prices, adjust air temperature setpoints and exchange lighting components for LED to achieve ambitious energy retrofitting programmes (Krarti et al., 2020).

In addition, Krarti et al. (2020) paper is unique because it is the first published paper in the field that implemented the bottom-up engineering technique to advance the energy efficiency of the KSA's housing stock. It discussed different EERMs on a large scale in the Kingdom. Its impact is also significant due to the sample representation of the housing stock as three archetypal housing units. Conversely, the paper assumed an infiltration rate at 0.8 air change per hour (ACH) for all housing types and only considered 19 EERMs. Other types of envelope thermal insulation, window glazing and shading devices can be applied not only to the five regions, but also to all the KSA's provinces. Although the result of this study reflects the entire housing stock, it might not be accurate due to the infiltration rate assumption.

Indeed, one particular concern was observed in the KSA's energy simulation studies that markedly impacts energy performance, model forecasts and the current state of dwellings. Most field research on housing energy performance in the KSA constructs energy baselines without envelope thermal insulation. Even though the Saudi energy census report states that 61% of all the KSA's buildings lack thermal insulation (GAS, 2019), this is neither evidently nor scientifically approved as applicable to all residential energy baselines. In other words, this high proportion comprises all building types, regardless of type or age. Therefore, the assumption is inaccurate that residential baselines can be extrapolated without thermal insulation. The reason is that the SEEC has developed minimum residential building requirements updated in 2018, which enforces the application of thermal insulation with alternative thermal resistance values (R-value) according to the climatic zone. The requirements have not been applied to the baselines, which may cause misleading results and deceptive reporting. The diversity of housing heterogeneity may require a parametric analysis using cluster analysis, which is an employed method for data extraction by machine learning to arrange associated information together. The purpose of cluster analysis is to detect trends in data by clustering data points collectively based on their shared and distinct characteristics.

3.1.5.4 Cluster analyses

Cluster analysis is a data mining approach that permits researchers to combine and classify large amounts of data into smaller units. It is important for evaluating a large dataset with a collaborative filtering identification (Adolfsson et al., 2019). It may be used to assess all feasible alternatives of houses involving thermal insulation types or thicknesses to multiple levels, which can then be evaluated independently or combined. Cluster analysis is significant for developing housing archetypes and has two techniques, hierarchical and partitional clustering. The *hierarchical clustering* technique consists of a cluster tree wherein each cluster reveals a portion of the dataset. It uses algorithms to divide data to generate the cluster tree. In contrast, the partitional clustering technique divides the dataset into a specified number of clusters. Subsequently, algorithms minimise clusters in a step that optimises problems (Saxena et al., 2017).

The hierarchical clustering technique is usually applied to categorise large data into separate twigs or clusters to form a tree. It can be shown in two algorithmic forms, divisive and agglomerative hierarchical clustering techniques. Divisive clustering techniques employ algorithms to split data to process the shape of the cluster tree, while the agglomerative technique merges data clusters to generate the cluster tree. The partitional techniques, though, classify the dataset into a specific cluster amount to optimise numeric problems. Partitional techniques are more common because clusters do not overlap and patterns may move from one cluster to another. However, it requires the number of groups (K-means) to minimise the total mean squared error (MSE). Minimising the MSE leads to consistent estimations of models' variables. The larger the MSE, the higher the error. The MSE and R^2 are statistical indicators often employed to describe the quality of the linear regression relationship (Omran et al., 2007).

3.2 Indoor Environmental Quality

IEQ is the perceived acceptability of air by a large proportion of people. Humans spend more than 80% of their lifetime indoors. Correspondingly, they inhale significant quantities of unidentified substances that harm their health. The perceived air should be healthy and refreshing, with no deleterious influence on human health, because air affects human health, productivity and learning capabilities. Poor IEQ is contributed by two major factors: a low level of air change or air infiltration and new building materials. Low levels of air change keep unknown contaminants indoors, while new building materials consist of polymers, which double the incidence of allergy and asthma. Possible influences from acceptable IEQ include cost reductions for medical treatment, as well as learning and productivity improvements. Additionally, accieiving acceptable IEQ increases the energy efficiency of buildings by applying suitable energy retrofitting measures. There are a little amount of studies in the KSA that identify the impact of energy-saving measures on acceptable IEQ. Hence, his can be initially assessed by predicting the air infiltration rate of the KSA housings. Research has proposed four solutions for better IEQ: source control, air cleaning, personalised ventilation and cool and dry air (Fanger, 2006). These strategies are able to increase the energy efficiency as well as achieve acceptable IEQ. On the other hand, IEQ has different effects on human health, summarised in Table 3.6, and on other than human, summarised in Table 3.7.

IEQ has been divided into four key sections; Section 3.2.1 summarises IEQ's effects on human health. Section 3.2.2 highlights IEQ's effects on other than human health, Section 3.2.3 compares IEQ studies in the KSA, and Section 3.2.4 describes IEQ treatment methods.

3.2.1 IEQ effects on people

Previous studies have explored the relationship between IEQ and its effects on human health; see Table 3.6. Two early studies were conducted by Samet et al. (1987) and Samet et al. (1988), who presented IEQ evaluations, control technology, research demands and clinical applications. The varying degree of human health effects attributable to indoor contaminants is linked to various health conditions including allergies, lung cancer, cardiovascular disease and others, and recently was associated with dementia (Wong et al., 2014). Indoor air pollution (IAP) is the presence of dust, filth or chemicals in enclosed spaces, including dwellings, which may be hazardous to inhale. The effects of human exposure to IAP have been classified into seven categories encompassing clinically evident illnesses and increased disease risks. However, other forms of IAP have not been characterised or identified by researchers and have unrecognised impacts on human. The literature on IEQ agrees that the dominant reason for human health issues due to IAP exposure is time spent indoors. Accordingly, more research is demanded to detect IAP from new construction materials and its association with illnesses. Additionally, poor IEQ is a common reason for sick building syndromes, or SBS (Samet, 1993).

IAP appears to be related to poor IEQ and human health risks. Therefore, Jones and Molina (2017) recently described the symptoms, indicators and treatment methods of IEQ. They provided IEQ effects on occupants' thermal comfort in residential, commercial and leisure buildings. Pollutants can be emitted indoors by various building substances, including materials, finishing, furniture and occupants' activities, while external contaminants enter the building through openings, gaps or cracks in the envelope through air ventilation or infiltration. This raises economic concerns because poor IEQ affects human behaviour and health on a national scale. Increases in healthcare spending on a national scale influence the country's performance and economy (Jones and Molina, 2017). They identified poor IEQ symptoms as building-related illness (BRI) and SBS. BRI symptoms can be clinically identified; they include infectious diseases, hypersensitivity diseases

TABLE 3.6: Relevant IEQ studies on people health effects.

Author (yar)	Area of study
Samet et al. (1987)	IEQ assessment to control reduce IAP
Samet et al. (1988)	IAP and its connections to various people health conditions
Samet (1993)	Association of construction materials and different illnesses
Husman (1996)	Categorization of indoor microorganisms and health effects symptoms
Jones (1999)	Health effects of exposure to combustion products inside
Emmerich et al. (2001)	Dampness in buildings and associated IAP
Sundell (2004)	people exposure to IAP effects and illnesses
Mendell and Heath (2005)	IAP effects on thermal conditions and productivity
Li and Niu (2007)	transmissions of airborne pollutants to indoors
Weschler (2009)	Differences in past and present IAP
Peretti and Schiavon (2011)	Brief literature review using indoor environmental survey
Fisk (2015)	climate change influences on people health
Tham (2016)	Critical review on IEQ and people health
Jones and Molina (2017)	IEQ symptoms, indicators, and treatment methods

and toxic reactions. Simultaneously, SBS symptoms include upper respiratory, lower respiratory, neurophysiological and skin irritation. SBS decreases when far from the indoors. Efforts have also been made to reduce energy demands and CO_2 emissions involving three approaches: laboratory experiments, controlled human laboratory studies and epidemiology. Health risks have been dichotomised into two exposure types: chronic and acute. Chronic exposure occurs after long-term exposure, whereas acute exposure occurs for short-term exposure. A ventilation rate of 9 l/s per person reduced odours to acceptable levels for receivers. Even though the concentration of indoor CO_2 is a helpful index of odour producers, such as bio-effluent emissions, the authors believe that it is incomplete for IEQ because it does not relate to many other IAP emissions, including formaldehyde, a toxic outdoor gas that may access a building through cracks, gaps or infiltration (Jones and Molina, 2017).

3.2.2 IEQ effects on energy efficiency

Table 3.7 summarises relevant studies of IEQ effects on other than people. Brown et al. (1994) reviewed 50 studies on the indoor concentrations of volatile organic compounds (VOC) found in new and old buildings. The authors asserted that concentrations in new buildings are much greater than in old buildings; many VOCs are attributed to new materials. However, the study did not extend VOCs to occupants' exposure and health because of the lack of a definition of VOC. Batterman and Burge (1995) investigated the influence of HVAC system emissions on IEQ and classified diverse emission sources associated with HVAC components. The exacerbated concerns about IEQ are due to two main factors: the accumulation of dust and the existence of fibrous insulation. It was recognised that an HVAC system distributes interior pollutants via entrainment, migration and infiltration. The good design of intakes, local exhaust air, and the operation and maintenance of HVAC systems were observed, as they enhance IEQ. The research was constrained by a lack of information on inadequate filtration.

Melikov (2016) investigated the impact of modern air distribution strategies of HVAC systems and concluded that the total volume of air distribution indoors is not a consistent and efficient strategy to promote IEQ and decrease energy use. The reason is that the method used was drafted based on strategies that included designing indoor environments for an entire space rather than designing it for individual occupants. Individual HVAC system controls for each occupant were proposed, though delivering high-quality air to occupants remains limited. Kumar et al. (2016) classified three IEQ sensors: gas, practical and packages of sensors. They aim to enhance current IEQ regulations and risk awareness. The development of air pollution sensors is a discovery for IAP monitoring that offers numeric measurements for better assessment, although the accuracy and credibility of data and integration of technologies are evolving. Ortiz et al. (2020) conducted a recent review to identify human threats due to poor IEQ. They classified and associated IEQ with the building envelope, heating, ventilation and air-conditioning (HVAC) systems and occupants. The recommendation was made to incorporate human behaviour and needs to improve energy efficiency and IEQ through multidisciplinary research.

The effects of IEQ on energy performance may be linked by the air pollutants that enters the buildings through the thermal envelope gaps, cracks and thermal bridges. This gaps increases heat gains in buildings, reduces the energy efficiency and changes the payback periods. This should be investigated in more depth as it shows clear data shortage in the KSA's IEQ studies.

3.2.3 IEQ in the KSA

The KSA has no IEQ guidelines, and existing standards have been adopted from international agencies like the Environmental Protection Agency (EPA). The

TABLE 3.7: Relevant IEQ Studies on energy efficiency and others

Author (year)	Area of study
Cooke (1991)	IAP indoor and outdoors
Brown et al. (1994)	50 study reviewed for VOC measurements
Batterman and Burge (1995)	Emissions by HVAC
De Dear and Brager (1998a)	AC and N.V. thermal adaption
Fisk and De Almeida (1998)	Sensors for controlling ventilation
Monn (2001)	PM, NO2, and Ozon forms and exposures
Destaillats et al. (2008)	Emission of IAP by office equipment
Zhang and Yeung (2012).	Enhancement of IEQ by air cleaning
Yang et al. (2014)	Green buildings requirements for IEQ
Luengas et al. (2015)	IEQ treatment review
Kumar et al. (2016)	Sensor of IEQ
Melikov (2016)	Air distribution developed techniques
Ortiz et al. (2020)	Human behaviour health factors

majority of IEQ research in the KSA has focused on pollutant concentrations and characterisation rather than mitigation measures as a result of pollutants' exposures (Amoatey et al., 2018a). Preparing national regulatory codes to enhance energy, IEQ, thermal comfort and the economy is an essential step to develop the KSA's housing. IEQ research areas should be investigated and incorporated into the evaluation of national energy demands. There are only seven housing studies concerning IAP in the KSA. This indicates a substantial data shortage, especially for homes. Consequently, this section reveals IEQ studies in various building types in the KSA, summarised in Table 3.8.

Al-Rehaili (1999) investigated 30 housing units in urban areas in Riyadh for two years. He utilised passive monitors to measure distinctive concentration levels of emissions that harm human health. Concentration levels of lead (Pb), carbon monoxide (CO) and total suspended particulate matter (TSP) have recorded 0.01-2.13, 143 and 6 - 478 mg/m^3, respectively. The Pb and TSP, both harmful pollutants, have exceeded the standard values of 1.5 and 80 mg/m^3, respectively, and the CO pollutant was less than expected. TSP is considered a major cause of smog formation, contamination and air pollution. The TSP levels were extremely high due to typical local dust storms. Al-Rehaili (2002) investigated 30 buildings, offices, hospitals, schools and libraries. He utilised a semi-movable drager to record IAP concentrations and found that the sulphur dioxide (SO_2), ammonia (NH_3) and formaldehyde (HCHO) concentrations were 1.09, 1.3 and 29.1 mg/m^3, respectively. This indicated extremely high levels of pollutants because the SO_2 and NH_3 surpassed the international yearly standard mean values of 80 and 0.5 mg/m^3 (0.072 ppm). The HCHO recorded moderate pollution because a few sites' values have passed the international values of 120 mg/m^3 (0.1 ppm).

Al-Jarallah (2005) evaluated 12 homes in Qatif and found that the radon concentration level in a single unit was as high as $535 \pm 23\,\mathrm{Bq\,m^{-3}}$, which is higher than the the National Radiological Protection Board of the UK (England, 1992). Radon is a toxic, colourless gas that is not usually recognised when inhaled because it has no scent. Al-Jarallah (2005) implemented active techniques that require electrical power to capture radon and passive techniques that do not require electrical power to measure radon. Such techniques included the AlphaGUARD 2000 PRQ analyser for radon concentration levels and the CR-39 passive radon indicator. The results showed radon concentrations vary according to the room and space. However, large quantities of radon were generated by underground diffusion delivered by the infiltration found in the envelope. Al-Saleh (2007) examined radon levels for homes in Riyadh. Unlike Al-Jarallah (2005), Al-Saleh (2007) observed that the concentration levels are less than international concentration values. The World Health Organization (WHO) requires sets of international values for hazardous concentrations (WHO, 2001). He also expected that radon health hazards are negligible in the KSA, confirming Mohamed et al. (2014). The conflicts in the literature about radon concentrations in the KSA might be due to varied measuring techniques and locations.

More recently, Vohra (2011) investigated formaldehyde (HCHO) levels in a laboratory at King Saud University located in Riyadh. Exposure to HCHO in buildings is a major reason for respiratory health effects or skin, eye, nose, or throat irritation. Vohra (2011) concluded that instructors and students have more exposure to HCHO than the general population. This is may due to the construction materials of the university's buildings. El-Desoky et al. (2014) investigated Lead (Pb) concentrated in the dust for homes located in Riyadh. Pb is a significant deleterious contaminant in the environment, and long-term exposure can cause anaemia, weakness, kidney and brain damage. It is especially dangerous to children since their developing body systems absorb more of it (Jones, 1999). A significant association of Pb concentration levels between indoors and outdoors were observed.

A remarkable survey including 786 homes was conducted in Riyadh to evaluate the levels of radon indoors (Alghamdi and Aleissa, 2014). Radon is an isotopic, diverse radioactive gas that is both colourless and odourless that is formed in the soil surrounding a building because of radium decomposition. The International Agency for Research on Cancer has identified radon as a human carcinogen (Group I). The danger of lung cancer from radon is demonstrated by residential epidemiological research showing a direct linear association between radon exposure and lung cancer (WHO, 2010). Radon levels in the Saudi dwellings surveyed were 98% less than the levels recommended by the WHO (2001) of $100\,\mathrm{Bq\,m^{-3}}$. The results varied substantially due to buildings' types, construction materials, ventilation or HVAC systems. El-Sharkawy (2014) and El-Sharkawy and Noweir (2014) conducted two studies for a hospital and 16 elementary schools in Dammam. The TSP was observed in both studies, including M, SO_2 O_3, CO and NO_2. TSP is considered a major cause of smog formation, contamination and air pollution. TSP levels in the hospital were higher than the levels recommended by the Air Quality Guidelines (AQG), while they were lower in schools (WHO, 2010). Most of the KSA IEQ studies recorded unacceptable IAQ of dwellings, and this might be due insufficient ventilation.

Amoatey et al. (2018b) reviewed IEQ for GCC, and they suggested that IAP might be reduced by developing air purification and ventilation technologies. Yousef and Zimami (2019) quantified indoor radon concentrations and investigated seasonal fluctuations to estimate the overall optimal dosage received by residents. They argued that radon levels are lower than the values recommended by the International Commission on Radiological Protection (ICRP Protection, 2007). The high levels of IAP concentrations encouraged researchers to apply or integrate various IEQ treatment techniques.

3.2.4 IEQ treatments

Occupational activities have been advanced due to changes in human lifestyles, including rapid urbanisation. People tend to spend more time indoors. Therefore, higher rates of occupants' exposure to various IAP have been recorded, which raise the SBS, BRI and Multiple Chemical Sensitivity (Li et al., 2001; Lan et al., 2011; Mallawaarachchi and De Silva, 2013). According to Kuehn (2014), air pollution caused seven million premature deaths in 2012, while about 4.3 million other deaths

TABLE 3.8: Summary of relevant IEQ studies in the KSA (Amoatey et al., 2018b).

Author (year)	City	Type	Units	IAP
Al-Rehaili (1999)	Riyadh	Homes	30	TSB
Al-Rehaili (2002)	Riyadh	Various	30	SO2, NH3, HCHO
Al-Jarallah (2005)	Qatif	Homes	12	Radon
Al-Saleh (2007)	Riyadh	Homes	NA	Radon
Vohra (2011)	Riyadh	Laboratory	1	HCHO
El-Desoky et al. (2014)	Riyadh	Homes	NA	Pb
Alghamdi and Aleissa (2014)	Riyadh	Homes	786	Radon
El-Sharkawy and Noweir (2014)	Alkhobar	Hospital	1	TSP, PM, SO2, O3, CO
El-Sharkawy (2014)	Dammam	School	16	TSP, CO, NO2, SO2
Mashat (2015)	Makkah	Mosque	5	Bacteria, Fungi
Salama and Berekaa (2016)	Dammam	Home	1	PM, CO, VOCs
Al-Khateeb et al. (2017)	Riyadh	Hospitals	6	Radon
El-Sharkawy and Javed (2018)	Dammam	Resturants	44	CO_2 No2, PM, CO, VOCs
Amoatey et al. (2018b)	GCC	various types	44	CO_2 No2, PM, CO, VOCs

were related to poor IEQ. Thus, the WHO attempted to decrease the impact of IEQ on public health in 1979, and by 2010, the WHO proposed guidelines to reduce IAP and increase international human health (WHO, 2001). Previous studies have discovered treatment methods for poor IEQ, including energy use, as compared in Table 3.9.

Asbestos, a toxic material, has been used in construction and various building substances for centuries due to its flexibility, strength and resistance to heat and electric energy (Strohmeier et al., 2010). France has regulated the use of asbestos since 1997, and the processing of asbestos fibre was controlled in 1999 by the Commission Directive 99/77/EC (Luengas et al., 2015). This commission prohibits the purchase or trade of Chrysotile asbestos and its byproducts. A new guideline for householders was published by the Australian government's Environment Health Standing Committee in 2013 and the US Environmental Protection Agency (EPA). The guidelines listed regulations governing asbestos (Judson et al., 2012).

Authors have classified various agents affecting IAP as biological, physical and chemical. Biological pollution includes animal allergens, bacteria, fungi, spores and endotoxins (Casset and Braun, 2010). Physical pollution is divided into temperature and electromagnetic fields. Chemical pollution comprises the more than 400 chemical compounds in indoor air that can be subdivided according to their concentrations and properties (Gale et al., 2009). Conversely, treatment methods were proposed to reduce IAP that were classified into three groups. First, the control source controls the pollution source throughout the removal, confinement or replacement of the source (Liebana and Calleja, 1998). The ventilation system is the second treatment method that allows in more outside air to dilute the number

TABLE 3.9: IEQ technological treatments (Luengas et al., 2015).

Treatment Technique	Waste production	Energy use level
Mechanical filtration	Spent filters	Moderate
Electronic filtration	Spent cleaning plates	Moderate
Adsorption	Spent adsorbent	Moderate
Ozonation	Nil	High
Photolysis	Depleted lamps	High
photocatalysis	Catalyst/lamps	Moderate
Plasma	Nil	High
Membrane separation	Clogged membranes	High
Botanical purification	Organic waste	Low
Bio-filtration	Biomass	Low

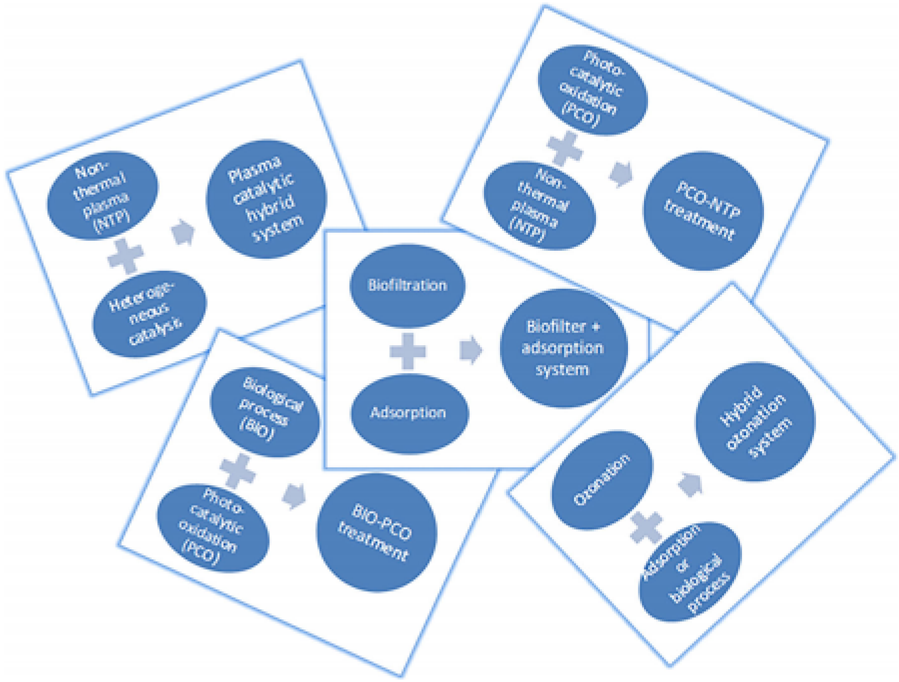

FIGURE 3.5: IEQ technological treatments integration (Luengas et al., 2015).

of pollutants inside (Zaatari et al., 2014). Purification and treatment technologies are the third IEQ treatment method; they use filters to improve indoor air. Multiple treatment techniques have been observed, and four are briefly mentioned below.

An IEQ assessment includes two evaluation approaches, that are modelling and actual measurements. Indoor concentrations can be modelled using a software tool that estimates the transfer and concentration of indoor pollutants known as CONTAM (Dols, Polidoro, et al., 2015). CONTAM was created by the US National Institute of Standards and Technology to analyse airflow and pollution. CONTAM is a useful tool for measuring pollution, though it cannot evaluate thermal envelope loads. Thus, researchers rely on EnergyPlus because it can predict energy loads (DoE, 2020). The actual measurement of IAP concentration is essential for calibration or verification. Measuring tools can be expensive. However, CO_2 measuring tools are inexpensive. Widely common CO_2 measuring tools use Non-Dispersive InfraRed (NDIR) gas sensors. NDIR measures the lengths of infrared light waves to estimate the concentration of CO_2 indoors. Light scattering technology is also applied to estimate the mass of air volume known as particulate sensors, but it is only convenient for temporary measurements. In addition, gas chromatography is a mechanism to evaluate the VOCs found indoors. This method is pricey, but provides precise measures (Jones and Molina, 2017).

3.3 Infiltration Rate

Countries attempt to reduce buildings' energy demands and GHGs to mitigate the potential for global warming. This is frequently accomplished by establishing optimal building requirements or codes for energy performance, IEQ and thermal comfort. Infiltration influences building energy demand and pollutants transfer to indoor air, which consequently effects GHGs. Infiltration may account for about 30% of winter heating loads (Kalamees, 2007; Meiss and Feijó-Muñoz, 2015; Jokisalo et al., 2009), and it effects thermal insulation performance, IEQ, thermal comfort, and ventilation system performance (Thébault and Bouchié, 2015; Robert and Piotr, 2015; Anis, 2001; MacPhaul and Etter, 2010). For instance, the UK plans to lower its energy demands 80% by 2050. Through a variety of measures, one technique attempted is to lower the energy demands of the housing sector, which uses more than 25% of the UK's total energy (DECC, 2013). Most of the UK's housing energy demands account for heating loads during heating seasons. Reducing domestic heating loads can be achieved by decreasing air infiltration and exfiltration rates through the thermal envelope (Jones et al., 2015).

Buildings' infiltration and exfiltration may be assessed with an airtightness evaluation. Even though infiltration has a major influence on housing energy demands, it has never been tested or measured in the KSA, and assumptions for building's infiltration rate have been made.

TABLE 3.10: Key air-leakage pathways (Sherman and Chan, 2006).

Source and Year	Air leakage	Notes
Pittomvils et al. (1996)	Walls and Roof connection	Thermal bridges
Stephen (1998)	Building materials	highly effects tightness
Leblanc (1991)	Windproof sheets	Dust blocks the holes
Wilcox and Weston (2001)	Polyethylene air barrier	External finishing
Petrie et al. (2002)	Insulated concrete	Tighter than timber
Elmahdy (2003)	Window and doors	Condensation
Sherman and Dickerhoff (1998)	Conditioned basement	tighter than unconditioned
Fugler (2001)	Garages	13% of leakage
Sherman and Chan (2006)	air barrier connection	Thermal bridges

3.3.1 Air-tightness

Airtightness is the fundamental feature of a building's envelope that directly impacts infiltration (Sherman and Chan, 2006). Most intercontinental building standards impose minimum requirements for the construction of new buildings to guarantee acceptable airtightness (Mees and Loncourt, 2015; Carrié et al., 2012). In recent years, a lack of experience and equipment has made the implementation of airtightness requirements more difficult, expensive and time consuming. Therefore, researchers have developed predictive models to test buildings' infiltration rates for building codes' compliance and to reduce energy and associated costs (Prignon and Van Moeseke, 2017), and defined most air leakage areas summarized in Table 3.10.

Infiltration is the transport of air through leaks, fractures and other unintended gaps in a building envelope. This airflow is dependent on pressure difference across the building envelope (Sherman, 1980). The difference in pressure occurs due to the stack effect and wind pressure. *The stack effect* is a gradient across the height of the building and caused by temperature difference while the wind pressure is attributed by the the movement of air around the building (Prignon and Van Moeseke, 2017). On the other hand, air-tightness is the fundamental envelope property that effects infiltration, and is defined as how the building's thermal envelope resists air infiltration through it at a defined pressure difference across it (ΔP), usually at 50 Pa, without ventilation. Infiltration occurs depending on temperature, wind movement, and location; and air-tightness is dependent to weather variations. If the air-tightness rate rises, the infiltration rate reduces. Researchers have utilized several methods for estimating airflow rate by actual air-tightness measurements using blower door test or Pulse test, and by modeling techniques using DOMVENT3D model (Zheng et al., 2020; Jones et al., 2015).

$$\dot{V} = a(\Delta P)^b \tag{3.1}$$

Equation 3.1 represents the relationship between the pressure difference occurs in the thermal envelope and the airflow rate through it, see Jones et al. (2015). a and b are determined by regression shown in the British Standards Institution (2015) and the Standard Test Method for Determining Air Leakage Rate by Fan Pressurization ASTM (1999) representing a flow coefficient ($m^3/h/Pa^b$) and flow exponent, respectively. The interpolation of $\dot{V}$ at 50 Pa is a common method through different measurements and it is recognized as Air Leakage Rate (ALR), $\dot{V}_{50}$ (m^3/h). Additionally, Orme et al. (1994) discovered that using the average exponent (b) of 0.65 from large data-sets is generally adequate. Therefor, the use of average flow exponent value, often 0.65, is sufficient. If the pathways are due to an orifice, the exponent value would be closer to 0.5, and if the leak is due to a long pathway, the exponent value would be closer to 1 (Sherman and Chan, 2006), see Section 5.3.2.2.

Airflow rate does not have a unified and standardized reporting method, different countries report it in distinctive approaches. This prevents easy comparisons and evaluations among other buildings or even countries. Reporting airflow can be normalized by the building volume to represent ACH, Air Change Per Hour, N_{50} (h^{-1}), like the USA, or normalized by the area of the thermal envelope to represent an air permeability, Q_{50} ($m^3/h/m^2$), like the UK (Sherman and Chan, 2006; Jones et al., 2015).

Researchers rely on airtightness rates to physically measure airflow rates in buildings using the blower door test, which is the most common approach, and the Pluse test, which is an additional and recent advanced physical approach to measuring airflow developed by the University of Nottingham (Nottingham Technology, 2019). The blower door is a mechanical device that blocks the main entrance of a building and requires all the intended ventilation openings to be sealed. While the Pluse test releases a less-than-two-second pulse of air inside the building from a compressed air vessel. This initially causes an instantaneous rise in the building pressure and gradually lowers the pressure until a quasi-steady state is achieved, See Figure 3.6.

Blower Door Kit Pulse Kit

FIGURE 3.6: Blower door kit (Keefe, 2010) vs. Pulse kit (Nottingham Technology, 2019).

More recently, airflow rates can be computationally predicted using DOMVENT3D model, which implies ASHRAE Standard Atmospheric conditions to predict constant airflow (ASHRAE, 2009). Aprimary infiltration and ex-filtration model through different amounts of exterior surfaces was theoretically developed the first time by Lyberg (1997), followed by Lowe (2000), and then extended more recently by Jones et al. (2015). This model is known by DOMVENT3D and was applied to the UK housing stock to predict total airflow rate through facades by integrating the airflow rate in the vertical plan using a generic MATLAB code (MATLAB, 2010). DOMVENT3D assumes that all exterior facades are uniformly porous and have linear distribution of pressure over the vertical surfaces, as seen at Jones et al. (2014). It assumes that the indoor resistance of airflow is negligible because the rooms are connected, as mentioned by Etheridge (2011). A separate flow exponent function, Equation 3.1, is applied for each vertical surface of exterior facades and then, all equations are coupled by a continuity function, Equation 3.2, to speed up run-time. Interior air pressure is equal for all conjoined dwellings because identical environmental states are assumed. Thus, interior airflow through inner surfaces is not considered (Etheridge, 2011). The model's data can be unique inputs for dwellings comprise dwelling type, location, flow exponent, density of air, surfaces' dimensions, wind speed (height and buildings terrain), and wind pressure coefficients; or general dwellings' inputs including altitude, exterior temperature, wind speed and orientation, see Section 5.3.2 of Chapter 5.

$$\sum_{i=1}^{j} \dot{V}_i = 0 \tag{3.2}$$

Concerns have been raised about the steady state of parameters that are independent to weather variations. These parameters were utilized to predict weather dependent parameters including wind speed, which requires estimations of calculations' uncertainties. The uncertainties assessments of airflow rates in models predictions was used for the UK conjoined homes for multi family use (Jones et al., 2013b). They agreed that uncertainties are unable to distinguish between infiltration of conditioned or unconditioned ambient air required for heating systems or the air delivered from attached dwellings. This issue has been raised by guarded zone test, which refers to analysing a specific component of a building to detect air leaks inside the structure with and without taking inner leakages into account. A guarded zone test might fail, however, if there are massive internal leakages (Kaschuba-Holtgrave et al., 2020). The guarded zone test was performed to measure airflow through party walls in apartments and found that party walls account for 31-58% of total ALR (Shin and Jo, 2013).

The UK's government adopted a rule of thumb to predict the infiltration rate, dividing the airtightness value by 20 (Pasos et al., 2020). This could be useful because the KSABC mandates a building airtightness value of 4 ACH (Saudi Building Code, 2018). According to the GAS (2019), concrete is the most-used Saudi building construction material at 89%. Intuitively, one presumes the KSA's homes are airtight due to the *in-situ* use of concrete and its high thermal mass. However, airflow rate and heat loss calculations must be operated in the KSA's context to obtain an in-depth assessment of the building stock's airtightness and its implications, which should be linked to buildings' energy performance studies. This allows the building of a national database similar to those of the USA, the UK and France that can be employed for further research and decision making. In addition, this would enable data comparison between national building stocks.

It is essential to emphasise that the KSA has not conducted infiltration rate studies, recorded measurements or performed modelling techniques. The infiltration rate substantially influences a building's energy demand and heat loss predictions. Researchers often assume varied air change rate values for buildings' energy performance analyses in the KSA due to a lack of data. A recent energy performance modelling study for the KSA's housing stock (Krarti et al., 2020) assumed a $0.8\,(\mathrm{h}^{-1})$ airflow rate for all housing archetypes. This may only work in limited cases, but not always, particularly if multiple housing types in different climatic zones are introduced.

3.4 Research gaps

This chapter distinguished research gaps and formulated the research hypothesis, questions, objectives and the research's major aim. It identified five research gaps that require further investigations to contribute to knowledge. The first research gap is defining housing archetypes that represent a proportion of the housing stock, which highlights a lack of a critical method like clustering for developing a set of housing archetypes that can be representative to a major proportion of the housing stock. The second research gaps is establishing archetypal energy baselines according to the minimum requirements of the KSABC, which allows code evaluation and sights different areas for improvements. The third research gap is detecting various sensitive key parameters in the buildings energy performance research that have not been investigated well and may have direct effects on the energy models' outputs. The fourth research gap is to predict the airflow rate of the KSA housing stock, which allows for the assessment of both infiltration rates and heat gains. The airflow rate study is the first pioneering investigation in the KSA that evaluates these factors. The fifth research gap is reducing the energy demands, carbon emissions and electrical billing costs of the KSA housing stock, which meets the international targets set by Paris Agreement and the overall research aim. Figure 3.7 summarises this research gaps and novelty.

Filling these research gaps assesses to inform the KSA's policy and decision making process, helps clarifying opportunities for resource optimisation and energy

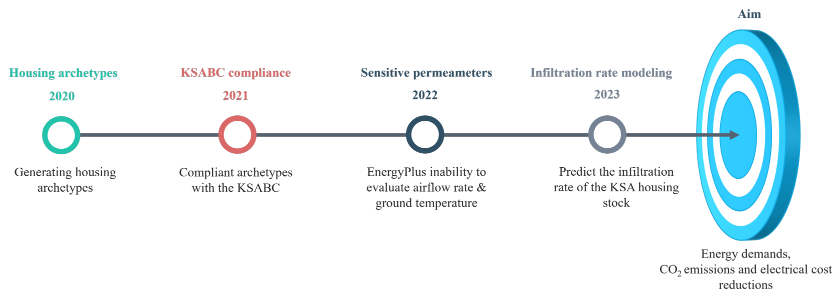

FIGURE 3.7: Research novelty.

efficiency, accelerates the economic progress, protects environmental sustainability to reduce global warming potential, enhances data and existing knowledge and encourages for international cooperation and competitiveness.

3.5 Summary

Buildings' energy performance modelling is useful for evaluating the building energy demands of a given stock, described in Section 3.1. This can be accomplished with a bottom-up or top-down approach, as detailed in Section 3.1.4, using the development of representative housing archetypes, as described in Section 3.1.5. The development of these housing archetypes assists with simpler and quicker energy performance assessments and decision-making processes. This archetype can then be modelled through various energy modelling tools, described in Section 3.1.2.3, to predict the energy performance of buildings. This raises the uncertainties highlighted in Section 3.1.2.1 and creates the need to obtain definite construction specifications, including data variations. The infiltration rate and heat loss addressed in Section 3.3 is responsible for 30%–51% of the UK's energy demands, but no infiltration rates or heat loss calculations have been conducted for the KSA's buildings. Thus, real census data were obtained from national sources and systematically presented in Chapter 4. These data should be versatile and comprehensive to mimic the real conditions of the existing housing stock.

Chapter 4

Data analysis and housing representation in the KSA

Chapter 3 defined the significance of detailed building specifications and the data variances in distinct stocks. In recent decades, the KSA's housing stock has experienced increases in energy demands, leading to excessive carbon emissions. This extreme housing energy demand is a concern due to the socio-economic and environmental impact of buildings (Bayar and Gavriletea, 2019). Scientific investigations must prioritise and support such concerns so the required procedures can be undertaken to reduce current housing stock energy demand, cost and carbon emissions, which answers the aim of this research. This will certainly meet the KSA's international obligations specified in the Paris Agreement, described in Chapter 1, to decrease the potential for global warming.

To improve expertise in this field, it is necessary to define the uncertainties associated with the energy demands of the KSA's housing stock. This may be described using an assessment tool that can perform probabilistic evaluations in an affordable manner to disclose relevant cases or settings and to assist with decision-making processes and policies. To predict mass transfer in dwellings, a broad variety of parameters is required to develop representative housing archetypes. Such data may not even exist in the KSA, or it may exist in incomparable or aggregated documentation formats. This issue demands data collection from several sources, notably governmental censuses, the literature and the building code. This operation may be time intensive and result in systemic inaccuracies, particularly when data monitoring is not recognised. Data credibility is essential

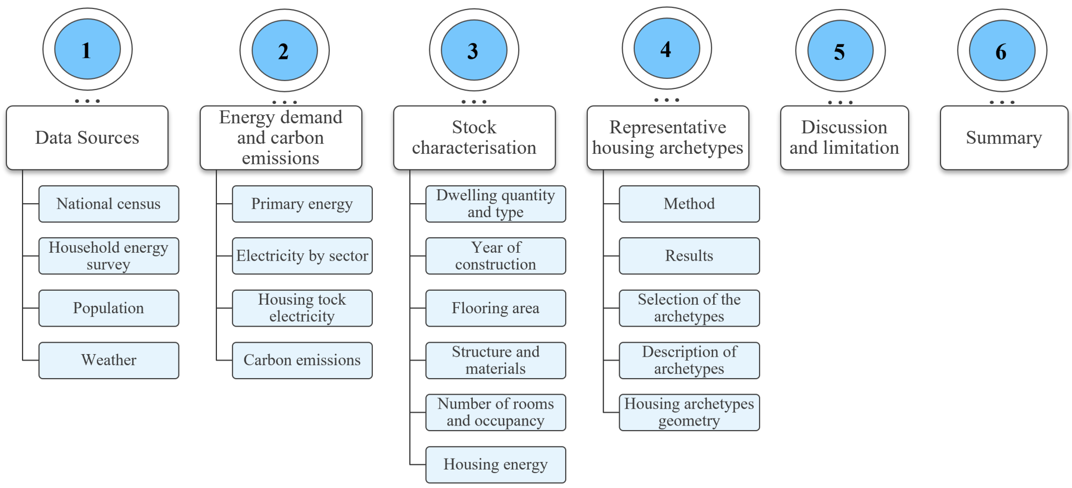

FIGURE 4.1: Chapter structure.

for most energy modelling tools to better inform the decision-making process. Section 4.1 of this chapter fulfils such requirements by reviewing all relevant and reliable data on the KSA's housing stock to develop housing archetypes for energy performance assessment, infiltration rate estimations and overall energy analysis purposes. Section 4.2 reviews historic and current energy use by different sectors of the KSA and their associated carbon emissions. Section 4.3 characterises and defines the KSA's housing stock. Section 4.4 develops a set of representative housing archetypes that mimic the existing conditions of the KSA's housing stock. Figure 4.1 summarises this chapter's structure.

4.1 Data sources

This section describes data sources collected by the KSA's agencies and related non-governmental organisations. This section attempts to reveal and categorise the necessary housing characteristics for modeling energy and mass transfer of the KSA housing stock. These data include large-scale national and local censuses, socio-economic surveys, energy censuses, building codes and the literature.

4.1.1 National census

The national census is a process of collecting, processing, disseminating and evaluating demographic and socio-economic information on individuals and distributing it to various geographic regions in a specified timeframe. This initiative is commissioned by governmental ministries directly related to the Ministry of Interior, which is responsible for the KSA's stability and security. Previously, the KSA lacked sufficiently accurate data for economic and demographic analyses. Accordingly, to gain the Kingdom's demographic data, it conducted actual censuses by employing real visits to individual dwellings. The censuses were conducted through face-to-face meetings utilising written forms that proceed through several phases before approval. This makes it a comprehensive and reliable source of data since it attempts to emulate statistics about population size (GAS, 2019).

The General Authority for Statistics (GAS) is responsible for censuses, and it interprets statistics for official disclosure. The original data are publicly available upon request and are summarised in Table 4.1. These data illustrate the progression of population and housing units since 1998. Housing units decreased from 2007 to 2016 due to the recent shifts of housing surveys. More recent versions only presented households occupied by Saudis rather than Saudis and non-citizens (GAS, 2019).

TABLE 4.1: A comparison of Censuses by Year and the Availability of Data (GAS, 2019).

Variable	Aggregated Data Base							
Source	General Authority for Statistics (GAS, 2019)							
Sample	Full population							
Year	Category	1998	2000	2007	2016	2017	2018	2019
Housing (Geometry)	Type	×	✓	✓	✓	✓	✓	✓
	Materials	×	✓	✓	✓	✓	✓	✓
	Age	×	×	×	✓	✓	✓	✓
	floor material	×	×	×	✓	✓	✓	✓
	Stories	×	×	×	✓	✓	✓	✓
	Rooms nu.	×	×	✓	✓	✓	✓	✓
	Bedrooms nu.	×	×	✓	✓	✓	✓	✓
	Floor area	×	×	×	×	×	✓	✓
Location	Region	×	✓	✓	✓	✓	✓	✓
	Urban/Rural	×	✓	✓	✓	✓	✓	✓
Occupants	Male/female	×	✓	✓	✓	✓	✓	✓
Energy Source	Water	×	✓	✓	✓	✓	✓	✓
	Electricity	×	✓	✓	✓	✓	✓	✓
	Cooking	×	✓	✓	✓	✓	✓	✓
	Cooling	×	✓	✓	✓	✓	✓	✓
	Heating	×	✓	✓	✓	✓	✓	✓
Operation	Lighting	×	×	×	×	✓	✓	✓
	Equipment	×	×	×	×	✓	✓	✓
Socioeconomic	-	×	✓	✓	✓	✓	✓	✓
Tuner	-	×	✓	✓	✓	✓	✓	✓
Houses (million)	-	×	3.4	4.2	3.4	3.5	3.5	3.6
Population (million)	-	0.1	20.8	23.9	13.7	32.6	33.4	34.2

The socio-economic data are essential for determining an accurate picture of the KSA's state of living, spending habits and household incomes. Consequently, an additional fundamental survey investigating households' socio-economic levels and societal well-being was conducted in 2019 by the GAS. The primary goal of this survey was to systematically deliver data about the distribution of household expenditures and demand, education, employment, life expectancy and health (GAS, 2019).

4.1.2 Household energy survey

Household energy demand is known to be a function of occupant behaviour. The Household Energy Survey (HES) offers information about housing distribution, households' energy status, energy performance and housing components that need cooling or heating, energy sources and the number of operating hours (GAS, 2019). It clarifies the housing type, age, flooring materials, construction materials, tenure type, number of rooms, kitchens, number of bathrooms and sources of services for water, electricity, sanitation and cooking fuel. This allows researchers to identify patterns of energy demand and its forms to study the impact of the current domestic housing stock and surrounding environment on large-scale developments. The survey indicates that concrete dominates buildings' construction materials by 89%, while more than 60% of the housing stock's energy demand is consumed for cooling purposes (GAS, 2019). This has resulted in continuous, extreme energy demand increases per person in the KSA since 2000, compared to international data. See Figure 4.2.

The data were acquired by field researchers using multiple questionnaires to interview 33,350 households across the country and provide a statistically representative sample. However, the available data were aggregated, giving parameters by region rather than by single housing units. Hence, greater disaggregation is required to increase its utility.

4.1.3 Population

In the 1950s, the KSA's government was urged by local developers to provide statistics so future population changes could be anticipated. In July 1974, the government conducted its first population census of seven million people, 46% of whom lived in cities and 54% lived in villages. The population had more than doubled to 16.95 million people when the second national governmental census

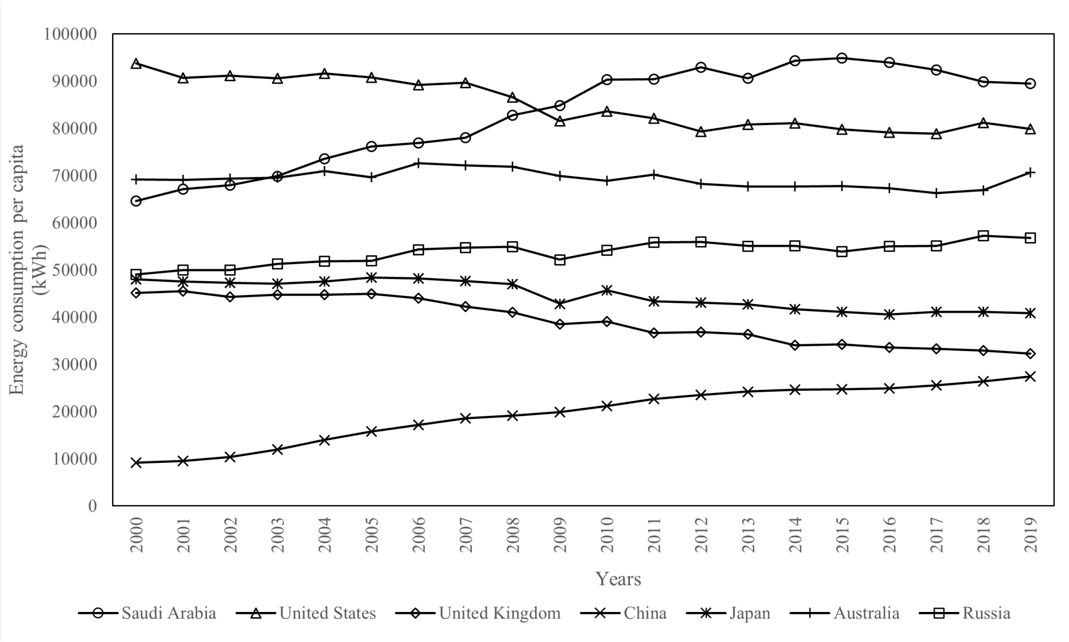

FIGURE 4.2: International energy demands per capita (Roser et al., 2013).

was conducted in 1993, indicating an annual growth rate (AGR) of 3.7% (Ashwan M., 2012). By 2004, the population had risen to 22.7 million, indicating an AGR of 2.9%, while the AGRs of the world, the USA and the UK were 1.2%, 0.8% and 0.6%, respectively. The AGR of the KSA was more than double that of the world and three times higher than the USA and the UK. Over the same period, a reduction in the KSA's mean household size from 5.8 to 5.5 was also observed (Al-Mayouf and Al-Khayyal, 2011; Roser et al., 2013).

In 2010, the population was found to be unequally distributed in the central, western and eastern regions, where 65% of the total population live. This is due to governmental offices' relocation from all regions to the capital city, Riyadh, to facilitate faster communication and to access utilities and services (Ashwan M., 2012).

The most recent census was conducted in 2019 and revealed that the population had increased to 34.2 million people (GAS, 2019). Although the AGR has reduced, the KSA's population is still expected to double by around 2060 (Roser et al., 2013), which increases demands for food, energy and houses when environmental threats are likely to increase. Figure 4.3 summarises the historic and future changes of the KSA's population compared with the AGR. Additionally, the KSA's population

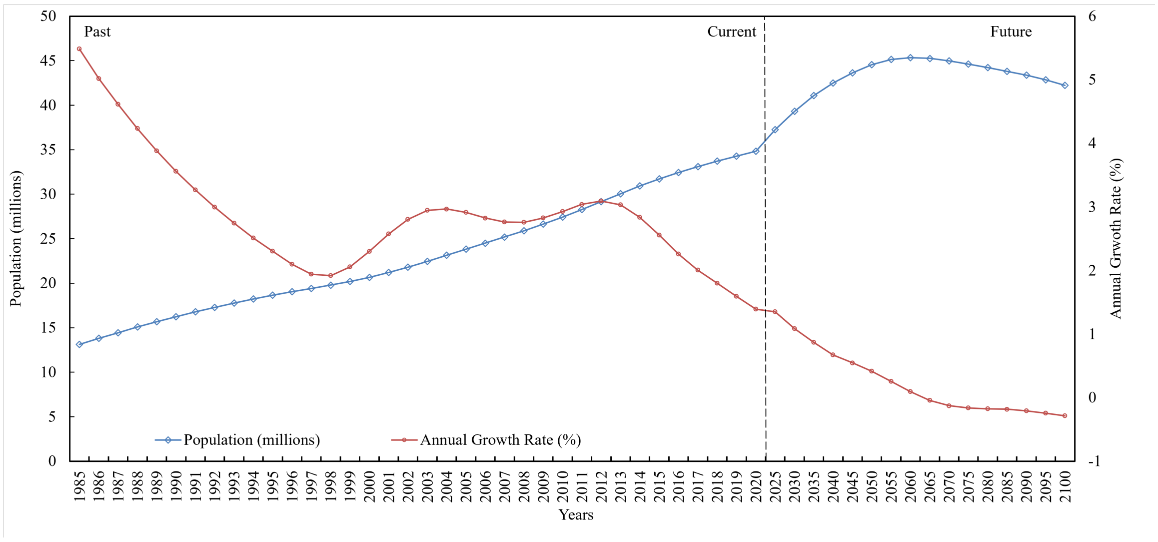

FIGURE 4.3: Annual population growth of the KSA, data from (Roser et al., 2013).

density increased until 2020 and was expected to drop a little in the future, although the KSA still has low population density compared to international countries. The population density in 2022 of the UK, the UAE, Iran, the USA and the KSA are 279, 133, 54, 37 and 17 people/km^2, respectively. This low population density has resulted in large housing areas per capita and is potentially due to the relatively massive size of the KSA, which was inhabited by only 34.2 million people in 2019 (Roser et al., 2013). This vast geographic territory is subjected to a variety of meteorological conditions involving extreme temperature swings.

4.1.4 Weather

The KSA occupies around 80% of the Arabian Peninsula and has a total area of 2×10^6 km^2. It is bounded on its eastern and western sides by the Persian Gulf and the Red Sea, respectively. Parallel and adjacent to the West Coast is the Sarawat mountain range, which rises to over 3 km in altitude. Around a quarter of its land area is the Rub al-Khali Desert, the world's largest area of uninterrupted sand (GAS, 2019), known as the *empty quarter*. This diverse geography corresponds with varied climate conditions.

Several studies have related regional climate with construction materials or dwelling design (Al-Naimi, 1989a; Alrashed and Asif, 2015; Almehrej, 2015; Calaqutit et al., 2015; Saudi Arabia, 2020; Talib, 1984a). An early effort demonstrated vernacular architecture depending on the use of local materials in relation to climate and region (Talib, 1984a). Climate zones had a significant role in determining the construction materials to maintain an acceptable indoor air temperature; in the hot–dry region, vernacular houses were made of mud with wooden beams to adapt to extreme temperatures in the summer and winter. Meanwhile, in the hot–humid region, houses were made from straw and palm tree leaves to adapt to high humidity levels for a more comfortable indoor environment (Almehrej, 2015). An alternative climatic classification study in 2015 showed the obstacles that confront sustainable housing adoption in the KSA and claimed that the climate contributes to buildings' designs (Alrashed and Asif, 2015). The study divided the KSA into six climatic zones, which contradicts the most recent version of the KSABC. See Table 4.2. The most recent edition of the KSABC was published in 2018 and states that KSA includes three climatic zones, Zone-1, Zone-2 and Zone-3 (Saudi Building Code, 2018). Figure 4.4 demonstrates the climate zones and major cities.

Building performance simulation tools are often utilised by engineers to estimate energy demands for heating, cooling, ventilation, lighting, electrical equipment and hot water usage in buildings. One such tool, EnergyPlus, collects weather data from actual measurements gathered by international meteorological stations for 20–30 years to prepare typical meteorological year (TMY) data. TMY data depends on actual weather measurements to describe the best representation of median climatic conditions in single-year hourly forms. The KSA's data available from EnergyPlus Weather Data (DoE, 2022) reveal the KSA has a wide range of OAT variations among the regions. See Figure 4.5. The mean summer temperature exceeds 33°C in most of the Kingdom due to high levels of solar radiation. Mean winter temperatures drop to 15°C in the southern and northern regions, while dropping to 14, 15 and 24°C in the eastern, central and western regions, respectively. Even though daytime temperatures may spike to 37°C, they can drop to less than 10°C in the winter.

In addition, the annual average air temperature has been collected from 25 meteorological stations across the KSA since 1978 (Almazroui, 2020). These data prove that air temperature increases at a rate of 0.71°C every decade (Almazroui et al., 2012). Temperature rates increase the highest in the central, eastern and southwest provinces, respectively, due to higher rates of global concentrations of

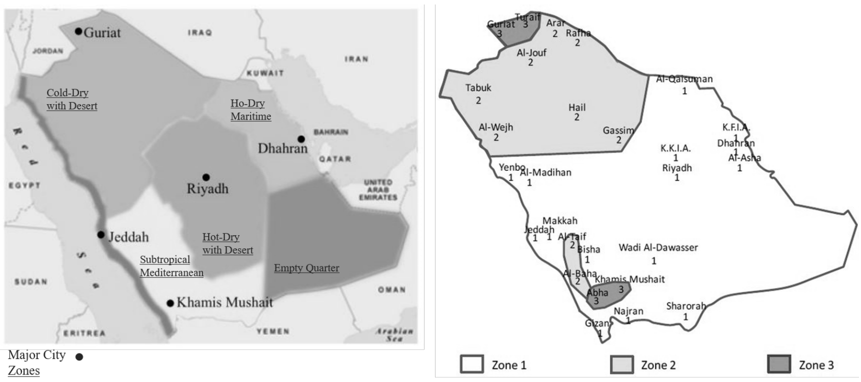

FIGURE 4.4: Climate Classification (Alrashed and Asif, 2015) (left) vs. KSABC zoning (Saudi Building Code, 2018) (right).

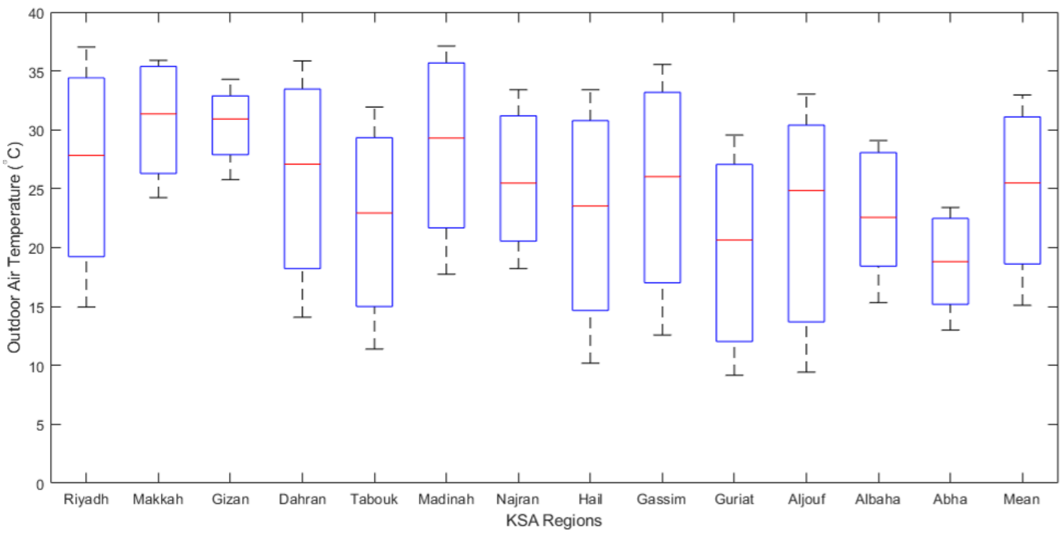

FIGURE 4.5: Mean temperature swing of the KSA regions.

heat-trapping GHGs in the earth's atmosphere, such as carbon dioxide, methane and nitrous oxide (Agency, 2016). Humidity, however, is very low overall except in two regions, eastern and western, where coastlines are. Rainfall levels are minimal: 65, 75 and 480 mm of rain for the western, central and eastern and southern regions, respectively (Said et al., 2003; Almehrej, 2015).

TABLE 4.2: Relevant studies about the KSA climates.

Author (year)	**Scope**	**Note**
Al-Naimi (1989a)	Early climate zones summary	3 Climate zones, comply with KSABC
Alrashed and Asif (2015)	Important Climate classification	Compare 5 climate zones, in-comply with KSABC
Almehrej (2015)	Vernacular architecture	Local construction materials and climate
Calaqutit et al. (2015)	Wind towers designs	Hot dry climate to reduce cooling energy
Saudi Arabia (2020)	residential building regulations	Only 3 climatic zones for the KSA

4.2 Energy demand and carbon emissions

Since the beginning of the Industrial Revolution, fossil fuels have predominated the energy portfolios of most nations throughout the globe. This has significant repercussions for the environment across the world as well as for the health of people. Burning fossil fuels for energy purposes is responsible for around 75% of the world's total GHG emissions. The burning of fossil fuels results in massive levels of air pollution around us, which is a hazard for human health. In fact, air pollution is responsible for at least five million premature deaths each year (Roser et al., 2013). It is imperative that the globe swiftly transition to low-carbon sources of energy, such as nuclear and renewable technology advancements, to reduce carbon emissions and air pollution. In future decades, the decarbonisation of international energy systems will be significantly aided using renewable sources of energy. However, how quickly are the methods evolving to produce renewable energy? What kinds of technology have the greatest potential to revolutionise our energy mix?

This section considers the KSA's Primary Energy (PE) exports and uses, housing electrical energy demand and associated CO_2 emissions. It compares the KSA's energy and carbon emissions data with those of Middle Eastern countries.

4.2.1 Primary energy

PE is derived from the resource in a direct manner and has several sources, including petroleum and other liquids, natural gas (NG), nuclear and renewable energy and coal production. The KSA is one of the highest PE producers and consumers in the Middle East (ME) due to high oil-based expenditures. In 2018, the KSA produced about 12,419 TWh and consumed about 3,079 TWh. From 1990 to 2018, energy production and consumption rose by 80% and 268%, respectively, resulting in a marked increase in energy demand. Most of the KSA's PE is produced from oil, accounting for 65% of total energy production, while 35% is from NG (Roser et al., 2013).

The disparity in total energy demand often reflects differences in population size; nations with larger populations consume more energy. In 2019, the per-capita energy demand of the KSA was 89.4 MWh, four times higher than the world average, 21 MWh. Figure 4.6 compares the PE production and demand of the highest energy producers and consumers in the ME. The KSA is among the top five consumers of oil in the world. Its NG production is also significant and has been increasing since 2006. Only Qatar and Iran have produced more NG than the KSA in the ME (statistics and analysis, 2019). In 2017, the KSA held 303 trillion cubic feet of NG and was ranked with the fifth-highest reserves globally. Indeed, the KSA has proven reserves equivalent to 79 times its annual consumption (statistics and analysis, 2019).

4.2.2 Electricity by sector

Electrical energy is a practical and regulated source of energy used to supply cooling, heating, lighting and power to buildings. The electrical energy production of the KSA is transmitted to buildings through public distribution networks, which are managed by the SEC. The SEC is the primary source of electricity distribution, maintenance and service charges (Matar, 2017). The KSA produces electrical energy by burning fossil fuels; it is ranked the highest among the ME and North African (MENA) countries; see Figure 4.7. The KSA's national electrical energy production and consumption in 2018 were 359 and 299 TWh, respectively (GAS, 2019). See Figure 4.8. According to the SEEC, 90% of the KSA's domestic PE use is consumed

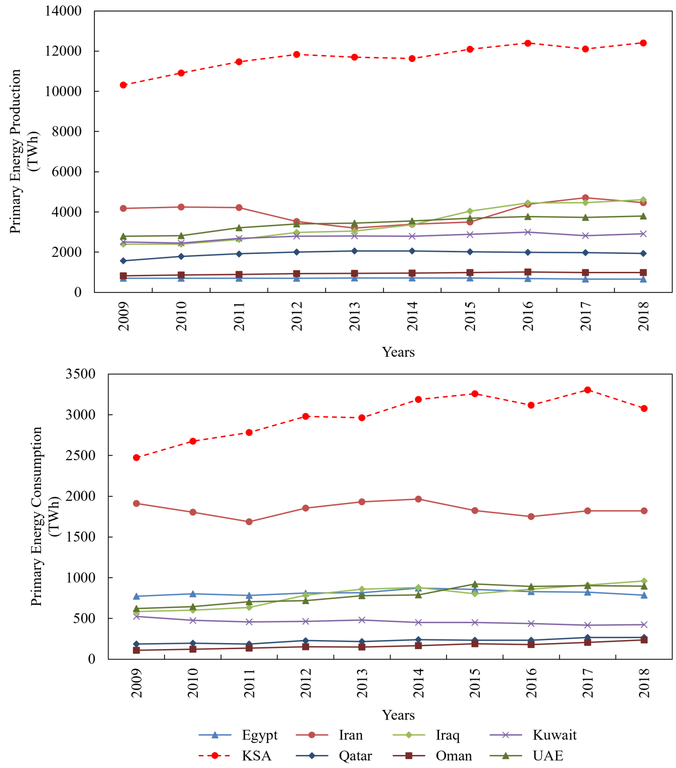

FIGURE 4.6: Highest PE production and demand in MENA countries (statistics and analysis, 2019).

by three major sectors, industrial (47%), construction (29%) and transportation (21%). The building sector's energy use alone is equivalent to 75% of the total PE production (AlGhamdi et al., 2020), and the demand for electrical energy has increased almost every year since 2010. See Figure 4.9. This increase is potentially due to growth in both the population and residential construction permits (Amran et al., 2020).

4.2.3 Housing stock electricity

The housing stock is responsible for about 50% of the total energy demands of the KSA (Abuhussain et al., 2018). This excessive energy demand is anticipated to continuously grow due to population growth and the issuance of more building permits for dwellings (Alrashed and Asif, 2012). Most of this residential energy consumption, 60%, is attributable to cooling, followed by 20% for lighting, 12% for appliances, 5% for heating and 3% for other uses; see Figure 4.10 (Hamid et al., 1990; Alaidroos and Krarti, 2015).

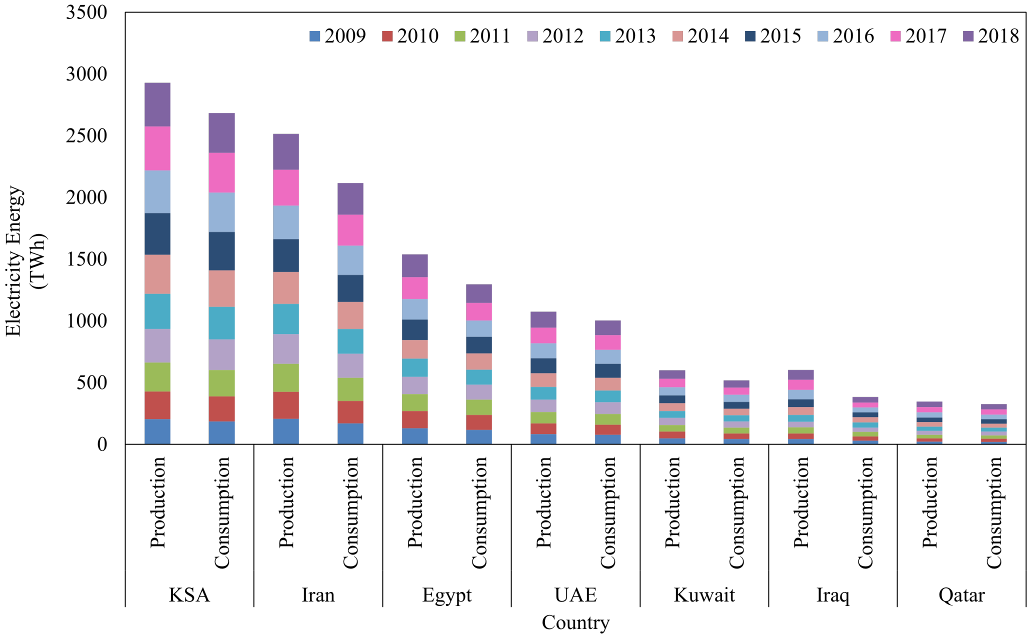

FIGURE 4.7: Highest electricity energy producers and consumers in MENA Area, (statistics and analysis, 2019).

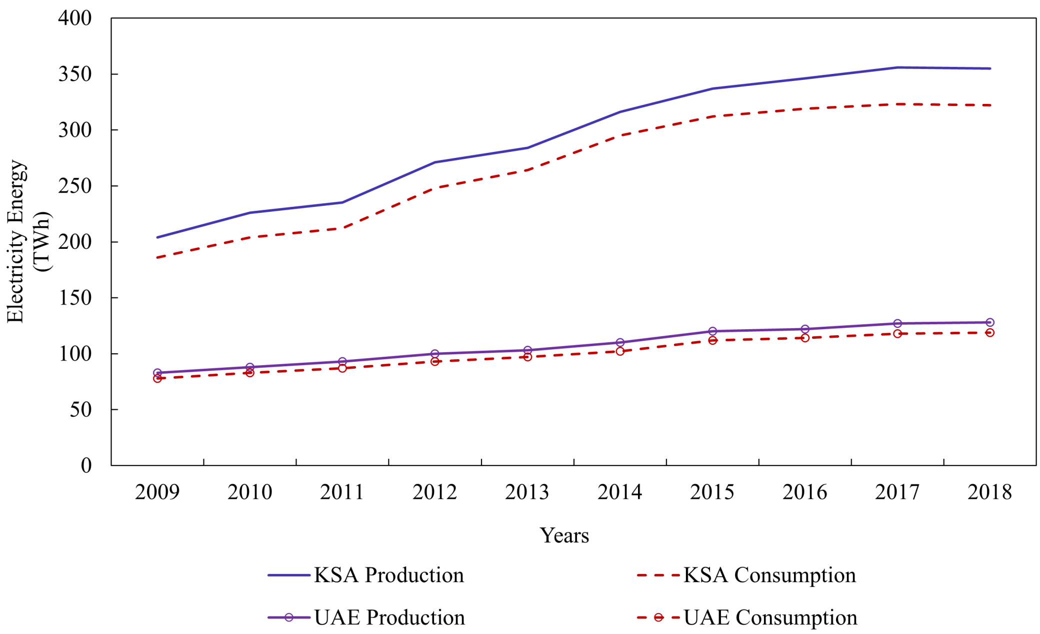

FIGURE 4.8: Two highest electricity production and usage for the gulf countries (data from (statistics and analysis, 2019)).

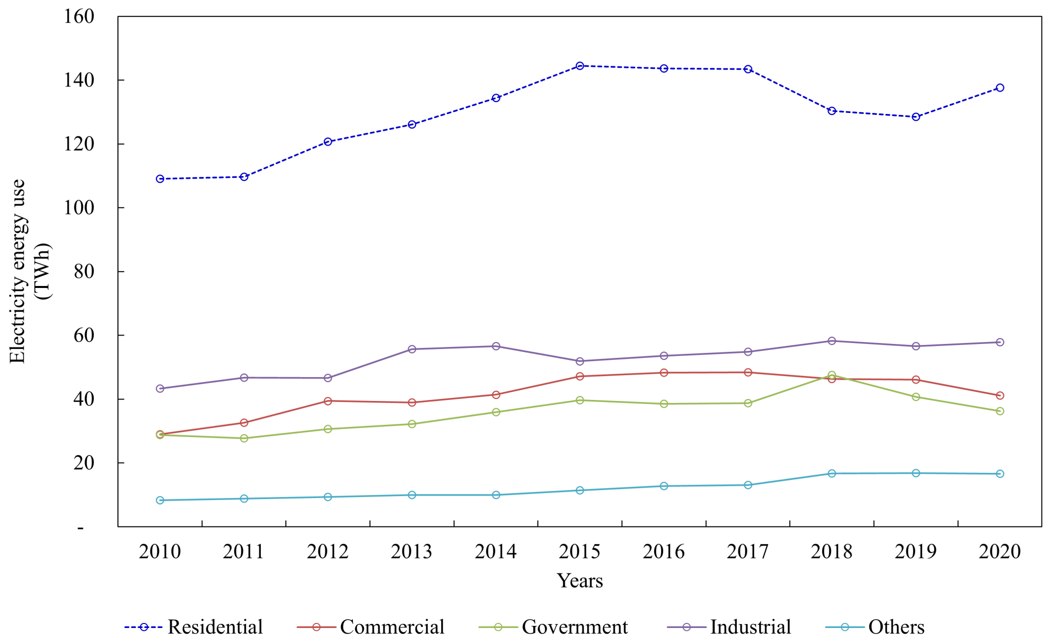

FIGURE 4.9: Electrical energy demand by sector (GAS, 2019).

Population growth is a potential reason for this high electrical energy demand; see Figure 4.11. Other potential reasons include extremely harsh weather and low energy prices that enable housing occupants to attain thermal comfort by using air-conditioning. Table 4.3 summarises the electrical energy demand by sector and population growth over the years, and the Sankey chart in Figure 4.12 summaries current energy production and consumption by sectors. The electrical energy use of the KSA's housing stock contributes to the total proportion of the carbon emission rates of the country. These energy demands and carbon emissions can be quantified and reduced to mitigate their environmental emissions.

This shows the significance of this research for predicting the energy demands and associated carbon emissions of the KSA's housing stock and how they can be reduced.

4.2.4 Carbon emissions

Among the most significant problems facing the environment currently is climate change, particularly global warming. It is believed that carbon dioxide is the primary component responsible for the greenhouse effect, which is the process of how greenhouse gases retain heat near the surface of the Earth (Bolin and Doos,

TABLE 4.3: Summary of Population and Energy Usage in the KSA (Amran et al., 2020; statistics and analysis, 2019; GAS, 2019).

Year	**Population** (million)	**Population growth rate** (%)	**Peak** load	**Power Sold Billion (kWh)**		**Costumers** (million)	**Total** Power (kWh)	**Avg. demand per consumer** (kWh/year)
				Residential	**Industrial**			
1980	9.7	5.9	0.3	10,611	6,841	0.8	17,452	20,014
1985	13.2	5.5	9.4	28,733	11,586	1.7	40,319	22,885
1990	16.3	3.6	12.1	42,305	16,667	2.3	5,872	24,915
1995	18.7	2.3	17.7	46,520	21,388	2.9	85,908	29,357
2000	20.8	2.3	21.6	86,504	27,657	3.6	114,161	31,819
2005	23.9	2.9	1.6	119,483	33,800	4.7	153,283	32,425
2010	27.4	2.9	41.2	158,818	34,654	5.7	193,472	33,934
2015	31.6	2.6	60.7	198,153	35,508	6.6	233,661	35,443
2018	33.4	1.8	80.3	237,488	36,362	7.6	273,850	36,952

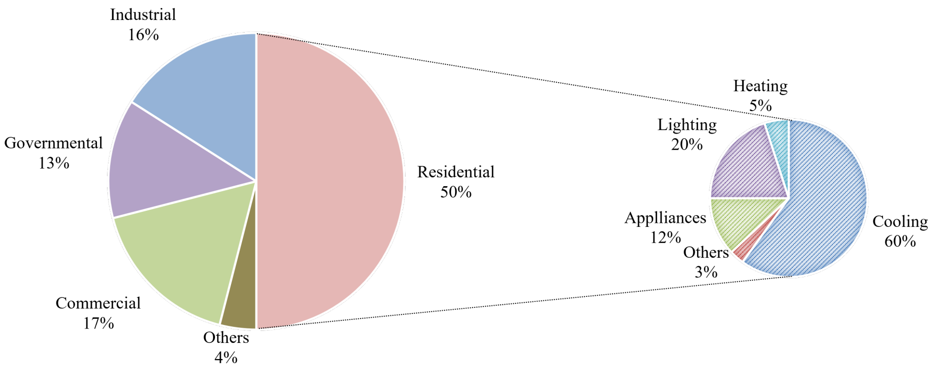

a) Electricity use by sector (Awad et al., 2018)

b) Residential buildings electricity use (Alaidroos and Krarti, 2018)

FIGURE 4.10: Residential buildings energy consumption in the KSA (Abuhussain et al., 2018; Alaidroos and Krarti, 2015).

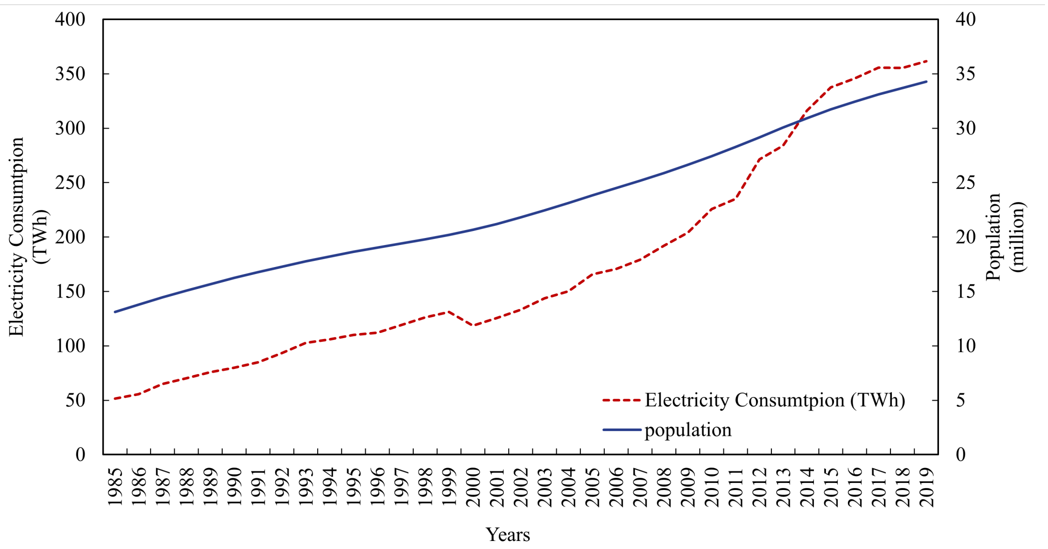

FIGURE 4.11: Population growth and electricity energy demand increase (Roser et al., 2013).

1989). The aim of lowering GHG emissions and slowing the global warming potential (GWP) has been at the centre of both academic and practical research. Researchers often compare nations' contributions to climate change by annual emission estimates. However, this statistic often reflects the disparities in population size that exist around the globe (Zhang and Cheng, 2009).

The KSA is obligated to decrease its carbon emissions to comply with the Paris Agreement since its total carbon emissions are four times greater than the world average (Scott et al., 2016). See Chapter 1. Scientists refer to per-capita carbon emissions to predict the typical person's footprint in a specific nation. The per-capita carbon emissions of the KSA is 17.9 tonnes, which is four times higher than the world average of 4.4 tonnes. The annual carbon dioxide that Middle Eastern countries emit is high due to the reliance on oil as the major source for a thriving economy. Reviews of current carbon emissions focus solely on present emissions. However, they also ignore previous nations' historic responsibility for carbon emissions. Figure 4.14 displays the cumulative annual carbon emissions for Middle Eastern nations, with only Iran emitting more carbon than the KSA. Population and total housing permit growth are two probable causes for the KSA's substantial carbon emissions. Since 1987, carbon emissions and the total number of the KSA's housing licences issued by the government, citizens or the private sector to construct residences have been rising, as described in Figure 4.13. The drop in housing permits in 2017 resulted

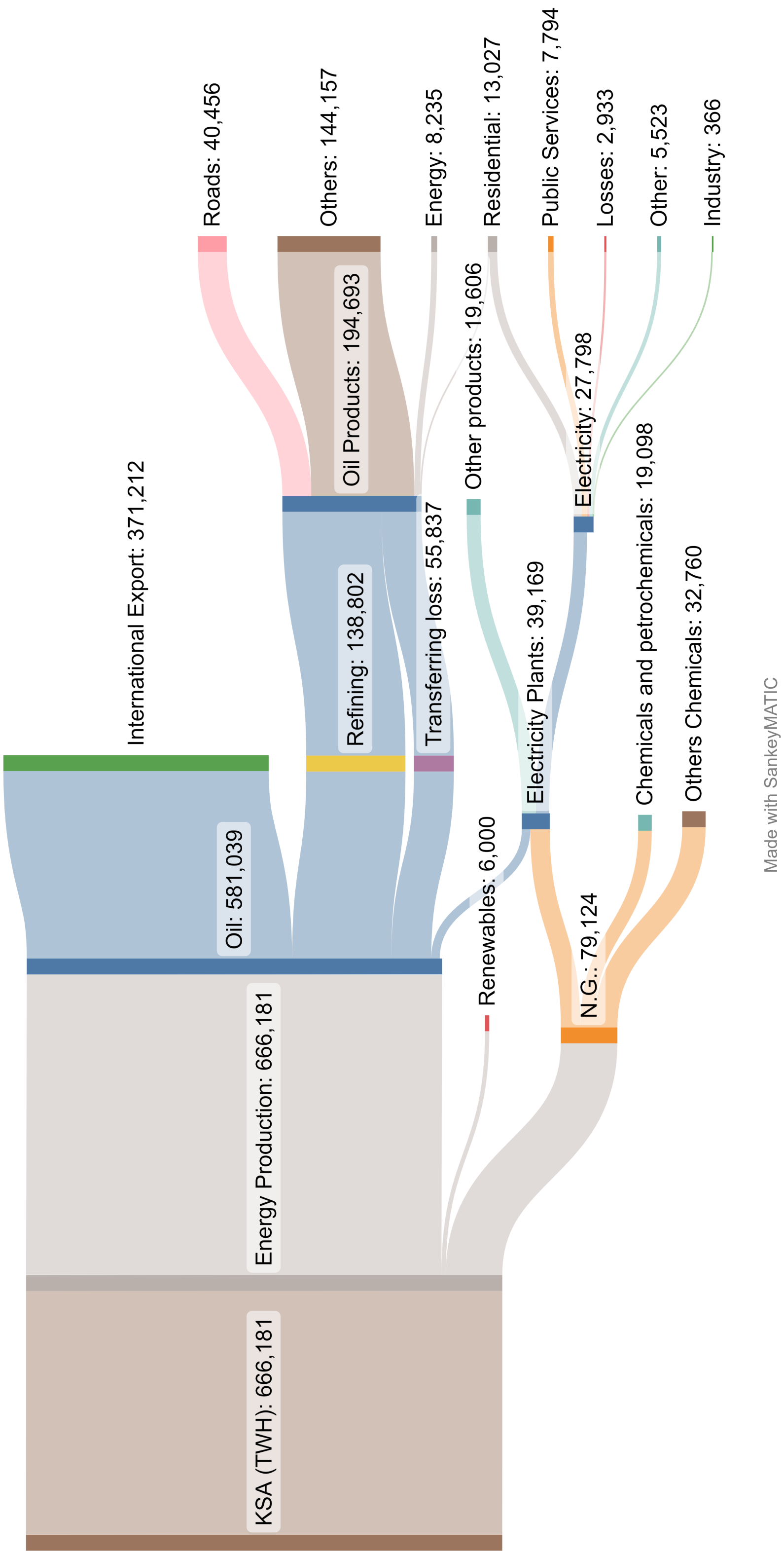

FIGURE 4.12: Summary of the KSA energy production and consumption by sector.

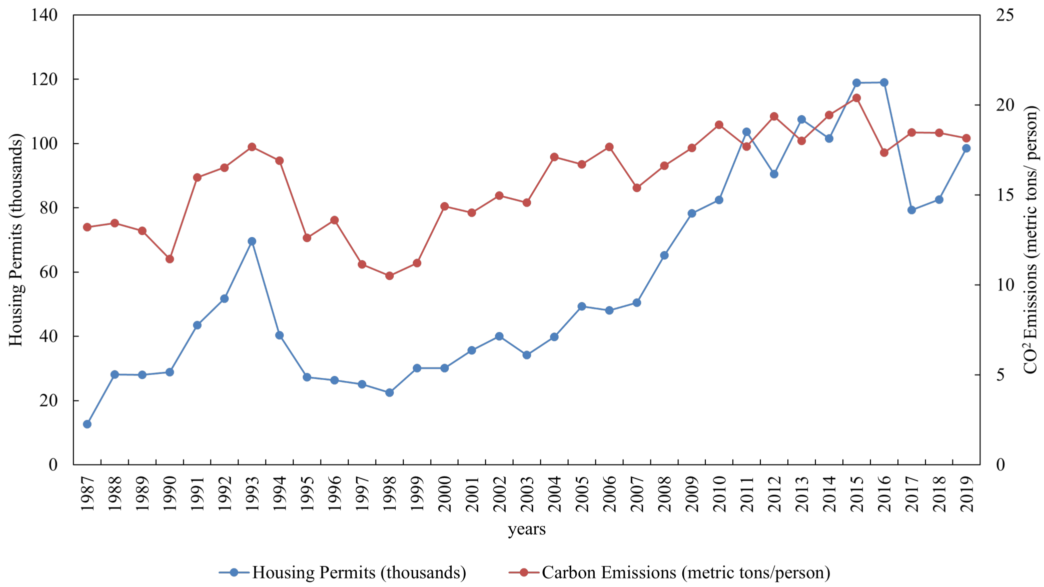

FIGURE 4.13: Housing permits and carbon emissions growth (Roser et al., 2013).

from the Vision 2030 declaration, which introduced new regulations and policies for the housing stock and the entire kingdom's economy. Moreover, since 1960, carbon emissions have been rising with the population, which highlights the relevance of this research's aims and objectives to reduce the KSA's housing energy demands, carbon emissions and costs.

4.3 Stock characterisation

This section describes the details of building components and the data sources mentioned in section 4.1.

4.3.1 Dwelling quantity and type

Most information on housing in the KSA can be obtained from the housing national census statistics collected by the GAS. Figure 4.15 indicates that the KSA's housing stock accounts for 3.6 million dwellings, the bulk of which are apartments at 44%, followed by villas accounting for 30% and traditional houses (TH) at 18%. The remaining proportions, 7% and 1%, are for a floor in a villa and a floor in a TH, respectively. The plurality of house types was constructed over the last 10 to 20 years, while the minority were constructed within the last five years. Most of the

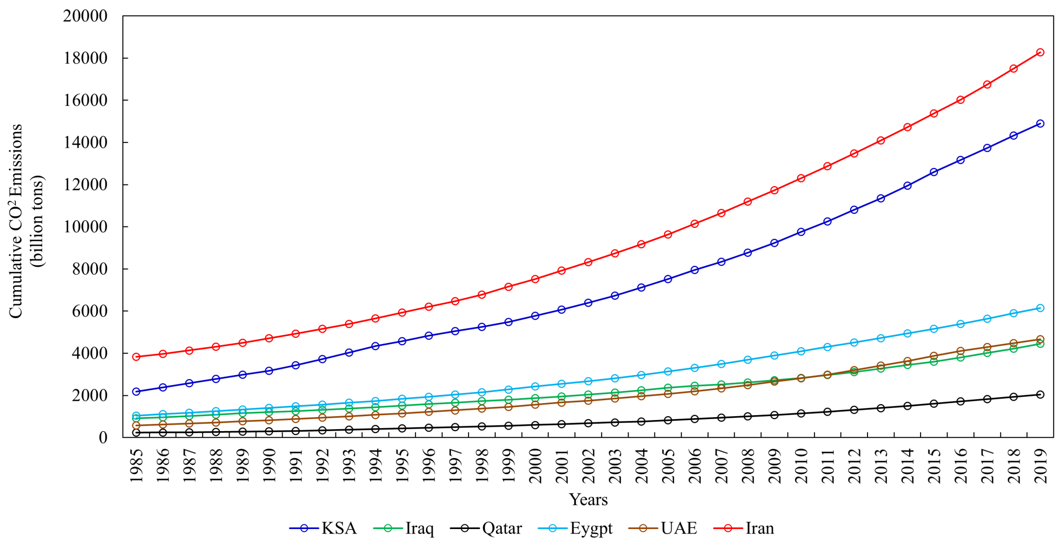

FIGURE 4.14: Cumulative weighting factor of carbon emissions (Roser et al., 2013).

housing is in the three most populous regions of the nation, Makkah, Riyadh and the Eastern Region (GAS, 2019).

Most details concerning housing data in the KSA are obtained from the housing census; see Table 4.1. The housing statistics indicate the housing types and quantity, but geometry and volume are not available. Flooring area, on the other hand, is only available in regionally aggregated forms. Unfortunately, housing surveys in the KSA lack required level of detail. This data insufficiency is unsatisfactory because it restricts data modification and prevents data comparisons with international housing stocks such as those of the UK and the USA.

4.3.2 Year of construction

Dwellings' ages are supplied by the GAS (2019), which splits ages into five groups. See Figure 4.15. Most housing is 10 to 20 years old, comprising 31% of the total housing, and this indicates that the condition of dwellings is fair. The 20–30-year-old age group comprises 25% of the total housing, and this indicates poor dwelling conditions. The third largest age group, 5–10 years old, accounts for 21%, which indicates a new building condition. Owned and rented dwellings account for 61 and 36%, respectively.

Most dwellings in the Kingdom have been built utilising in-situ concrete, which

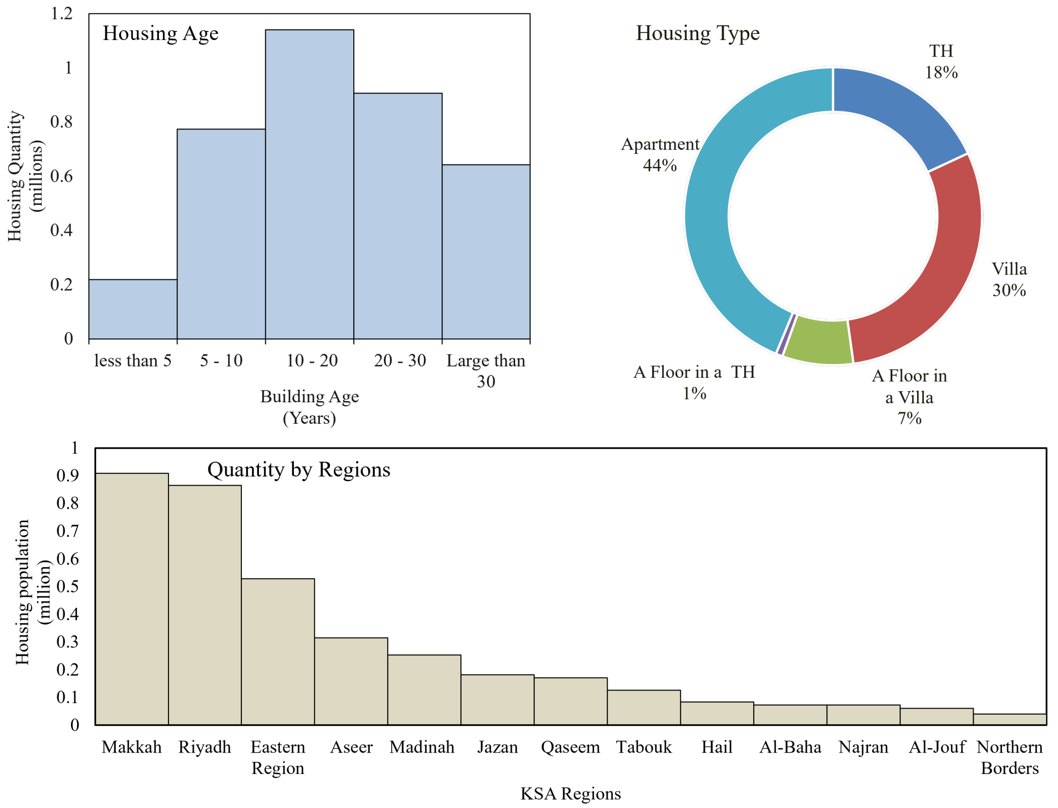

FIGURE 4.15: Housing type, age, and location (GAS, 2019).

accounts for about 90% of all housing construction materials. Block or bricks were only used for traditional houses and occupy 10% of all housing units. Common flooring materials are ceramic, plain tiles, cement tiles, marble and parquet, which account for 63%, 28%, 6%, 2% and 1%, respectively. It is evident that most construction materials are cement-based, with a typically high thermal mass.

4.3.3 Flooring area

Before 2019, little data described dwelling floor areas in aggregated or disaggregated forms. The KSA housing permit data were neglected in this research because they were only found in aggregated forms and sometimes integrated commercial and residential building areas, which made comparisons tedious. Figure 4.16 illustrates the total and per-capita housing flooring areas in the KSA. The drops of areas in 2019 were due to new building regulations updated and implemented in 2018 that lower housing contraction rates.

Recently, the MMRAH specified data for housing flooring areas, designs and

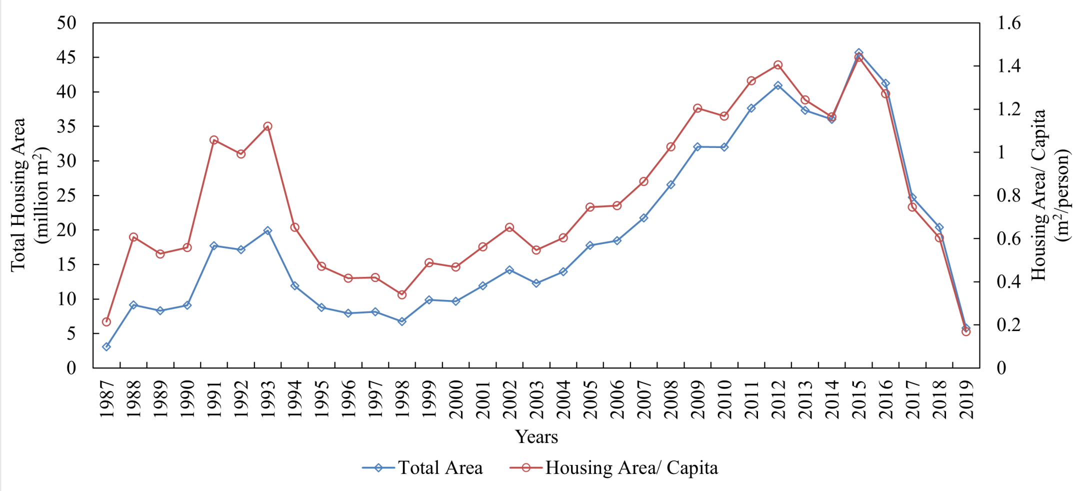

FIGURE 4.16: Total and per capita housing flooring areas (GAS, 2019).

TABLE 4.4: Descriptive statistics for the KSA housing flooring areas.

Flooring areas description	Villa	Apartments	Total
Mean	311.8	190.8	261.4
SE	9.4	10.5	9.9
Median	297	188	273.5
Mode	279	125	279
SD.	61	57.8	84.4
Sample Variance	3726.4	3336.9	7119.3
Kurtosis	7.5	-0.9	1.4
Skewness	1.9	0.4	0.4
Range	387	198	450
Minimum	188	125	125
Maximum	575	323	575
Count (groups)	42	30	72
CI (95.0%)	19	21.6	19.8

locations for new or recently constructed homes (Housing, 2020). The data were collected from 140 housing developments, known as *projects*, comprising 182,923 housing units. The MMRAH funded and led the construction of 30% of the projects whereas the private sector, managed by the MMRAH, constructed 70% of them. Around 50% of the projects were granted to the public before January 2019. Villas comprised 45% of total housing units, with a mean flooring area of 311 m^2, and apartments accounted for 51%, with a mean flooring area of 190 m^2. The total mean flooring area for the KSA's dwellings was 261 m^2. This mean flooring area is one of the largest globally, higher than the USA and more than double that of the UK, which might be due to gender segregation. Figure 4.17 and Table 4.4 summarise descriptive statistics for KSA dwellings' flooring areas. Figure 4.18 displays floor area frequencies of the KSA's homes and depicts that houses are massive structures, with an average household occupancy of 5.4 persons. See Figure 4.19.

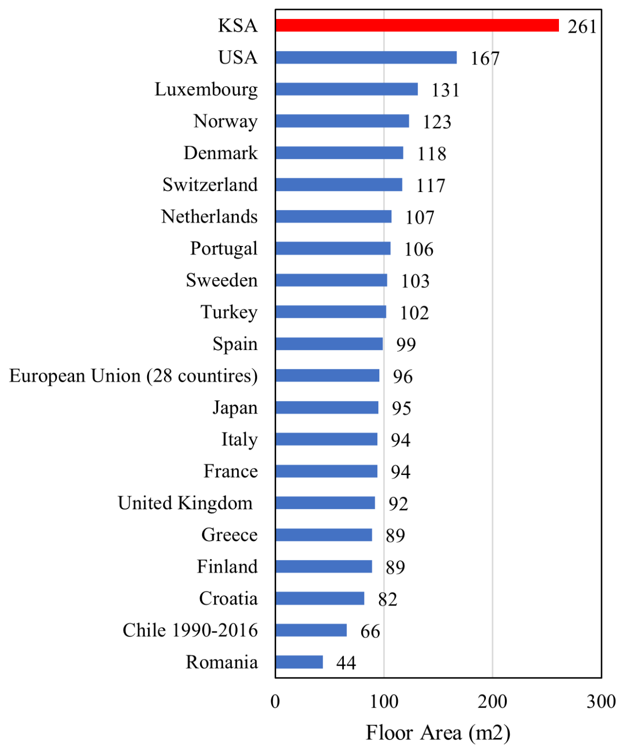

FIGURE 4.17: Mean housing flooring areas by country (INE, 2014; *Eurostat statistics database* 2012; Moura et al., 2015; Molina et al., 2020).

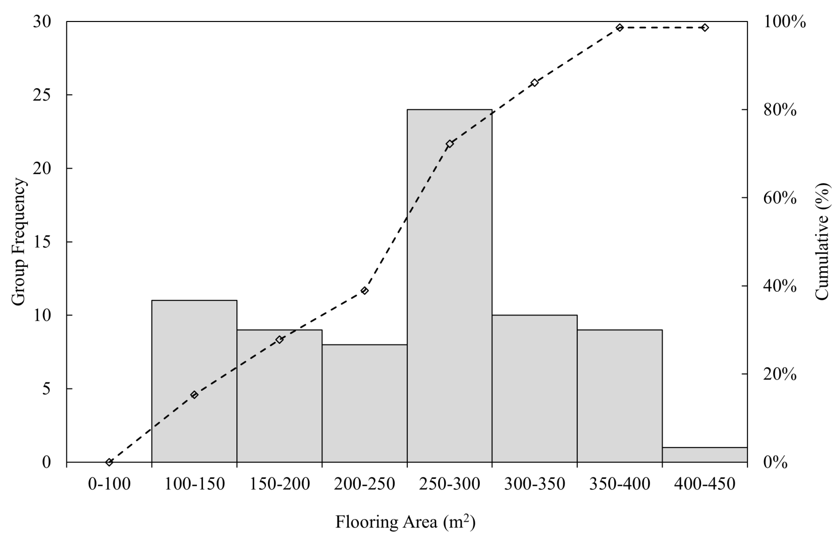

FIGURE 4.18: Flooring Areas Frequency of Modern Housings in the KSA (Housing, 2020).

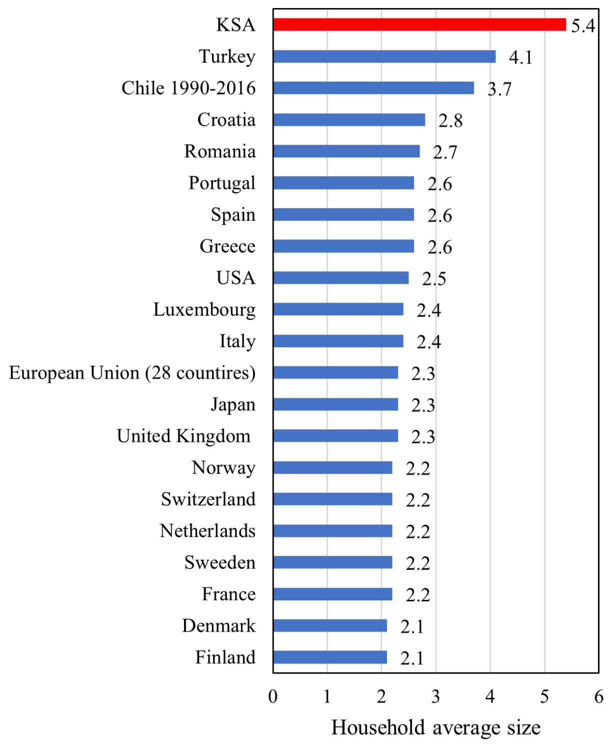

FIGURE 4.19: Mean household size by country (*Generating power* n.d.).

4.3.4 Structure and materials

The KSA established its building code in 2007 and updated it in 2018 (Saudi Building Code, 2018). It sets minimum requirements for residential buildings as a function of its local climate and then sets region-specific envelope U-values. KSABC classifies the KSA as having three climatic zones; however, it does not state detailed material thicknesses or layers of the envelope configuration.

Dwelling construction materials are generally concrete, block or clay brick, or stone materials. Portland cement concrete is the predominant building material in the KSA; it is made of cement, water, coarse aggregates and sand (Alhozaimy, 2008). Concrete is found in 90% of dwellings; blocks or bricks are found in 10% of dwellings. A negligible number of homes are constructed using stone or other materials (GAS, 2019). Modern houses are built using diverse imported and non-natural construction materials, such as concrete blocks, terrazzo, glass tiles (Bahammam, 1998) and aluminium (Talib, 1984a). Most construction materials are not available in the KSA, so they are mostly imported (Almehrej, 2015). This is due to

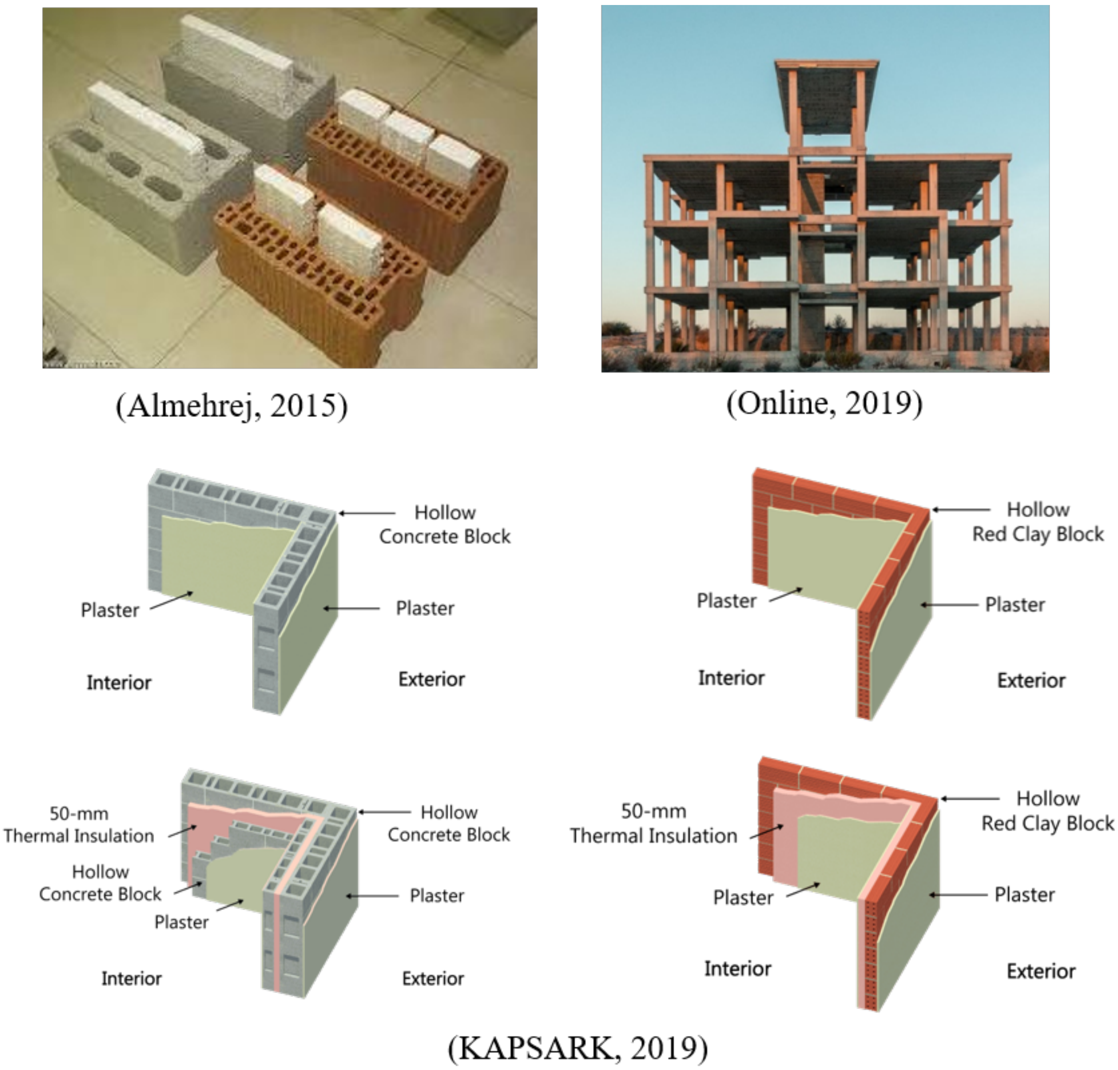

FIGURE 4.20: Walls construction materials of the villas in the KSA (KAPSARC, 2021; Almehrej, 2015).

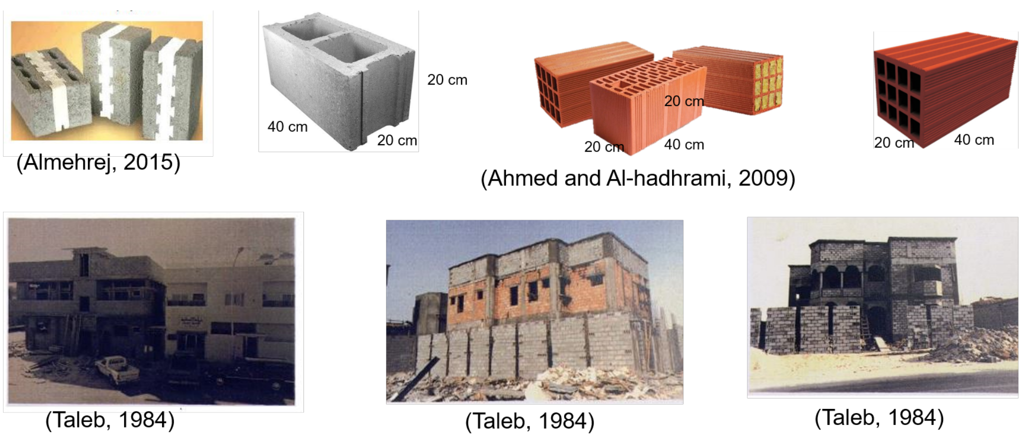

FIGURE 4.21: Different sizes and applications of blocks and bricks, data from Almehrej (2015) and Talib (1984a).

the high cement consumption demand for construction purposes (Alhozaimy, 2008). Conventional frames for building systems comprise columns and beams to attain long spans. Walls are more commonly constructed employing hollow concrete or clay blocks with heat insulation filling or placed on the inner or outer surface of the thermal envelope; see Figure 4.20. External walls are thicker than interior walls and occasionally are made of compressed polystyrene. Concrete blocks and clay bricks are found in two sizes; see Figure 4.21 (Almehrej, 2015).

Glazing areas have a clear impact on the indoor air temperature of buildings due to high solar radiation. The KSABC relies on U-values and solar heat gain coefficients (SHGC) to regulate windows, which limits the amount of solar gains from direct sunlight. The advantage of pre-determining glazing criteria is to set the level of solar reflectance and visual transparency. The code states that the window-to-wall ratio should not exceed 25% of the total exterior wall area for each air-conditioned space (Saudi Building Code, 2018).

4.3.5 Number of rooms and occupancy

The total number of rooms and bedrooms were specified in the most updated version of the governmental survey (GAS, 2019). It was categorised into three groups, which are one to three rooms occupying 14%, four to six rooms comprising the majority with 62% and seven rooms or more counting for 24%. Housing units usually have one to three bedrooms, four to six bedrooms and seven or more bedrooms, accounting for 77%, 21% and 2%, respectively. See Figure 4.22.

4.3.6 Housing energy

The KSA's government is responsible for delivering electrical energy through public networks to buildings, while a negligible number of buildings rely on private networks. Housing energy use in the KSA is the highest compared to other sectors. See Figure 4.23. Most of this energy is unfairly distributed and mainly used by three major regions: central, western and eastern. See Figure 4.24. Identifying all the systems used in the KSA's dwellings is essential because it improves statistical analyses to develop representative housing archetypes for

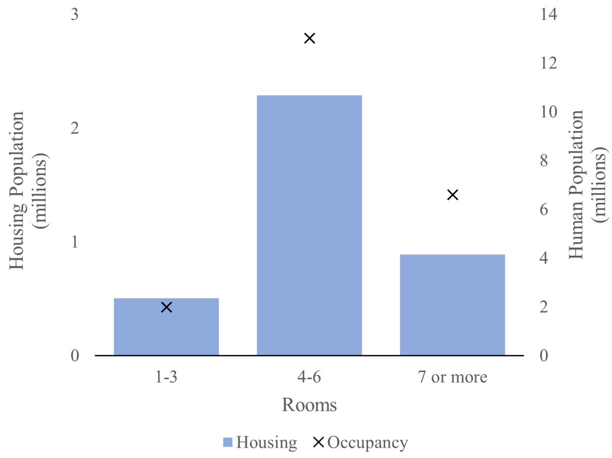

FIGURE 4.22: Number of rooms and occupancy (GAS, 2019).

energy modelling assessments. This excessive energy use is due to cooling, lighting and various housing machinery, including kitchen appliances.

The KSA is one of the largest consumers of AC units internationally due to cooling purposes. The most frequent types of AC units in dwellings are window AC and split systems, which account for 40% and 34%, respectively. The AC systems used are cheap due to their low energy-efficiency rates (EER). Figure 4.25 describes all the cooling equipment used and its hours of operation in KSA dwellings. Regardless of the type of AC unit, households usually operate cooling systems for more than 60% of the summer in all regions.

Lighting equipment is found in four types: regular, energy saving, fluorescent and side lamps. Most are regular lamps at 49%. See Figure 4.26. A fluorescent bulb is used for less time than regular lamps, and it may radiate less heat. This helps inform housing energy modelling assessors about which lighting system should be more realistic to represent the KSA's context.

Table 4.5 summarises the electrical equipment types and hours of operation of the KSA's dwellings. There is a minimum of 15 pieces of equipment in each dwelling, including TVs, washing machines and vacuums. The primary source for cooking fuel in dwellings is predominantly gas at 93%, compared to only 7% of dwellings that use electricity.

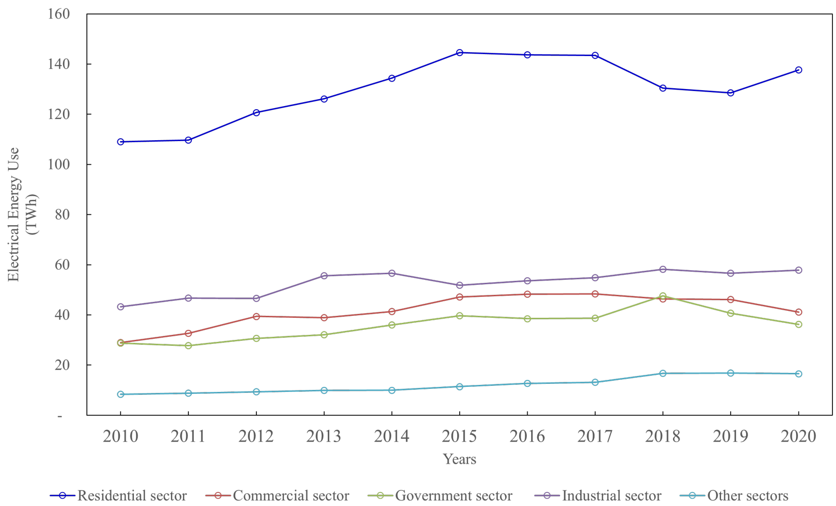

FIGURE 4.23: The KSA consumed energy by sector.

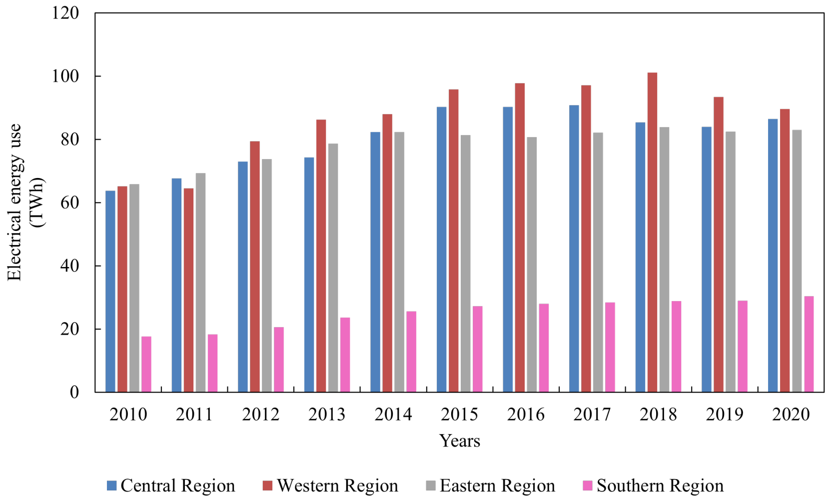

FIGURE 4.24: The KSA consumed energy by region.

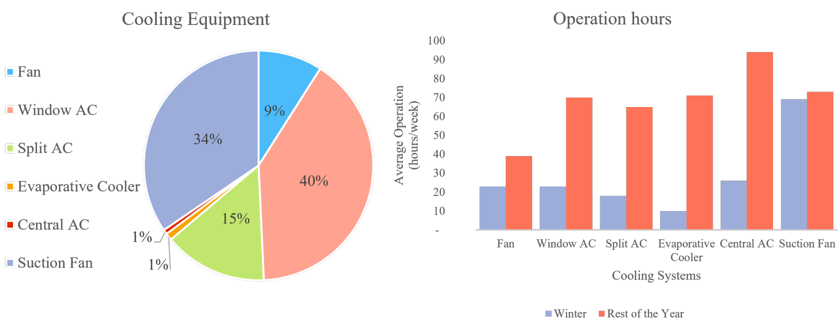

FIGURE 4.25: Cooling equipment and operation hours in the KSA (GAS, 2019).

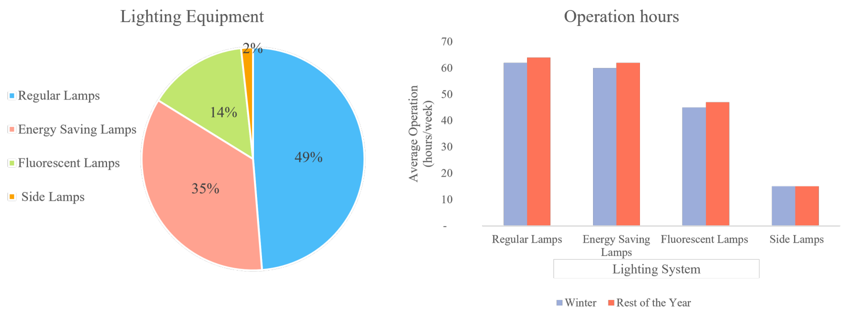

FIGURE 4.26: Lighting, equipment and operation hours in the KSA (GAS, 2019).

TABLE 4.5: Usage of electrical energy and average of operation hours in the KSA (GAS, 2019).

Variable	Aggregated Data Base		
Source	General Authority for Statistics (GAS, 2019)		
Sample	Full population		
Type	quantity	Winter operation (hours/week)	Rest of the year operation (hours/week)
TV	8.2	41	43
Washing Machine	5.7	7	8
Iron	4.7	5	5
Vacuum Cleaner	4.4	5	5
Dishwasher	0.2	9	9
Water Cooler	2.9	95	152
Water Bump (Dynamo)	3.7	11	12
PC	2.7	14	15
Gaming Devices	1.8	22	24
Other	9.3	17	18
Fridge	6.4	166	166
Freezer	2.6	166	166
Microwave	2.5	5	6
Electrical stove	1.2	1	12
Electrical heater	0.1	35	11

4.4 Representative housing archetypes

Modelling the energy performance of a given housing stock is less complicated and less expensive than real field studies and measurements. This is advantageous due to the ability to forecast potential stock exchanges. Modelling individual buildings is typically problematic due to the quantity and heterogeneity of a massive housing stock. Thus, they can be clustered by similar characteristics into representative buildings, called archetypes (Persily et al., 2006), which answers the first research question.

When a home is allocated to an archetype, its distinguishing attributes are replaced with representative values. This statistical representation of a national stock using a set of typical dwellings applies a robust method previously defined by Das et al. (2014). This enables a housing representation of the stock using generic inputs, including geometry, fabric, equipment and operation. This, however, raises uncertainty across the stock model and emphasises the significance of tracing information sources.

The extrapolation method is usually employed to assess the overall energy performance of a stock. Sousa et al. (2017) previously used this technique. When homes share common attributes, they may be assigned to clusters to make a dataset more comprehensible and to allow extrapolation about a stock of homes (Kavgic et al., 2010; Swan and Ugursal, 2009; Swan et al., 2008; Sousa et al., 2017; Yao and Steemers, 2005; Lee and Yao, 2013; Loga et al., 2016; Molina et al., 2020; Sousa et al., 2018). This defines a stock by employing relevant variables governed by the same rules and procedures.

4.4.1 Method

The KSA's housing stock can be categorised into archetypes using the same method as Persily et al. (2006), Mata et al. (2014), Shi et al. (2015) and Molina et al. (2020). The information provided in this chapter was classified into categorical (housing types) or discrete (flooring areas) and compared by common factors to generate a collection of archetypes. This selection of factors relied on the accessibility of the data and, most importantly, on their expected impact on buildings' energy demands. This increases the model's uncertainty; therefore, a Monte Carlo sampling technique was employed (Das et al., 2014). Figure 4.27 shows the methodology for developing the housing archetypes.

A key independent variable of relevance, which affects both energy demand calculations and mass transfer, is flooring area. Flooring areas were classified into five ranges. This variability changes the length and width of the building, which results in an overestimation or underestimation of the building's volumes. Building and ceiling heights are additional influential factors. The Saudi building code's minimum requirement for ceiling height is 3 m for occupied rooms, and the total residential building height should not exceed 12 m (Saudi Building Code, 2018). It is important for future censuses to identify housing areas and heights in dis-aggregated forms. The classification of different occupancy levels for different archetypes were not accounted in this archetypes generation because it is determined by the GAS to be an average family size of 5.4 person/house, regardless the housing type, due to lack of data. Additionally, the variation of occupancy, lighting and equipment use were not considered in this research stage because they are only found in identical values like the occupancy level of 5.4 persons/house or found in aggregated forms without specifying the exact lighting or equipment systems and not linked to housing types but to the overall region. This shows a clear data deficit and encourages future surveys to include these data to assess future research. Furthermore, no ventilation use have been found in the national censuses and infiltration rate is missing from all governmental sources, but the censuses briefly mention the HVAC systems in aggregated forms, and desegregation of such systems is not available to date.

The literature demonstrates that field or simulation studies often associate their outcomes with ventilation system types, air change rates, building location, construction year, location of contamination sources, occupants' activities, environmental variables, unit type, volume and geometry shape and size, building airtightness, thermal envelope configuration, orientation and the number of storeys (Jones et al., 2015; Shi et al., 2015; Persily et al., 2010; Molina et al., 2020; Krarti et al., 2020). Dominant factors in dwellings are determined to aggregate data inputs and divide them into clusters according to similar properties. Some values appear more

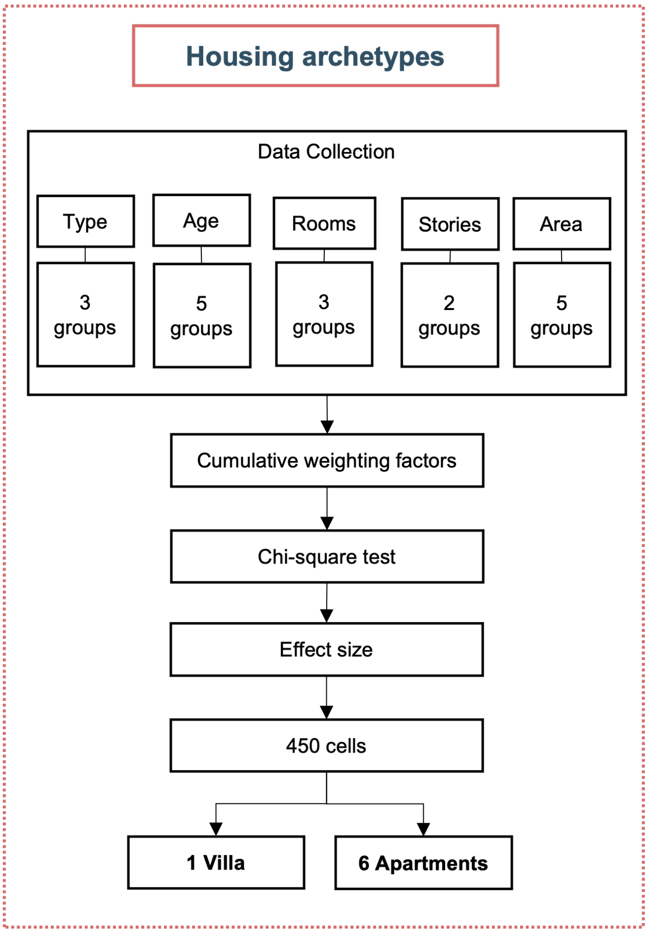

FIGURE 4.27: The housing archetypes method.

frequently, resulting in the development of bigger cells.

The quality and importance of the data was ranked according to source, and official government resources were prioritised. However, not all information is included in official censuses or only found in aggregated forms, such as building flooring areas. Thus, additional sources include the literature, the Ministry of Housing (2020) and the Saudi Building Code (2018). These data are derived from the most updated version of the KSA's census in 2019. See Section 4.1.1 of this chapter. The data was categorised to create the archetypes. The most significant data involve these housing types: villa (33%), apartment (44%), traditional house (19%) and vintage (less than five years (8%); five to 10 years (23%), 10–20 years (31%), 20–30 years (22%) and older than 30 years (16%); number of rooms, (1–3), (4–6) and (+7) rooms; number of storeys (1 and 2) and five groups of flooring areas, (0–100), (101–200), (201–300), (301–400) and (401–500) m^2. It resulted in groups of (3 (housing types) × 5 (vintage) × 3 (number of rooms) × 2 (number of storeys) × 5 (flooring areas)) and produced a fractional total number of 450 cells.

The 450 cells were utilised to include the variety of housing data: geometry, age, flooring area, number of rooms and number of storeys. The database was created and then aggregated by weighting each category according to the housing type and vintage. Increasing the number of cells eventually gets to a point where the sample size's growth becomes insignificant. As sample size increases, the heterogeneity of each sampling distribution diminishes, making the sample highly leptokurtic, meaning that the sample distribution is narrower than the population distribution. Leptokurtosis is a statistic that measures how much a distribution of probabilities is peaked or squeezed around its mean in comparison to the normal distribution. A high leptokurtosis distribution features a stronger peaks and tails that are heavier than a normal distribution.

The stock was then classified into housing archetypes using the 450 cells. See Figure 4.28. The total housing stock was weighted based on the proportion of homes in each combination cell. Even though the housing was classified, many archetypes require high-performance computers to simulate them. This is seen in Sousa et al. (2018), who simulated 1,000 archetypes. In addition, Mata et al. (2014) and Persily et al. (2006) simulated only a few hundred archetypes because it was more computationally efficient. Thus, the use of fewer archetypes might be more feasible when a loss of precision is recognised.

The represented archetypes' percentages of the stock and null hypothesis significance testing were employed to define groups of archetypes. The variations between the frequencies of the archetypes were used for comparisons by applying the chi-square (χ^2) test following Field et al. (2012) and Molina et al. (2020), see Equation 4.1. This procedure compares the whole dataset to identify statistically meaningful groups against the archetypes with less observed frequencies.

$$\chi^2 = \sum \frac{(obsereved_{ij} - model_{ij})^2}{model_{ij}} \tag{4.1}$$

The effect size, φ, utilised an estimation technique to measure the magnitude of effects between parameters. The effect size provides a more precise indication of the correlations between variables. It is often used for assessing the validity of a statistical assertion (Ferguson, 2016). The determined effect size indicator of less important groups for comparisons is provided by Kim (2017) and was more recently applied to the Chilean housing stock by Molina et al. (2020). The total number of observations is signified by n in Equation 4.2. The significance is then calculated using the Ferguson method (Ferguson, 2016), in which three effect boundaries are proposed: weak (≥0.2), medium (≥0.5) or strong (≥0.8). See Table 4.6. The weak effect size, ≥0.2, has no observed relevancy and, thus, is negligible.

$$\varphi = \sqrt{\frac{\chi^2}{n}} \tag{4.2}$$

The two most frequent housing archetypes with a 'strong' effect size represent 10% of the KSA's housing stock. They have been utilised for energy demand evaluation using the energy modelling tool known as EnergyPlus.

TABLE 4.6: Predicted housing archetypes effect sizes.

Effect Size Ferguson, 2016	Amount of Archetypes	Stock representation
Weak	18	21%
Medium	134	74%
Strong	192	85%

4.4.2 Results

This section highlights the results from the sampling technique described in Section 4.4 of this chapter. An evaluation of a multitude of housing with a systematic statistical method is applied to allow overall evaluations and extrapolation. This section summarises the results of the sampling technique by defining and describing the housing archetypes.

4.4.3 Selection of the archetypes

The number of housing archetypes required to evaluate a fraction of the KSA's housing stock and the associated effect size are presented in Figure 4.28. The first 18 archetypes show a weak effect size on the housing stock, which represents about 21% of the entire housing stock, while 134 archetypes show a medium effect size, representing 74% of the stock. Finally, 192 archetypes represent 85% of the stock, presenting a strong effect size.

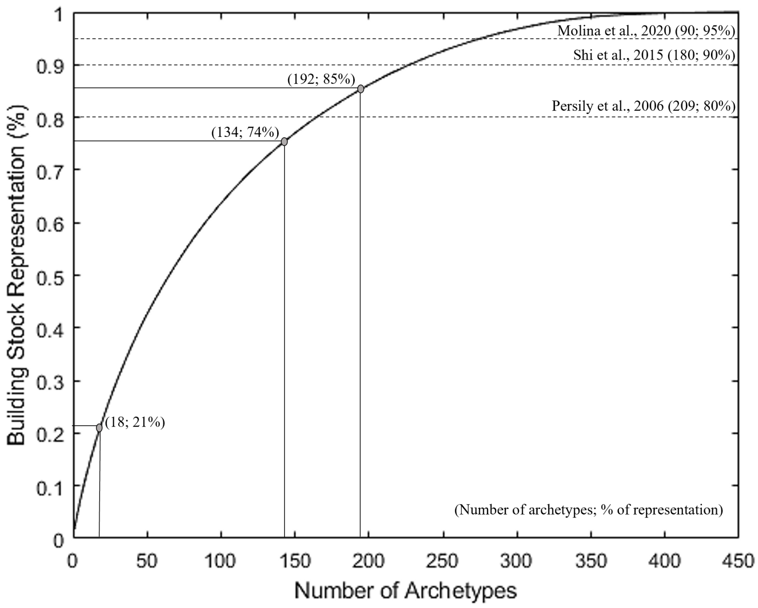

FIGURE 4.28: The housing archetypes representation for the KSA housing stock.

The χ^2 test was employed to assess the effect size variations between the most prevalent and each lower-classified archetype. The curve in Figure 4.28 depicts the fraction of the current housing stock and is not significantly increased when archetypes with lower weights are incorporated. Consequently, it may be used to select a suitable set of archetypes that corresponds to the stock's share with the computational resources available for the development and energy assessment of the archetypes. Table 4.7 displays critical variables in ascending order to represent the first 30 housing archetypes. The table reveals that villas and apartments are the most frequent housing archetypes with different construction periods.

4.4.4 Description of the archetypes

Throughout the dataset, the most common housing archetype is the apartment, and it is a single-block building consisting of six individual apartments, two for each floor and constructed by in-situ concrete. The villa archetype, however, is a detached single-family housing unit that usually consists of a larger living floor than in apartments and a second floor for sleeping purposes. The apartment archetype recently appeared in the last 10 to 30 years, while the villa archetype is a new building type from the last five to 10 years. The construction materials include clay

TABLE 4.7: Housing archetypes inputs of architectural variables for the first 30 housing archetypes.

Order	Statistical ID	Stock Representation (%)	Type	Construction (years)	Stories Nu.	Rooms Nu.	Flooring Area (m^2)	Houses Nu.	Weighting Factor	Cumulative weighting factor	Effect size
1	83	1.7	Apartment	10 - 20	1	2	3	62530	0.017	0.017	0.00
2	308	3.3	Apartment	10 - 20	2	2	3	56518	0.016	0.033	0.00
3	8	4.8	Apartment	10 - 20	1	2	3	51587	0.017	0.048	0.02
4	233	6.1	Apartment	10 - 20	2	2	3	46627	0.016	0.061	0.04
5	82	7.3	Apartment	5 - 10	1	2	3	46393	0.013	0.073	0.04
6	84	8.6	Apartment	20- 30	1	2	3	44376	0.012	0.086	0.05
7	307	9.7	Apartment	10 - 20	2	2	3	41933	0.012	0.097	0.06
8	98	10.9	Villa	5 - 10	1	2	3	41411	0.012	0.109	0.08
9	309	12.0	Apartment	20- 30	2	2	3	40109	0.011	0.120	0.09
10	7	13.1	Apartment	5 - 10	1	2	3	38275	0.013	0.131	0.11
11	323	14.1	Villa	5 - 10	2	2	3	37429	0.011	0.141	0.11
12	9	15.1	Apartment	20- 30	1	2	3	36610	0.012	0.151	0.13
13	158	16.1	Apartment	5 - 10	1	2	3	35955	0.017	0.161	0.14
14	232	17.1	Apartment	5 - 10	2	2	3	34594	0.012	0.171	0.15
15	23	18.1	Villa	10 - 20	1	2	3	34164	0.012	0.181	0.15
16	234	19.0	Apartment	20- 30	2	2	3	33090	0.007	0.190	0.18
17	383	19.9	Apartment	10 - 20	2	2	3	32498	0.011	0.199	0.18
18	85	20.8	Apartment	Older than 30	1	2	3	32274	0.006	0.208	0.19
19	248	21.6	Villa	10 - 20	2	2	3	30879	0.007	0.216	0.22
20	97	22.5	Villa	5 - 10	1	2	3	30724	0.006	0.225	0.22
21	88	23.3	Apartment	10 - 20	1	3	3	30187	0.006	0.233	0.23
22	99	24.2	Villa	20- 30	1	2	3	29388	0.006	0.242	0.23
23	310	25.0	Apartment	Older than 30	2	2	3	29170	0.005	0.250	0.25
24	322	25.7	Villa	5 - 10	2	2	3	27770	0.005	0.257	0.26
25	313	26.5	Apartment	10 - 20	2	3	3	27284	0.005	0.265	0.26
26	157	27.2	Apartment	5 - 10	1	2	3	26676	0.009	0.272	0.27
27	10	28.0	Apartment	Older than 30	1	2	3	26626	0.006	0.280	0.27
28	324	28.7	Villa	20- 30	2	2	3	26563	0.005	0.287	0.29
29	113	29.4	Villa	Older than 30	1	2	3	25703	0.005	0.294	0.30
30	159	30.2	Apartment	20- 30	1	2	3	25516	0.005	0.302	0.30

bricks or hollow concrete bricks applied to interior and exterior walls while ceramic is used for flooring. The archetypes consist of four to six rooms with a flooring area of 210 m^2 for each apartment and 525 m^2 for each villa.

Electrical energy sources are SEC for cooling or heating fuels and public networks for sewage and water. Gas is used for cooking fuel. The archetypes are predominantly found in the western, central and eastern regions. The apartment building is commonly rented (63%) by six families in each building block, while villas are mostly owned (67%) by one single family. There are 44% (1.6 million) and 37% (1.3 million) apartments and villas, respectively. Both archetypes have the same mean family size of 5.6 (person/unit).

Even though various architectural elements are distributed differently throughout the country and within archetypes, the archetypes have common characteristics, such as construction materials and electrical energy source. The variables were all based on the proportions of observations in each dwelling. The most sensitive variable in the dataset is the construction year and the flooring area of dwellings because it significantly increases the proportion of the building stock due to high variances.

4.4.5 The housing archetypes geometry

The representative housing archetypes generated from the sampling technique described in Section 4.4.2 of this chapter share similar characteristics involving construction materials and scheduling, as well as HVAC, lighting and equipment systems and occupancy. These common characteristics have been gathered as they possess typical housing features. Identical features include weather data by region or the U-values of envelope materials such as walls, while nonidentical features include building design, dimensions, window-to-wall ratio, heights and interior or exterior surface areas. Archetypal floor plans and zoning are summarised in Figures 4.29 and 4.30.

The first archetype is a detached two-storey villa occupied by a single family with a total height of 6 m. The ground floor includes the kitchen, the guest room, the dining room, the living room and a corridor, while the second floor involves three bedrooms and a lounge open to the second-floor corridor. All rooms are separate;

TABLE 4.8: Archetypes floor plans and zoning.

Space	Villa dimensions Depth × Width (m)	Area (m^2)	Flat dimensions Depth × Width (m)	Area (m^2)
Guestroom	8.7 × 6.7	58.2	6.1 × 6	36.6
Dining	6.5 × 6.5	42.9	4.1 × 5	20.5
Living-room	7.8 × 6	46.8	4.1 × 4.3	17.6
Kitchen	6.8 × 6	40.8	4.1 × 3.9	15.9
Corridor	-	32.3	-	53.4
Master Bedroom	8.7 × 8.8	76.5	4.4 × 4.1	18
Bedroom-2	7.8 × 6	46.8	4.2 × 4.4	18.4
Bedroom-3	6.8 × 6	40.8	-	-
Corridor/lounge	-	81.6	-	-
Total	17.5 × 15	525	10.5 × 25	262.5

thus, every room has its individual zone and two additional zones for two corridors on both floors. In contrast, the apartment building archetype is a detached building block including six apartments, two for each floor, with a height of 9 m. Every apartment includes three bedrooms, one guest room, a kitchen and a living room. All rooms are connected to the living room by doors, allowing all rooms to function as a single volume to which all other rooms are attached. The two apartments on each floor are separated by a corridor. Thus, every floor includes two zones for the two apartments and one zone for the corridor.

4.5 Discussion and limitation

4.5.1 Information sources

Representative archetypes are often employed in building energy performance research to evaluate buildings' energy demands because they are simpler and faster than physical measurements. The housing archetype dataset should be versatile and diversified to obtain representative housing archetypes that allow the total energy performance to be predicted and reflective of the actual conditions of the stock. The dataset, described in Chapter 4, is collected using sources involving national censuses conducted by the government, the literature, the building code and official organisations such as housing ministries or municipalities. The national censuses are usually large surveys and have a degree of uncertainty regardless of the sample size, precision and accuracy (Baker et al., 2016). This occurs due to the diversity of data collection techniques, instruments' utilisation and expertise, which limit

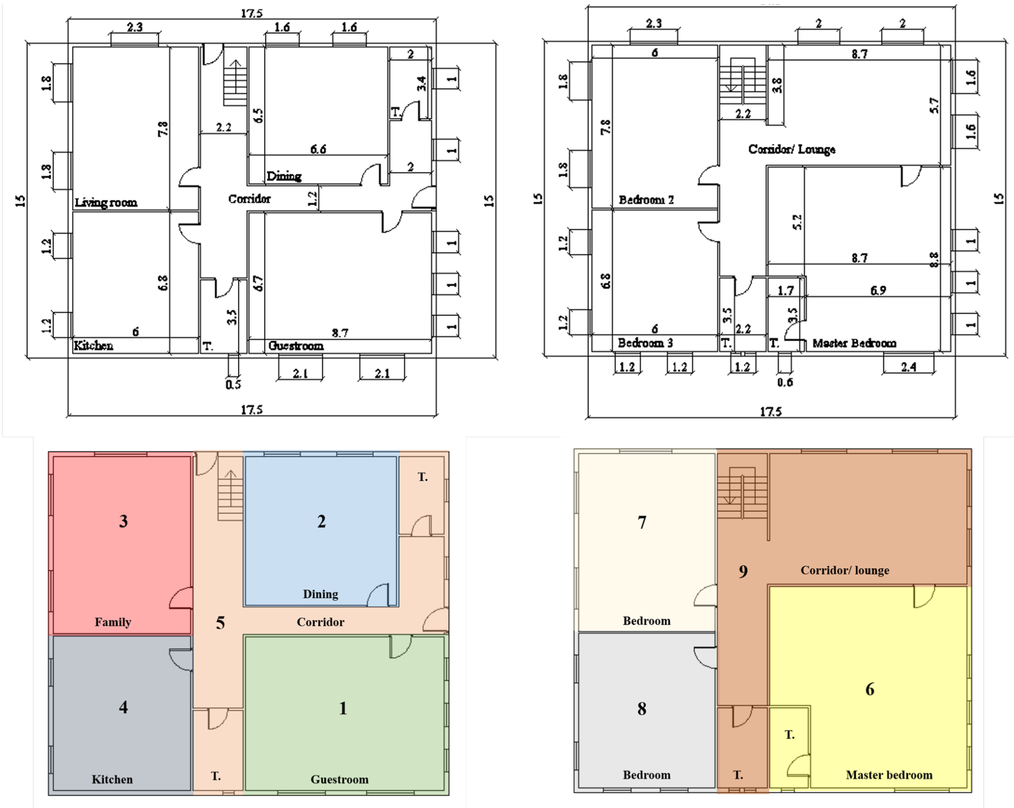

FIGURE 4.29: Typical floor plans (top) and zoning (bottom) of the villa archetype (Ahmad, 2004)

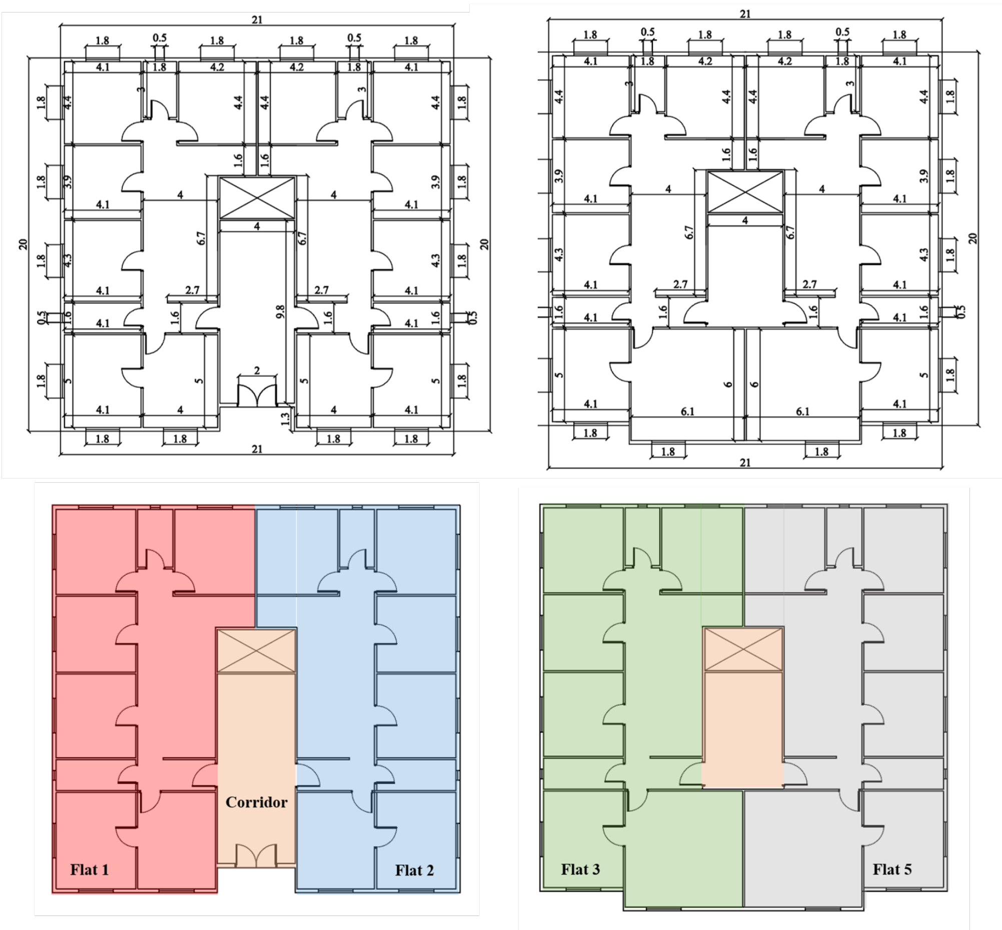

FIGURE 4.30: Typical floor plans (top) and zoning (bottom) of the apartment building archetype (Taleb and Sharples, 2011).

the usability of data. Large datasets often amplify uncertainty and may require sensitivity analyses.

The KSA's national censuses lack important factors useful for building energy modelling assessments. The housing dataset's description reveals detailed information on categorical and numerical data; categorical data include characteristics involving the residence year of construction, housing types, holding type and cooling and cooking energy sources, whilst physical characteristics are not available, such as residence volume, window-to-wall ratio and glazing type, infiltration rate, number of storeys and envelope thermal insulation and orientation. Additionally, occupancy patterns, IAT, thermostat setpoints, lighting and equipment power densities and scheduling are critical to housing energy performance and are not obtainable from governmental surveys.

The modelling process becomes a complex task when evaluating a massive housing stock since it requires a large dataset, and the accuracy of model outputs is contingent on these data being available. The housing archetype method is one of the more practical and convenient ways for modelling a stock because it captures data variability. The establishment of the KSA's housing stock energy archetypes should be a fundamental and basic energy model, such as the Cambridge Housing Model in the UK (Jones et al., 2015; Sousa et al., 2018) or the Chilean housing stock model (Molina et al., 2020). Moreover, official governmental organisations in the KSA hold unique information that is unavailable or inaccessible in the surveys. This includes housing geometry, the window-to-wall ratio, dimensions and flooring areas, orientation and cooling or heating setpoints. This encourages the use of alternative sources to collect important data that directly impact the energy model's prediction. For example, the IAT setpoint is not available in censuses. Therefore, it was provided from the building code requirements.

Further national surveying is required to collect important data related to different building assessment tasks involving energy demands, thermal comfort, IEQ and infiltration rate. This can be done by defining occupancy behaviour and activities, cooking and equipment scheduling, airflow rate and the concentration of indoor pollutants. This is essential for building a database which can be employed to distinguish the impact of building variables on the total housing stock's energy demands. This might be developed theoretically, but it would be more intriguing and realistically reflective if it were physically measured. However, this illustrates the importance of applying the bottom-up modelling approach to develop housing archetypes rather than following a physical measuring approach due to COVID-19, time and research expenses. This additionally shows the significance of this research by using the housing archetypes to assess and reduce energy demand, CO_2 emissions and cost of the KSA's housing stock. This meets this research aim. Nevertheless, modelling approaches occasionally raise the likelihood that data cannot be readily merged or integrated. Hence, this work becomes incomparable. This is seen in the flooring areas, described in Section 4.3.3 of Chapter 4 and in the infiltration rate model in Section 5.3 of Chapter 5. This allows the development of a large housing dataset for evaluation purposes. This data deficiency is problematic since it prohibits data comparisons with worldwide housing stocks, such as those of the UK and the USA.

4.5.2 Archetypes

This chapter identified the contemporary KSA's housing stock using archetypes. The archetypes' development process employed all accessible sources of descriptive data for dwellings. This was adopted to develop housing archetypes that represent 10% of the total housing stock of the KSA.

The housing archetypes become highly dependent on existing data and the variety of sources that characterise the KSA's dwellings and their inhabitants, and the data are of sufficient quality to infer meaningful and conclusive results. The precision of models' estimates is influenced by the quality of its input variables. Nonetheless, there are a few settings where the existing data may be substantially upgraded, extended or improved. There is an evident contradiction in the KSA's housing statistics, as they overlap or contrast, predominately due to the adoption of diverse data collection techniques. This indicates a clear opportunity for data integration or sharing among the surveyed institutions' estimates by cultivating a collaborative approach. This may also decrease estimation uncertainties.

The findings indicate that 450 archetypes may adequately describe the whole collection of the KSA's housing stock. The total amount of archetypes is proportional to the degree of precision offered by the dataset and the distinguishing features of the selected parameters. It is anticipated that the quantity of cells and, hence, the number of archetypes will vary proportionally when the major factors fluctuate or as the knowledge regarding them evolves. The classification of the stock may then be suitably selected according to the evaluation of its key attributes. This classification is then determined based on a thorough examination of its essential characteristics Because energy use was addressed throughout the determination process for this research, it is essential that these factors be included when other criteria are evaluated.

The level of this volatility is assessed by employing a stochastic technique because it was expected that some archetypal traits would exhibit variability and the effect of this variability would depend on the model being used. The findings may then be applied to the whole collection of archetypes; however, they cannot be applied to other sets until their input parameters and dispersion are comparable. The volatility of every factor is evaluated by varying them across known boundaries and performing simulations to obtain a range of results. This enables housing energy modelling assessments to reduce energy demands, CO_2 emissions and cost, which fulfils the aim of this research. This stage may require data extrapolation to reflect the total housing stock or to compare it with international housing archetypes such as the UK's or the USA's. The housing archetypes developed for the KSA are eventually utilised to assess the energy demands and airflow rates of the stock, but because the energy modelling tool used cannot properly predict the airflow rate, the DOMVENT3D_KSA model is applied. See Section 5.3.

4.5.3 Archetypes comparison

The representative archetypes developed in this research are suitable because they reveal the most parameters with highest variance among the archetypes, and this involves age and flooring area. This is important for capturing data variance and for accounting for alternative housing types or scenarios. The archetypes may be simply and quickly extended to evaluate additional environmental housing concerns including IEQ, occupants' thermal comfort, life cycle cost and economic analysis; nonetheless, this demands the inclusion of more diverse parameters relevant to the topic being discussed. The archetypes can estimate, for instance the KSA housing's indoor pollutants, but this requires additional data inputs involving the concentration of various pollutants or the use of CFD to estimate indoor pollution. Adding parameters to investigate other housing concerns, such as IEQ, increases the amount of archetype representation and associated effect size. In other words, the archetype representation may vary depending on the objective of the research and the variables included in the process.

In contrast, the three housing archetypes developed primarily by Krarti et al. (2020) to reflect the existing housing stock of the KSA only considered three main housing criteria throughout the archetype's generation process involving housing type, vintage and location. The archetypes included three housing types: villas, apartments and traditional houses. The archetypes' generation used the KSA's national censuses, GAS (2019) and the literature, including (Taleb and Sharples, 2011), (Alaidroos and Krarti, 2015), (Aldossary et al., 2014a) and (Algarni and Nutter, 2013a), to develop three archetypal housing models. The overall condition of the units was assumed by the buildings' age. The *new building* is typically built less than five years ago, with new building conditions, while the *recent building* ranged from five to 10 years old with a fair building condition, and the *old building* was built more than 10 years ago with poor building condition. Here, the housing archetypes comparison allows the results verification.

Although this is important for the KSA context to evaluate housing energy demands, the archetypes should be derived from a suitable and robust sampling approach. The location of the energy models' archetypes was also considered by Krarti et al. (2020), but the energy models do not comply with the building code (Saudi Building Code, 2018). In fact, most of the KSA's housing energy research does not apply thermal envelope insulation to energy model baselines or base cases. This may be understandable to reflect a proportion of the stock, but it is neither statistically nor evidentially accurate to state that all residential structures lack thermal insulation. Although the GAS indicates that 61% of the KSA's total buildings lacks thermal insulation, this estimate comprises residential, commercial and other building types. The remaining 39% is comparable, which depicts significant data insufficiency.

In addition, the supplied archetypes of this research included data on the number and types of rooms, bedrooms, storeys, flooring areas, the type and source of cooking, cooling and heating fuels and the water supply. The values of the systems' power densities will be calculated and detailed using the first-order approximation described in Section 5.2.9 of Chapter 5. The calculation will be performed for all housing systems employing real data provided by the GAS that accounted for cooking, equipment, lighting and energy loads. Nonetheless, Krarti et al. (2020) did not, and this may be due to the use of the PD values found in the literature or assumed, which does not capture the real systems characteristics.

4.6 Summary

This chapter highlighted the available data for the KSA housing energy demands using official governmental resources. This emphasised a clear data deficit in different areas including housing flooring areas, geometries, power densities, electricity bills, energy loads and others. Most of the data does not capture individual buildings' observations and leads to loss of detailed information because the data is not available or only accessible in aggregated forms.

The available KSA's housing data showed that the energy demands of housing sector is high and mostly consumed by the cooling systems. This resulted in massive carbon emissions. The housing characteristics of the KSA can be similar or varied, but the available data was used to apply a suitable statistical technique like clustering to categorise the housing stock and to define housing archetypes that can be able to represent a major proportion of the total housing stock. Employing two housing archetypes; one villa and six apartments in one building block can represent about 10% of the KSA housing stock.

Chapter 5

Methodology

Chapters 3 and 4 clarified the data requirements for evaluating the physics of buildings' energy performance using a simplified energy analysis model to rapidly estimate the energy use of the KSA's housing stock. This chapter addresses these needs for using the data to develop analytical housing energy models that explicitly include energy performance as part of their modelling methodology. In general, housing energy performance can be actually measured under controlled (Fisk and De Almeida, 1998; Karjalainen and Koistinen, 2007; Avci et al., 2013b) or uncontrolled (Wigo, 2008; Wigo, 2013) environmental conditions or modelled following the top-down (Edmonds et al., 1994; Wiesmann et al., 2011) or bottom-up (Edmonds et al., 1994; Krarti et al., 2020; Swan and Ugursal, 2009; Oladokun and Odesola, 2015), approaches for individual buildings (Alaidroos and Krarti, 2015; Algarni and Nutter, 2013a) or a proportion of a housing stock (Krarti et al., 2020).

Scientists have developed alternative procedures to conducting research by identifying three broad methods for answering researchers' questions: quantitative, qualitative and mixed. The qualitative method is associated with categorical data and a descriptive narrative for data analysis, whilst the quantitative method concerns numeric values and uses statistical methods to analyse data. The mixed method incorporates both (Soiferman, 2010; Creswell and Clark, 2017). This research methodology employs a deductive quantitative approach (Trochim and Donnelly, 2001), beginning with the broad and progressing and moving towards the specific. This technique is distinguished by its organised and systematic nature, since researchers strive to rigorously and objectively evaluate a certain hypothesis or theory. Deductive quantitative research results are often generalizable to a

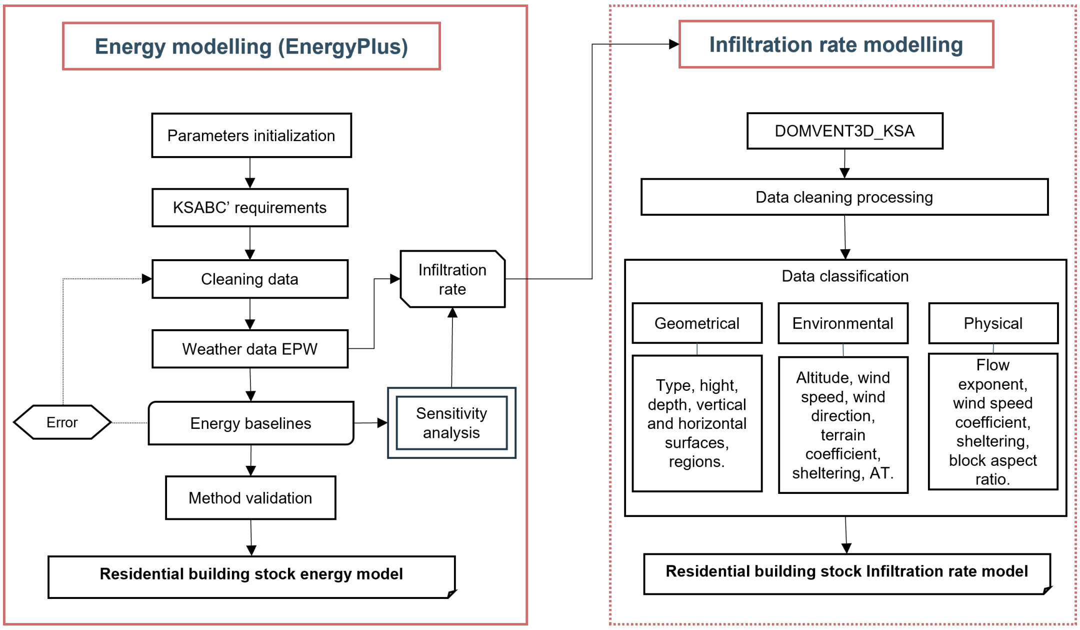

FIGURE 5.1: The methodology flowchart.

broader population, since the study is frequently conducted. This is used to describe a cause-and-effect relationship between two variables using mathematical, computational and statistical approaches.

The sampling technique described in Section 4.4 of chapter 4 developed a set of seven housing archetypes that represent 10% of the total housing stock of the KSA, which answers the first research question. These housing archetypes may be employed to develop housing energy model baselines for the energy assessment of the KSA's housing stock. Section 5.1 defines the energy modelling tool selected to analyse the internal environmental conditions and energy performance of the housing archetypes, hence answering the second research question. Section 5.2 develops housing archetypes' energy models based on the minimum requirements of the KSA's residential building code, answering the third research question. This evaluates archetypes' internal environmental conditions to estimate uncertainties and to define the most influential factors affecting energy performance. Section 5.3 establishes an infiltration rate model to assess the airflow of the KSA's housing stock, which thus answers the fourth research question. Figure 5.1 summarises the methodology chapter.

5.1 Energy modelling and analysis tool

Section 3.1.1 of Chapter 3 discussed building energy demand calculation approaches and classified them into steady state and dynamic. According to *Fundamentals of Engineering Thermodynamics* (2010), a wide range of building energy simulation tools and building regulations have been developed since the 1970s by adhering to theoretical models established in accordance with the First Law of Thermodynamics. The Energy Conservation Law argues that energy cannot be lost during the process of converting one form of energy to another and that energy must always be preserved (Moran et al., 2010). Consequently, the energy performance of the KSA's housing stock is assessed by applying the KSABC's minimum requirements to housing archetypes to identify the most influential factors and their sensitivity to overall energy demand to reduce it.

In this study, the dynamic approach was determined to predict the KSA's housing stock's energy demands over the steady-state approach because it is more suitable for reflecting energy flows and dynamics by varying building parameters. It involves additional variables that cannot be effectively and accurately presented by the steady-state approach, for example complex building system controls (Kim et al., 2013). This requires the use of a dynamic energy simulation tool such as EnergyPlus, described in 3.1.2.3, to predict the KSA's housing stock's energy demands. EnergyPlus is a popular energy building simulation tool used by engineers for modelling building heating, cooling, lighting, ventilating and other equipment. This requires detailed inputs to generate output files. EnergyPlus is often used to predict the energy use of buildings to lessen peak energy demands (Krarti et al., 2020; Krarti and Howarth, 2020; Alaidroos and Krarti, 2016; Aldubyan et al., 2021). EnergyPlus was selected among alternative simulation tools because it is white-box and transparent, with an engineering interface. This means that models are able to clearly describe how the energy performance is operating, how they produce predictions and what variables influence them (Fung et al., 2021). It is freely available, so the results can be replicated and compared to the housing stocks of other nations. The engineering interface makes EnergyPlus easier for engineers to enter building's data and parameters. Additionally, EnergyPlus presented lower standard deviation ranges and smaller data variation than previous approaches, resulting in more precise findings. Using EnergyPlus to evaluate the internal conditions and energy performance of the KSA's housing stock answers the second research question.

EnergyPlus was developed in 1996 by the United States (US) DOE Building Technologies Office (DoE, 2020). This is a new-generation building energy simulation tool formed from the integration of the greatest capabilities of two earlier modelling tools, known as Building Load Analysis and System Thermodynamics (BLAST) from the Department of Energy (Drury et al., 1999). It offers scalable self-sizing of certain parameters for every component in the system, such as cooling and heating capacities and supply air flow rate. This is helpful because it refines the accuracy of the outcomes and avoids sever errors. Self-sizing is frequently used to handle fluctuating server allocation. Numerous autonomic controllers must coexist to regulate the overall system using a self-sizing approach to solve diverse challenging tasks such as air-loops or water-loops, nodes and HVAC airflow volume to meet cooling or heating setpoints. However, coordination methods are required to avoid contradictory administrative selections (Gueye et al., 2014). All HVAC equipment can size itself within EnergyPlus, and every subsystem module contains a scaling procedure. When a module is executed for the first time in a simulation, it initially receives its user-specified input data before starting the sizing process. This function computes the necessary information and validates the auto-sizable mandatory fields for any incomplete information. This scaling subroutine employs a variety of high-level variables if necessary to size different HVAC components, including duct sizing for cooling, heating and other (DoE, 2020).

EnergyPlus can calculate the heating and cooling loads required to maintain thermostat setpoints, HVAC conditions and the energy use of major equipment defined by the user's description. See Figure 5.2. A variety of user descriptions or data inputs include building geometry, construction materials, usage, systems, scheduling, equipment power densities, occupancy, orientation, infiltration rate, ground temperature and location, all of which are required to perform simulations. It requires intensive data inputs to run the model with no server errors and, therefore, to gain the model's outputs. The outputs include the energy demands

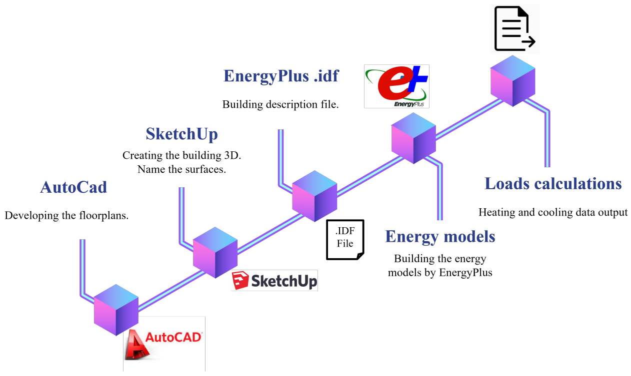

FIGURE 5.2: Summary of EnergyPlus simulation process.

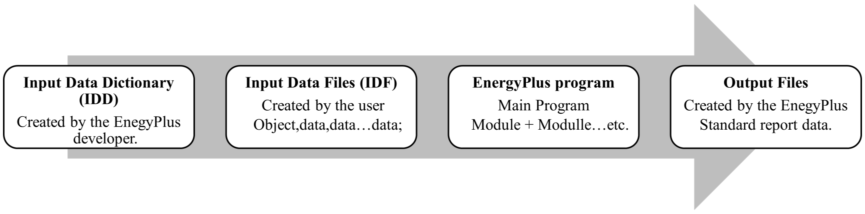

FIGURE 5.3: Summary of inputs and outputs of EnergyPlus modeling tool.

of the building with summarised or time-step variables. See Figure 5.3. EnergyPlus iteratively calculates the impact of any heat transfer time delay, and it employs the heat balance method. This method determines how much energy is needed to offset heat gains and loss at any temperature (McMullan, 2017). EnergyPlus uses four coupled heat transfer components: conduction via building components, convection to the air, absorption of short- and long-wave radiation and reflections (DoE, 2020; Spencer, 2010).

5.2 Energy performance modeling

The information supplied in chapters 3 and 4 is used to develop a collection of nationally representative archetypal dwellings for the KSA to be simulated using an engineering bottom-up approach and building physics models (Swan and Ugursal, 2009; Swan et al., 2008; Kavgic et al., 2010; Grandjean et al., 2012). Even though the engineering bottom-up approach is complex and requires more data input, it was adopted to model the energy performance of a stock over a top-down approach because it delivers individual dwellings' energy consumption at hourly time steps and allows an individual or regional energy performance evaluation.

The outcomes from the sampling technique shown in Section 4.4.2 of Chapter 4 demonstrate that an evaluation of 10% of the KSA's housing stock can be performed by defining the seven most frequent housing archetypes.

5.2.1 Energy model baselines

The energy baseline approach is commonly used because it is easier and less expensive than monitoring actual buildings (Swan and Ugursal, 2009; Swan et al., 2008; Kavgic et al., 2010; Grandjean et al., 2012). The baseline must be identified to assess the magnitudes of peak electricity demands of residences and their probable energy performance and CO_2 emissions. The expected new baseline is a metric of performance testing against which all uncertainties can be compared. It predicts energy use, estimates indoor conditions and forecasts future exchanges. It requires a variety of data inputs, which may be divided into geometrical, environmental and physical parameters. Geometric parameters include the shape of the building, dimensions, heights and orientation, while environmental parameters involve weather variations such as outdoor air temperature (OAT), humidity, wind speed and other physical parameters, including wind pressure coefficients.

The seven housing archetypes can be employed to develop seven energy model baselines using EnergyPlus to evaluate energy demands, CO_2 emissions and the cost of the KSA's housing stock. The energy baselines are constructed following a bottom-up engineering technique previously detailed in Section 3.1.4 of Chapter 3. The baselines employ the data described in Chapter 4, the results from the sampling method explained in Section4.4 of Chapter 4 and the building code. The level of detail in the available input data may vary significantly, which supports alternative modelling methods for maximising the use of current data. The baseline technique's advancement should eventually undergo a validation stage, demonstrating its energy behaviour is similar to real buildings, often through statistical regressions (Lee et al., 2016). The validation stage of this research method is described in Section 5.2.11 of this chapter.

In this thesis, seven representative housing archetypes represent 10% of the KSA's housing stock, shown in Section 4.4.2. This was determined to create energy baselines to quantify the energy demands of the KSA's housing stock. The archetypes include a separate villa and six apartments in one building block. The baselines were constructed according to the minimum requirements of the KSABC, and this allows code evaluations (Saudi Building Code, 2018). The archetypes are utilised as reference tools that enable energy performance comparisons before and after modifications to the baseline, against which improvements may be assessed. The baselines create a 'before' picture by collecting the overall energy usage of a building prior to making adjustments for evaluation purposes (Agency, 2018). Modelling housing archetypes using the EnergyPlus simulation tool require the setting of the environment according to the simulation's controls.

5.2.2 Simulation control

EnergyPlus requires setting up the environment for energy modelling by defining simulation parameters. One of the simulation parameters is the time step for heat transfer and load calculations. The *time step* is the time interval required for the equations to be solved for the building zone surface simulation and is measured per hour. It presents an identified point in time for calculating time zones. It assesses the simulation's run time and model predictions, and it can be reported hourly or sub-hourly. The time step default setting of 6 directs EnergyPlus to use a 10-minute zone time step. Its maximum and minimum values are zero and 60 seconds, respectively. Long time steps have more lags and require more dynamic responses because they are coupled with short output intervals that generate a large amount of data. This significantly impacts the simulation process since it slows it and may cause failure. The DoE (2020) recommends using a short time-step value of 4 seconds because it enhances the numerical solution of the Zone Heat Balance Model by coupling the surface temperature and zone air temperature to improve the model's overall predictions (DoE, 2020).

EnergyPlus requires the historic temperature data of a zone's surfaces to start the simulation process. EnergyPlus reports the first 24 hours of the environment according to the zone's data, temperature and loads. This reporting must undergo a convergence process. *Data convergence* is when the indoor conditions, temperatures and energy load values of each iteration are satisfied, meeting convergence tolerance.

There is a default maximum limit of 25 warm-up days to determine the minimum number of 'warmup' days until EnergyPlus verifies the convergence agreement to begin the simulation process. If the limit is exceeded, a severe warning message will display in the error file, which terminates the simulation. This emphasises an issue within the model. The structure might be oversized, or the building might be overcooling or overheating each day. *Warm-up convergence* defines the converging criteria for each run period. This convergence occurs when the lowest and greatest air temperatures throughout the warm-up day are almost identical between two successful iterations, marking periodic conditions. When stable periodic conditions are not met, simulation results may be incorrect. Thus, EnergyPlus runs the first few days until convergence tolerance is achieved or until the number of warm-up days is reached. This occurs before the actual simulation begins. Having too-loose tolerance convergence values would cause the energy code to be satisfied early, which leads to inaccurate predictions. Higher tolerance values may cause inaccurate data and systematic errors because convergence tolerance is applied to each step. If the tolerance is not tight enough, errors may accumulate over a series of iterations. This convergence process relies on four variables, maximum and minimum IAT°C and maximum heating and cooling loads (W). Once convergence is achieved, the actual simulation will start. These tolerance values should be left at the default. Loads, temperature convergence tolerance values and warm-up days were set according to the DoE (2020). The tolerance value for loads is a fraction of the total load, and it was set to 0.04, while the temperature convergence value was set to 0.4°C.

Full interior and exterior solar distribution was applied to quantify solar radiation with surface reflectiveness. This was determined to calculate the absorbed, reflected, transmitted and radiated heat to the zones and to account for the effect of exterior shading.

The baselines will be in the five most-populated regions of the KSA that have different weather variations. This is required to account for wind pressure, speed and direction. The surrounding terrain within the model was determined to be a city in all regions as determined by the GAS (2019). This is critical because it defines how wind would impact a building, which is usually defined by Bernoulli's equation if height remains constant and there are no pressure losses (Qin and Duan,

TABLE 5.1: Wind speed profile coefficients (ASHRAE, 2009).

Terrain Description	Exponent, α	Boundary Layer Thickness, $\delta(m)$
Open country	0.14	270
Rough, wooded country	0.22	370
Cities and towns	**0.33**	**460**
Ocean	0.10	210

2017), see Equation 5.2.2. However, EnergyPlus uses a Pressure Coefficient Method that determines the external pressure coefficients (C_p) to represent the relationship between the wind pressure and the static pressure outside the building.

$$p_w = C_p \rho \frac{V_{ref}^2}{2} \tag{5.1}$$

C_p varies because it is a function of the position on the building's envelope and the direction of the prevailing wind. The employed reference for local wind speed calculations is expressed by (V_{ref}), and the mean air density between indoors and outdoors is presented by $\bar{\rho}$ (kg/m^3). The equation for calculating local wind pressure and speed would have a different flow exponent value depending on the terrain of the location, thus influencing the model's prediction. See Table 5.1. The external wind speed in the weather data influences the model's energy parameters, which is presumed to have been recorded at a weather station in an empty field at a 10 m height. The local wind speed is predicted by accounting for terrain variances in the location and at the height of the building's surface. Equation 5.2 adjusts the wind speed from the reported meteorological wind speed data (Handbook, 2001).

$$U_\infty = V_{met} \left(\frac{\delta_{met}}{z_{met}} \right)^{a_{met}} \left(\frac{z}{\delta} \right)^{a} \tag{5.2}$$

Where z is the system's central height, z_{met} is the height of the reported typical climatic wind speed and a and δ are the coefficients of the terrain. Moreover, δ is the thickness of the boundary layer for the determined terrain type.

5.2.3 Weather data

The weather is a key data input with a basic text-based format. EnergyPlus uses formatted weather data known as EnergyPlus Weather (EPW) files, which are a simple text-based format known as comma separated values (CSV). These formatted weather data describe the environmental conditions of a particular site: location (name, state/province/region, country), information sources, latitude, longitude, time zone, altitude, peak heating and cooling design conditions, holidays, daylight savings period, typical and extreme periods, two comment lines and period covered by the data (Crawley et al., 2004). The EPW files have hourly weather data for certain regions involving the dry-bulb temperature, relative humidity (RH), wind speed, sky cover, atmospheric pressure, precipitation and others. The major source for these historic data is the US National Climatic Data Center (center, n.d.), which collects this information from actual meteorological stations from different countries. The US DOE created the EPW file format, which is used by simulation tools similar to ESP-r (*Energy Systems Research UNITESP-R, University of Strathclyde* n.d.), IES (*Building Energy Modeling with IESVE* n.d.) and TAS (Sawford, 2019). The US DOE presently possesses 2,590 weather datasets from around the world (DoE, 2020).

The EPW file is produced by cumulatively analysing a typical meteorological year (TMY) file that contains 20–30 years of hourly solar radiation and other meteorological variable records (Herrera et al., 2017). In this thesis, the EPW weather files were selected over other weather file types since they are derived from historical data and statistical analysis rather than a single year's hourly data (Maklad, 2014). It is created from a multi-year time series that was specifically designed to demonstrate the location's unique weather fluctuations while offering yearly means that are consistent with long-term patterns (Argiriou et al., 1999; Bulut, 2004; Bulut, 2003). Thus, five separate climate datasets in EPW format were obtained from the USDoE and applied to the associated five regions of the KSA (DoE, 2020). Even though the KSABC provides only three climatic zones for the KSA, five regions were determined in this study to capture weather variations. The orientation of the archetypes is an important factor, as it may affect energy use.

5.2.4 Orientation

The buildings' orientation describes the angle of the site plan relative to the North axis. The highest intensity of solar radiation falls on East- and West-facing walls in summer, while most of it falls on South-facing walls due to latitude. North-facing

TABLE 5.2: Meteorological data for the KSA locations (Algarni and Nutter, 2013a).

Region	Province	CDD (°C-days/year)	HDD (°C-days/year)	Annual mean global horizontal radiance	Mean OAT (°C) (Wh/m2)	KSABC
Middle	**Riyadh**	**5688**	**291**	**6352**	**26.4**	**Zone-1**
	Hail	4428	601	6253	23.9	Zone-2
	Qassim	5361	389	6154	26.3	Zone-2
East	**Dhahran**	**5953**	**142**	**5831**	**29.2**	**Zone-1**
	Al-Jouf	4128	859	6272	25.3	Zone-2
	Turaif	3395	1168	6107	24.8	Zone-3
West	**Makkah**	**7549**	**0**	**5946**	**34.2**	**Zone-1**
	Tabuk	**5359**	**571**	**6324**	**23.2**	**Zone-2**
	Madinah	6680	9	6188	32	Zone-1
South	**Abha**	**3132**	**486**	**5971**	**20.2**	**Zone-3**
	Jizan	7347	0	5586	33.1	Zone-1
	Najran	5605	12	6623	28.4	Zone-1
	Al-Bahah	5543	11	6180	29.8	Zone-2

walls receive the least amount of solar radiation; therefore, it is wise to plan for main facades to face the North (Wahl, 2017). This keeps the indoors relatively cooler during the summer while maintaining a large portion of natural light. The most solar radiation falls on the south-facing walls, and it can be used for heating purposes. The KSABC's orientation requirements encourage orienting the building towards the Northern axis to avoid unnecessary solar heat. Therefore, the baselines were oriented towards the North to minimise solar radiation's effects on rising energy use demands and other orientations were not considered. Accordingly, the physical properties of archetypes are required to evaluate energy performance (Saudi Building Code, 2018).

5.2.5 Baselines physical properties

The physical properties applied for archetypal energy baselines are stipulated according to the minimum requirements of the KSABC (Saudi Building Code, 2018). The minimum requirements are based on the climate zone and the surfaces of the envelope; therefore, envelope U-values may differ, from an exterior wall's surface to a roof. The KSABC classifies the climate into three zones with nonidentical envelope U-values. See Table 5.3.

The construction materials' names and types used for the envelope configuration must be specified in the materials object in EnergyPlus. EnergyPlus will connect every construction layer to its detailed material in the construction object. The materials object includes materials specifications, such as name, thermal

TABLE 5.3: KSABC U-values (W/m^2.K) requirements for residential buildings and the developed energy baselines.

Component	Walls	Roofs	Floors	Doors	Windows	Glazing SHGC
KSABC	0.34	0.27	0.47	2.83	2.66	0.25
Baselines	0.34	0.27	0.47	2.90	2.70	0.25

conductivity, thickness, density and specific heat, while the construction object details its layers in the order of the exterior to the interior surface of the envelope.

The building code does not demonstrate in detail materials' thicknesses, layers or insulation locations; however, it states the total exterior wall's U-values depending on the climatic zone and location. Thus, an analysis of the optimal exact location and layers of envelope thermal insulation was performed for the baselines. The main construction material of the exterior wall is concrete, and it consists of four layers, as follows: 10 mm plaster, 75 mm board thermal insulation, 200 mm medium-rough concrete block and 10 mm plaster finish. The baseline U-value of the exterior wall is 0.34 (W/m^2.K) in accordance with the KSABC. Figure 5.4 represents a section of the exterior wall, showing the layers, including their thicknesses and U-values. Notably, concrete is the most common construction material in the country, and it covers about 90% of all buildings due to harsh weather and the lack of wood (GAS, 2019).

Roof construction materials consist of five layers: 10 mm built-up roofing, 20 mm sand, 10 mm membrane, 100 mm medium-rough rigid thermal insulation and 150 mm lightweight concrete. According to the KSABC, the total roof U-value is 0.27 (W/m^2.K). The roof is 100% exposed to sun rays, and external shading is not required. Roofs receive the most solar radiation, which may be highly effective for models' predictions.

The KSABC's minimum U-value requirement for ground floors is 0.47 (W/m^2.K), which was applied to the baseline. It consists of a 10 mm smooth carpet, 200 mm slab on grade and 55 mm medium-rough insulation board, as shown in Figure 5.4. This building's ground floor is attached to the site's ground and features a thermally insulated outer surface with a carpeted inner surface. The interior floor separating levels is not insulated because it is not required by building regulations.

Window glazing has a clear impact on the IAT of buildings in the KSA due to the high solar radiation. To define and regulate window performance, the KSABC prescribes a U-value and a solar heat gain coefficient (SHGC). The SHGC is a

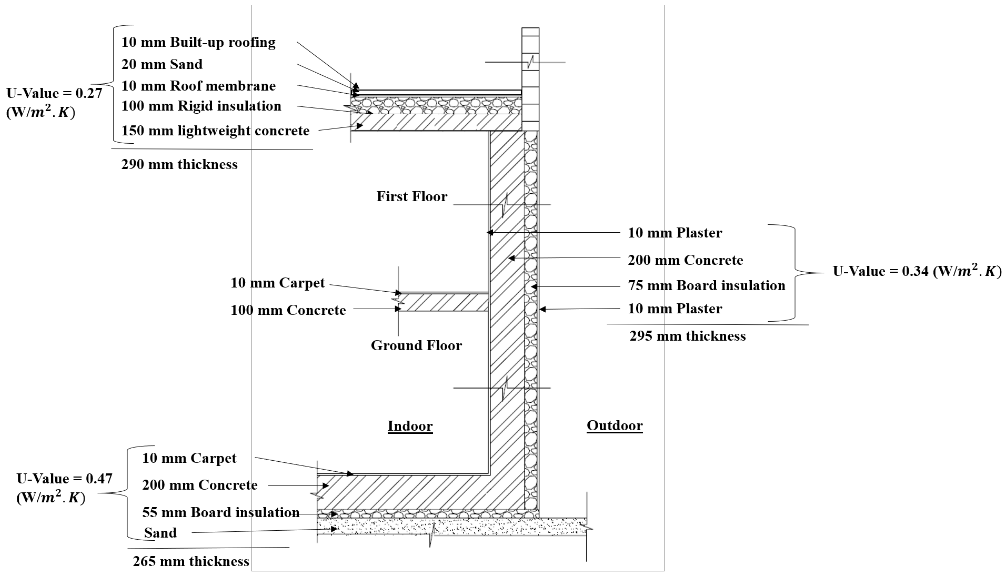

FIGURE 5.4: Construction materials' layers of the housing archetypes

fraction of how much solar energy can pass through a window. It defines how a window responds to sunlight and solar heat, which is often affected by the climate and position (*Solar heat-gain coefficient ratings for Windows* n.d.). This SHGC rating is a metric for measuring the window's energy efficiency and is often required by building codes. The KSABC's minimum requirement is aluminium-frame double-pane windows with a total U-Value of 2.67 (W/m^2.K) and glazing SHGC of 0.25 for all locations. The code also states that the WWR should not exceed 25% of the total exterior surface area for each air-conditioned space. In this study, the WWR is 13% for the villa and 15% for the flats, which complies with the building code. The building code does not mention critical factors, such as ground temperature, and this requires the use of sensitivity analysis to determine the changes in the results.

5.2.6 Sensitivity analysis

The sensitivity analysis (SA) of modelling approaches can be used to mitigate risks by identifying the most critical exposures or risk factors. Baker et al. (1999) identified SA as one of the key quantitative approaches used in risk management. Moreover, Jones (2000) mentioned that SA may be used to build climate change adoption strategies because it can identify the most crucial uncertainties in a model, which allows further investigation (Cullen et al., 1999). Additionally, SA may be used to verify and validate a model while the model is being built and refined

(Kleijnen, 1995; Kleijnen and Helton, 1999; Kleijnen and Sargent, 2000; Fraedrich and Goldberg, 2000; Phillips et al., 2000; Ward and Carpenter, 1996). It is possible to perform a SA for decision-making purposes, as it can help in understanding how robust the model's results are (Limat et al., 2000; Christopher Frey and Patil, 2002).

According to Christopher Frey and Patil (2002), SA techniques have been widely utilised in research areas such as difficult engineering systems, economics, physics, the social sciences and medical decision making. They classified SA into three alternative approaches: mathematical, statistical and graphical. In this thesis, the mathematical SA was utilised to evaluate the sensitivity of a model's outputs to a range of input values following the method mentioned by Brun et al. (2001). The statistical SA was separately applied, in which data variables are assigned probability distributions and the influence of variations in inputs on the outcome distribution are measured by changing one or more input at a time, using the method suggested by Andersson et al. (2000). Finally, the graphical SA is applied because it provides a data representation of its sensitivity in visual graphics or charts, adopting the approach employed by Geldermann and Rentz (2001). Furthermore, a regression analysis was applied at different stages of this research because it describes the relationship between two variables, controls the predictor variables for a particular response parameter value and predicts responses via predictor variability. SA may be performed for different factors, such as ground temperature or infiltration rate, to investigate their influence on energy performance.

5.2.6.1 Ground temperature

The EnergyPlus zone model is based on an hourly time scale, whereas ground heat transfer is based on a monthly time scale. An ability to connect ground heat transfer estimates to the model is required. Due to a shortage of GT data and studies globally, nominal range sensitivity (NRS) was applied, as explained by Christopher Frey and Patil (2002). The NRS is a basic approach that can be easily implemented, though it cannot show changes is all inputs together. The NRS is adopted in this research by applying a selection of a random range of GT values to the energy baseline models – 13, 18, 23 and 28 °C – to explore their sensitivity. This is a primary modelling phase to evaluate the variability of GT and its effects on indoor air conditions.

The reason for this absence of GT requirements for energy simulation studies in the KSA is that most studies do not mention GT or its values, such as Alrashed and Asif (2012) and Taleb and Sharples (2011). A noticeable number of studies utilise EnergyPlus to simulate energy for the KSA's housing (Alaidroos and Krarti, 2016; Krarti et al., 2020; Al-Homoud and Krarti, 2021; Aldubyan et al., 2021; Alaidroos and Krarti, 2015). However, EnergyPlus must include GT to simulate the energy model. If GT is not specified, EnergyPlus assumes it to be 18 °C for the entire year (DoE, 2020), and this may have a significant impact on energy predictions.

EnergyPlus handles GT for different calculation methods: the slab processor, object the Site: Ground Domain and slab on grade. The slab processor is another tool that is integrated with EnergyPlus; it calculates the slab temperature with a numeric method that requires EPW weather data, the features of the building and its soil and various operational conditions of the tool such as surrounding terrain. In the Site: Ground Domain method, different floor levels with different thermal zones are in contact with the ground. It calculates slab temperature by adopting implicit formulations to provide undistributed GTs. Studies of residential buildings recommend the use of a monthly mean OAT for GT, such as Papst et al. (1999) and Lima (2007), as auto cited in Costa et al. (2017). However, the original sources of the studies are only found in the Portuguese language and are not recent. Finally, in the slab-on-grade method, GT can be directly inputted into the ground temperature's building surface object in the energy model. It calculates the heat exchange between the building's floor, which relates to the site's ground. This method is suggested by different studies, including the Manual Auxiliary Programmes in EnergyPlus Documentation, which suggest a temperature of 2 °C less than the mean IAT for artificially air-conditioned commercial buildings.

The Auxiliary Programme does not suggest using the GT from the weather data, as it is undisturbed. These values are far too high for the soil beneath an air-conditioned structure. Conversely, it suggests the use of normally disturbed GTs to make the simulation robust by preventing the parameter from returning negative values. Therefore, distributed monthly mean IATs minus 2 were given to the GT that are inputted directly into the baseline energy model depending on the location to check their sensitivity (DoE, 2020). This SA conveys how important GT is for the energy model's evaluations. In addition, the NRS is a useful technique for testing the sensitivity of infiltration rates.

5.2.6.2 Infiltration rate

The infiltration rate of a dwelling directly affects cooling and heating loads due to the uncontrolled airflow through gaps and cracks within the building's thermal envelope (Sherman, 1980; Sherman, 1980; Sherman and Sherman, 1986). Common sources of infiltration are usually caused by opening and shutting outside doors, gaps surrounding windows and even small cracks in building materials. The infiltration quantity is translated from air changes per hour (ACH) and integrated into the zone's air heat balance using the external temperature at a specific simulation time step (DoE, 2020). EnergyPlus uses Equation 5.3 to determine the design infiltration rate (I_design), schedule fraction ($F\_schedule$), temperature difference between the thermal zone and external air (ΔT) and wind speed. The equation involves four default coefficients, A, B, C and D, to account for the effect of micro-climate environmental variations, including temperature and wind speed, through each simulation time step. These defaults were determined by the infiltration rate relationship evaluation provided by the ASHRAE Handbook of Fundamentals (ASHRAE, 2010).

$$Infiltration = (I_{design})(F_{scheduling})[A + B|(T_{zone} - T_{odb})| + C(WindSpeed) + D(Windspeed^2)] \tag{5.3}$$

Modelling the infiltration rate in EnergyPlus requires two types of data. First, the design infiltration rate (I_design) is described as the volume flow rate for every internally air-conditioned zone. This requires an infiltration schedule ($F\_schedule$) that is defined to reflect infiltration rates' variability according to time. Second, infiltration model coefficients are utilised to predict thermal loads according to three factors: the airflow rate, the temperature and the wind speed. The standard infiltration prediction method in EnergyPlus applies default coefficient values of 1, 0, 0 and 0 for calculating a constant airflow volume in all conditions. This is not sufficient because it does not consider weather variations such as temperature, wind speed and the pressure difference across the thermal envelope.

Additionally, EnergyPlus provides two common infiltration models usually utilised for modelling building infiltration: the DOE-2 and BLAST models. The DOE-2 and BLAST infiltration techniques employ reference wind speed values of 10 and 7.5 mph, respectively. Yet, this is done without ΔT across the thermal envelope. Yielding these conditions for both models makes the infiltration rate equal to (I_design). The DOE-2 and BLAST models consider weather variations and have different coefficient values.

However, the typical values for the coefficients are a subject of controversy. Ideally, a full study of the infiltration condition should be performed first, followed by the determination of a customised set of coefficients using methods such as those described in Chapter 26 of the ASHRAE Handbook of Fundamentals (ASHRAE, 2010). In addition, EnergyPlus is a tool for dynamic thermal modelling, not a computational fluid dynamics (CFD) tool for investigating airflow in buildings. This reveals the need for modelling the airflow rate of the KSA's housing stock utilising an alternative approach. See Section 5.3 of this chapter.

The design flow rate calculation of EnergyPlus can be performed using five methods: flow per zone, flow per area, flow per exterior area, flow per exterior wall area and air change per hour. In this thesis, the design flow rate was predicted following the air change per hour method. This method uses the total amount of air change per hour to represent the infiltration quantity. However, the infiltration rate has never been measured in the KSA's housing, and researchers have assumed 0.8 ACH is a sufficient value for all housing types (Krarti et al., 2020; Alaidroos and Krarti, 2016; Aldalbahi, 2020), whereas the KSABC requires an airtightness value of 4 ACH at 50 Pa for residential buildings (Saudi Building Code, 2018). According to Jones et al. (2016), Sherman (1987), and Persily (1982), the dimensionless ratio constant (N) in equation 5.4 may be assumed to be 20 and should vary according to environmental parameters. Dividing the air change rate (n_{50}) (h^{-1}) recorded during a pressurisation test by 20 yields the air infiltration rate (n_I) (h^{-1}) under normal conditions. See Equation 5.5; this is known as the divide-by-20 rule of thumb (Pasos et al., 2019).

$$n_{50}/n_I = N \tag{5.4}$$

$$n_{50}/20 = N_I \tag{5.5}$$

Currently, the infiltration rate of the KSA's housings is in conflict. It could be 0.8 or 0.2 ACH, but by performing a sensitivity analysis, one can see that such an assumption can lead to great uncertainty. Thus, an NRS analysis is preferred to understand infiltration rates for the KSA's housing (Østergård et al., 2016), and this would clarify how important the infiltration rate is to energy loads (Saltelli and Annoni, 2010). A random range of infiltration rates (0, 1, 2, 3, 4, 5, 6, 7 and 8 (h^{-1})) has been input into the baseline model to capture the impact of varying infiltration rates on energy loads.

5.2.7 Ideal load air system

The building energy performance calculation in EnergyPlus can be analysed using the Ideal Load Air System (ILAS). The ILAS can run with infinite capacity or schedules to meet space energy loads. The ideal system is typically utilised for evaluating the energy performance of a building without designing a full HVAC system package for simplicity. The user does not need to specify air loops, water loops and other mechanical components; it only requires zone controls, equipment and thermal loads. The system's predictions consider variables involving the maximum or minimum zone supply air temperature and humidity ratio. It sufficiently supplies heating or cooling loads to the zones without overheating or cooling, and it can be set up to meet cooling or heating setpoints. In this model, the system capacity was determined to keep the zone thermally comfortable at a constant 20 °C, as required by the KSABC (Saudi Building Code, 2018).

The ILAS object is modelled to represent an ideal variable air volume terminal unit with the capability of supplying temperature and humidity. The supply airflow rate is adjusted between zero and the maximum to accommodate the zone's required energy, humidity controls, outside air requirement and other stated constraints. The ILAS inputs include naming and linking the inlet node, outlet node, exhaust node and a plenum, if applicable, for each zone. Wang and Song (2012) and the Auxiliary Programme of EnergyPlus (DoE, 2020) suggest using a maximum cooling supply air temperature of 50 °C, a minimum heating supply air temperature of 13 °C, a maximum heating supply air humidity ratio of 0.0156 (kg water/kg dry air) corresponding to 42% RH and a minimum cooling supply air humidity ratio of 0.0077 (kg water/kg dry air) corresponding to 10 °C of the dew point that is the temperature at which air becomes saturated with water vapour, forming condensation. The heating and cooling capacity (W) of this system can be set to its limits or to infinite. A constant sensible heat ratio (CSHR) indicates that the system will be adjusted to match the sensible cooling load, while the latent cooling rate will be calculated using the CSHR, as explained by Equation 5.6. The supplied air mass flow rate must meet cooling or heating loads utilising Equation 5.7. The sensible heat recovery effectiveness is 'the change in supply temperature divided by the difference in entering supply and relief air temperatures', while the latent heat recovery effectiveness is 'the change in supply humidity ratio divided by the difference in entering supply and relief air humidity ratios'. As recommended by the DOE, sensible and latent energy were left at the default values of 0.70 and 0.65, respectively.

$$SHR = Sensible\,cooling \div Total\,cooling\,(sensible + latent) \tag{5.6}$$

$$Q_{sys} = m_{sys} C_p (T_{sub} - T_z) \tag{5.7}$$

Where Q_{sys} represents the system energy delivered to the zone, m_{sys} (kg/s) presents the supply air mass flow rate, C_p stands for zone air-specific heat, T_{sub} is the supply air temperature and T_z is the desired air temperature. All systems in the baselines can have individual operational schedules or be integrated.

This ideal system has a few limitations as it is not able to specify system-level control by assuming instantaneous and perfect control over temperature and humidity. This is done without considering the HVAC system real abilities to interact with the indoor space. The ideal system sometimes oversimplifies the air distribution and does not consider the detailed data inputs of the system, but it is acknowledged and used by researchers for modeling simplifications.

5.2.8 Scheduling

Scheduling consists of a set of objects that enable users to regulate the schedules of a wide range of variables, such as occupancy, lighting, thermostatic controls and occupancy activity. Schedules frequently refer to the profile components (PC) object in EnergyPlus to describe how an operation will run and for how long. The PC is often employed to distinguish a quantity's variability over a day.

Schedules are used to individually control systems such as lighting, equipment or HVAC using specified values, from 0 (no operation) to 1 (full operation). It includes day, month or year descriptions, and each sub-level of information depends on prior levels. The day description involves the name assigned to a range of 24 hours, and each day is defined by a name, a holiday, a summer and a winter design day and two additional adjustable days (DoE, 2020).

The values for scheduling were not conducted through actual interviews and surveys similar to the primary data; instead, they were collected from previous research, as were the secondary data. Due to COVID-19 restrictions, time and cost, the author defined seven housing energy modelling studies, from 1989 to 2020, that include lighting, equipment and occupancy schedules (Ahmad, 2004; SAID and Abdelrahman, 1989; Maziad, 1999; Ahmed, 1991; Al-Saadi and Budaiwi, 2007; Alaidroos and Krarti, 2015; Krarti et al., 2020). All scheduling numeric values were combined to generate an approximate representation of the data distribution. Figure 5.4 divides the frequencies into weekdays and weekends. It illustrates that only the lighting scheduling has identical values, with a mean value of 40% of operation per day. This is because most of the studies utilised one lighting schedule for weekdays and weekends. The most frequent scheduling values were determined to be applied in the baselines based on the type, name and associated system. This scheduling technique indicates only systems' operation times; however, it requires more data analysis to include systems' power density for lighting and equipment. This stresses the importance of employing the first-order approximation approach.

Although this scheduling was assumed based on previous studies and applied to all the housing archetypes, it may not be able to realistically represent the actual occupants' behavior. This scheduling technique has limitations as it fails to reflect

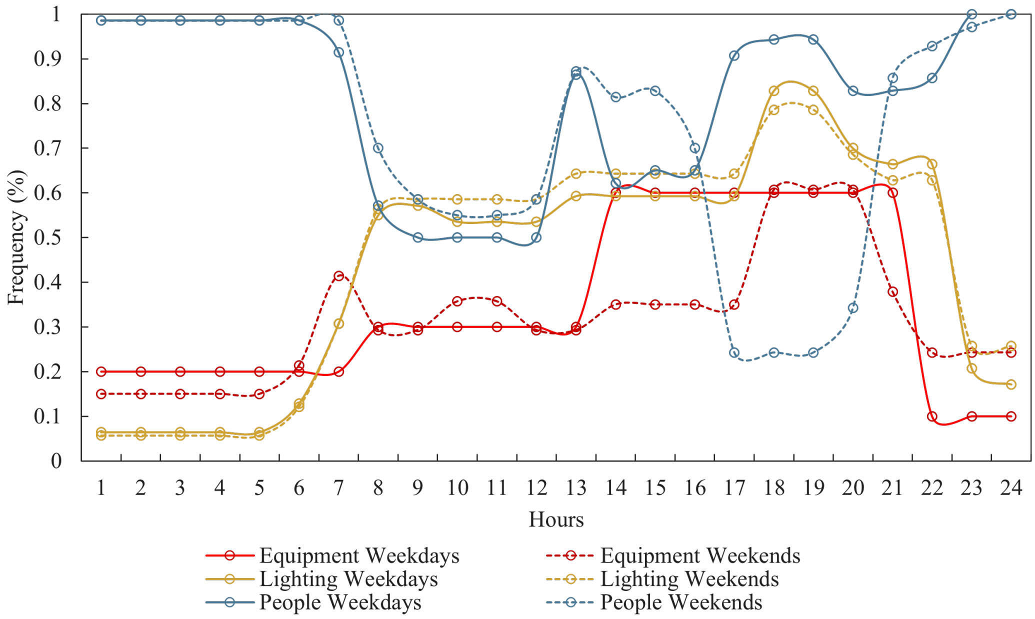

FIGURE 5.5: Scheduling frequencies of lighting, equipment and occupancy.

all event attributes and cannot accommodate for intricate timing flexibility and constraints because it assumes that events occur at fixed frequencies at precisely defined intervals and cannot involve additional modifications unless they are specified.

5.2.9 First order approximation

When investigating numerical calculations, several heuristic techniques can be used to generate an approximated answer. This approximated answer can be refined to a result. The fundamental reason for this approach is to estimate a model with stochastic parameters (Wu and Shen, 1999). Starting with an initial estimate of the answer, one can develop an algorithm that converges more quickly on the true value. Scientists refer to a first-order approximation to simplify assumptions when a number is required. It only applies if one number is precisely and accurately stated. In quantitative research such as engineering, the order of approximation refers to formal or informal phrases expressing how precise an approximation is (Wu and Shen, 1999).

The energy baselines of this study require a first-order approximation of an energy-efficiency evaluation, although additional accuracy improvements are feasible. The research uses a basic paradigm in which technology, lighting systems and kitchen equipment are separated into possible expansions. This approximation can be utilised separately to represent the power density of lighting and equipment.

5.2.9.1 Power density

The values of lighting power density (LPD) and equipment power density (EPD) vary among studies, with a mean of 11.4 and 9.8 (W/m^2), respectively. Figure 5.6 presents a negative relationship of the PD over the years, and this is due to electrical systems' improvements to become more efficient. A recent study of Saudi housing energy modelling applied an LPD and an EPD of 4 and 3.5 (W/m^2), respectively (Krarti et al., 2020). Nevertheless, the values are not representative because they were derived through assumptions, not through a detailed analysis. It is extremely important for analyses to centre on reliable sources of data. Thus, the author employed the most up-to-date housing and energy surveys in the country to analyse internal gains (GAS, 2019). See Table 5.4.

5.2.9.2 Lighting and equipment

The most-used lighting and equipment systems in the KSA's dwellings were specified in the Saudi housing and energy censuses in 2019 (GAS, 2019). The censuses included the quantity of each lighting and equipment type with average operation hours. However, the data were only aggregated. Figure 5.7 summarises the system in the KSA's dwellings.

TABLE 5.4: The utilised amount of systems in the KSA homes (data from (GAS, 2019)).

Type	Total Amounts (million)	Average number by home
Home	3,681,927	-
Equipment	43,486,748	11.81
Lighting	248,549,376	67.51
Cooking Appliances	13,206,525	3.59

The collected data must be disaggregated by system type and home to attain representative values. The mean amounts of lightbulbs, equipment and kitchen appliances per single dwelling were calculated separately by employing equation

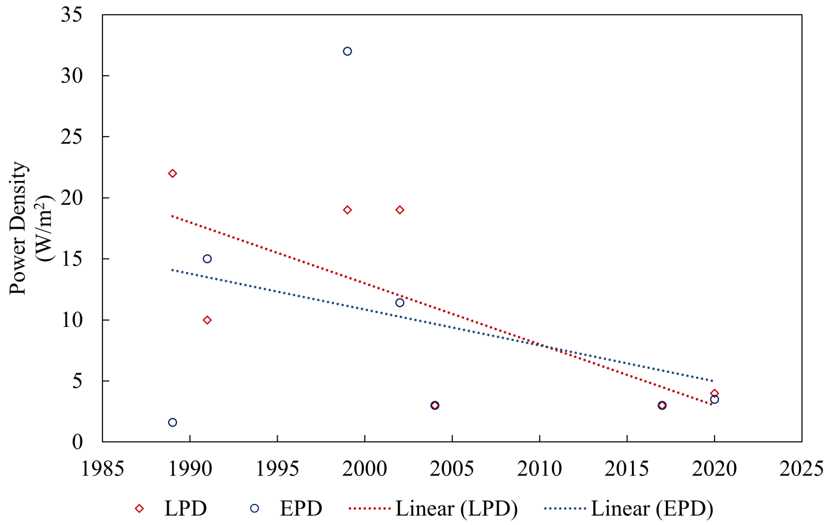

FIGURE 5.6: LPD and EPD from the KSA housing energy modeling in the KSA.

5.8 for each system type. The equation resulted in 68 lightbulbs, 11 equipment types and five kitchen appliances per house. The values are sufficient for lighting homes and involve the needed equipment.

$$f(\bar{x})_{(system\ type\ per\ house)} = \sum_{S=i}^{S=\infty} (system\ amount) \div \sum_{H=i}^{H=\infty} (Housing\ amount) \tag{5.8}$$

Where S represents the number of lightbulbs or equipment, and H stands for the total number of housing units.

Determining the utilised types and numbers of lightbulbs, equipment and kitchen systems is critical due to the variability of radiated internal heat from each system. The systems used in the KSA and their associated internal heat gains have been individually calculated for each type, utilising Equations 5.9 and 5.10. Equation 5.11 was finally employed to gain the system PD per square meter (McMullan, 2017). This was done to quantify how much internal heat can be added to the space per year from each system. For example, using only a regular lamp-type bulb contributes to 22,338 (kWh/year) of internal heat gain. This is five times higher than using energy-saving lamps, which only contribute 3,971 (kWh/year) of internally radiated heat.

Consequently, the author of this research individually calculated the PD for each

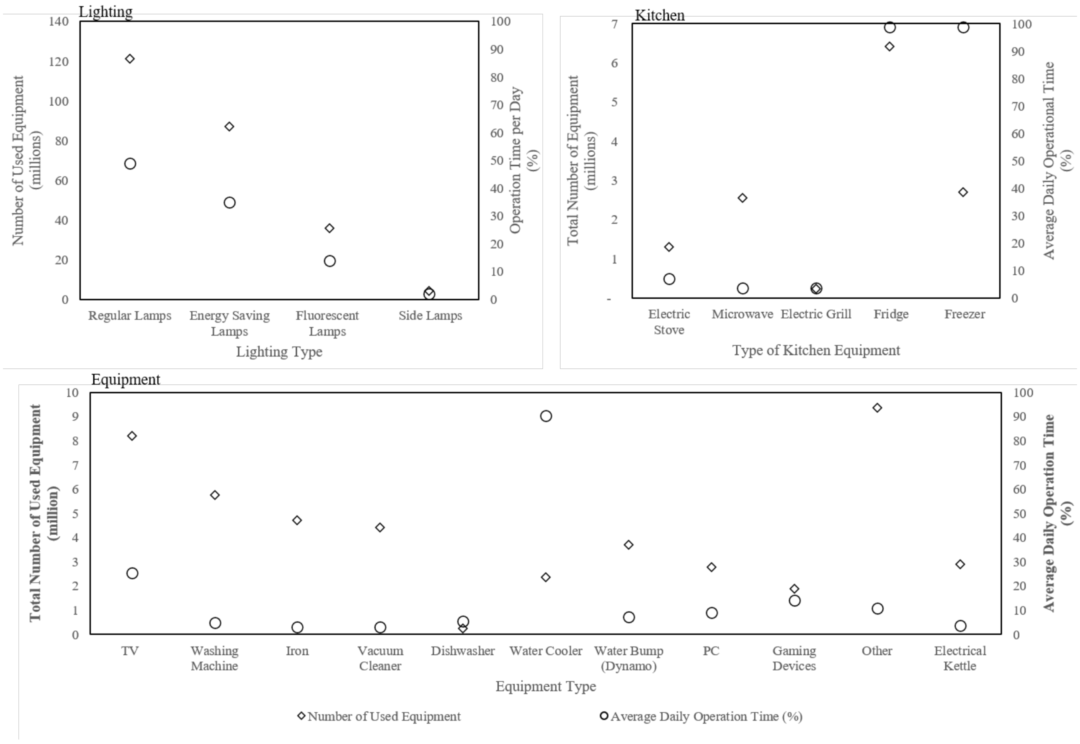

FIGURE 5.7: Lighting, equipment and kitchen systems in the Saudi homes (GAS, 2019).

lighting type and then integrated them for a mean value of 2.9 (W/m^2). This is an acceptable mean value because lighting accounts for less than 25% of a household's energy use in the KSA. This is less than the recent housing energy study by Krarti et al. (2020) with a LPD of 4 (W/m^2), which might be due to the use of inefficient lightbulbs. Figure 5.8 summarises LPD and the associated internal heat gains for each lighting type.

$$f_{(\overline{PD})} = \sum_{S=i}^{S=\infty} (system * Operation\ (h) * Wattage) \div 24\ (h) \tag{5.9}$$

$$f_{(\overline{PD})/year} = \sum_{Watts=i}^{Watts=\infty} (Wattage * Hours) \div 1000 \tag{5.10}$$

$$f_{(\overline{PD})W/m^2} = PD\ (Watts) \div \sum_{HA=i}^{HA=\infty} (HouseArea) \tag{5.11}$$

Where S represents the total number of lighting or equipment systems, H stands for the total amount of homes, HA is the housing area (m^2) and PD is the power density (W/m^2).

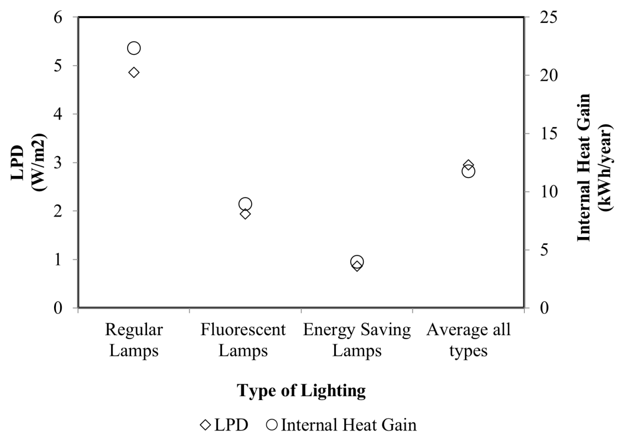

FIGURE 5.8: LPD and associated internal heat gains by lighting type.

The electrical systems were broadly mentioned by the energy censuses. See Section 4.3.6 in Chapter 4, with no electrical capacity or consumption. Therefore, this research's author collected the electrical capacities of each system from the Saudi Electricity Company (SEC), which is the only organisation responsible for distributing energy to buildings (SEC, 2018). The company indicates the most often used electronic systems in the KSA's housing, which conforms to the census's broad statistics. They additionally included information about the type, system and capacity of various electronic devices.

Furthermore, the cooking PD was separately calculated because it has an individual input object with different scheduling values in EnergyPlus. Then, it was added to the EPD to gain the total value of the kitchen PD. However, EPD and kitchen PD have been calculated following the previous process and equations. Figure 5.9 summarises all PDs of the systems in a single housing unit in the KSA. The total internal gains must also involve the occupants, as they radiate heat to the space depending on their activity.

5.2.10 People

The amount of heat emitted from occupants affects spaces and may alter cooling or heating loads (Parsons, 2000). This can be calculated through people's activity level (W/person), scheduling, metabolic ratee (met) and clothing value (clo). The activity level is given in watts per person, and it usually ranges from 100–150 (W/person) for light activities. It may reach 900 (W/person) for heavy

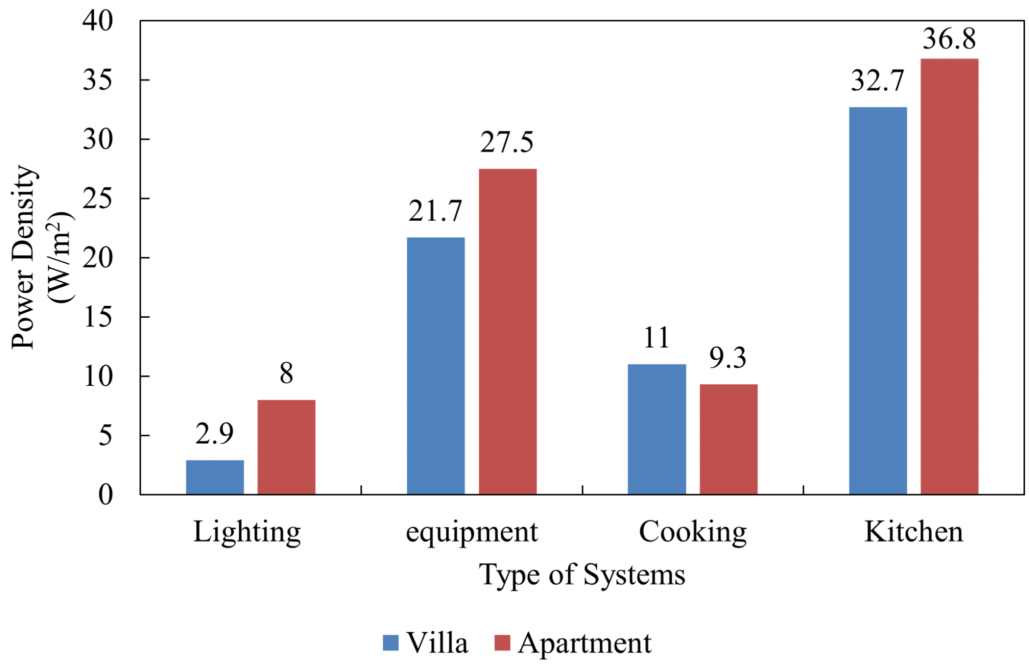

FIGURE 5.9: Electrical power density of all system in the ksA dwellings.

physical activities, such as wrestling. The values for the activity level were provided from the ASHRAE Handbook of Fundamentals (2005), which utilised a standard adult body surface area of 1.8 m^2. The activity schedule was preliminarily assumed by the author and represented in Figure 5.9. The assumed dynamic values have a mean of 120, which matches the ASHRAE thermal comfort standardised fixed value (ASHRAE, 2009). If activity level values fall from normal ranges at any hour, EnergyPlus will alert users with warnings or severe errors. This is essential when dealing with thermal comfort modelling, which is beyond the scope of this research

The clothing value describes the amount of clothing worn by occupants in a typical zone. Different clothing values are provided by ASHRAE (2010), but were not applied in this model due to clothing materials and culture in the KSA. The clothing values were attained from clothing insulation research in the KSA (Al-Ajmi et al., 2008). Figure 5.11 conveys typical Arabian Gulf clothing for all genders. The value of this clothing varies from summer to winter due to the covered body area. See Figure 5.12. The average clothing values used are 1.33 and 1.45 (clo) for summer and winter, respectively. This value is more reasonable for the KSA's context and is relatively high due to the amount of clothing insulation. Occupants' amount was set

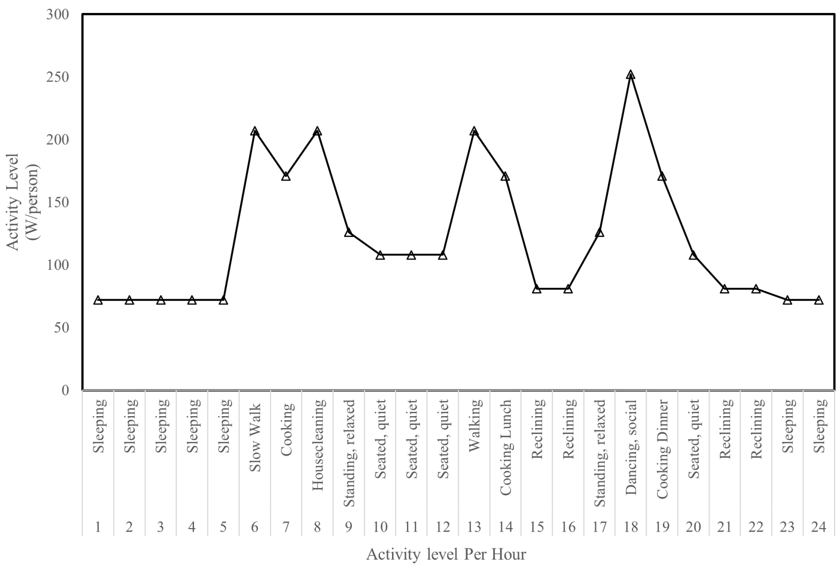

FIGURE 5.10: Activity schedule of people for both archetypes.

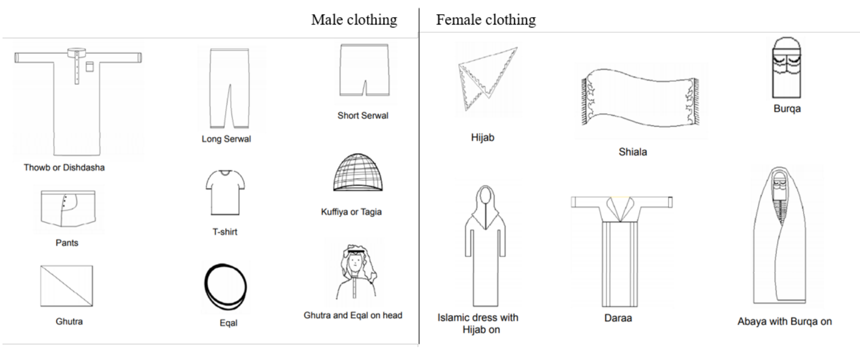

FIGURE 5.11: Typical gulf countries traditional clothing Al-Ajmi et al. (2008).

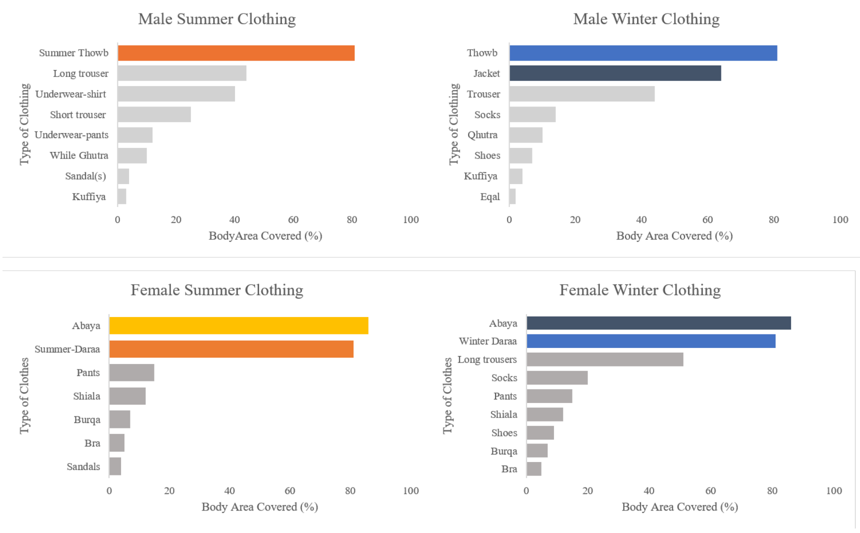

FIGURE 5.12: Area body covered by typical gulf countries clothing Al-Ajmi et al. (2008).

to 6 according to the average household size of the KSA (GAS, 2019).

5.2.11 Energy model validation

Model validation is the process of verifying that a model successfully fulfils its purpose. This shows whether the model is predictive in the context of its intended application (Merwe et al., 2018). The validation of numeric models employs three techniques: analytical solutions, empirical data and peer models (Ryan and Sanquist, 2012).

In this thesis, the validation stage was conducted through an empirical analysis by comparing model predictions with reported data. Initially, the validation was done using existing data from the literature. First, the validation has been initially developed with existing data to validate the research method. The existing data of the villa energy performance was collected from previous research conducted by Krarti et al. (2020) to develop an energy model using EnergyPlus simulation tool. The predicted energy model used the data, provided in Figure 4.29 and Tables 4.8 and 5.5, for the villa housing unit. This resulted in similar monthly energy behavior, see Figure 5.13, with a coefficient of determination of R^2 =0.98 within the range of ASHRAE of $R^2 > 0.75$, see Figure 5.14. This resulted in a Mean Base Error (MBE) of -319.1 kWh and a Nominal Mean Base Error (NMBE) of -3.2%, within the range of value of ASHRAE ±5, see Equation 5.13. The Root Mean Square Error (RMSE) is 1154 kWh with a Coefficient of Variations (CV) of RSME of 11.5%, within the range of ASHRAE of 15% (Guideline et al., 2014), see Equation 5.18.

$$MBE = \frac{\sum_{i=1}^{n}(m_i - s_i)}{n} \tag{5.12}$$

$$NMBE = \frac{1}{m} \cdot \frac{\sum_{i=1}^{n}(m_i - s_i)}{n - p} \times 100\,(\%) \tag{5.13}$$

Where m_i is the measured observations and s_i is the simulated value and n is the measured observation data points. p is adjustable parameters in the model.

Secondly, the validation was performed using actual electricity bills of three villas in the KSA for the years 2017–2019 were collected from the (SEC, 2018) and averaged. The SEC is the only organisation in the KSA that distributes energy to

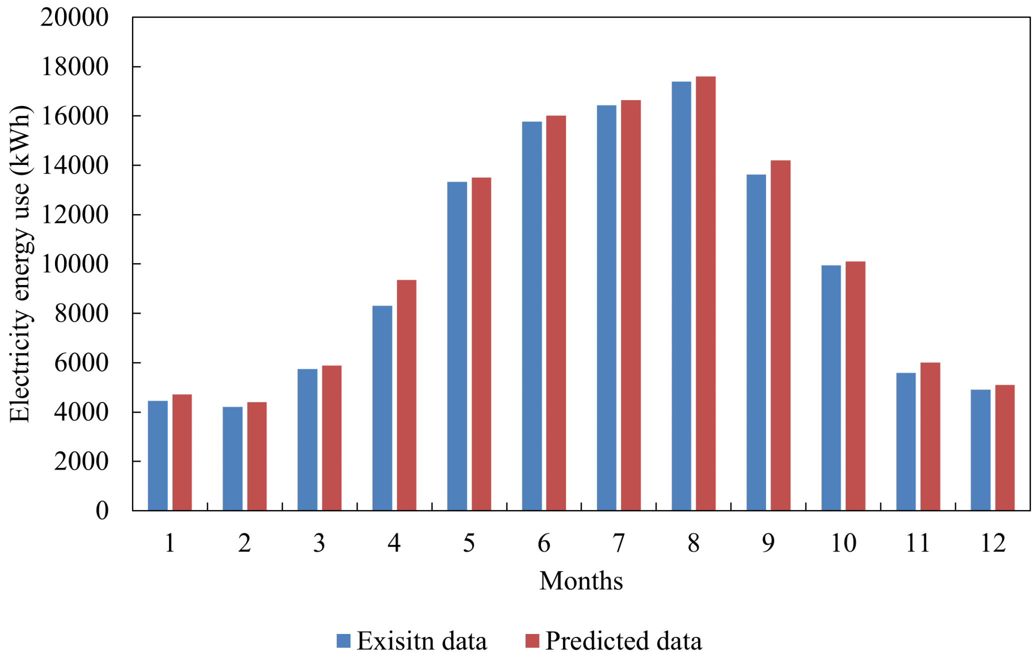

FIGURE 5.13: Comparison of existing data (Krarti et al., 2020) and the simulated model.

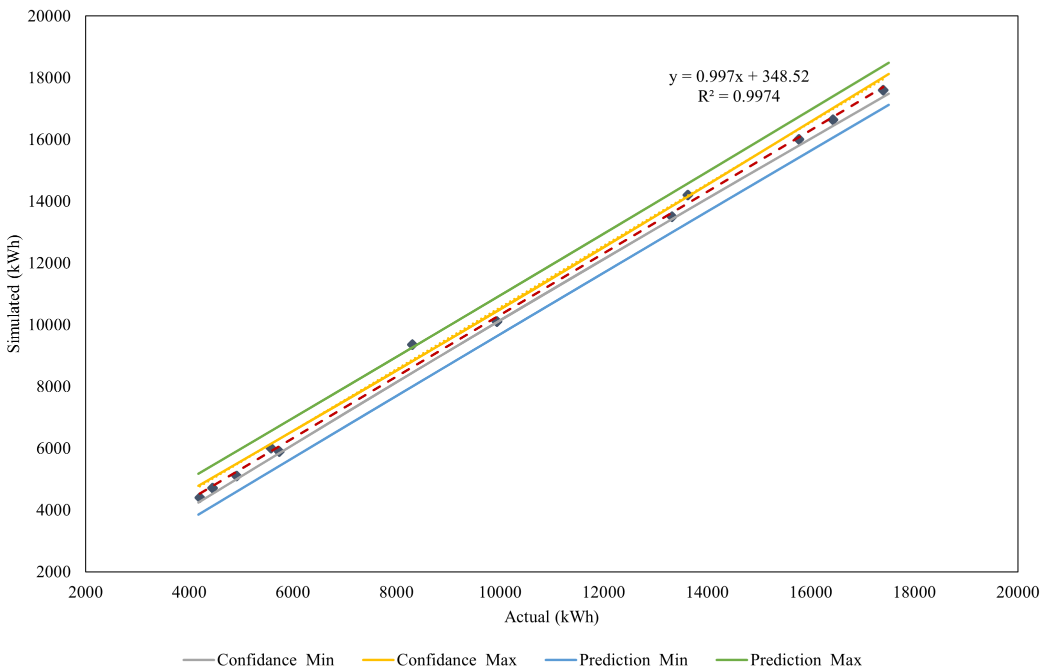

FIGURE 5.14: The existing data (Krarti et al., 2020) and the simulated model coefficient of determination.

TABLE 5.5: Building model details (Krarti et al., 2020).

Villa building type details	
Number of Floors	2
Total Floor Area	525 m^2
Wall Construction	20 mm plaster outside, 150 mm concrete hollow block, 20 mm plaster inside
Roof Construction	10 mm built-up roofing, 200 mm concrete roof slab, 13 mm plaster inside
Floor Construction	Ceramic tiles, 100 mm concrete slab on grade
Glazing	Single-Clear with Wood Frames
Window-to-Wall Ratio (WWR)	13%
Air Infiltration	0.8 ACH
Number of Occupants	6
Lighting Power Density	4.0 W/m2
Equipment Power Density	3.5 W/m2
Cooling Set Point	23 °C
HVAC System	Split DX
Energy Efficiency Ratio (EER)	7.5
Heating and Cooling Period	24-h/day

buildings. The energy model of this research was compared to the reported data. See Figure 5.15.

It is important now to perform a statistical inference method on the KSABC's compliant energy model to examine the experimental variable against a hypothesis of no influence or no relationship based on a predefined observation (Frick, 1996). Since its development by Fisher (1956), researchers have referred to null hypothesis testing to determine whether two measurable observations are related. It informs the user whether the results were obtained by chance or by affecting an event (Fisher, 1956). Testing the null hypothesis that a correlation is zero requires p-value calculations. The P-value is a statistical measure utilised to indicate how a relationship between two variables is statistically significant (Marasini et al., 2016). If the p-value is below 0.05, it refers to a 5% probability that the results occurred by chance. This means there probably is a real difference in energy consumption between the actual and the simulated model. In addition, if the p-value is 0.001 or less, it informs researchers of a 0.1% probability that the results occurred by chance. This means the result is highly significant and there is a strong energy consumption relationship between the actual and the simulated model. For more details, see Table A.2 in the Appendix A.

Prediction intervals (PI) illustrate that 95% of the values will be within the PI range. See equation 5.14. This means that, if one uses another sample from the same population, 95% of the found values will fall in the specified PI range. Confidence intervals (CI), however, provide a narrower data range and describe how large the

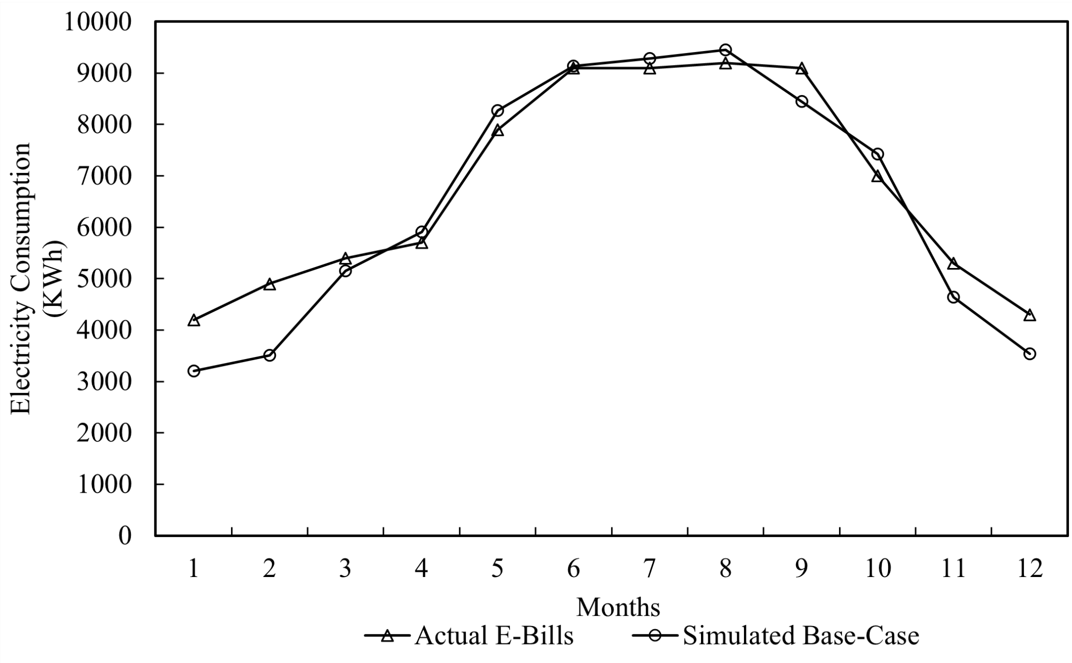

FIGURE 5.15: Comparison of actual electricity bills and simulated model.

difference might be in the compared data. See equation 5.15. This is important because it demonstrates a 95% probability that the best-fit line of the population falls within the CI range. Standard error (SE) is the sample mean standard deviation (SD), a measure for determining how representative a sample of the population is. See equation 5.16. A large SE value from a sample mean implies many variations between the two means, which indicates that the sample does not represent the population. Simultaneously, a small SE indicates that most sample means are similar to the population's mean. In the simulated model, the statistical analysis showed that our sample is likely accurate. Figure 5.16 summarises the statistical linear regression of the actual and simulated electricity consumption.

$$X = Y \pm t_a SE \sqrt{1 + \frac{1}{n} + \frac{(X - X_m)^2}{SS_{xx}}} \tag{5.14}$$

$$X = Y \pm t_a SE \sqrt{\frac{1}{n} + \frac{(X - X_m)^2}{SS_{xx}}} \tag{5.15}$$

Where t_a presents the student distribution, n is the sample size, X_m is the sample mean, and SS_{xx} is the sum of squares of the deviations of data points from their sample mean.

$$SE = \sqrt{\frac{SS_{res}}{n-2}} \tag{5.16}$$

Pearson's r was calculated because it measures the linear correlation between the actual and simulated data. It is a normalised measurement of the covariance, which has a value between -1 and 1. An absolute value of 0.1 is considered modest, 0.3 is considered medium, and 0.5 is considered significant (Cohen, 2013). In this comparison, the Pearson's r is 0.981, which represents a strong relationship between the variables. Finally, the root mean square error (RMSE) was calculated to represent the SD residuals, that is a measure of the variation or inaccuracy between a building's predicted and actual energy use (the difference between actual and predicted values) (Chai and Draxler, 2014). This is useful because it reveals the dispersion of the predicted data from the actual data, and it calculates the differences using equation 5.17. The RMSE is 3,054 due to overheating in the actual buildings at the beginning and the end of the year, which might be due to factors including low-efficiency heating and cooling systems, a high infiltration rate value and varied GT.

$$RMSE = \sqrt{(\frac{1}{n}\sum_{i=0}^{n}(y_i - y_{i(estimated)})^2} \tag{5.17}$$

$$CVRMSE = \frac{1}{m} \cdot \sqrt{\frac{\sum_{i=1}^{n}(m_i - s_i)^2}{n-p}} \times 100\,(\%) \tag{5.18}$$

5.3 Infiltration rate modeling

Buildings account for a significant share of international energy use; 40% of the European Union's energy use is consumed by the building sector alone (Cao et al., 2016). Similarly, the KSA's building sector is responsible for about 50% of the nation's energy use (Alaidroos and Krarti, 2016), 80% of which is consumed by cooling and lighting systems, at 60% and 20%, respectively. Heat can infiltrate a building through gaps and cracks in the envelope due to pressure differences between the indoors and outdoors, ΔT and the moisture content in the envelope. This unintentionally accessed heat impacts homes' energy loads and CO_2 emissions.

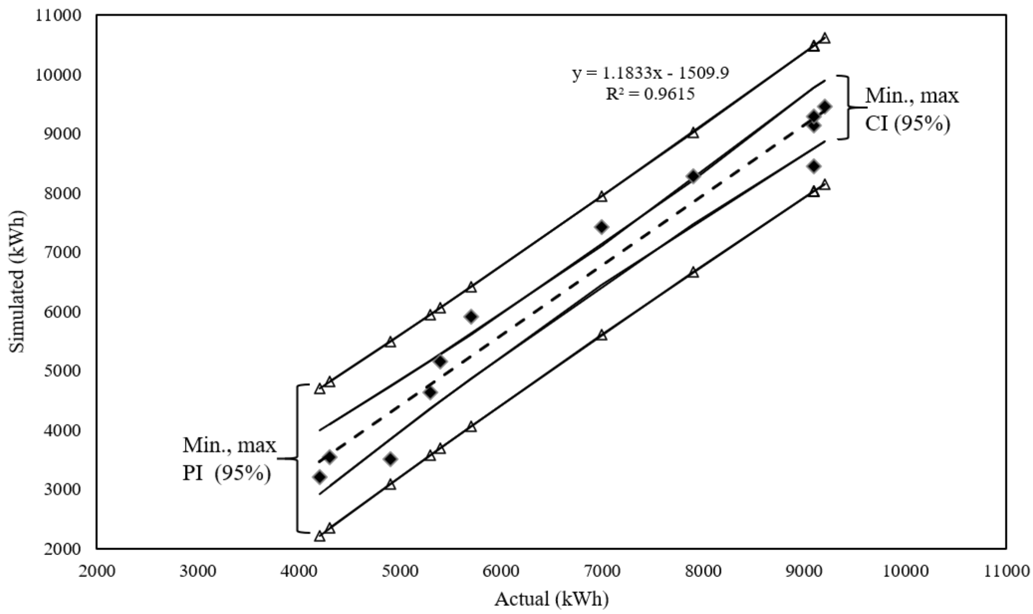

FIGURE 5.16: Statistical analysis of the actual electricity bills against the simulated model.

Currently, countries are attempting to reduce their energy demands worldwide and to meet international GHG emission requirements (Waisman et al., 2019). This is the first study that predicts infiltration rate distributions during cooling hours for the KSA's housing stock, which answers the fourth research question.

External air that enters the house by infiltration is mixed with the zone's air. It is difficult to calculate the amount of air infiltration, which is loaded with uncertainties. EnergyPlus provides constant infiltration rates after external and internal environmental condition exchanges, and it accounts for wind and stack effects. However, it utilises typical values for coefficients in the empirical function of the infiltration equation. Even though these typical coefficient values were initially provided in Chapter 26 of the ASHRAE Handbook of Fundamentals (ASHRAE, 2009), they are not practically applicable to mid- or high-rise residential buildings. The modelling of airflow in EnergyPlus is debatable and requires advanced capabilities for the energy model to allow models' integration. This can be accomplished by using the multi-zone airflow network capability inherent in EnergyPlus for airflow calculations. However, airflow can be modelled using a generic mathematic model utilising MATLAB (2010) software.

In this section, an air infiltration rate model is applied that follows the same method as Jones et al. (2013a), Jones et al. (2013b), Jones et al. (2014), and Jones et al. (2015) for modelling the airflow rate of the KSA's housing stock, see Section 3.3.1. It models airflow heat gain by introducing the DOMVENT3D_KSA model to create hourly infiltration rate distributions for the existing KSA residences. This development of an infiltration rate model to predict airflow answers the fourth research question. This requires different data input that can be categorised as geometrical, physical and environmental metadata. Finally, a stochastic technique is applied to produce mean infiltration rate distributions of the KSA's housing stock during cooling hours and the associated heat gain.

DOMVENT3D_KSA method was applied over other modelling techniques like CONTAM due to lack of data in the KSA (Dols, Polidoro, et al., 2015). CONTAM requires unavailable data of the KSA existing housing stock to allow airflow rate evaluation like air leakage height, width, area and relative air leakage area.

5.3.1 Modelling airflow heat gain

The model will develop mean frequency distributions of infiltration rates during cooling hours for the residential stock of the KSA. It employs a simplified statistical probability approach for predicting infiltration and ex-filtration heat gain in the KSA's current housing stock. The model is called DOMVENT3D_KSA and it looks at the airflow through an air leakage path which is conveniently modelled using a power law, see Equation 3.1. The power law relates the airflow rate to the pressure difference (ΔP) across the air leakage path. DOMVENT3D_KSA assumes that there are an infinite number of air leakage paths uniformly distributed over the facade in the absence of their locations. This assumption enables the integration of the power law equation over the height of the facade, and this allows to use one equation for a single facade. It also assumes a linear distribution of pressure over the vertical surfaces, as seen at Jones et al. (2014), and the indoor resistance of airflow is negligible because the rooms are connected, as mentioned by Etheridge (2011).

The modelling infiltration rates of a large-scale housing stock are performed instead of actual measurements due to COVID-19 restrictions and because of the need to reduce cost, effort and time. The requirements for infiltration models include comprehensive generic infiltration and ex-filtration modelling techniques for multiple dwelling types, defining a large set of statistics for dwellings' properties and appropriate statistical analysis that supports dwellings' variability to run parametric tests. The data for DOMVENT3D_KSA inputs were collected from different sources including governmental censuses and surveys, literature review and the building code, so we were to investigate all the relevant features for modelling energy and heat gain in the KSA. See Section 4.4. Data inputs include national and municipal censuses, socio-economic surveys, energy censuses, construction regulations and the literature (GAS, 2019; Housing, 2020; Saudi Building Code, 2018). The housing archetypes previously described in Section 5.2.1 of this chapter have been utilised to identify the housing stock's geometric and physical details, while environmental inputs were gathered from the EnergyPlus Weather (EPW) file format (Hirsch, 2018; DoE, 2020).

5.3.2 Infiltration rate model inputs

A prime determining factor of modelling the infiltration rate of a large-scale housing stock requires divergent data inputs, including housing variations, locations and weather conditions. The model should be sufficiently versatile to overcome data variations and to generate proper predictions. Accordingly, archetypes should be representative of a large sample size. The model inputs are classified to three major characteristics; geometrical, physical and environmental metadata, see Section 3.3.1.

5.3.2.1 Geometrical metadata

The housing archetypes described in Section 4.4.2 share a cubic shape with nonidentical proportions and no neighbouring outside walls with other blocks. The typical apartment unit in a building block shares one vertical surface with a neighbouring apartment. Six individual apartments, two for each floor, make up the total structure. The two apartments on each floor are separated by an inner vertical surface. Due to the building's entryway, the ground floor units have a narrower main elevation than the rest. The horizontal surfaces of the second storey apartments, the ceiling and floor, are shared with the residences above and below. The quantity of apartments in each block is significant because it directs the code to calculate physical variables such as wind pressure coefficients, as demonstrated in Section 5.3.2.2. This is also essential for calculating the Aspect Ratio, the fraction of the width to the depth of structures or blocks. According to Jones et al. (2013b), the original DOMVENT3D model estimated the number of apartments by giving a range of three to 20 units in each block, because English housing stock does not specify it.

Conversely, the villa is a detached building block, and it has no shared walls with neighbours due to the structure's inherent position in the centre of the site plot. The plot's sides are often fenced due to building code compliance. Local government setback standards vary based on dwelling type, surrounding streets' sizes and location (Saudi Building Code, 2018). The orientation of the archetypes is not given by housing surveys, the building code or the literature. Therefore, a uniform random variable distribution was assumed within a range of values $0 \leq a < 360°$. The geometric information is summarised in Table 5.6.

TABLE 5.6: Geometrical metadata for the KSA infiltration model (edited from (Jones et al., 2015)).

Input	**Unit**	**Value, comment, or PDF assumed**	**Source**
housing surfaces width, depth, height, and top and bottom heights above the ground level (w,d,z_s,z_{max},z_{min})	m	Defined by the statistical analysis for housing archetypes for each story and surface. Constructed following the Krarti et al. (2020) model and the KSABC.	(KSABC 2018)
Block aspect ratio	-	Integration of (w/d) and the amount of dwellings in the block.	
Apartment block floors	-	Amount of floors in a block of apartments.	(Krarti et al., 2020)
Number of dwellings in a block	-	U(1) for villas, U(6) for apartments.	(Krarti et al., 2020)
Location in an apartment block, (X,Y)	-	Apartments only, X: if the unit has 3 sides or 2 perpendicular sides, the apartment is assumed to be located at the edge of the block. If the apartment has one facade or two opposite facades then the dwelling is a uniformly random location along block's width. Y: a uniformly random variable between the lowest (ground) to the highest storey.	
Dwelling orientation (a)	°	U(0,360)	
Dwelling height (z_u)	m	Ceiling height of the top floor of the dwelling	(KSABC, 2018)
Dwelling type	-	Villa, apartments	Sampling Analysis

5.3.2.2 Physical metadata

There are no large- or small-scale infiltration rate studies or real measurements in the entirety of the KSA. New studies assume the infiltration rate to be 0.8 (h^{-1}) for all housing units regardless of type, location or climate. A common feature of the

KSA's homes is that they share similar if not identical construction materials with similar exterior shapes (GAS, 2019), which are often cubical.

The system of airflow through air leakage paths is demonstrated by the flow exponent, b, and it is the foundation for the roughness of the surfaces and their geometric shape. The flow exponent is critical because it impacts the airflow through air leakage paths and, therefore, changes the pressure differential across the envelope. It is usually assumed to have a constant value of $b = 0.66$, as demonstrated by Orme et al. (1998). However, Sherman and Dickerhoff (1998) performed a Gaussian distribution, which statistically showed a mean value of $\mu = 0.65$ and a standard deviation of $\sigma = 0.08$, representing a large sample of dwellings, 1,900, in the USA. The measurement administered a blower door test to all units to generate infiltration rate distributions. Sherman and Dickerhoff (1998) flow exponent value is almost identical to the database of the international AIVC (Orme et al., 1998). This allows the flow exponent to be a random variable with a normal distribution to safeguard the parameters from having negative values (Sherman, 1980).

A normalised average wind pressure coefficients for the exterior walls of low-rise residential buildings were given by Swami and Chandra (1987). They considered the angle of the wind's direction, exterior walls and local shelters, where a nonlinear relationship was confirmed with a correlation coefficient of 0.80. The wind pressure coefficient was determined because both KSA housing archetypes are low-rise dwellings with a 9 m maximum height for the apartment building archetype and a 6 m for the villa archetype. The wind pressure coefficient is a function of wind angle, wind direction and block aspect ratio, see Section 5.3.2.1, and local sheltering, see Section 5.3.2.3. This permits wind pressure coefficient scaling for building shielding. A uniform random variable distribution is generated depending on the location of the dwelling and pressure coefficient. According to Sherman (1980), horizontal surfaces have no wind effects because they are considered fully shielded. Meanwhile, exterior vertical surfaces are given a wind coefficient based on the disparate effective factors, such as angle, orientation and location. Finally, the wind coefficient is scaled to represent local shielding. Table 5.7 summarises the physical inputs.

TABLE 5.7: Physical metadata for the KSA infiltration model (edited from (Jones et al., 2015)).

Input	Unit	Value, comment, or PDF assumed	Source
Residence age	Years	GAS parameter indicating housing age	(GAS, 2019)
Permeability (Q_{50})	$m^3/h/m^2$	Assumed normal distribution	
Party wall relative permeability ($\tilde{Q}$)	-	Party wall have a permeability equivalent to a dwelling when $Q = 1$ and are impermeable when $Q = 0$.	
Airflow exponent (b)	-	$N(0.651, 0.077)$	(Sherman and Dickerhoff, 1998)
Facade wind pressure coefficient (C_p)	-	$f(0, w, z_u, d, C_{p0})$ low-rise dwelling.	(Swami and Chandra, 1987)
Wind pressure coefficient for house's front surfaces with normal wind C_{p0}		$f(sheltering)$. Product of 0.6 and the LBL shielding factor.	(Swami and Chandra, 1987)

5.3.2.3 Environmental metadata

The national census of the KSA described in Section 4.1.1 of Chapter 4 indicates that the KSA has 13 regions. The weather data of the regions were attained from an EnergyPlus dataset (DoE, 2020). EPW files, described in Section 5.2.3 as a Typical Meteorological Year (TMY) weather dataset, provide a representative full year's weather data for all the KSA's regions. These data have been collected for 20–30 years from typical meteorological weather stations in the KSA in .epw files. The weather files' data include longitude, latitude, elevation, wind speed, wind direction and mean air temperature. The files were transferred to a Comma Separated Values (CSV) file to be organised and connected with the proper census's region. Every weather file is randomly selected (having an equal chance) and linked to the specific region. Wind speed is scaled depending on building heights and terrain by employing the power law function described in BS (1991). The building's height is attained using the cubic shapes of the dwellings, while the terrain is a city, regarding the regions stated in the (GAS, 2019).

The internal air temperature is treated as an external variable because DOMVENT3D_KSA is not a thermal load model. The IAT (T_int) was determined with a normal distribution attained from Shipworth et al. (2010), with a mean of $\mu = 21.1°C$ and a standard deviation of $\sigma = 2.5°C$. Table 5.8 summarises the environmental inputs.

TABLE 5.8: Environmental metadata for the KSA infiltration model (edited from (Jones et al., 2015)).

Input	Unit	Value, comment, or PDF assumed	Source
Dwelling location	-	GAS regions (National censuses)	(GAS, 2019)
Altitude (h)	m	$f(location)$. Given by weather file.	(DoE, 2020)
Wind direction (θ)	°	$f(location)$. Given by weather file.	(DoE, 2020)
Weather station wind speed (u_0)	m/s	$f(location)$.	(DoE, 2020; GAS, 2019)
Terrain coefficients (k,m)	-	$f(location, sheltering)$	(BS, 1991; GAS, 2019)
Wind speed at dwelling height (u)	m/s	$f(u_0), z_u, k, m, location)$	(BS, 1991)
Sheltering	-	GAS sheltering LBL shielding coefficient	(Sherman and Modera, 1986; GAS, 2019)
		[BSI terrain coefficients]. City, heavy shielded	(Deru and Burns, 2003; BS, 1991)
Internal dry bulb (T_int)	°C	N(21.1,2.5)	(Shipworth et al., 2010)
External dry bulb (T_ext)	°C	$f(location)$. Given by weather file.	(DoE, 2020)

5.3.3 The applied statistical technique

Predicting distributions of infiltration rates and heat gain of houses during cooling season was generated applying a Monto Carlo approach, following the method of Das et al. (2014). This involves producing an amount of random samples for every input variable and then executing the simulation for each sample combination. This approach utilizes a random probability determination process to generate and analyse data. In DOMVENT3D_KSA, five major data inputs were selected; housing and region variations, selected by using housing cumulative weighting factors, residence orientation (a), air permeability (Q_{50}), and the flow exponent (b). A Latin Hyper-Cube Sampling (LHC) technique was determined because it is a stratified sampling approach, often adapted to reduce run-time and speed up the simulation process in assessing uncertainties. The LHC was applied for 100 sets of the five variables and every set is randomly implemented to the model to predict mean infiltration rates $(\bar{N_I})$ (h^{-1}) during cooling season, and total heat gain (H_I) (MWh).

Distributions of infiltration rates and the heat gains of houses during cooling season were predicted applying a Monto Carlo approach, following Das et al. (2014). This approach utilises a random probability determination process to generate and analyse data. In DOMVENT3D_KSA, five major data inputs were selected – housing and regional variations – using housing cumulative weighting factors, residence orientation (a), air permeability(Q_{50}) and the flow exponent (b). A Latin Hyper-Cube Sampling (LHC) technique was determined because it is a stratified sampling approach often adapted to reduce run time and speed up the simulation process when assessing uncertainties. The LHC was applied for 100 sets of the five variables. Every set was randomly implemented in the model to predict mean infiltration rates ($\bar{N_I}$) (h^{-1}) during cooling season and total heat gain (H_I) (MWh).

The sample size becomes larger when increasing the number of sets, which was selected to reduce run time. Predictions of the μ and σ of $\bar{N_I}$ and H_I were continuously made after every run of the dataset for each housing type. Then, the entire sample was integrated to assess if the stopping criterion had been met. Stopping criteria are often used to record a procedure's progress across iterations to make decisions based on the long-term behaviour of the algorithm being observed rather than the outliers. The minimum accuracy requirements of the typical ventilation and indoor air-quality sensors were used to select the lower limits of the stopping criterion (Jones et al., 2015). The sample size was determined depending on the 0.2% stopping criterion for each set of μ and σ to the following set of individual housing types and the entire housing stock. The sample size was selected to guarantee every housing type is incorporated into each dataset.

5.3.4 Infiltration rate model validation

The validation of the infiltration rates model was performed against the infiltration rates of the UK, four models (DOMVENT3D of the UK, BREDEEM, L=20 and SAP), because there is no available or accessible data for infiltration rates in the KSA. The model validation findings showed a substantial relationship between predicted and observed infiltration rates in the literature, with high coefficient of determination (R^2) values indicating a high degree of accuracy and dependability. The validation showed R^2 values of 0.94 with SAP model, 0.95 BREEDEM model, 0.95 with L=20 model and 0.96 with the UK DOMVENT3D model, see Figure 5.17. This implies the extent to which the regression model accurately matches the observed data and evaluates the quality of the model's fit.

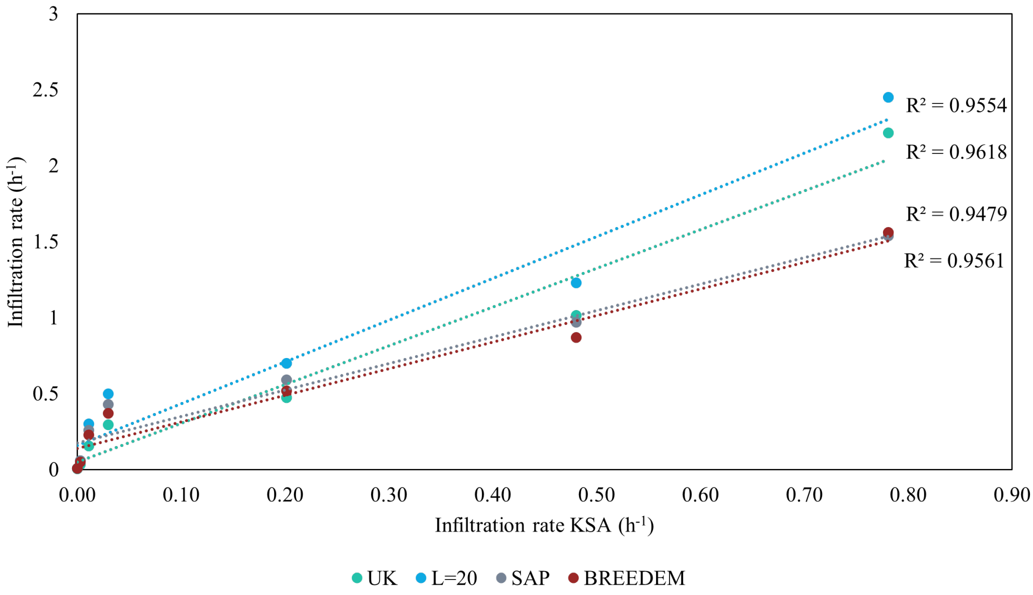

FIGURE 5.17: Infiltration rate model validation.

5.4 Summary

This chapter demonstrated the applied bottom-up engineering modeling approach for assessing the energy performance of the KSA housing stock using the dynamic EnergyPlus simulation tool. It showed the development process for the housing archetypal energy baselines by defining various building data inputs and parameters. It defined where and why the sensitivity analysis is used and what are the most influential parameters to the energy models' outputs. The sensitivity of two major parameters, infiltration rate and ground temperature, showed clear data variances when they are not involved in the energy model establishment process, hence, they impact the results. The energy modeling process has been carried out for validation process using existing data and showed a similar behavior with a coefficient of determination of R^2=0.98, within the range of ASHRAE of R^2> 0.75.

EnergyPlus assumes a deterministically constant air pressure for the entire year in order to simulate the model and predict the energy performance. This limitation in EnergyPlus tool encouraged the developement of an airflow rate model to predict the infiltration rate of the KSA housing stock using a generic coding tool, MATLAB. The infiltration modeling procedure and all required data inputs were described and validated against existing data of four infiltration rate models and showed a coefficient of determination of R^2= +0.94.

Chapter 6

Results

Chapter 4 highlighted the KSA's housing data and the generation process of the housing archetypes that may represent 10% of the entire housing stock in Section 4.4; hence, the first research question is answered. Chapter 5 described the two applied modelling approaches: modelling housing energy performance using the dynamic EnergyPlus simulation tool to evaluate the typical internal environmental conditions of the dwellings in Section 5.1 and to assess their energy use in Section 5.2 and modelling the air infiltration rate of the KSA's housing stock in Section 5.3.

Chapter 6 employs descriptive and inferential statistics to reveal the outcomes from the models by applying different evaluation schemes, such as sensitivity analysis, associations (relationships or correlations) between variables and regressions. This identifies the inputs that had the greatest influence on the energy performance of the stock. This chapter is classified into four sections, as follows: Section 6.1 analyses the energy performance findings of the housing archetypes' energy baselines to answer the second research question. Section 6.2 evaluates the applications of different energy measures to reduce housing energy demands, which answers the third research question. Section 6.4 presents the results from the infiltration rate model, answering the fourth research question and Section 6.3 demonstrates the total energy demands, cost and CO_2 emissions reductions of the KSA's housing stock, thus, answering the fifth research question and fulfilling the overall aim.

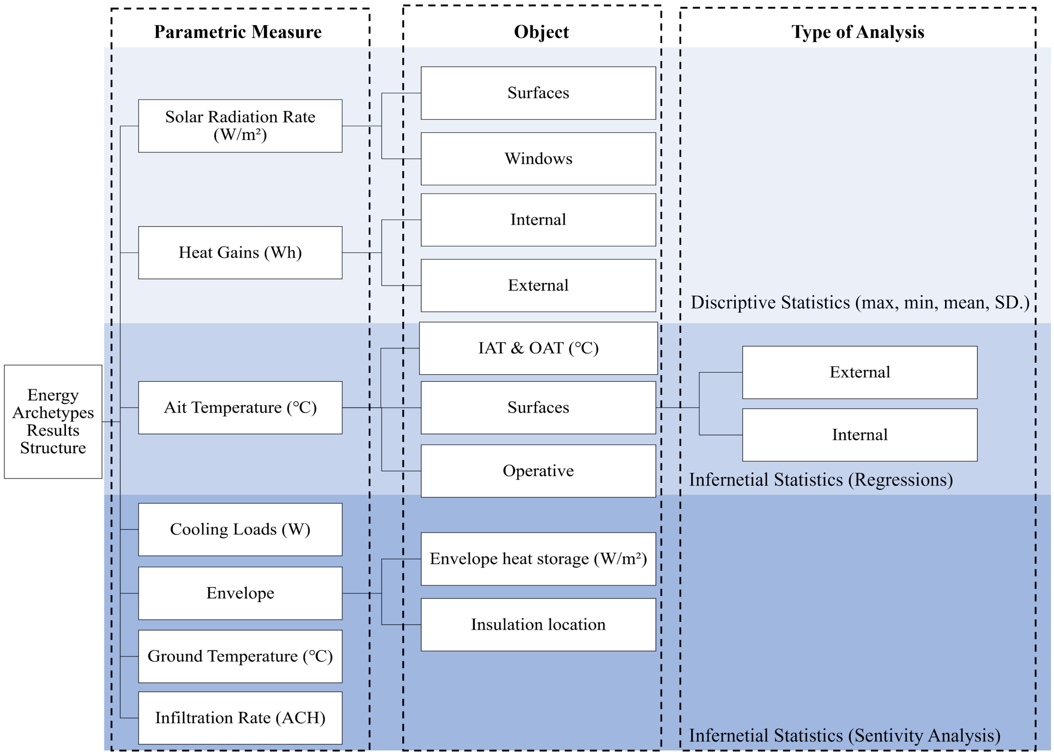

FIGURE 6.1: Energy analysis section scheme.

6.1 Archetypes energy baselines

The evaluation of the archetype's energy performance included seven housing archetypes: one villa and six apartments in one building. The archetypes were in the five most populated regions with weather fluctuations, which are Riyadh, Dhahran, Makkah, Abha and Tabouk. This to ensure that the archetypal baselines reflect the energy demands of each region and the overall stock. Figure 6.1 describes energy analysis sections and the parameters of this research.

6.1.1 Solar radiation rate

This section quantifies solar radiation rates that strike exterior surfaces and windows according to location and building orientation. This allows the identification of the amounts of added heat from the sun according to each surface and window oriented towards the thermal zone and, accordingly, the evaluation of external heat gain sources. The analysis for this section encompasses two days with extremely varied environmental conditions. The winter day refers to 20 January and the summer day refers to 1 July.

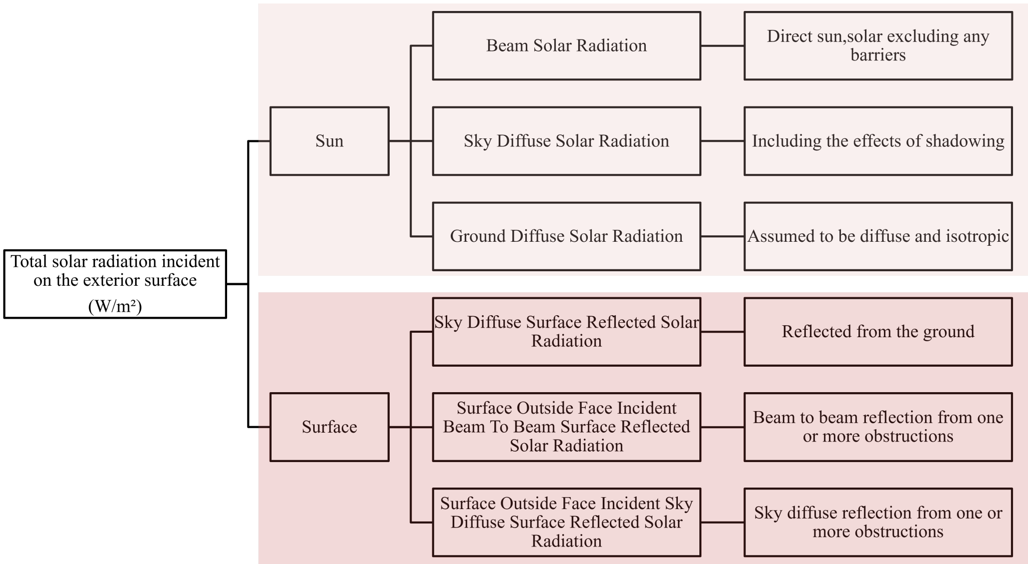

FIGURE 6.2: Total solar radiation incident on the outsider surfaces.

6.1.1.1 Surface solar radiation rate

According to the literature review, the KSA's high solarradiation rate is a major influence of excessive cooling energy use (Tinker and Buijan, 1998; Rehman, 1998; Almasoud and Gandayh, 2015). This can be assessed by the surface group object in EnergyPlus. Diverse surface heat transfer variables are arranged around the interior and exterior faces of each surface. The zone heat balance approach generates energy balances on each side of a surface, resulting in two pairs of findings for each surface. The inner face of a heat transfer surface is the side that faces the thermal zone while the outer side faces the outdoors and is exposed to the sun. The integrated outside face incident solar radiation rate per area (W/m^2) includes factors such as direct, beam or reflected solar radiation. See Figure 6.2. This is to compare the difference in quantities between the surface solar radiation rates of the archetypes according to the building's orientation.

Solar radiation rates in the KSA are higher in the summer than in the winter due to the sun's movement. On a summer day, Abha has the greatest mean solar radiation rates of $\mu = 139\,W/m^2$ ($\sigma = 46$) for the villa and $\mu = 165\,W/m^2$ ($\sigma = 91\,W/m^2$) for the apartment building. See Tables 6.1 and 6.2 as well as Figures 6.3 and 6.4. These higher rates in the apartment building are due to the larger surface area exposed to the sun, building size and volume. Tabouk received the second-highest solar radiation rates in the villa and the apartment building with

TABLE 6.1: Predicted solar radiation rates of the archetypes surfaces and windows in the winter-day.

		Villa Facade (winter-day)							
Regions	Object	North	South	East	West	Roof	max	Mean	SD.
Riyadh	Surfaces	47	165	101	96	153	165	112	48
	Windows	47	47	87	165	0	165	69	62
Dhahran	Surfaces	37	95	38	72	88	95	66	27
	Windows	37	39	76	72	0	76	45	31
Makkah	Surfaces	37	76	38	72	88	88	62	23
	Windows	72	39	76	72	0	76	52	33
Abha	Surfaces	53	121	67	78	148	148	93	40
	Windows	53	72	121	78	0	121	65	44
Tabouk	Surfaces	44	167	82	96	139	167	106	48
	Windows	44	84	167	96	0	167	78	62
Total	Mean	47	91	85	90	62	127	75	42
	SD.	11	47	38	29	68	40	22	14
		Apartments Facade (winter-day)							
Regions	Object	North	South	East	West	Roof	max	Mean	SD.
Riyadh	Surfaces	47	165	101	96	153	165	112	48
	Windows	47	87	165	96	0	165	79	61
Dhahran	Surfaces	37	72	76	39	88	88	62	23
	Windows	37	39	76	72	0	76	45	31
Makkah	Surfaces	50	94	164	101	163	164	114	49
	Windows	50	101	164	94	0	164	82	61
Abha	Surfaces	53	78	121	72	148	148	94	39
	Windows	53	72	121	78	0	121	65	44
Tabouk	Surfaces	44	167	96	84	139	167	106	48
	Windows	44	84	167	96	0	167	78	62
Total	Mean	46	96	125	83	69	142	84	47
	Max	53	167	167	101	163	167	114	62

TABLE 6.2: Predicted Solar radiation rates of the archetypes surfaces and windows in the summer-day.

		Villa Facade (summer-day)							
Regions	Object	North	South	East	West	Roof	Max	Mean	SD.
Riyadh	Surfaces	91	70	158	136	153	158	122	39
	Windows	136	91	136	70	0	136	87	56
Dhahran	Surfaces	90	92	132	141	88	141	109	26
	Windows	90	137	73	141	0	141	88	57
Makkah	Surfaces	90	73	132	141	88	141	105	30
	Windows	141	137	73	141	0	141	99	62
Abha	Surfaces	139	62	165	182	148	182	139	46
	Windows	139	175	62	182	0	182	111	79
Tabouk	Surfaces	95	80	146	151	139	151	122	32
	Windows	95	151	80	151	0	151	95	62
Total	Mean	110	107	116	144	62	153	108	49
	SD.	24	40	39	31	68	17	17	17
		Apartments Facade (summer-day)							
Regions	Object	North	South	East	West	Roof	max	Mean	SD.
Riyadh	Surfaces	91	70	158	136	271	271	145	78
	Windows	91	136	73	136	0	136	87	56
Dhahran	Surfaces	90	141	73	137	274	274	143	79
	Windows	90	137	73	141	0	141	88	57
Makkah	Surfaces	95	141	69	115	249	249	134	70
	Windows	95	115	69	132	0	132	82	52
Abha	Surfaces	139	141	62	175	310	310	165	91
	Windows	139	175	62	182	0	182	111	79
Tabouk	Surfaces	95	80	151	151	278	278	151	78
	Windows	95	151	80	151	0	151	95	62
Total	Mean	102	129	87	146	138	212	120	70
	Max	139	175	158	182	310	310	165	91

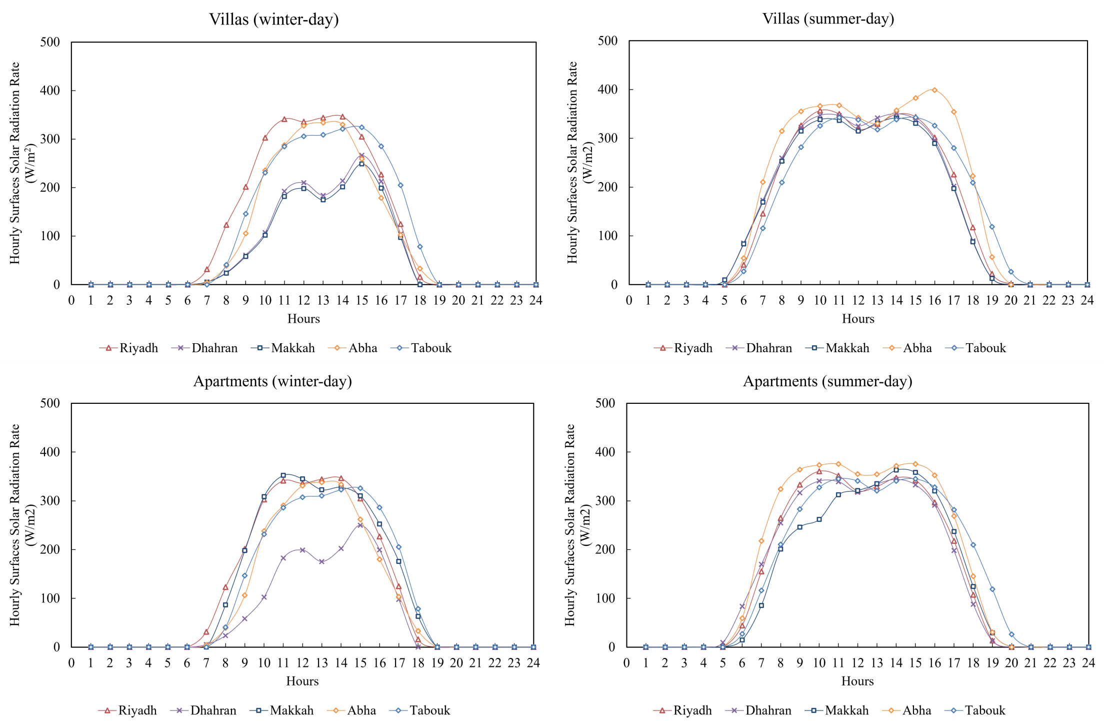

FIGURE 6.3: Predicted surfaces solar radiation rates for the archetypes.

total means of $\mu = 122\,\mathrm{W/m^2}$ ($\sigma = 32\,\mathrm{W/m^2}$) and $\mu = 151\,\mathrm{W/m^2}$ ($\sigma = 78\,\mathrm{W/m^2}$), respectively. On a winter day, Riyadh received the highest proportions of solar radiation rates for both buildings with an identical total mean of $\mu = 112\,\mathrm{W/m^2}$ ($\sigma = 48\,\mathrm{W/m^2}$). Tabouk received the second-highest total mean solar radiation rate with an identical value of $\mu = 106\,\mathrm{W/m^2}$ ($\sigma = 48\,\mathrm{W/m^2}$). Roofs usually have the highest solar radiation rates over all surfaces in both seasons for archetypes, which may exceed $\mu = 310\,\mathrm{W/m^2}$. See Figures A.1 and A.2 in the Appendix A for more detailed information.

Due to windows' transparency, more sun rays penetrate buildings and mostly have a detrimental influence on interior conditions (McMullan, 2017). Hence, the KSABC requires double-pane window glazing with aluminium frames (Saudi Building Code, 2018). Windows' solar radiation rates for both archetypes on a winter's day are much less than on a summer day. Figure 6.4 summarises the solar radiation rates of windows for the five regions of the KSA. See Figures A.3 and A.4 in the Appendix A. This increases buildings' heat gains from solar radiation.

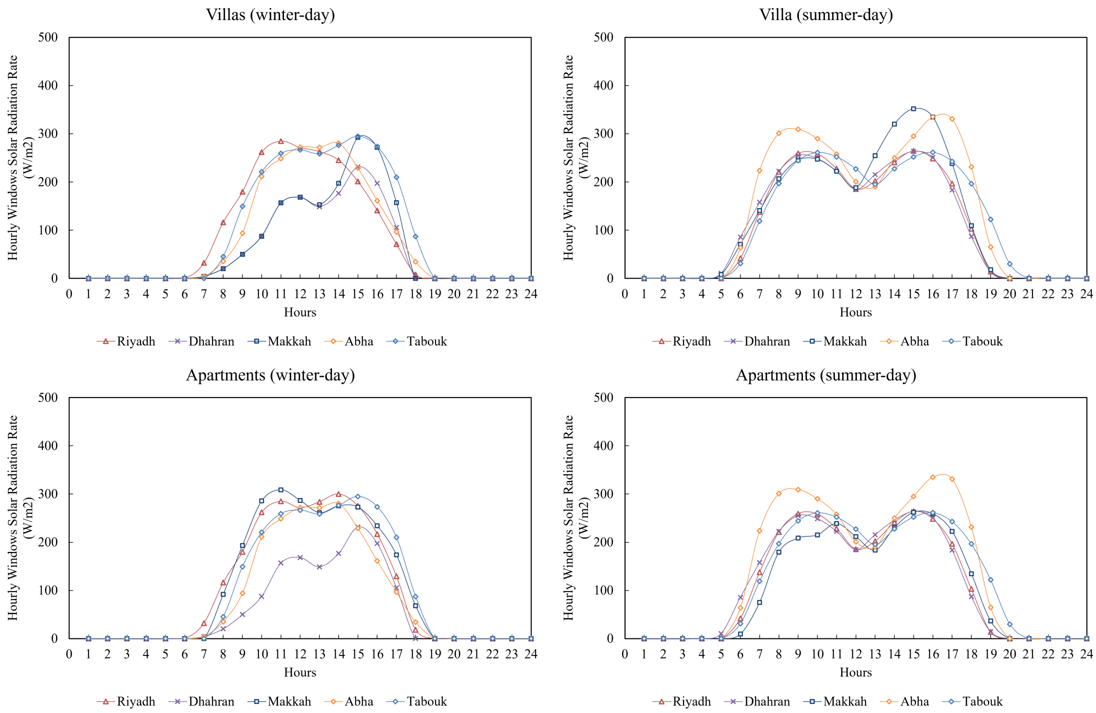

FIGURE 6.4: Predicted windows solar radiation rates for the archetypes.

6.1.2 Archetypes' heat gains

The literature reveals buildings have two major types of heat gains: external or internal. External heat gains originate from an outside source of energy such as the sun. Internal heat gains include radiated heat from internal sources, such as lighting, equipment and people (McMullan, 2017). This section distinguishes between these two possibilities of heat sources to determine the internal environmental conditions for energy assessment, hence answering the second research question.

6.1.2.1 External heat gain sources

The KSA's housing stock has three major sources of external heat gains: windows, surfaces and infiltration (Harding, 2018). Windows' heat gains represent the total amount of heat penetrating an exterior window and reaching the thermal zone. The surface heat gains describe the heat transported by the absorption of solar radiation incident at the outdoor surface face of the envelope. Finally, infiltration heat gains indicate the total amounts of heat transmitted to the zone air from external air transfers, such as infiltration (Jones et al., 2016). This condition exists if the overall zone infiltration heat gain energy is $\geq$ the all-zone infiltration heat gain energy.

The primary external heat source is windows due to extreme solar radiation with greater rates in the summer than in the winter for both archetypal buildings. Figure 6.5 illustrates mean values of external heat gains in the two days for both buildings. The mean amounts of window-absorbed heat gains on the winter's day and the summer day for the villa are 64 and 96 (Wh), respectively, while they are far higher in the apartment archetype with a mean of 178 and 372 (Wh), respectively. See Figures 6.6 and 6.7. The upper and lower bars reflect the greatest and lowest heat gain rate values, while the centre bar represents the mean value μ. One standard deviation from the mean is shown by the blue box. Window-absorbed external heat gains are more than double the heat gained from exterior surfaces. Exterior surfaces are the second major heat source in the villa with means of 25 and 8 (Wh) for cold and hot days, respectively, whilst they gain about 126 and 73 (Wh) in the apartment building, respectively. Importantly, surfaces on the winter's day gain heat at three times the rate of the summer's day because the rate at which a surface accumulates heat is determined by multiple variables, including the temperature differential between the surface and its surrounds, the thermal conductivity of the substance and the heat transfer coefficient of the air around it. Although the air temperature is substantially lower in the winter than it is in the summer, there is a greater temperature variations between the surface and the air around it, resulting in a more rapid rate of heat transfer. Furthermore, the air is frequently dryer in the winter, indicating that there is less moisture in the air to obstruct heat transmission. Because of the dry air, heat may flow more readily from the surface to the surrounding air, raising the rate of heat transfer. As a consequence of these combined effects, surfaces on a winter day may acquire heat at three times the rate of surfaces on a summer day. The infiltration rates present heat loss from the building to the external environment; the villa infiltration's heat loss for the winter's day and the summer's day are -29 and -13 (Wh), respectively, while for the apartments are 126 and 7 (Wh), respectively. Here, the minus sign represents heat being removed. See Figures A.5 and A.6 in Appendix A.

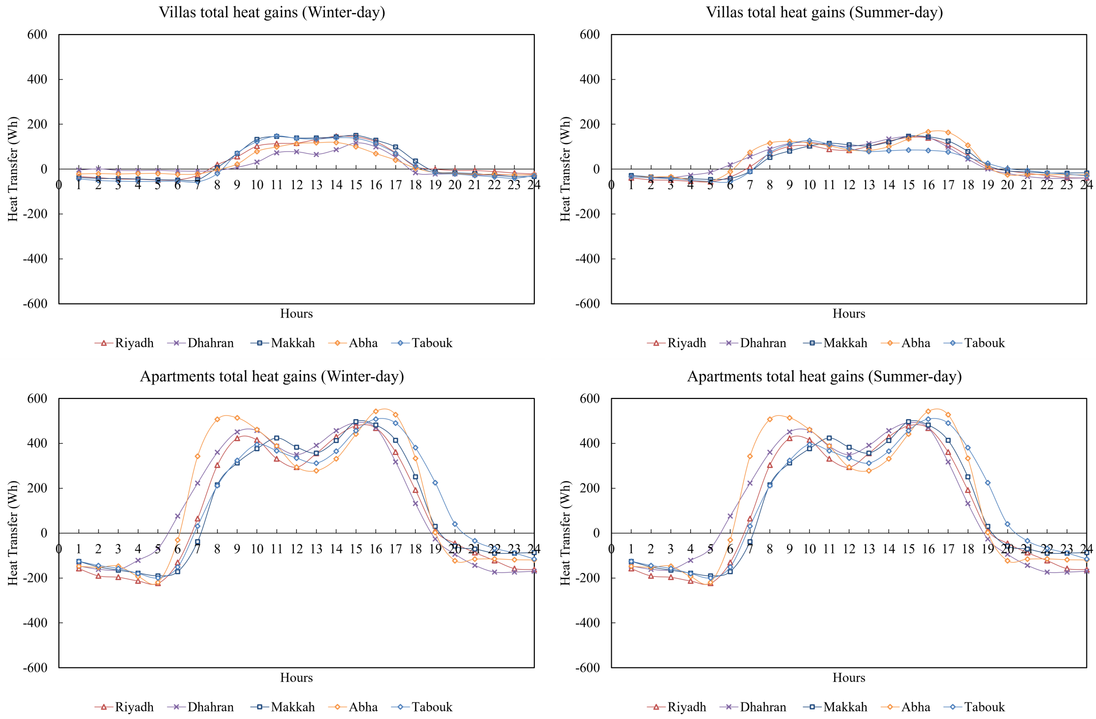

FIGURE 6.5: Predicted external heat gains for the archetypes.

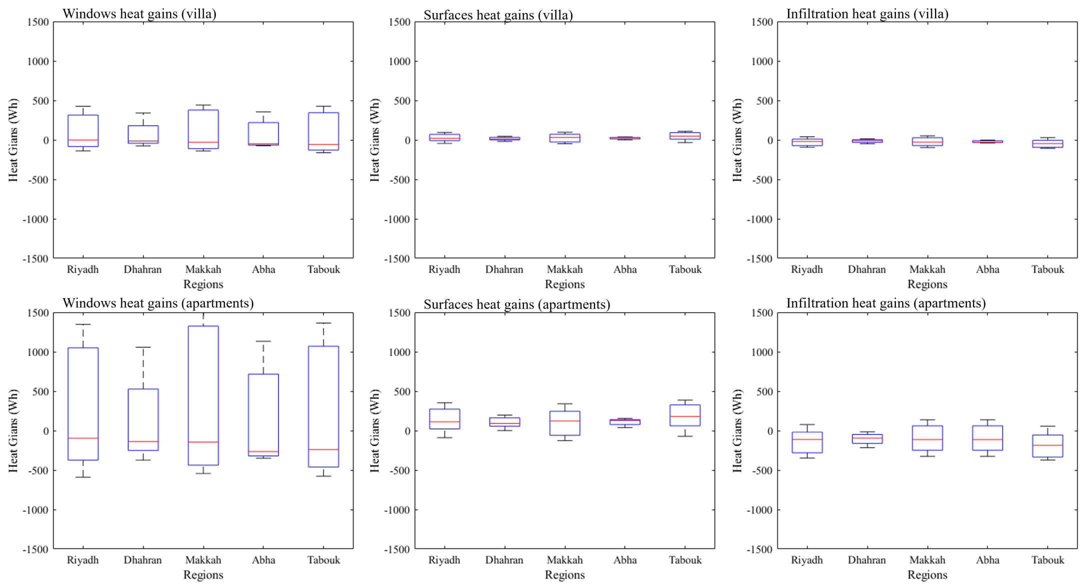

FIGURE 6.6: Predicted heat gain rates of the archetypes in the winter-day.

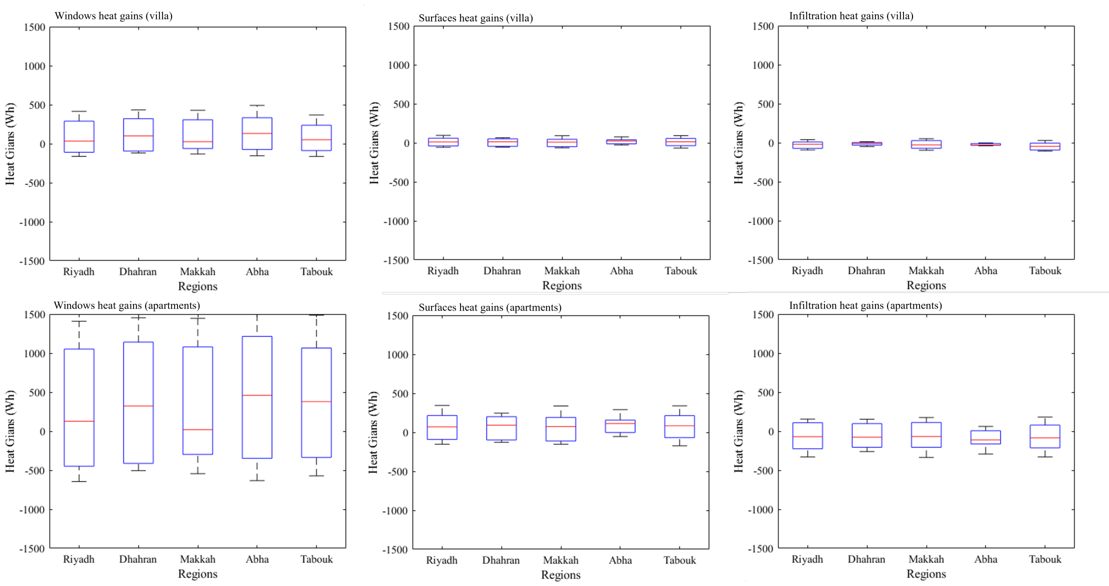

FIGURE 6.7: Predicted heat gain rates of the archetypes in the summer-day.

6.1.2.2 Internal heat gain sources

Internal heat gain sources include lighting, equipment and occupancy, and they account for varied proportions of convective, radiant and latent gains (McMullan, 2017). According to the surface's heat balance, convective gains are immediate rises in the temperature of the zone's air (DoE, 2020). Radiant gains are dispersed throughout the zone's surfaces, where they are initially absorbed and subsequently reflected into the thermal zone. In addition, cooling systems can control latent gains from people. Hashim et al. (2018) defines latent heat gains as 'the energy added to the space when moisture is added to the space by means of vapor emitted by the occupants, generated by a process or through air infiltration from outside or adjacent areas'. Electrical equipment contributes to 69% of total internal heat gains, followed by people with 16% and lighting with 15%. See Figure 6.8. Electrical equipment internal gains are the highest due to the application of systems with higher power densities in the KSA's dwellings, which impacts internal heat gains and raises the IAT. People's internal heat gains are far less due to the number of occupants in each dwelling, six people, while the lighting is lower because it has lower power density due to the use of more efficient lightbulbs than the literature's average and equipment. See Figure 5.6 (p. 139).

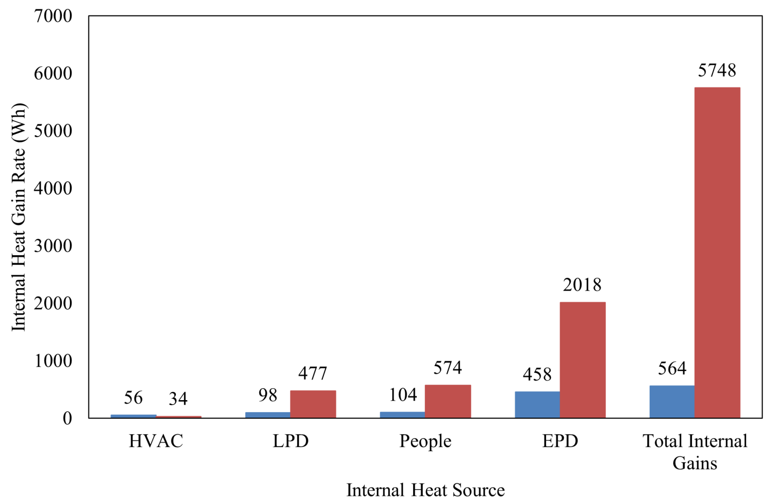

FIGURE 6.8: Predicted internal heat gain rates for the archetypes.

6.1.3 Air temperature

Summertime air temperatures in the KSA's regions are generally high, whether outdoor or indoors, and this is also observable in the literature (Krarti et al., 2020; Aldalbahi, 2020; Algarni and Nutter, 2013a). Figure 6.9 depicts the most frequently predicted OAT for Riyadh and Dhahran is 31°C, whereas Abha, Tabouk and Makkah's most frequent OATs are 20, 25 and 32°C, respectively. See Figure A.7 in the Appendix A for individual histograms for each city. Riyadh, Dhahran and Tabouk have the widest range of OAT data variances, while Makkah and Abha have the shortest. The box plot in Figure 6.10 presents predicted OATs for the five regions of the KSA. The top and bottom bars represent the highest and lowest OAT values, respectively, while the middle bar indicates the mean value, (μ). The blue box represents one standard deviation (σ) from the mean. High variances are witnessed across the predicted data with values exceeding 45°C except in Abha, where the OAT never surpasses 34 due to its semi-arid climate, which is influenced by a higher altitude than the rest of the regions.

Generally, OATs and IATs have a direct linear positive relationship, as seen in Figure 6.11. See Figure A.8 in Appendix A for individual relationships in all regions. The increases in OAT result in warmer air accessing buildings and, therefore, raising the IAT. Even though the villa archetype has more surfaces exposed to direct sunlight, it has lower IAT than apartments everywhere due to the KSABC's thermal

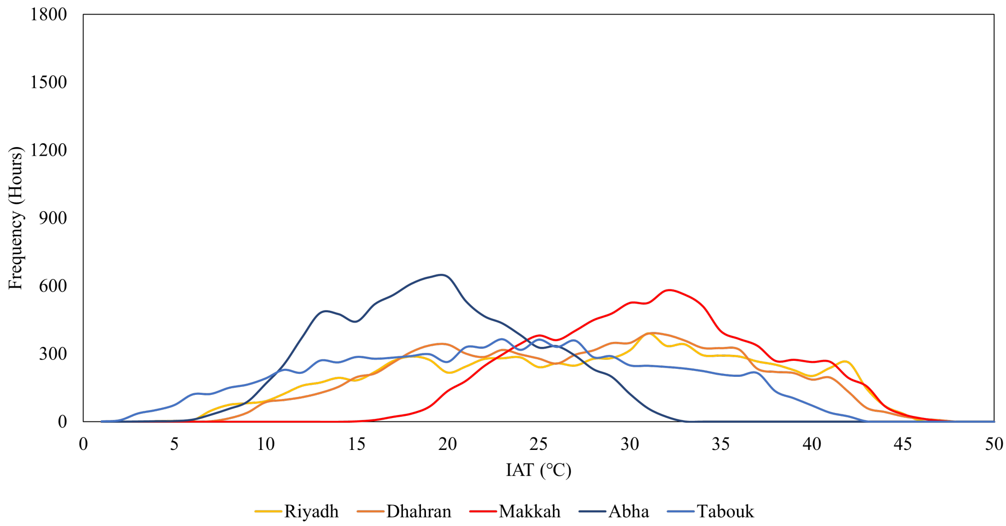

FIGURE 6.9: Predicted frequency of OAT for the five regions of the KSA.

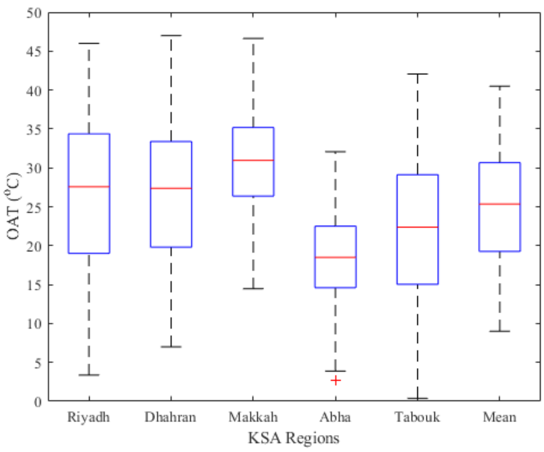

FIGURE 6.10: Predicted OAT of the five regions of the KSA.

insulation requirements for exterior walls.

The predicted data have no modes for both archetypes in all regions. Hence, line charts may be employed to describe the dispersion of the most frequently occurring values for IATs. Figures 6.12 and 6.13 show the predicted IATs for the archetypes in the five regions. On one hand, the most frequent IATs for the villa archetype in Abha, Tabouk, Dahran, Makkah and Riaydh are 26, 33, 37, 38 and 39°C, respectively. On the other hand, the most frequent IATs for the apartment archetype are 32, 40, 43, 44 and 45°C for Abha, Tabouk, Dhahran, Makkah and Riyadh, respectively. Riyadh and Dhahran have the largest data dispersion while Makkah and Abha have shorter ranges of data. See Figures A.9 and A.10 in Appendix A for histograms and more

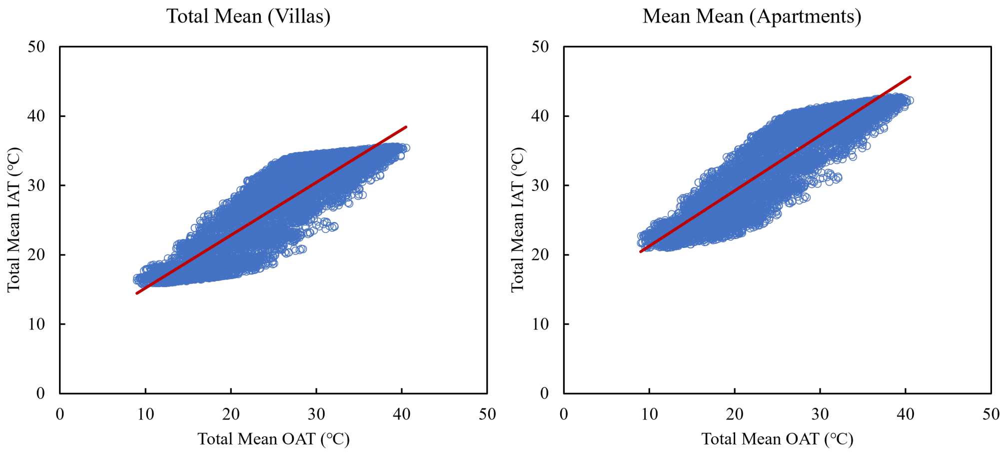

FIGURE 6.11: Predicted total mean IATs and OATs of the KSA housing stock.

details.

Figure 6.14 presents temperature predictions for the entire year in the five regions and the total mean. The dotted line signifies the KSABC requirement for IAT (Saudi Building Code, 2018). It shows that both archetypes have higher mean IATs than the required cooling setpoint of 20°C. The mean IATs for the villa are less than the apartments in the five regions. Makkah has the highest mean IAT of 32.5 and 38.8°C for the villa and the apartments, respectively, and Abha has the lowest mean IAT of 23.9 and 28.6°C for the villa and the apartments, respectively. Figure 6.15 compares hourly OATs and IATs without systems for the archetypes in the regions. The cooling setpoint required by the building code is shown by the dashed black line. Abha has better indoor and outdoor environmental conditions compared to the rest of the regions. However, the indoor environment of the other regions is extremely uncomfortable most of the year. Not only is cooling required during the summertime, but heating is also required during wintertime for all regions except Makkah. This elevated IAT is influenced by the surface temperatures of the envelope.

6.1.3.1 Surfaces' temperature

The surfaces' temperatures instate to the internal or external face temperature of the surfaces, °C. The surface heat transfer variables are arranged around the interior and

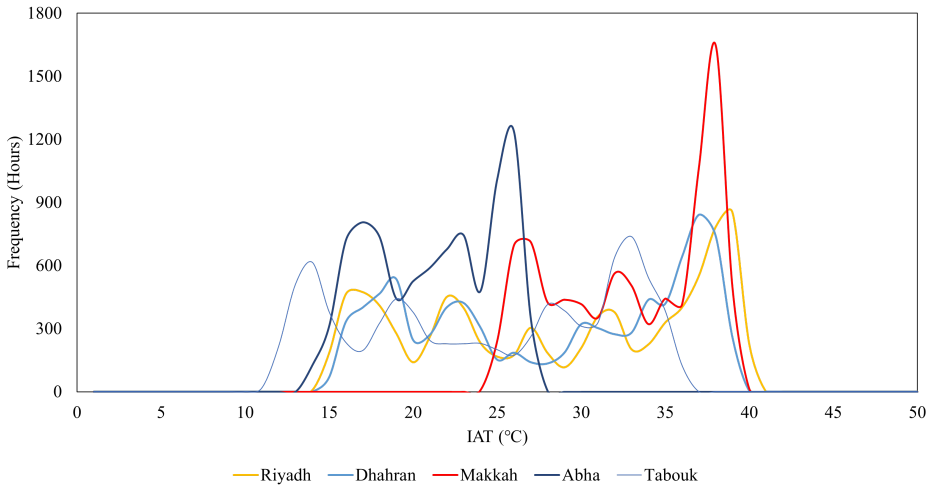

FIGURE 6.12: Predicted IAT frequency for the villa.

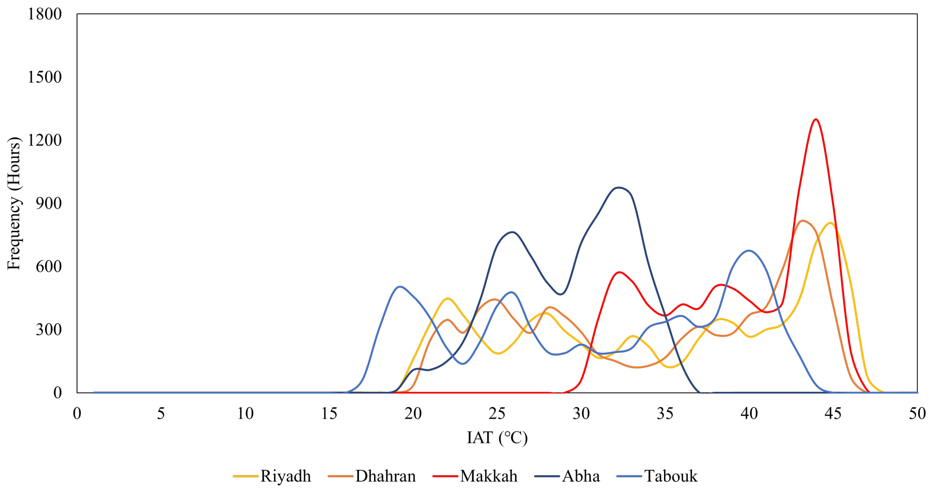

FIGURE 6.13: Predicted IAT frequency for the apartments' building.

exterior faces of each surface. The zone heat balance model creates energy balances on each face, resulting in two sets of findings for every surface.

Information about surfaces' temperatures in the KSA's building envelope is missing, neither evaluated individually nor as part of an energy performance analysis. Only one study in the KSA has considered the inner surface temperatures of buildings; it was conducted through actual measurements of three cases in three regions (Alwetaishi et al., 2017). The study only considered inner face surface temperatures, while the outer surface temperatures that receive heat from the sun were not included. Involving the outer surface in such a study is essential for three major reasons. It quantifies the time lag and the delay in the heat transfer between the surfaces. It indicates the difference between the conduction of both

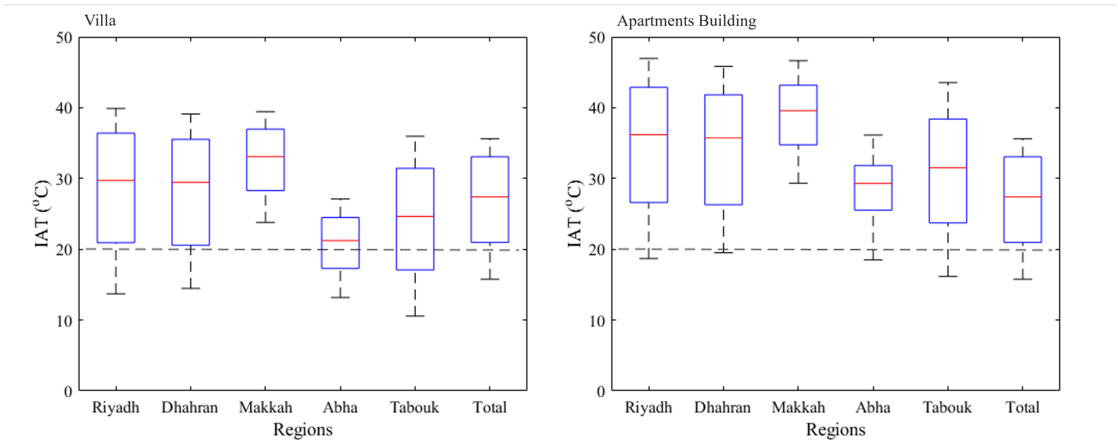

FIGURE 6.14: Predicted IAT of the archetypes.

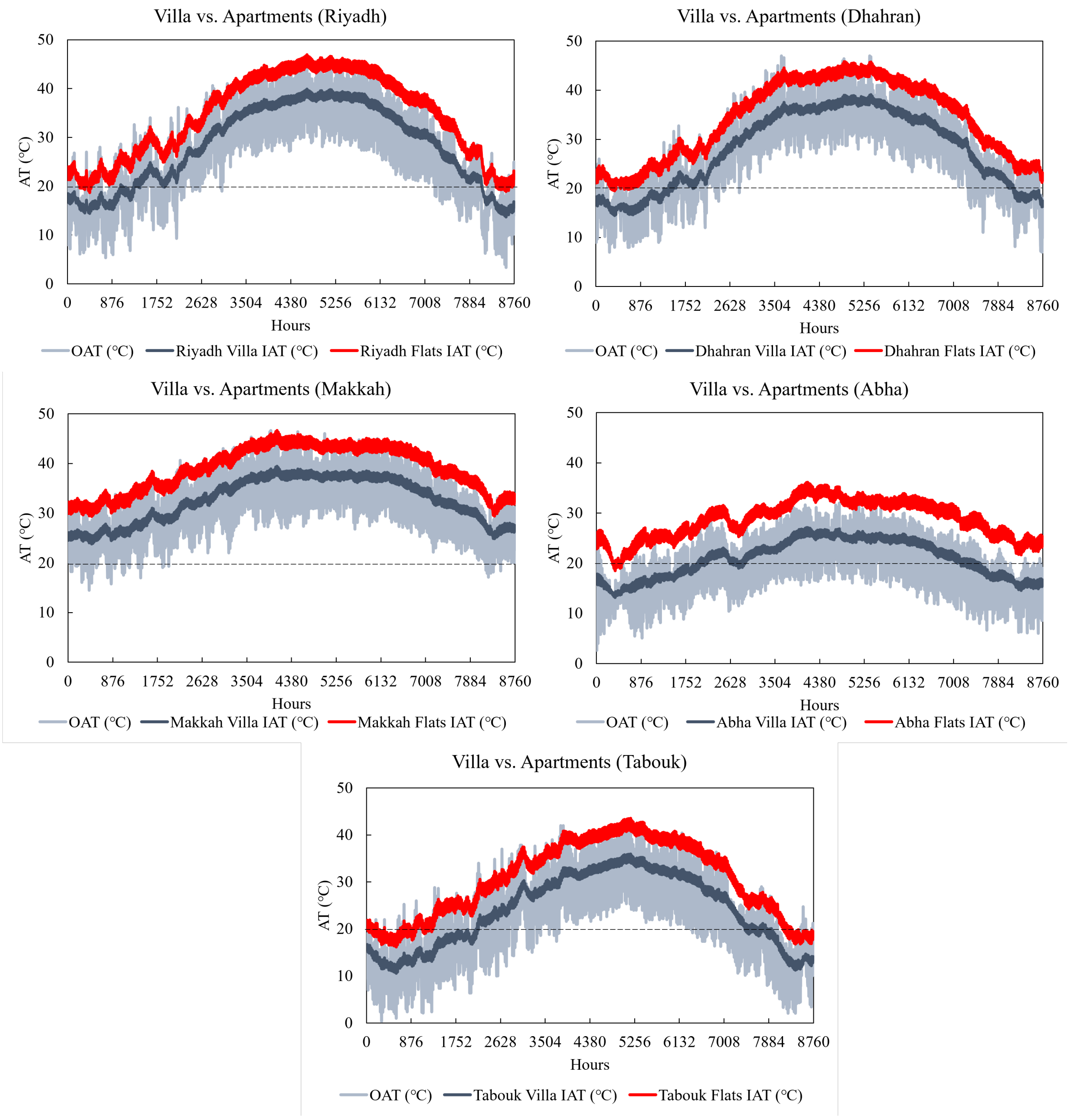

FIGURE 6.15: Predicted hourly IATs for the archetypes located in five regions of the KSA.

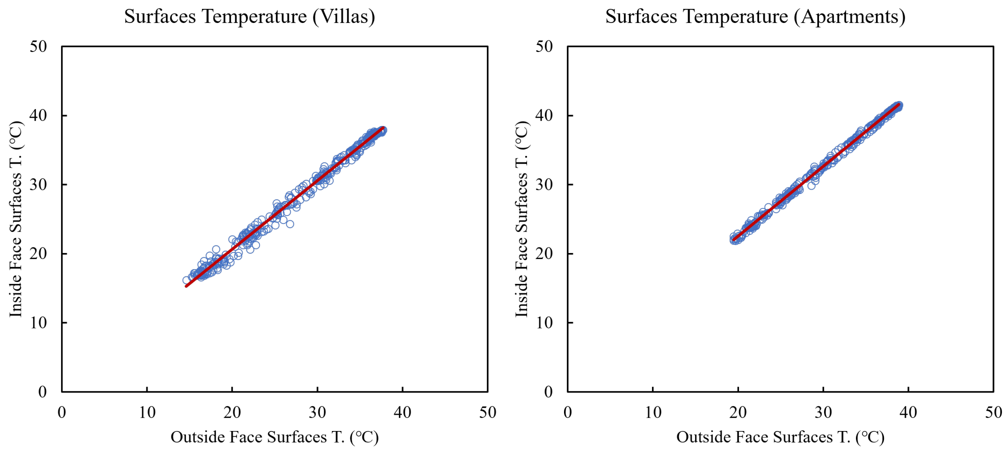

FIGURE 6.16: Linear relationships between surfaces faces temperatures.

surfaces, and it calculates how much heat is gained from the sun. Increasing the outer surface face's temperature by solar radiation results in transferring an amount of this absorbed heat to the inner surface and warms it. Thus, the surface radiates, adds heat to the thermal zone and raises the space's mean IAT (Smargiassi et al., 2008).

The results of this research showed a strong linear relationship between surfaces' faces. If the exterior surface's face temperature increases, so does the internal surface's face temperature. See Figure 6.16; more details are shown in Figure A.12 in Appendix A. Figure 6.17 showcases that both surfaces' temperatures are similar in the five regions except Makkah, where it never drops below 22°C. Overall, the villa has lower surface temperatures than apartments. The villa's outside surface face temperatures (OSFT) are 35.4 and 39°C for Tabouk and Makkah, respectively, while it is 39.1°C for Riyadh, Dhahran and Abha, with a total mean of 37.7°C. The inside surface face temperatures (ISFT) are 35.2 and 38.7°C for Tabouk and Makkah, respectively, and 39.2°C for Riyadh, Dhahran and Abha, with a total mean of 37.9°C. On the contrary, the apartments' OSFTs are 31.4, 39.6 and 42.2°C for Abha, Tabouk and Dhahran, whereas it is 43.1°C for Makkah and Riyadh, with a total mean of 38.9°C. The ISFCs are 34.6, 42.1, 44.5, 45.2 and 45.6°C for Abha, Tabouk, Dhahran, Makkah and Riyadh, respectively. The surface temperature has a direct correlation with the operative temperature.

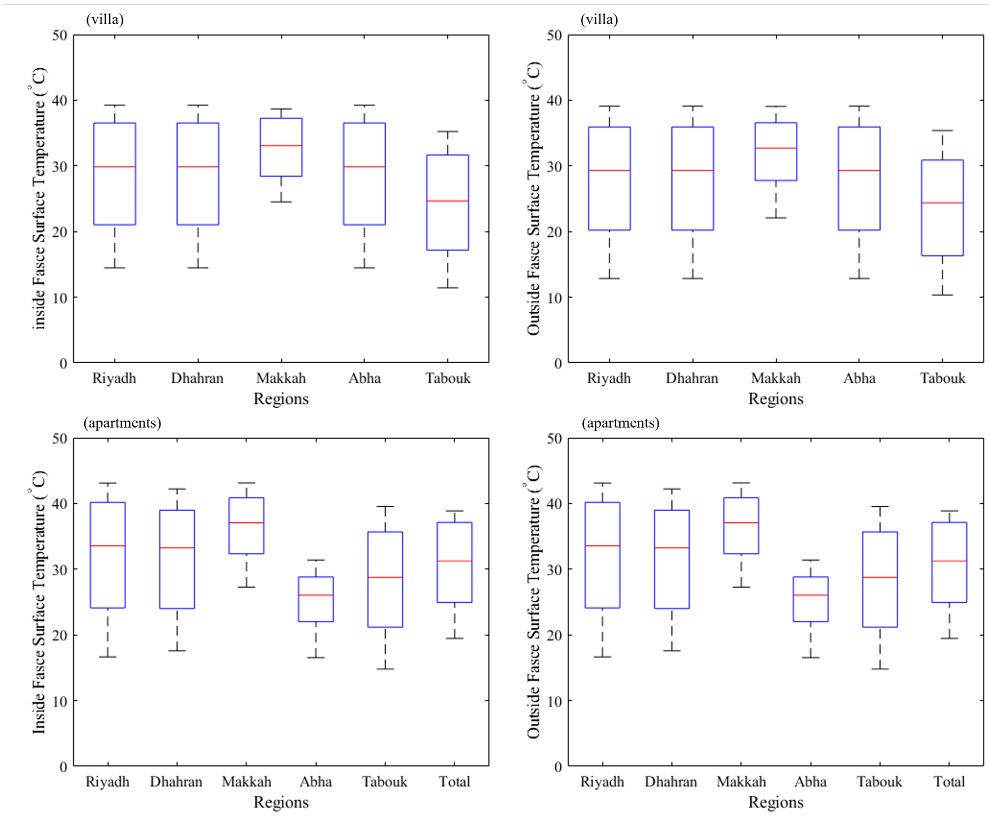

FIGURE 6.17: Predicted relationships between IFST and OFST for the archetypes located in five regions.

6.1.3.2 Operative temperature

The *operative temperature* (OPT) is the sum of the zone's mean air temperature (MAT) and mean radiant temperature (MRT) divided by two. See Equation 6.1. It is a simplified measurement that can be utilised to evaluate the thermal comfort of human occupancy. Real thermal comfort models have two types of influential variables. First, environmental variables include IAT, OAT, air velocity, RH and human behaviour. Second, personal factors involve clothing value, metabolic rate, human adoption and health conditions. Researchers have investigated OPT to develop thermal comfort models (Auliciems, 1981; De Dear and Brager, 1998a; De Dear and Brager, 1998b; Nicol and Humphreys, 1973; Nicol and Humphreys, 2002; Nicol and Humphreys, 2010; Humphreys et al., 2013). They rely on positive linear regression models related to IAT and OPT to achieve acceptable human thermal comfort and to predict OAT. In this research, a strong positive relationship was detected between IAT and OPT. See Figure 6.18. The OPTs of the archetypes in the five regions of the KSA are generally thermally uncomfortable and presented

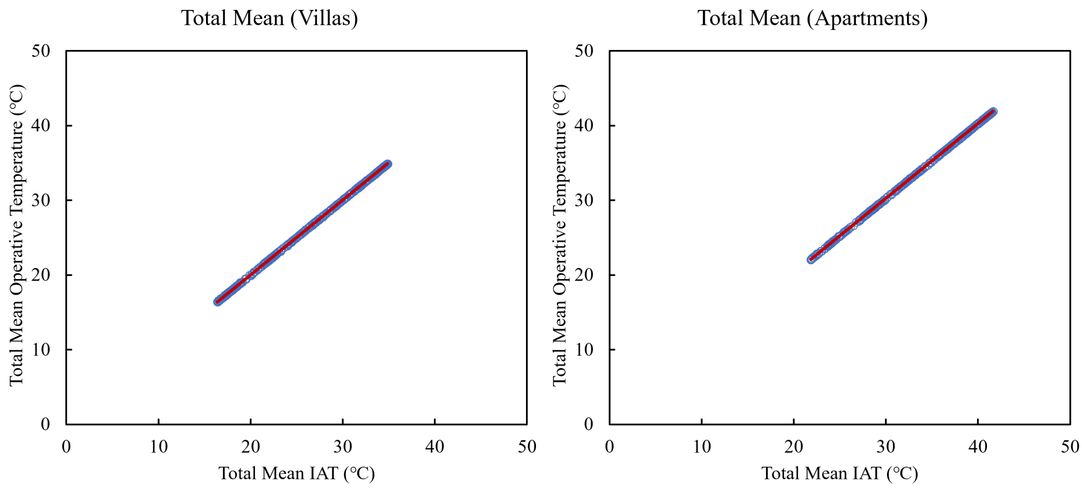

FIGURE 6.18: Linear relationships between IAT and OPT for the archetypes located in the five regions.

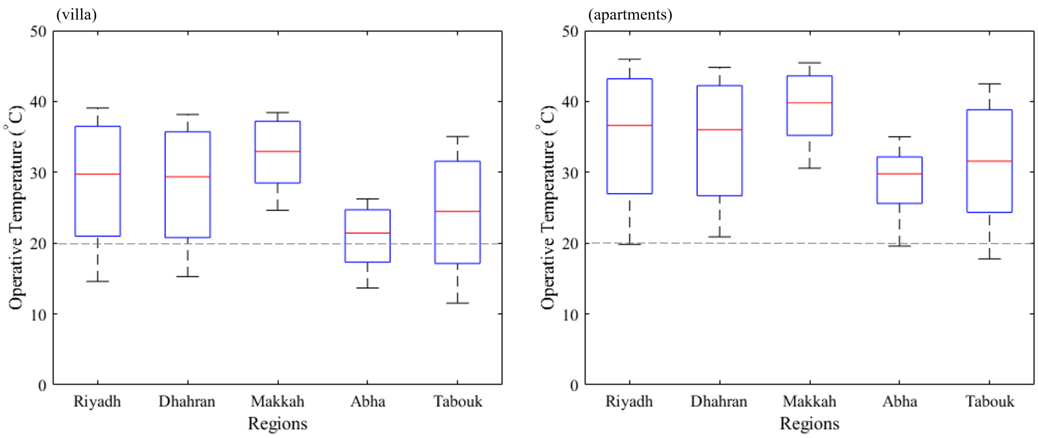

FIGURE 6.19: Predicted operative temperatures for the Archetypes.

in Figure 6.19. See Figure A.13 in Appendix A for more information. Achieving occupants' thermal comfort in the KSA's dwellings requires HVAC systems to meet the cooling setpoint required by the building code.

$$OPT = (MAT + MRT) \div 2 \tag{6.1}$$

6.1.4 Cooling and heating loads

The KSABC states that all occupied spaces in dwellings must have a fixed thermostat setpoint of 20°C (Saudi Building Code, 2018). This is to ensure that indoor occupied spaces are thermally comfortable and habitable, but this conflicts with Krarti et al. (2020). They applied two air-conditioning setpoints for the villas and the

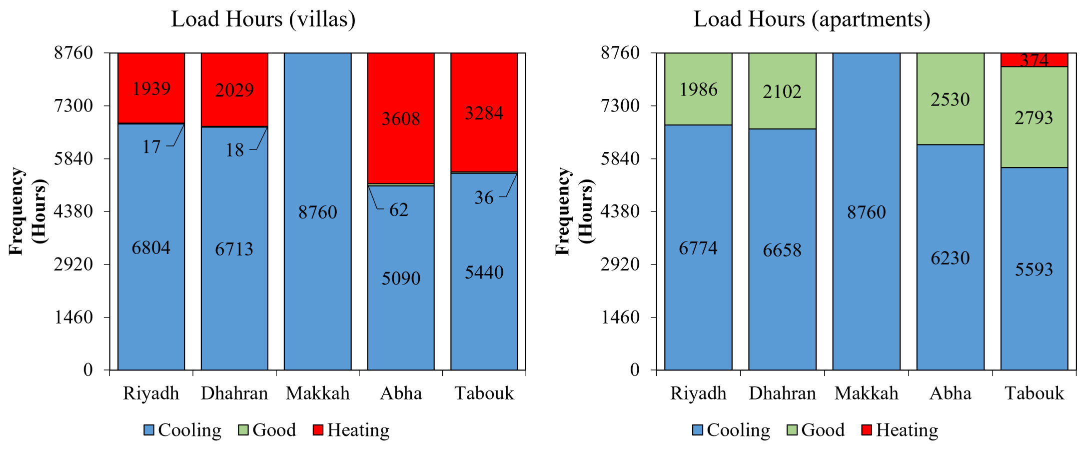

FIGURE 6.20: Cooling and heating hours for archetypes.

apartments: 23 and 24°C, respectively. In the KSA, having higher cooling setpoints reduces energy consumption because indoor spaces are extremely hot most of the year. See Figure 6.14 (p. 171).

Setting the model's cooling setpoint to 20°C following the building code, one can predict cooling or heating loads during a full typical year. The villa requires cooling or heating all year long to maintain acceptable indoor conditions, while apartments only require cooling in the hot seasons. The blue and red areas in Figure 6.20 represent cooling and heating hours, respectively, while the green area represents the cofortable hours. The green Apartments do not require heating mostly everywhere; nevertheless, their cooling consumption is high. Table 6.3 statistically compares the cooling or heating hours with associated energy loads. The villa achieves an acceptable IAT only if the HVAC system is running for cooling or heating purposes, while apartments do not require cooling or heating systems for about 25% of the time. The Makkah region, though, needs cooling the entire year, and no heating is required for both building types. The cooling system might be impacted by various building parameters due to the influences of IAT, and this demonstrates the importance of sensitivity analyses to evaluate the most influential factor for energy performance.

6.1.5 Sensitivity analysis

This section applies a sensitivity analysis to critical parameters of energy performance that are usually assumed or ignored by research.

TABLE 6.3: Predicted hours for energy loads for the KSA housing archetypes.

Archetype	Villa				Apartments Building			
Region	Cooling	Good	Heating	Energy load (kWh)	Cooling	Good	Heating	Energy load (kWh)
Riyadh	6804	17	1939	12678	6774	1986	0	29463
Dhahran	6713	18	2029	11355	6658	2102	0	38327
Makkah	8760	0	0	9247	8760	0	0	29603
Abha	5090	62	3608	3880	6230	2530	0	20376
Tabouk	5440	36	3284	5576	5593	2793	374	22486
Mean	6561	27	2172	8547	6803	1882	75	28051
SD	1444	24	1422	3743	1188	1101	167	7069
Min	5090	0	0	3880	5593	0	0	20376
Max	8760	62	3608	12678	8760	2793	374	38327

6.1.5.1 Envelope

In general, the envelope of the KSA's housing stock is a high thermal mass with a total thickness of 200 mm, as shown in Figure 4.21 of Section 4.3.4. The high heat capacity of the thermal mass causes a time lag for the heat transfer between the outer and inner surfaces, which varies IAT. This is because varying proportions of heat require more time to be absorbed by the outer surface, transferred to the inner surface and radiated to the thermal zone (Yu et al., 2022). Therefore, a sensitivity analysis was conducted in this research to reveal parameters' uncertainties and to investigate the most influential variables regarding heat transfer. The sensitivity analysis found a strong positive relationship between IAT and the building's total thermal mass. Figure 6.21 conveys a strong relationship between IAT and the total thermal mass proportion in both seasons. As a greater number of interior or exterior walls' increase, IAT rises for the five regions. Having more interior walls increases heat-storage elements in the dwellings, and this heat is absorbed and radiated to the indoor spaces, which raises IAT. This is also displayed in Figure 6.22, where a similar positive relationship appears when increasing the exterior wall's thickness in all regions in both seasons.

Increasing the thermal mass quantity or thickness results in a similar positive correlation. This indicates that adding more thermal mass to a building increases its ability to store more heat. Furthermore, integrating the conduction difference between the inner and the outer surfaces clarifies the envelope's capability to store heat. A positive value indicates that heat is being added to the surface mass and vice versa. A direct strong correlation is noticeable where raising the concrete thickness

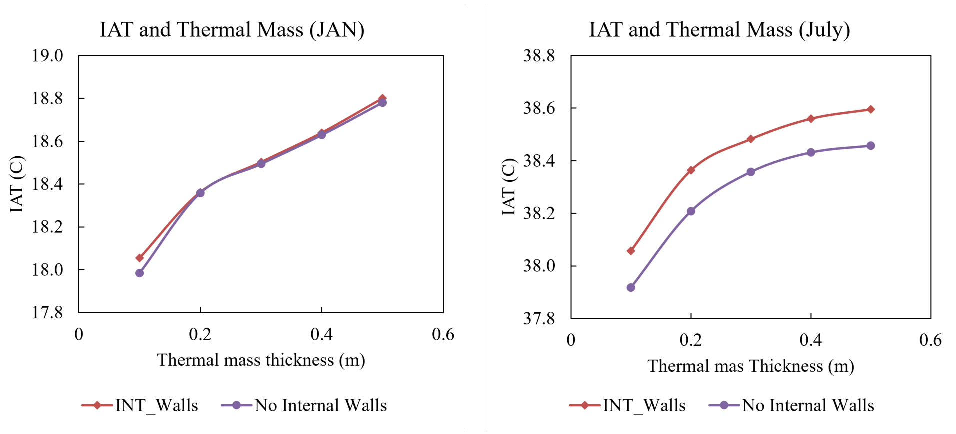

FIGURE 6.21: The sensitivity of IAT and extras interior walls.

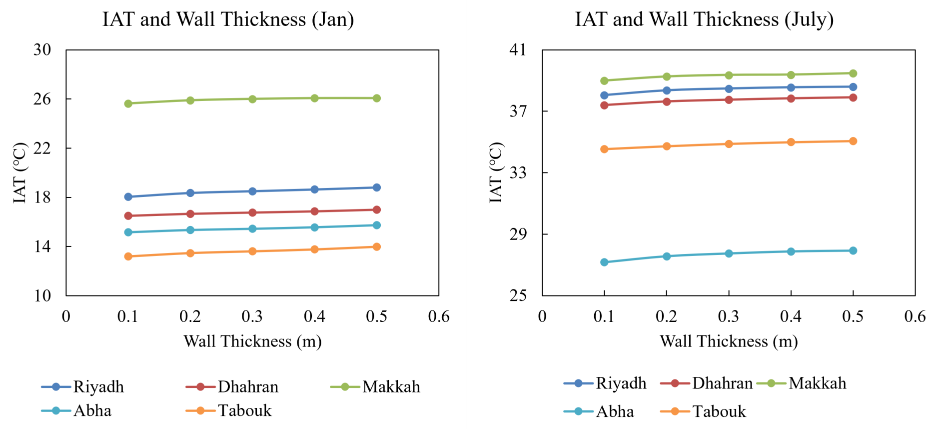

FIGURE 6.22: Sensitivity of IAT and thermal mass in the five regions.

results in increasing its ability to store more heat and, accordingly, raises the IAT. See Figure 6.23. The model is sensitive to other parameters including ground temperature.

6.1.5.2 Ground temperature

The GT is a critical parameter for investigating buildings' energy behaviour, as described in Section 5.2.6.1 of Chapter 5. There is a clear data scarcity about GT in the KSA and globally, and this may be due to the complexities of ground floor heat transfer and soil modelling techniques (Shi et al., 2021).

Testing the sensitivity of GT is essential, as it determines the sufficient values for proper energy performance assessments. The sensitivity analysis of GT in this research showed a significant impact on IAT and, consequently, cooling loads. Figure 6.24 presents the simulations performed for two days with extremely

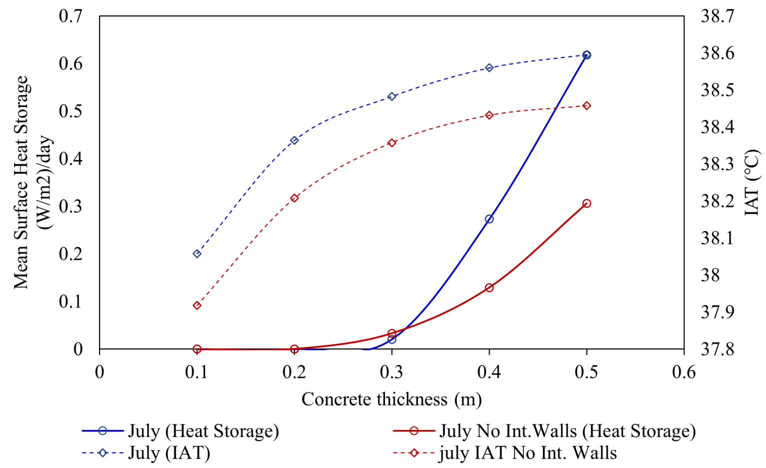

FIGURE 6.23: Envelope heat storage, concrete thickness, and IAT.

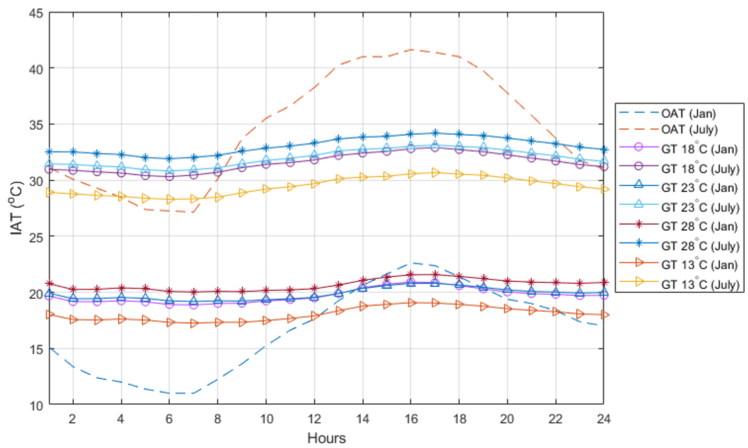

FIGURE 6.24: Sensitivity analysis of GT impacts on IAT.

different climate conditions, hot and cold. It emphasises the uncertainty of converting GT values, and it results in inconsistent model outputs. Here, most building energy research in the KSA does not identify or involve GT in the analysis process (Bahel et al., 1985; Bahel et al., 1989; Kinsara et al., 1996; Budaiwi and Al-Homoud, 2001; Almutairi et al., 2015), and this will be discussed in Section 7.3.2 of Chapter 7. This becomes more critical when using the EnergyPlus tool, because it assumes the GT value to be an undistributed 18°C all the time (DoE, 2020), and this can be observed in studies including Matar et al. (2013) and Krarti et al. (2020). However, the mean values of GT of the KSA's cities reveal that the peak GT for the entire year is in July, while the lowest GT is in January due to weather conditions. See Figure 6.25. An additional sensitive parameter that may have a significant influence on buildings' energy performance is the rate of air infiltration.

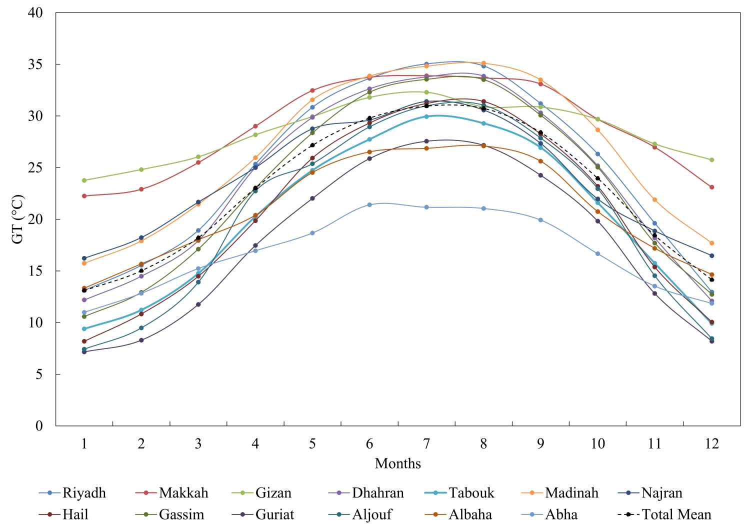

FIGURE 6.25: Ground temperature for the five KSA regions.

6.1.5.3 Infiltration rate

According to the literature review, infiltration rates are mostly assumed among researchers without considering their uncertainty and impact on energy loads. Only one study was found that considers the impact of infiltration rate on energy loads in the KSA. However, the study is outdated, and it does not represent the current housing stock (Said and Al-Hammad, 1993). Moreover, infiltration rate values conflict among researchers. Krarti et al. (2020) assumed an infiltration rate of 0.8 ACH for all buildings, while Said and Al-Hammad (1993) assumed a range of values, including 0.5, 0.75, 1 and 1.25 ACH. This illustrates significant uncertainty; consequently, a sensitivity analysis was performed.

The simulations in this section were performed for two days. The sensitivity was preliminarily applied to the baseline without thermal envelope insulation to capture airflow rates' uncertainties. Figure 6.26 reveals a negative relationship between IAT and infiltration rates. Increasing the airflow rate results in reducing the IAT. Nonetheless, by performing the same analysis on the KSABC-compliant baseline, one may observe the divergence in IAT. See Figure 6.28. Varying infiltration rates display critical IAT fluctuations, which directly impact energy loads. Furthermore, monotonic relationships are described to compare average IATs with a range of infiltration rates. See Figure 6.27. A reverse negative proportional relationship was noticed, and the curves of both days were fitted separately to link the data

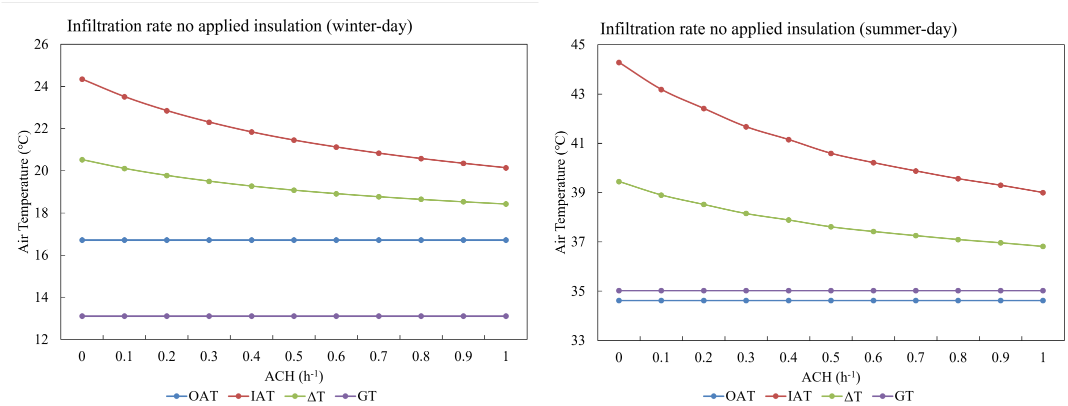

FIGURE 6.26: Predicted sensitivity influence of infiltration rates to IAT.

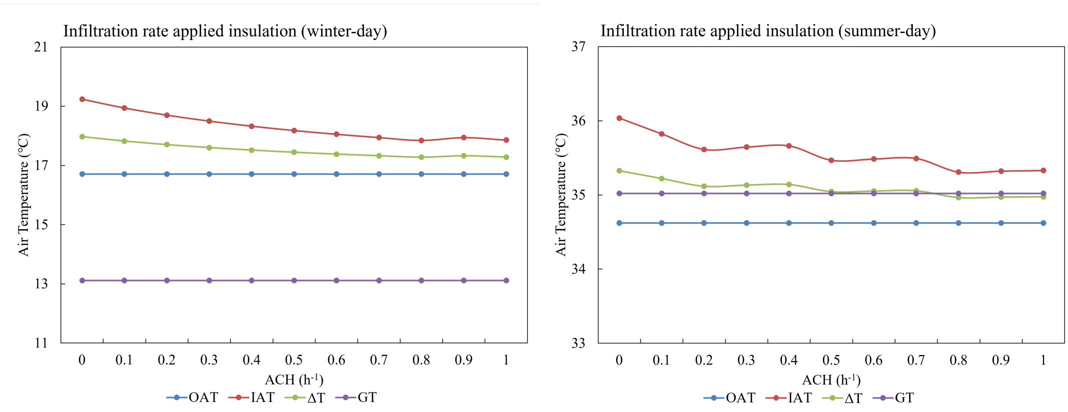

FIGURE 6.27: Predicted sensitivity influence of infiltration rates to IAT with thermal insulation.

points. Curves were split using spline interpolations and a polynomial line. The linear relationship only depicted the direction of the data. Nevertheless, as the infiltration rate increases, the IAT decreases for both days, and vice versa. The variations of the IAT in July are due to the application of 75 mm thermal insulation on the envelope. Thermal conductivity is non-linearly related to the temperature difference and causes a thermal mass lag. An individual airflow modelling approach is preferred, so DOMVENT3D_KSA is developed in Section 5.3 and the reported result is documented in Section 6.4.

The KSABC requires an infiltration rate value of 0.2 (h^{-1}) for all climate zones, and this value was applied to the energy baselines. This value is tight and more sufficient; however, the type of residential units and climatic zones should be considered.

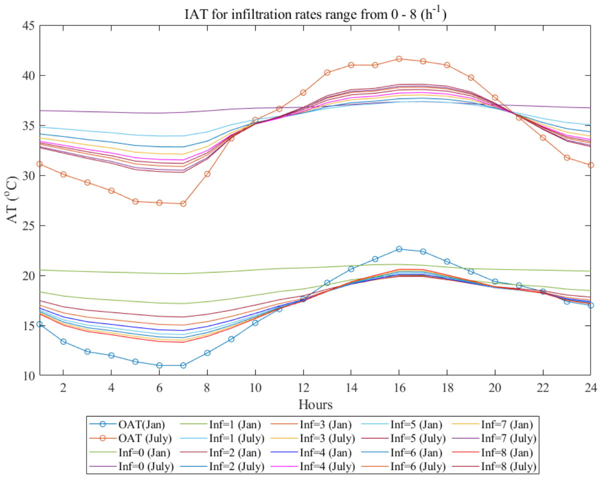

FIGURE 6.28: Variations of IAT to different infiltration rates.

6.1.6 The baselines energy use

The Sankey chart in Figure 6.29 was generated by adopting a systematic approach starting by collecting related energy performance data from the KSA housing sector using reliable and governmental resources to construct the data set, see Chapter 4. Followed by analysing the data to identify essential parameters that directly effect the energy consumption of the housing stock. These typical parameters involve cooling, heating, lighting and equipment energy use. This allows the use of a coding tool known as RStudio (Field et al., 2012) with the energy performance of actual buildings for data visualization by mapping out the energy flow among the parameters and the housing type. This formation provided clear and concise elaboration of the energy baseline model and highlighted the contributions of each housing type and there typical components energy performance.

The Sankey chart depicts the energy use of each housing archetype in the KSA's major regions. It demonstrates that the apartments use about 1,335 TWh of the total energy demands, and this is more than the villas, with 169.3 TWh. Most energy is consumed by cooling energy and accounts for 1,029 TWh. This is followed by equipment (329 TWh), lighting (76 TWh) and heating energy (0.3 TWh), respectively. This emphasises the need for reducing cooling energy by applying various energy retrofitting schemes.

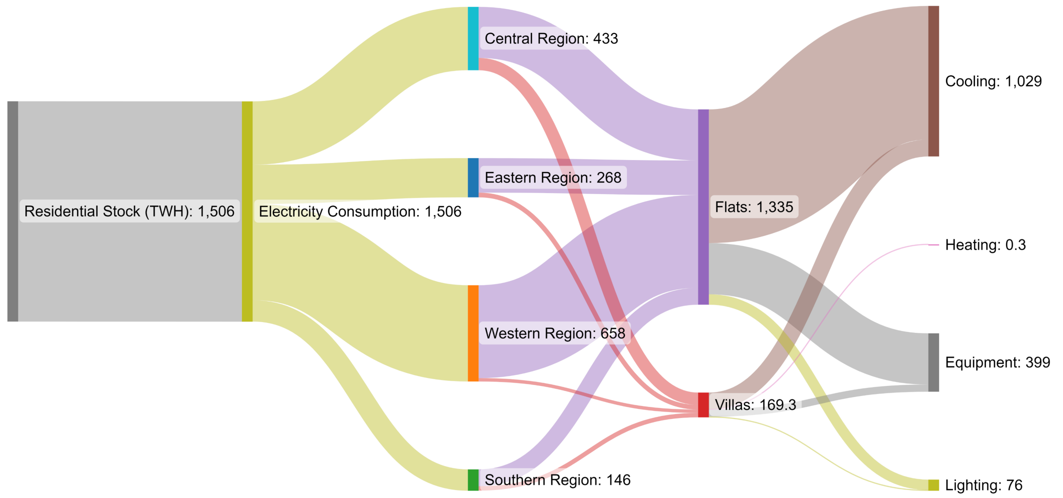

FIGURE 6.29: Sankey chart of the KSA housing archetypes.

6.2 Energy efficiency retrofitting measures

This section applied energy-efficiency retrofitting measures (EERMs) to the archetypes' energy baselines to reduce energy demands, costs and CO_2 emissions and, thus, meet the research's overall aim. The analysis was conducted for two extremely different weather conditions: a winter's day in January and a summer's day in July. The EERMs were initially applied individually to ensure energy performance reductions and capture the exchanging effects on energy use and IAT. This individual application is finally integrated with the most efficient EERM of each type to obtain the total energy reduction. Section 6.2.1 addresses the results of thermal insulation implementation on the exterior surfaces of the envelope. Section 6.2.2 describes lowering the IAT by applying exterior shading on the thermal envelope. Section 6.2.3 presents the quantity of energy production by applying a photovoltaic system on the exterior shadings. Section 6.2.4 highlights the installation of ENERGY STAR-certified light-emitting diode (LED) lighting and equipment appliances to reduce the dwellings' energy demands.

6.2.1 Thermal insulation

Thermal insulation is the first EERM that has been applied to the baselines. The thermal insulation involves the five most common types in the KSA: board, batt, cellular glass (GC), fibre glass (FG) and polystyrene (PO), with five varied thicknesses each. The baseline has an applied board thermal insulation of 0.75 mm

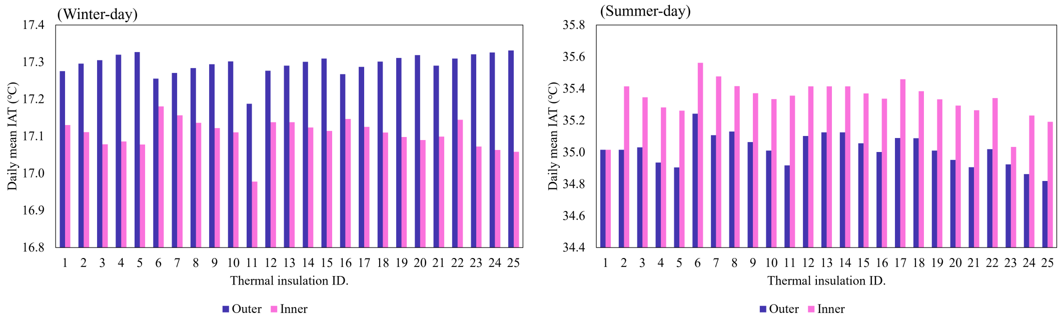

FIGURE 6.30: Sensitivity of envelope thermal insulation location.

on the exterior surfaces, and this insulation thickness is varied and associated with each insulation type, resulting in a total insulation thickness of 100, 125, 150, 175 and 200 mm. The location of the thermal insulation was not specified by the KSABC (Saudi Building Code, 2018). Therefore, a sensitivity analysis of the optimal location was performed. Figure 6.30 conveys the placement of five thermal insulation types with their five additional thicknesses on the exterior and the interior surfaces of the envelope. It resulted in a total of 100 simulations for the outer and inner surfaces of the envelope. Placing the insulation on the outer surface of the envelope performed more efficiently in terms of lowering IAT in the summer and maintaining relatively higher IAT in the winter. Furthermore, a negative reverse relationship was discerned between thermal insulation thickness and U-value. See Figure 6.31. As the thermal insulation thickness increases, U-value decreases; obtaining a lower U-value reduces the heat transference to the indoors. The regressions in Figure 6.32 evaluate the correlation between wall thicknesses and IAT; it illustrates a linear relationship, meaning that increasing the thicknesses of the thermal insulation results in lower IAT.

Figure 6.33 conveys the optimal thermal insulation for both archetypes and for two extreme designing days. The five thicknesses of the five types of thermal insulation have been individually employed at the baselines to allow IAT evaluations. The thermal insulation increases with each run by 25 mm, and this process is repeated for the five regions by varying the insulation type, thickness and housing archetype for the two days. This resulted in (5 (insulation types) · 5 (insulation thicknesses) · 5 (regions) · 2 (housing archetypes) · 2 (days)) 500 separate simulations. On one hand, the most achievable optimal IATs are attained by using

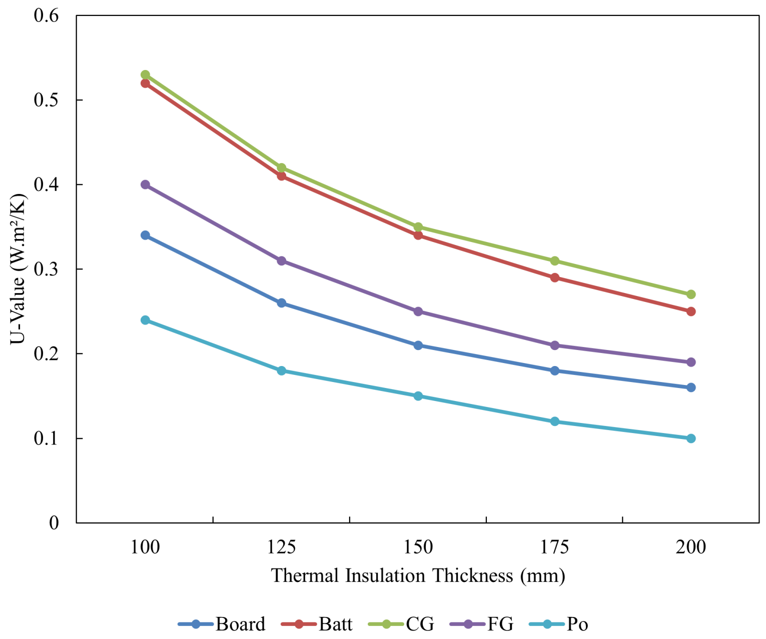

FIGURE 6.31: Sensitivity of thermal insulation U-Values.

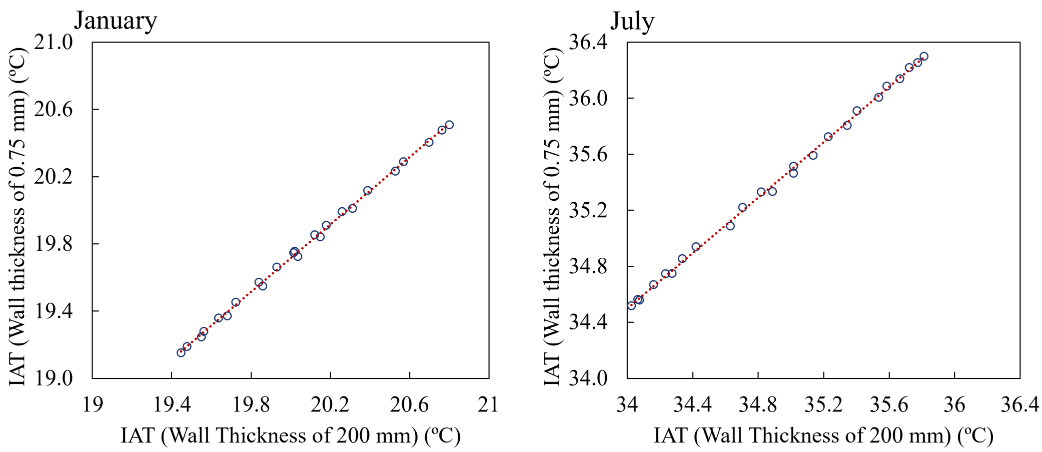

FIGURE 6.32: Linear relationship for wall thicknesses.

TABLE 6.4: predicted IATs of the optimum thermal insulation (PO) applications.

	Villa		Apartment	
Region	Winter-day (°C)	Summer-day (°C)	Winter-day (°C)	Summer-day (°C)
Riyadh	20	37.7	21	35.9
Dhahran	19.2	34.9	20	36.5
Makkah	23.8	35.5	24.5	37.1
Abha	17.8	24.8	19.3	25.9
Tabouk	15.3	31.8	16.4	33.4

the PO thermal insulation type of 200 mm for the villa archetype, and it reveals the coldest IAT is 15°C in January in Tabouk while it is 24.8°C in July in Abha. On the other hand, the optimal IATs for the apartments in January is 16.4°C for Tabouk, while in July, it is 25.9°C in Abha. See Table 6.4. The PO insulation cannot reduce the IAT of the archetypes in Makkah to less than 23.8 for all seasons.

6.2.2 External shading

External shading is one of the most effective EERMs due to the high solar radiation that strikes the building's envelope most of the year, as described in Section 6.1.2. According to Waheeb (2005), the KSA experiences high solar radiation, and shading can reduce energy demands depending on buildings' orientation, vegetation, trees and location. This section describes the implementation of exterior shadings on the exterior surfaces of the envelope to reduce energy demands, cost and CO_2 emissions, which answers the research aim.

The implementation of external shadings for both archetypes involved eight identities for each, which are shown in Figures 6.34 and 6.35. Each shading system has been analysed individually to capture its effects, after which the optimal application is chosen. Primarily, the application started by blocking the glazed areas from the sun, but the effect was negligible due to the small WWR the buildings possess. Hence, the application of external shading was applied to the envelope rather than windows only. External shadings (8) were applied to every housing archetype (2) for each region (5) for two days (2), resulting in $(8 \cdot 2 \cdot 5 \cdot 2)$ 160 individual simulations.

Figure 6.36 compares the IAT of all exterior shading systems' applications for both housing archetypes. Overall, the external shading ID7 was determined for the archetypes' application as the optimal shading system because it allows natural

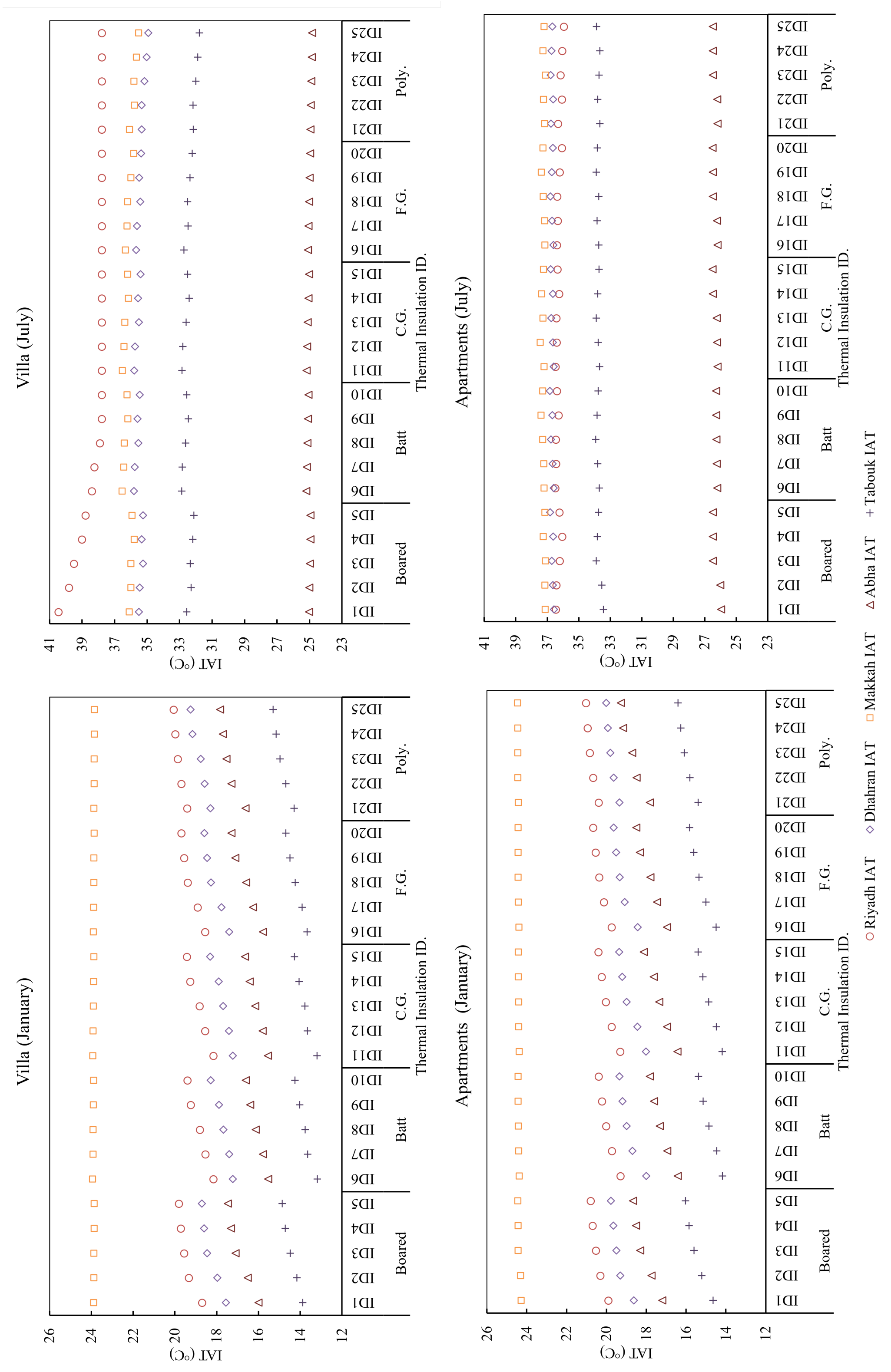

FIGURE 6.33: Predicted IAT for thermal insulation applications on the archetypes for two days.

light and vision. The villa's ID7 shading lowers the mean IAT of the winter day in the Makkah region from 23.9 to 23.1°C, while it drops it from 36.1 to 35.2°C of the summer day. Apartment buildings' ID7 shading reduced the winter-day mean IAT from 24.2 to 23.2°C, while it decreased the summer-day IAT from 37.1 to 36.1°C. This illustrates that Makkah buildings in the summer must have air-conditioning systems running most of the time to meet the KSABC's cooling setpoint. See Table 6.5 in Appendix A.

The application of ID7 shading to the villa and apartment building in Riyadh lowered the January IAT from 18.6 and 19.8 to 18 and 18.7°C, respectively, while it decreased the July IAT from 35.6 and 37.1°C to 34.7 and 34.9°C, respectively. The Dharan villa and apartments' archetypes behaved similarly when applying the ID7 shading; it reduced the winter IAT from 17.5 and 18.6°C to 17.2 and 18.1°C, respectively, while it lowered the July IAT from 35.5 and 36.5°C to 34.7 and 35.3°C, respectively. Dhahran has high levels of humidity because it is on the coastline. Adding ID7 shading to the archetypes in Abha achieved the highest daily IAT reductions because Abha has the highest solar radiation rates on exterior surfaces. The villa and apartment building IATs lowered from 16 and 16.9°C to 15.3 and 15.7°C, respectively. The IATs of July dropped from 25 and 25.8°C to 24.1 and 24.7°C, respectively. Tabouk has the lowest IAT in only January, while it has a relatively high IAT in July. Adding ID7 shading decreased the villa and the apartments' January IATs from 13.8 and 14.4°C to 12.6 and 12.9°C, respectively, while it reduced July IATs' from 32.5 and 33.4°C to 31.3 and 32.2°C, respectively. This exterior shading system may be utilised for installing the PV panels.

6.2.3 Photovoltaic

Photovoltaics (PV) is an intriguing strategy for utilising solar radiation to generate electricity that can be stored, transferred or credited to the customer (Irena, 2017). The primary motive behind its application in the KSA is to exploit the local climatic conditions for blocking solar radiation from striking buildings' envelopes utilising this free solar energy for usable electricity that feeds back to the building. The PV systems in the KSA have an observable positive impact on energy use, cost and CO_2 emissions and, hence, meet this study's aim.

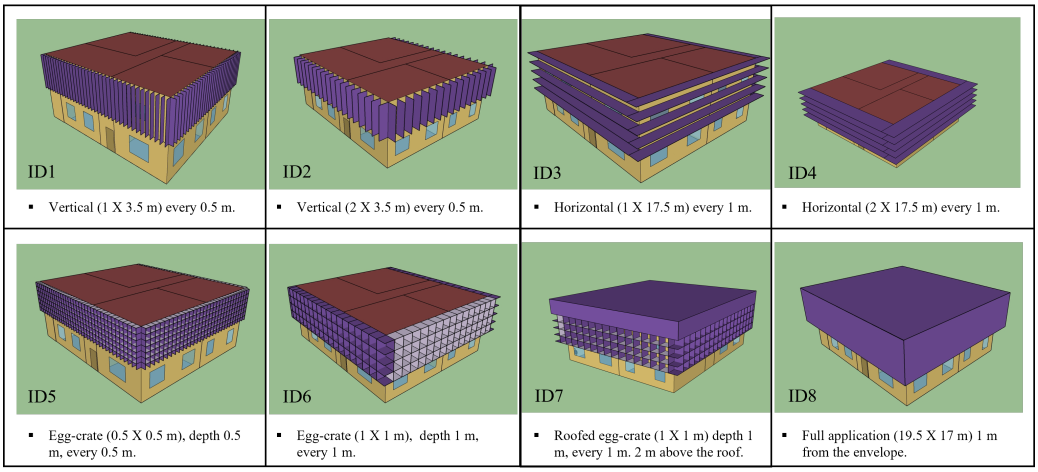

FIGURE 6.34: Eight external shading systems applications on the Villa Unit.

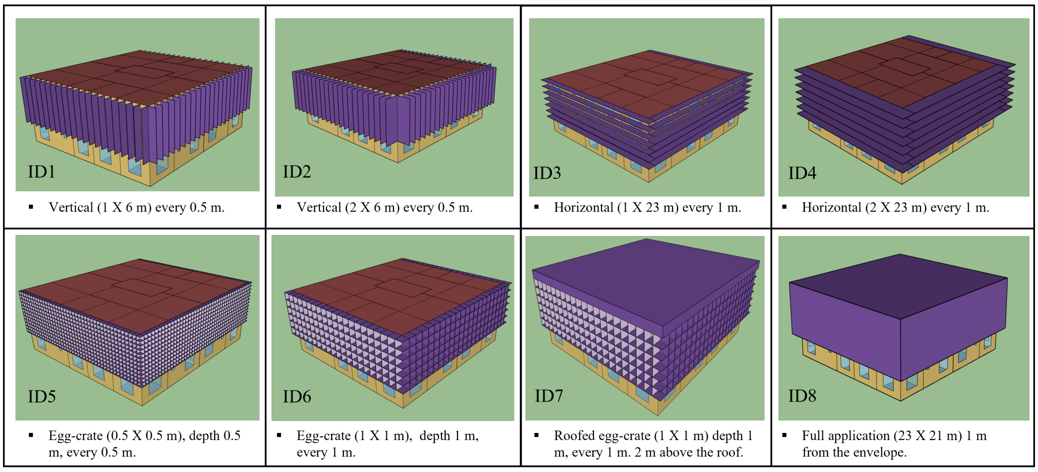

FIGURE 6.35: Eight external shading systems applications on the apartments building.

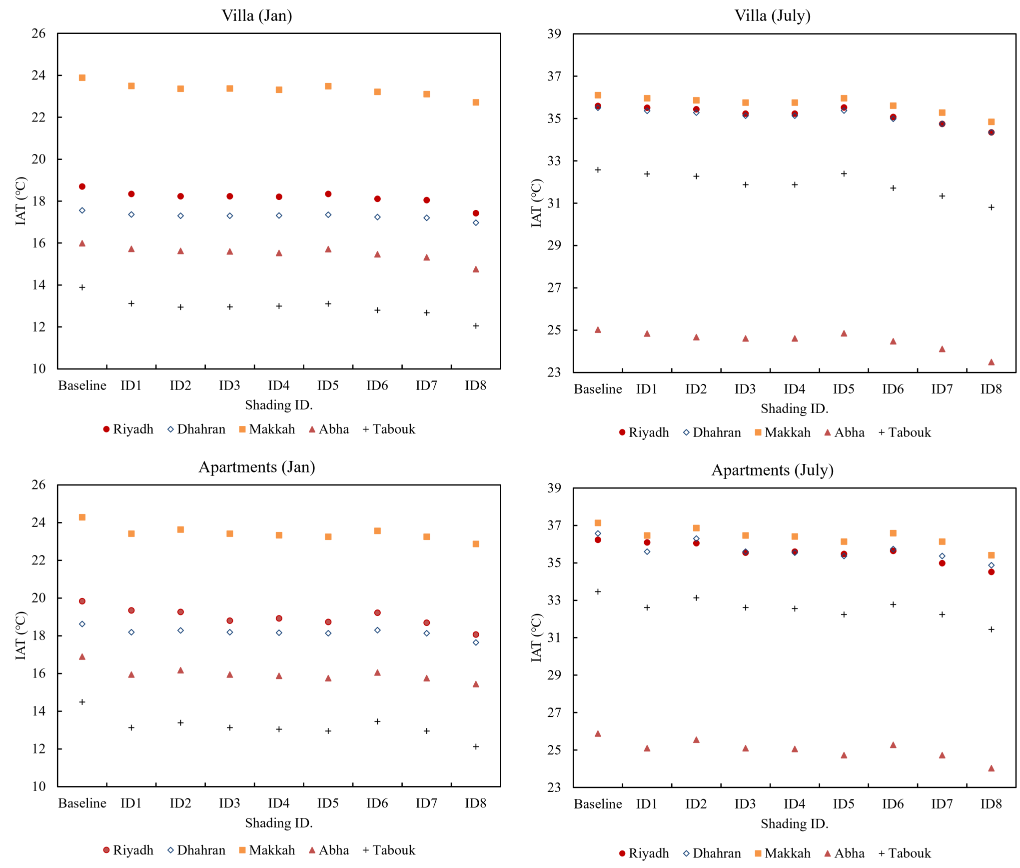

FIGURE 6.36: Predicted IAT for the exterior shading systems applications on the archetypes.

TABLE 6.5: Predicted IAT for external shading system applications on the Archetypes.

	ID	Baseline	ID1	ID2	ID3	ID4	ID5	ID6	ID7	ID8
		Villa IAT (°C)								
Villa (winter -day)	Riyadh	18.70	18.35	18.24	18.23	18.21	18.34	18.10	18.05	17.42
	Dhahran	17.56	17.36	17.30	17.31	17.31	17.35	17.24	17.21	16.97
	Makkah	23.90	23.51	23.38	23.38	23.33	23.50	23.23	23.11	22.73
	Abha	16.00	15.72	15.62	15.61	15.52	15.71	15.47	15.32	14.76
	Tabouk	13.89	13.11	12.95	12.96	13.00	13.10	12.79	12.67	12.06
Apartments (winter -day)	Riyadh	19.84	19.35	19.26	18.80	18.93	18.73	19.22	18.70	18.07
	Dhahran	18.62	18.19	18.29	18.19	18.16	18.14	18.30	18.14	17.65
	Makkah	24.29	23.41	23.63	23.41	23.33	23.25	23.57	23.25	22.87
	Abha	16.90	15.95	16.18	15.95	15.88	15.75	16.05	15.75	15.44
	Tabouk	14.49	13.13	13.39	13.13	13.05	12.95	13.46	12.95	12.12
		Apartments IAT (°C)								
Villa (summer -day)	Riyadh	35.61	35.53	35.45	35.24	35.24	35.53	35.09	34.76	34.35
	Dhahran	35.53	35.38	35.30	35.14	35.14	35.39	35.00	34.77	34.35
	Makkah	36.12	35.97	35.87	35.76	35.76	35.97	35.63	35.29	34.86
	Abha	25.03	24.84	24.67	24.61	24.61	24.85	24.48	24.11	23.49
	Tabouk	32.57	32.38	32.28	31.87	31.87	32.39	31.71	31.34	30.81
Apartments (summer -day)	Riyadh	36.23	36.09	36.06	35.54	35.60	35.48	35.65	34.98	34.52
	Dhahran	36.58	35.61	36.30	35.61	35.55	35.37	35.74	35.37	34.87
	Makkah	37.13	36.46	36.86	36.46	36.41	36.14	36.58	36.14	35.40
	Abha	25.88	25.10	25.54	25.10	25.05	24.73	25.27	24.73	24.03
	Tabouk	33.46	32.62	33.14	32.62	32.56	32.25	32.78	32.25	31.44

It is scientifically proven that the sensitivity of the electrical efficiency of solar panel cells is influenced by cells' temperature (Zhang et al., 2012). There is a negative reverse relationship; increasing cell temperature leads to decreasing electrical efficiency. See Figure 6.37. Raising the cell temperature by 1 K results in an efficiency reduction by 0.25%–0.5% depending on the type (Brinkworth et al., 1997; Krauter et al., 1999; Kalogirou and Tripanagnostopoulos, 2006). Furthermore, the overall energy efficiency of the PV cells can reach 45%, and this was tested in a controlled environment at standard test conditions (STC). This does not depict the real application of the panels under variable weather conditions. The PV system is extremely effective against climatic factors involving dust, temperature and moisture (Tyagi et al., 2013).

In contrast, a modest PV system was constructed in the KSA and recorded 18% energy efficiency (Bahaidarah et al., 2015). This 18% efficiency was applied to the archetypes of this research by installing PV panels on exterior shadings. This demonstrates that Abha has the largest proportion of energy production due to high solar radiation rates compared to other locations, and the rest of the locations behaved similarly. A roof surface receives the highest amount of solar radiation and is, therefore, the highest energy producer.

Figure 6.38 indicates possible quantities of electrical energy generated from the sun. Overall, a roof's mean electrical energy production is the highest compared to all other envelope surfaces with 14 and 20 kWh, respectively. This accounts for about 81% and 77% of total PV systems' energy production for the villa and apartments, respectively, which is not massive due to the low cell efficiency and the small application area. The rest of the surfaces generated much less energy due to solar radiation's striking angle on the PV unit and its orientation. The rest of the villa and apartments' building surfaces generate energy at around 0.5 and 1 kWh, respectively. The horizontal applications of the PV system, for all regions and both archetypes, produced more energy than the vertical applications. The second-highest PV energy producer is the horizontal PV application on the eastern surfaces of the villa, while it is the horizontal PV application on southern surfaces for the apartment building. See Table 6.6.

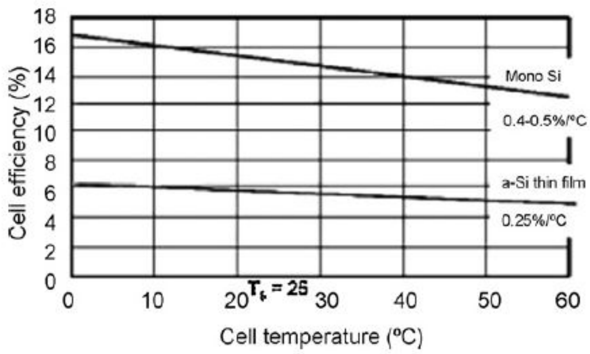

FIGURE 6.37: The relationship between Cell Temperature and Efficiency (Zhang et al., 2012).

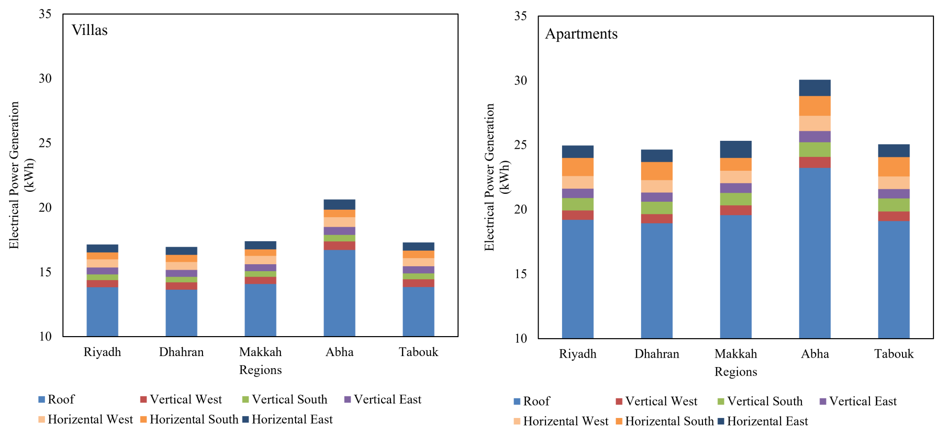

FIGURE 6.38: Electrical power generation from the photo-voltaic system and orientation.

TABLE 6.6: Predicted energy production by the PV system.

Months	Roof	Vertical Surfaces (kWh) West	South	East	Horizental Surfaces (kWh) West	South	East	Mean	Max	Min	SD.
Riyadh	13.83	0.56	0.44	0.54	0.62	0.54	0.62	2.45	13.83	0.44	5.02
Dhahran	13.64	0.56	0.43	0.54	0.62	0.55	0.62	2.42	13.64	0.43	4.95
Makkah	14.07	0.57	0.44	0.54	0.64	0.51	0.62	2.48	14.07	0.44	5.11
Abha	16.72	0.66	0.51	0.61	0.76	0.58	0.80	2.95	16.72	0.51	6.07
Tabouk	13.85	0.59	0.46	0.56	0.63	0.59	0.63	2.47	13.85	0.46	5.02
Mean	14.42	0.59	0.46	0.56	0.65	0.55	0.66	2.55	14.42	0.46	5.23
Max	16.72	0.66	0.51	0.61	0.76	0.59	0.80	2.95	16.72	0.51	6.07
Min	13.64	0.56	0.43	0.54	0.62	0.51	0.62	2.42	13.64	0.43	4.95
SD	1.29	0.04	0.03	0.03	0.06	0.03	0.08	0.22	1.29	0.03	0.47

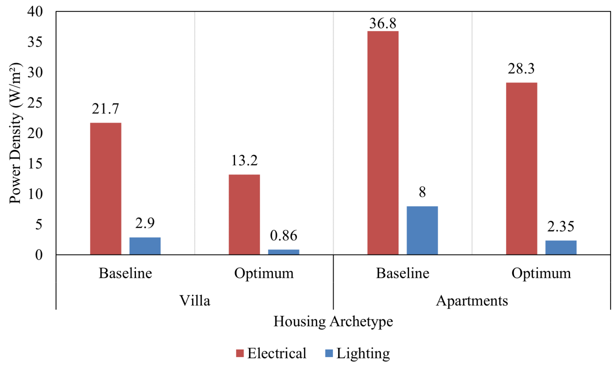

FIGURE 6.39: Lighting and electrical systems power densities reductions.

6.2.4 LED systems

Lighting and equipment power densities include simple and rapid adjustments to reduce energy demands, costs andCO_2 emissions. Thus, replacing the average installed lighting and equipment systems with LED appliances with efficient power densities may be desirable. This is done by converting the archetypes' systems to more efficient Energy Star appliances to evaluate possible energy reductions (Praprost et al., 2020). Figure 6.39 illustrates the power densities for electrical equipment and lighting for both archetypes. Table 6.7 summarises the applied Energy Star appliances, including operation hours and wattage for both archetypes.

In the villa archetype, lowering the mean lightbulb intensity from 2.9 (W/m^2) to 0.86 (W/m^2) reduces the villa's total mean energy use by about 19%, 22%, 25%, 27% and 51% annually for Makkah, Riyadh, Tabouk, Dhahran and Abha, respectively. Meanwhile, lowering the electrical power density from 21.7 to 13.2 (W/m^2) reduced energy demands by 27%, 31%, 35%, 36% and 60% for Makkah, Riyadh Tabouk, Dhahran and Abha, respectively. Integrating both low-power densities into the villa baseline reduces the corresponding stock's total energy use by μ = 40% with a σ = 13%. See Figure 6.40. Table A.5 in the Appendix A summarises energy reductions for all EERMs.

In the apartments, decreasing the lighting PD from 8 to 2.35 (W/m^2) lessened energy use by 35%, 36%, 41% and 45% for Abha, Makkah, Riyadh, Dhahran and Tabouk, respectively. Meanwhile, lowering the equipment PD from 36.8 to 28.3 (W/m^2) saved 38%, 42%, 43% and 47% for Makkah, Abha, Dhahran, Riyadh and Tabouk, respectively. Applying lighting and electric low PDs together reduces apartments' total energy demands by $\mu = 45\%$ with a $\sigma = 4\%$. See Table A.5 in Appendix A.

6.3 Total reductions

Section 6.3 integrates the application of the optimal EERMs to reduce energy demands and to offset usage by producing on-site energy. This section attempts to answer the fifth research question by comparing the achievable energy, cost and CO_2 reductions of the housing archetypes with the optimal energy models. The baselines were constructed according to the KSABC, which is efficient. This makes reducing energy and cost a more challenging task as it may already have applied most EERMs. For example, double-pane windows were already applied to the energy baseline to achieve the U-factor and SHGC values given by the KSABC or the installation of the envelope thermal insulation on the exterior surface. However, this section integrates the optimal EERMs to construct the optimal case for each housing archetype and region.

The optimal EERMs for each region and housing archetype are polystyrene thermal insulation of 175 mm applied on the exterior surface of the envelope, egg-crate external shading system, Energy Star lighting system and Energy Star equipment systems. The application of an egg-crate PV panel system generated a little energy compared to the consumed energy, so this reduced peak energy demands, electricity bills and the associated CO_2 emissions. See Figure 6.42. Table A.3 depicts individual and integrated applications of the EERMs over the five regions. It illustrates that the 200 mm of the polystyrene envelope's thermal insulation reduced mean energy use by about 9.5%, the external shading system decreased energy use by 14.7%, Energy Star lighting systems saved energy use by 32.5%, and Energy Star appliances conserved about 37.6% of the total energy use. Installing PV panels on external shading may produce small proportions of electrical energy of 0.16% and 0.07% of the total electrical energy use for the villa and the apartments, respectively. Integrating all the EERMs can reduce 42.6% and 36.9% of the villas' and apartments' total energy use yearly. The total mean energy savings

TABLE 6.7: Electrical and lighting power density for the archetypes.

ID	Name	KSA housing equipment Equipment/house (millions)	Mean equipment per house	Operation hours per day	Wattage (Wh) Baseline	Wattage (Wh) Optimum	Equipment Heat Gains (Wh) Average	Equipment Heat Gains (Wh) Annual
1	TV	8.2	2.2	6.1	150	15	9	75
2	Washer	5.7	1.6	1.1	700	500	37	327
3	Iron	4.7	1.3	0.7	1000	800	30	267
4	Vacuum	4.4	1.2	0.7	1500	650	23	204
5	Dishwasher	0.2	0.1	1.3	350	350	1	11
6	Water cooler	2.3	0.6	21.7	160	160	93	817
7	Water bum	3.7	1.0	1.7	350	350	25	221
8	PC	2.7	0.8	2.1	4000	2000	135	1182
9	Gaming devices	1.8	0.5	3.4	500	150	11	96
10	Other	9.3	2.5	2.6	1500	1000	273	2388
11	Electrical kettle	2.9	0.8	0.9	1200	1000	28	247
Total		46.3	12.6	42.4	11410	6975	666	5834
Villa Electrical Powere Density (W/m²)					21.7	13.29		
Apartments Electrical Powere Density (W/m²)					36.8	28.30		
Villa Lighting Powere Density (W/m²)					2.9	0.86		
Apartments Lighting Powere Density (W/m²)					8.0	2.35		

for the archetypes in the five regions may reach 39.8% of the total housing stock's energy use. Table A.4 summarises the five regions' energy use, electrical cost and CO_2 reductions. See Tables A.5 and A.6 in the Appendix A for more details.

6.3.1 Archetypes energy, carbon emissions and cost

The predicted energy savings of the housing archetypes in the five regions of the KSA are presented in Figures 6.40 and 6.41; the cost savings are presented in Figures 6.42 and 6.44. Carbon emissions are revealed in Figures 6.43 and 6.45.

Figure 6.40 compares the mean monthly energy use with individual and integrated applications of the EERMs, including PV energy generation. The mean predicted energy use shows that all housing archetypes in the five regions can reduce diverse amounts of energy. Most energy savings occur during the summertime due to extremely hot weather conditions. Figure 6.41 evaluates housing's energy use of the baselines and the optimal models. The predicted mean energy performance revealed that the energy use of the archetypes in the five locations behaved similarly, but Abha generally requires much less energy to obtain acceptable indoor conditions due to more comfortable weather conditions. Here, the predicted mean energy use reveals that the villa in Abha achieved the highest quantity of energy savings of 6,673 kWh/year (σ = 948 kWh/year), followed by the villas in Makkah, Dharan, Riyadh and Tabouk, with 5,240 kWh/year ($\sigma = 1,696$ kWh/year), 4,583 ($\sigma = 2,697$ kWh/year), 3798 ($\sigma = 2,788$ kWh/year) and 3,025 ($\sigma = 2,047$ kWh/year), respectively. The villa's savings are much less than the apartments' due to apartments' larger building size, which requires more energy load. The apartments' energy savings are 15,661 ($\sigma = 3,145$ kWh/year), 15,069 ($\sigma = 5,254$ kWh/year), 14,405 ($\sigma = 5,444$ kWh/year), 13,633 ($\sigma = 4,889$ kWh/year) and 7,944 kWh/year ($\sigma = 2,365$ kWh/year) for Makkah, Dhahran, Riyadh, Tabouk and Abha, respectively.

Table A.4 summarises energy, cost and carbon emission reductions for both archetypes in the five regions. The greatest yearly energy reduction of the villa is in Abha with $\mu = 61\%$ ($\sigma = 3\%$), cost savings of $\mu = 70\%$ ($\sigma = 1\%$) and CO_2 reductions of $\mu = 46\%$ ($\sigma = 3\%$). Consequently, more than half of the villa's energy use in Abha can be saved. The villa's second-greatest energy conservation is 40% ($\mu = 32\%$)

in Dhahran, with cost and CO_2 reductions of 66% and 37%, respectively. This is followed by Makkah, Riyadh and Tabouk, with energy savings of 40%, 37% and 35%; cost reductions of 48%, 43% and 42%; and associated CO_2 emissions reductions of 32%, 27% and 34%, respectively.

The apartments' energy savings in the five regions range from 32%−40% (μ = 35%, σ = 4%), while cost savings range from 35%−43% (μ = 38%, σ = 5%) and CO_2 emission reductions range from 25%−34% (μ = 32%, σ = 1%). The largest energy conservation of the apartments is 40% in Tabouk, with 43% cost savings and 34% CO2 emissions reductions. The apartments in Riyadh and Dhahran achieved similar energy and cost reductions of 36% and 39%, respectively. Riyadh and Dhahran's carbon emission reductions are 32% and 33%, respectively. The apartments' lowest proportions for energy conservation are 32% and 33% in Abha and Makkah, respectively, with cost savings of 35% for carbon emission reductions of 25% and 32%, respectively. The villas may save approximately 43% of mean energy use across the five locations, which is equivalent to 54% of cost savings and 34% of carbon emissions reduction. Meanwhile, the apartments may save approximately 35% of their energy consumption, 38% of their costs and 32% of CO2 emissions.

Additionally, the energy models may be extended to assess the total housing stock energy demands of the KSA by locating the archetypes in the rest of the KSA's regions. This requires setting the GT of each location. See Section 6.1.5.2, which applies the associated weather data.

6.3.2 The total KSA housing stock

The KSA's housing archetypal baselines may be used to establish the housing stock's energy model for the benchmarking and evaluation of the total energy demands of the stock. This requires locating the predicted archetypal energy baselines and the optimal models in all regions of the Kingdom with its associated weather data and setting the GT of each location. See Section 6.1.5.2. Table 6.8 and Figures 6.46 and 6.47 summarise the KSA stock model's baseline energy predictions and reductions. The highest energy savings was achieved in the Makkah region by reducing the total region's energy demands from 9.24 to 5.67 TWh, the total carbon emissions from 4

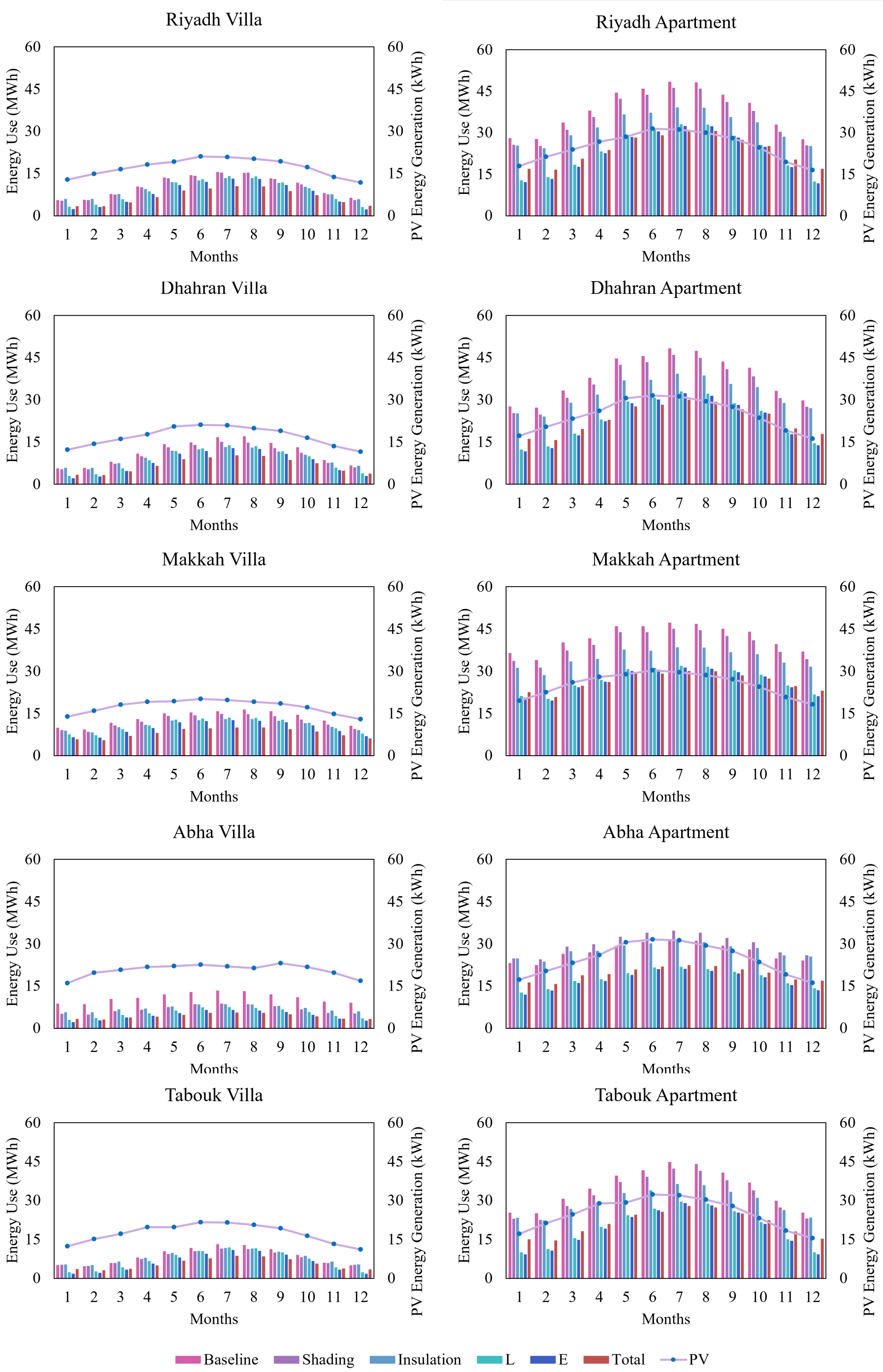

FIGURE 6.40: Predicted energy reduction for the KSA housing archetypes.

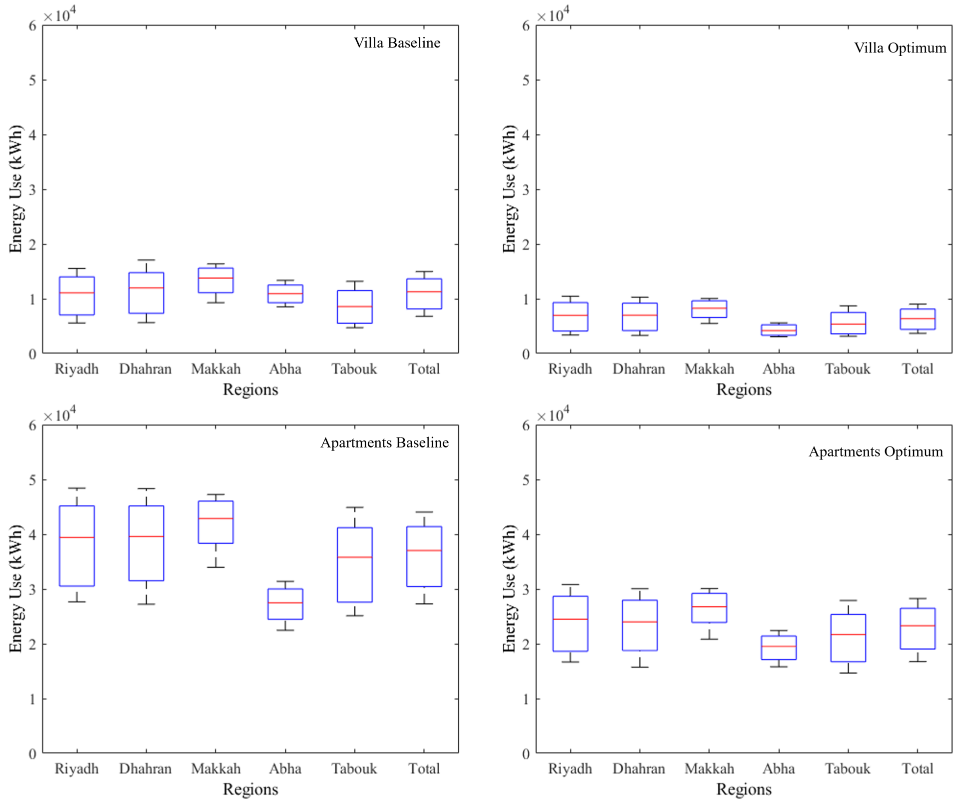

FIGURE 6.41: Comparisons of the archetypes energy use for the baselines and the optimum cases.

to 2.46 ($MtCO_2$ e) and the total cost from 564.62 to 289.54 million USD. Riyadh has the second-highest energy savings of 7.36 to 4.68 TWh, carbon emissions reductions of 3.19 to 2.03 ($MtCO_2$ e) and total cost reductions of 422.73 to 244.58 million USD. Most of the KSA's energy demands are consumed by the most populated regions and were initially used in this research to construct energy baselines and to assess the optimal energy solutions.

6.4 Infiltration rate model

Due to the absence of data in the body of the literature and the contradictory assumptions made by researchers for the KSA's housing, the infiltration rate was investigated in this study. This section predicts the air infiltration rate and total heat gain of the KSA's housing stock, which answers the fourth research question.

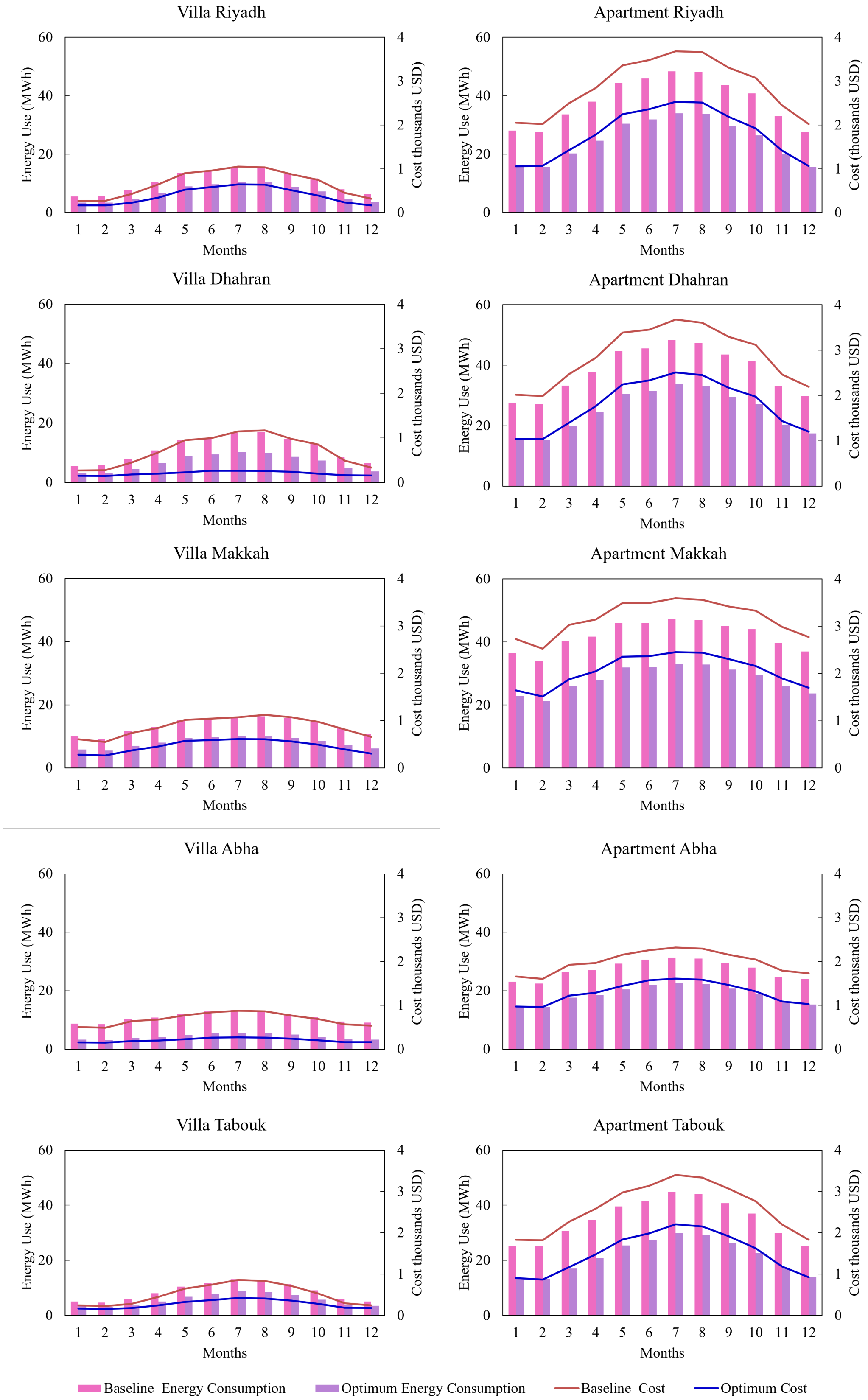

FIGURE 6.42: Comparisons of the archetypes energy use and cost for the baselines and the optimum cases.

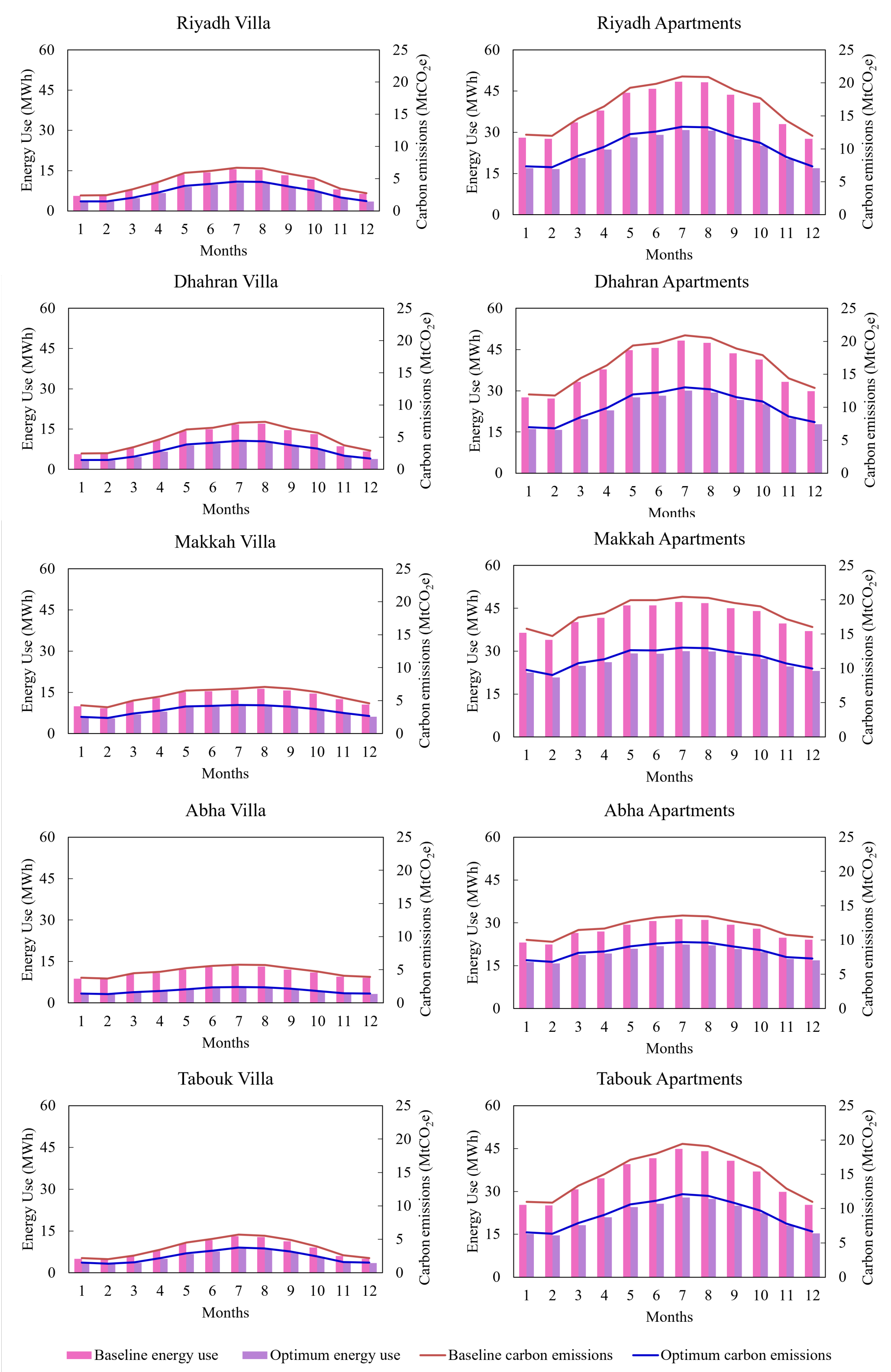

FIGURE 6.43: Comparisons of the archetypes predicted energy use and carbon emissions for the baselines and the optimum Cases.

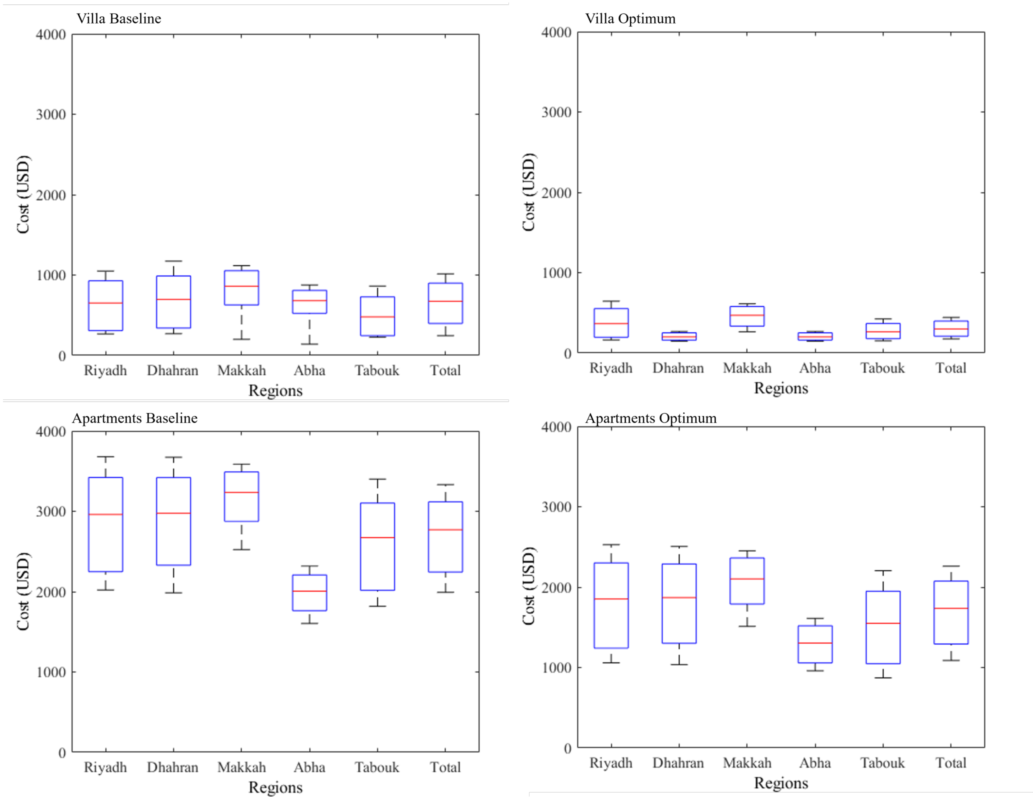

FIGURE 6.44: Comparisons of the archetypes energy use and carbon emissions for the baselines and the optimum cases.

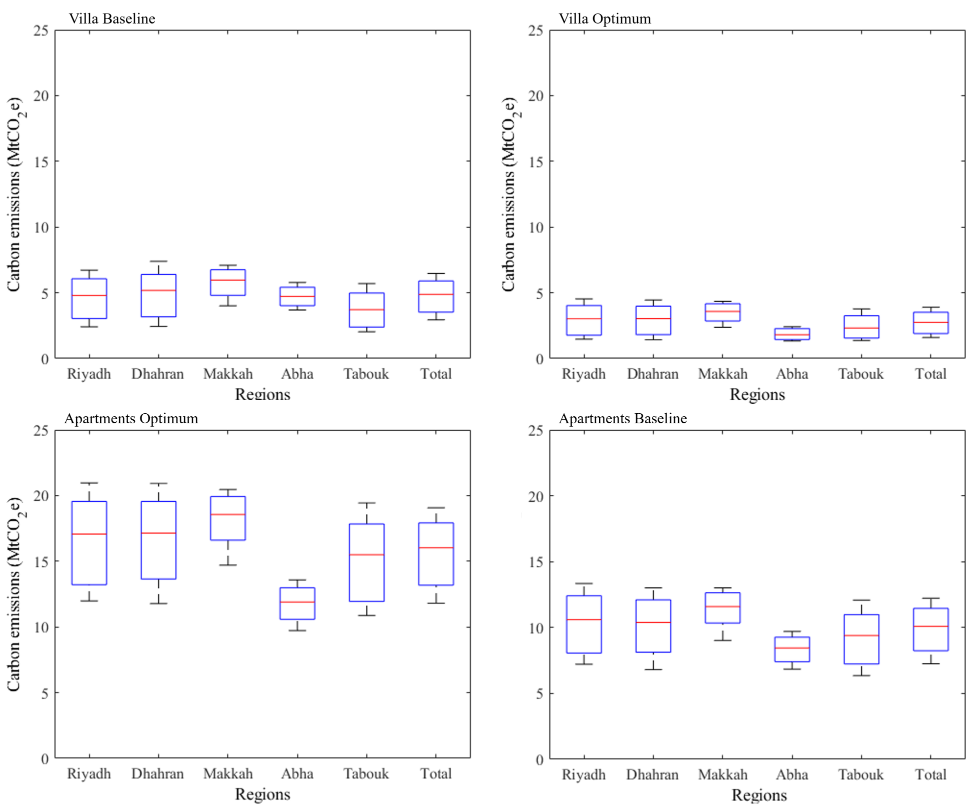

FIGURE 6.45: Comparisons of the archetypes energy use and carbon emissions for the baselines and the optimum cases.

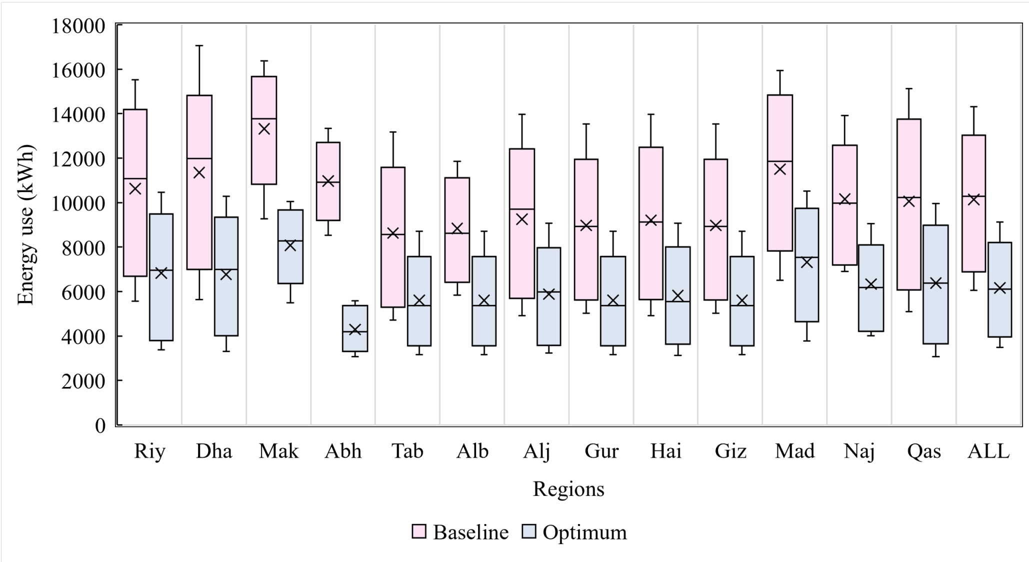

FIGURE 6.46: Comparisons of the villa energy use of the baselines and the optimum cases.

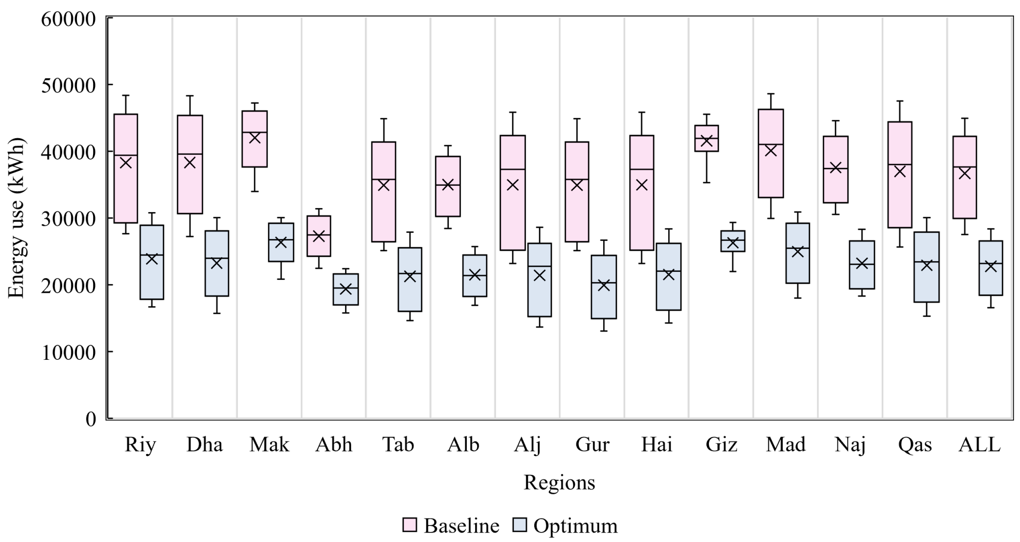

FIGURE 6.47: Comparisons of the apartments energy use of the baselines and the optimum cases.

TABLE 6.8: Summary of the KSA stock model predictions and reductions per month.

				Housing stock/region					
	Housing	Energy demand (kWh/unit)		Energy demands (TWh)		Carbon emissions million ($MtCO_2$ e)		Housing cost million (USD)	
Region	amount	Baseline	Optimum	Baseline	Optimum	Baseline	Optimum	Baseline	Optimum
Riyadh	865390	8506.10	5406.54	7.36	4.68	3.19	2.03	422.73	224.58
Makkah	909228	10162.32	6237.71	9.24	5.67	4.00	2.46	564.62	289.54
Madinah	253047	9093.71	5738.88	2.30	1.45	1.00	0.63	123.58	61.47
Qassim	170948	8112.72	5101.32	1.39	0.87	0.60	0.38	83.48	41.53
Dhahran	528214	8871.42	5324.09	4.69	2.81	2.03	1.22	273.46	134.99
Abha	315262	7759.35	3760.87	2.45	1.19	1.06	0.51	135.17	56.91
Tabouk	126112	7223.28	4574.56	0.91	0.58	0.39	0.25	48.66	27.69
Hail	84383	7518.81	4702.51	0.63	0.40	0.27	0.17	41.21	20.50
Northern	40531	7395.97	4462.91	0.30	0.18	0.13	0.08	19.79	9.85
Jizan	182421	7951.70	4993.48	1.45	0.91	0.63	0.39	89.09	44.31
Najran	72566	8207.64	5104.45	0.60	0.37	0.26	0.16	35.44	17.63
Al-Baha	72692	7334.31	4594.28	0.53	0.33	0.23	0.14	35.50	17.66
Al-Jouf	61133	7541.39	4723.74	0.46	0.29	0.20	0.13	29.85	14.85
Mean	3,681,927	8129	4979	2.49	1.52	1.08	0.66	146.35	73.96
Max	-	10162	6238	9.24	5.67	4.00	2.46	564.62	289.54
Min	-	7223	3761	0.30	0.18	0.13	0.08	19.79	9.85
SD	-	849	626	2.87	1.78	1.24	0.77	170.82	88.61

6.4.1 Results

The mean infiltration rate $\overline{N}_I$ (h^{-1}) and total ex-filtration heat gain H_I (MWh) of the KSA's dwellings during the cooling season are presented in the cumulative distribution functions and the probability distribution density in Figures 6.49 and 6.50, respectively. The dashed blue line depicts the KSABC's requirement for housing infiltration rate value. There is a strong correlation between infiltration rates and associated heat gain. See Figure 6.48. The increases in the infiltration rates will lead to more heat gain from the dwellings.

Table 6.9 and 6.10 display descriptive statistics of the total mean infiltration rate, associated heat gain and air permeability of the KSA's dwellings for each housing type. They are predicted to fall between $0.01 \leq N_I \leq 0.78$ (h^{-1}), $0.02 \leq H_I \leq 37.3$ (MWh), and $11 \leq Q_{50} \leq 20$ ($m^3/h/m^2$), respectively. The bottom and top bars in Figure 6.10 represent the second and 2nd and 98th percentiles, respectively, while the centre box demarcates the interquartile range, and the central bar represents the median. The required sample amounts were 650 villas and 765 apartments for data convergence. Table 6.9 and Figures 6.49 and 6.50 highlight that all distributions are right skewed, leading to the employment of the sample medians.

The villa infiltration rates are substantially larger than the apartments due to the sheer volume and external surface area of the villas exposed to environmental

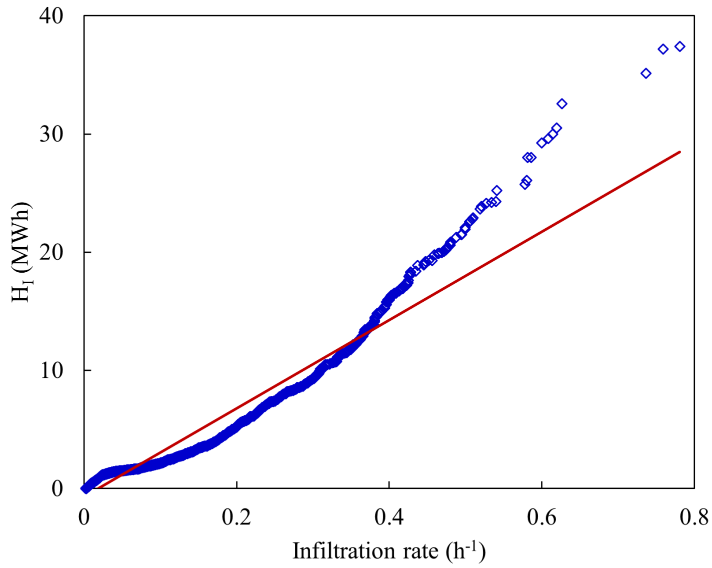

FIGURE 6.48: Infiltration rates and associated heat gain relationship.

conditions. The data dispersion of the villas' infiltration rates, which vary $0.01 \leq N_I \leq 0.78\,(\mathrm{h}^{-1})$, and total heat gain, which ranges from $0 \leq H_I \leq 23\,\mathrm{MWh}$, are displayed in Figures 6.51 and 6.52, respectively. The infiltration rates for most villas range from 0.1 to 0.2 (h^{-1}), practically meeting the KSABC's airtightness standards. However, the infiltration rates of the apartments are much tighter than the construction code, ranging from 0.01 to 0.05 (h^{-1}). An infiltration rate of 0.8 (h^{-1}) is a common value used in earlier research about the energy simulations of residential structures in the KSA, including (Krarti et al., 2020), which is not the correct representative value.

The results of the infiltration rate model for housing archetypes are presented as a cumulative density function shown in Figure 6.49. Most dwellings have low infiltration rates, from 0.01 to 0.4 (h^{-1}), perhaps due to extreme climatic conditions. The stock has airflow rates between 0 to 0.78 (h^{-1}), and about 78% of the dwellings' sample has less than the required infiltration rate value of 0.2 (h^{-1}) (Saudi Building Code, 2018). The villa archetype may occasionally record an infiltration rate of 0.78 (h^{-1}), while the apartments will never exceed 0.1 (h^{-1}). The results revealed that it is odd to have an airflow rate for apartments that is $\leq$ 0.1 (h^{-1}). See the distributed values in the histograms in Figure 6.53.

Published research assumes the infiltration rate of the KSA's dwellings is 0.8 (h^{-1}), regardless of housing type (Krarti et al., 2020; Alaidroos and Krarti, 2016;

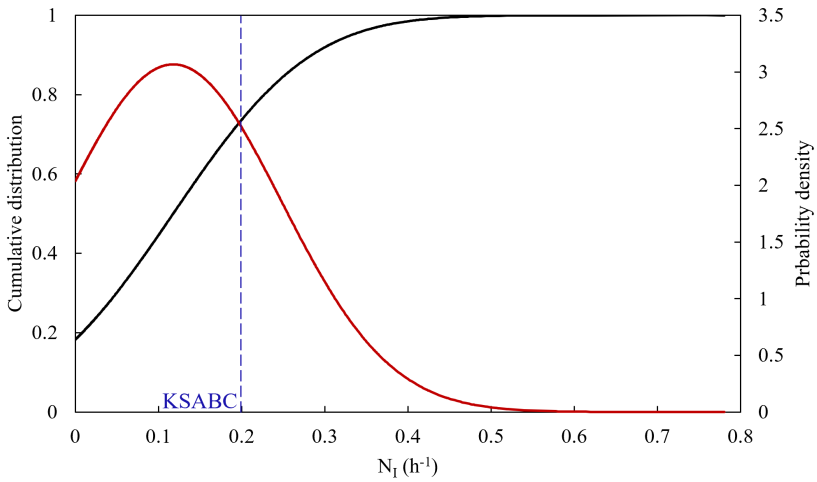

FIGURE 6.49: Infiltration rates of the housing stock of the KSA.

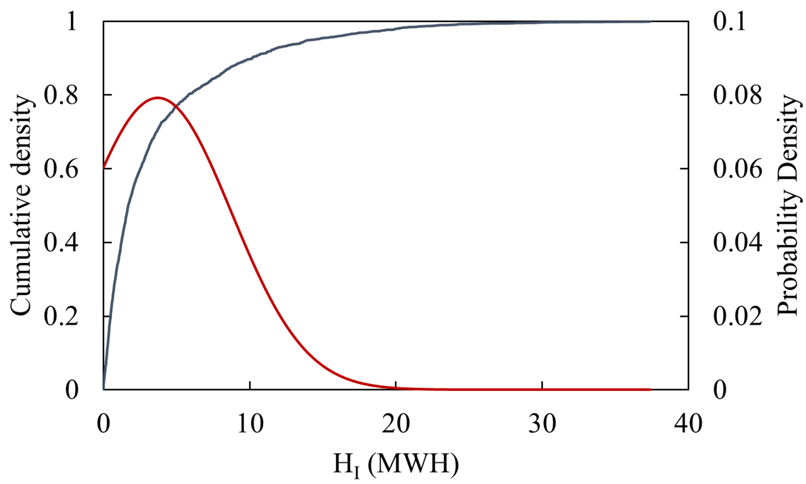

FIGURE 6.50: Heat gain rates of the housing stock.

TABLE 6.9: Statistical summary of mean cooling season infiltration rate (h^{-1}) by dwelling type and stock.

	Infiltration rate (h^{-1})			Heat gain (MWh)			Permeability ($m^3/h/m^2$)		
Type	Villa	Apartments	Total	Villa	Apartments	Total	Villa	Apartments	Total
Minimum	0.01	0	0	0.08	0	0	11.16	7	11
2%	0.07	0	0	0.12	0	0	5.10	3	4
25%	0.15	0.01	0.01	3.04	0.33	0.62	9.05	7.47	8.14
50%	0.22	0.01	0.03	6.19	0.82	1.97	10.63	9.73	10.29
75%	0.32	0.02	0.20	10.48	1.77	5.64	12.57	12.18	12.44
98%	0.54	0.04	0.48	25.21	4.77	20.84	16.64	16.52	16.62
Maximum	0.78	0.08	0.78	37.39	9.51	37.39	20.32	18.88	20.32
Mean	0.24	0.01	0.12	7.66	1.24	4.19	10.72	9.87	10.26
SD.	0.12	0.01	0.14	6.34	1.27	5.44	2.80	3.37	3.15
Sample	650	765	1415	650	765	1415	650	765	1415

TABLE 6.10: Median values of key descriptive parameters of sampled dwellings.

Type	Villa	Apartments	Total
Permeability, Q_{50} ($m^3/h/m^2$)	10.72	9.87	10.26
Volume, V (m^3)	1601.30	3780	5381.30
Envelope Area A (m^2)	1578	921.50	2499.50
A:V (m^{-1})	0.99	0.24	0.46
H_I	7.66	1.24	3.71
N_I	0.24	0.01	0.12

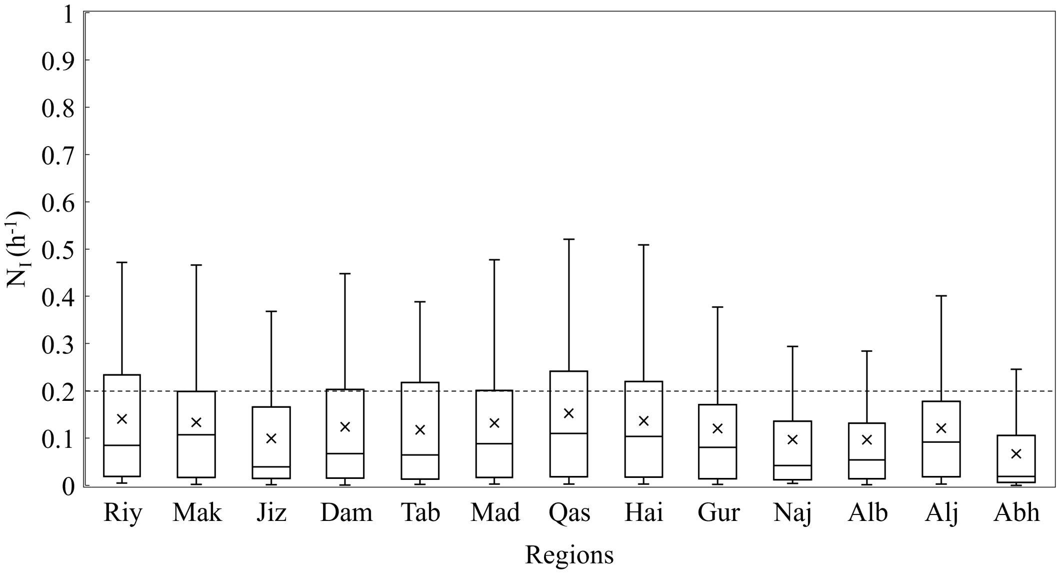

FIGURE 6.51: predicted infiltration rates of the KSA housing stock by region.

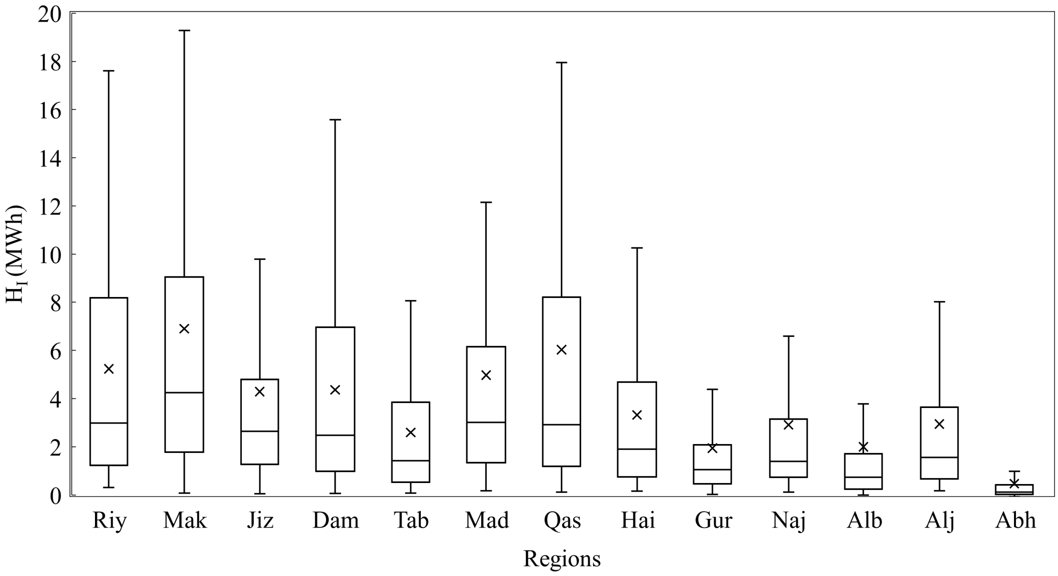

FIGURE 6.52: predicted heat gain of the KSA housing stock by region.

TABLE 6.11: Statistical summary of mean cooling season infiltration rate N_I, heat gain H_I, and air permeability Q_{50} by dwelling type and stock.

Housing Type	Villa			Apartments			Total		
Parameter	N_I	H_I	A_{50}	N_I	H_I	A_{50}	N_I	H_I	A_{50}
Mean	0.24	7.66	10.72	0.01	1.24	9.87	0.12	3.71	10.26
Standard Error SE	0.00	0.25	0.11	0.00	0.05	0.12	0.00	0.12	0.08
Median	0.21	6.18	10.62	0.01	0.82	9.73	0.07	1.69	10.29
Mode	0.19	11.50	10.21	0.01	0.24	13.59	0.01	1.57	12.04
SD.	0.12	6.34	2.80	0.01	1.27	3.37	0.13	5.04	3.15
Sample Variance S^2	0.01	40.20	7.84	0.00	1.60	11.36	0.02	25.39	9.92
Kurtosis	1.11	2.68	0.19	4.07	5.10	-0.38	1.78	8.10	-0.12
Skewness	0.97	1.46	0.07	1.46	1.86	0.01	1.39	2.56	-0.04
Range	0.76	37.46	18.33	0.08	9.52	18.67	0.78	37.46	20.12
Minimum	0.02	-0.08	1.99	0.00	-0.01	0.21	0.00	-0.08	0.21
Maximum	0.78	37.39	20.32	0.08	9.51	18.88	0.78	37.39	20.32
Sum	158.43	4981.27	6969.72	10.96	950.07	7547.31	204.78	6456.47	14517.03
Sample (n)	650.00	650.00	650.00	765.00	765.00	765.00	1740.00	1740.00	1415.00
CI (95%)	0.01	0.49	0.22	0.00	0.09	0.24	0.01	0.24	0.16

Aldalbahi, 2020). Researchers often accept this value since it is adequate for meeting the airflow rate criteria for housing units (ASHRAE, 2009). However, it contradicts the KSABC's airtightness requirement, which mandates the airtightness value to be 4 (h^{-1}) for all climate zones. According to the divide-by-20 rule introduced by the UK's Standard Assessment Procedure (UK, 2013), as explained by Pasos et al. (2020) and described in Section 5.2.6.2, the infiltration rate value should be ACH to meet the KSABC's requirement. The rule is to obtain the infiltration rate from the airtightness value by dividing the airtightness value by 20. Table 6.12 demonstrates a descriptive statistical summary of infiltration rates and the heat gain of the KSA's housing stock.

6.4.2 Energy and carbon emissions

Table 6.9 conveys that the cooling season infiltration demand in a Saudi dwelling is predicted to be $0.02 \leq H_I \leq 37.3$ MWh, and the total heat gain median is 1.97MWh. Villas' and apartments' medians are 0.82MWh and 6.17MWh, respectively. This total heat gain is equivalent to running approximately 12 lightbulbs of 20W for an entire year without stopping. This emphasises that the KSA's dwellings undergo from heat gain.

It is now achievable to employ the CDFs given in Figure 6.50 to predict the total H_I or the total KSA housing sector of 3.6 million units. This is accomplished by regularly sampling and utilising subsets of uniform random variables of a size equal to the number of Saudi units until the differences in the mean and SD of the total H_I changes by $\leq$ 0.01%. The total ex-filtration H_I for the entire KSA's housing stock of 3.6 million dwellings is estimated to be 40 TWh. This corresponds to carbon emissions of 9.9 ($MtCO_2$ e). The villa archetype is responsible for 84% of this, while the apartments are responsible for 16%. This is about 29% less than the carbon emissions predicted from the stock energy model with 14 ($MtCO_2$ e), but this is due to the varied ground temperature in the energy model that affects the model's predictions.

TABLE 6.12: Descriptive statistical summary of infiltration rates and heat gain of the KSA housing stock.

Housing Type	Infiltration rate			Heat Gain		
	Villa	Apartments	Total	Villa	Apartments	Total
SS	0.06	0.04	0.05	169.9	812.2	76.0
F	4.25	1507.78	3.00	4.2	1507.8	3
P-value	$p < 0.001$	$p < 0.001$	$p < 0.001$	$p < 0.001$	$p < 0.002$	$p < 0.003$
Multiple R	0.08	0.81	0.04	0.1	0.8	0
R^2	0.01	0.66	0	0	0.7	0
SE	0.12	0.01	0.13	6.3	0.7	5.0
Sample	650	765	1740	650	765	1740

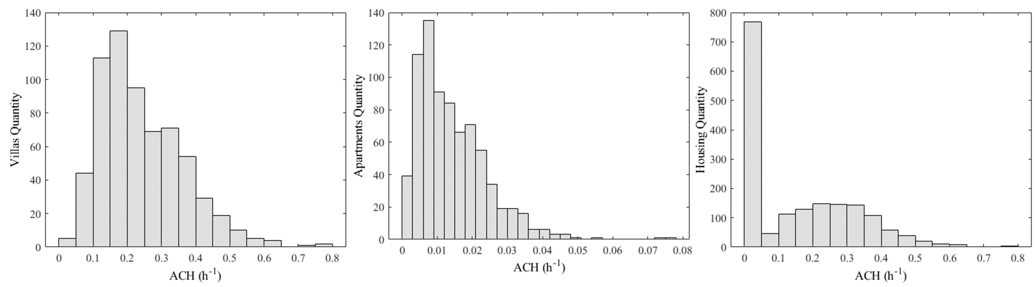

FIGURE 6.53: Infiltration rates of the housing stock by archetype.

6.5 Limitations

6.5.1 Energy model

The energy modeling tool has limitation involving the modeling of airflow rate and the ground temperature. The airflow rate in the modeling tool assumes a deterministically constant air pressure for all year to allow the energy performance simulation. The investigation of the airflow rate in EnergyPlus showed a strong correlation meaning that changing the airflow rate would result in different outputs. This area requires more investigation in order to apply distributed air pressure in EnergyPlus and to allow more accurate model results. The senstivity analysis showed a strong correlation between IAT and GT and this also effect the models output. this clarifies the needs for more investigation.

The modeled baselines were oriented towards the north because its the most efficient and other orientations were not considered. The energy baselines have been established according to the minimum building code requirements to allows code's evaluation. It showed that the code can be beneficial, but also emphasised areas for improvements. This involves the envelope thermal insulation application on the exterior surfaces to keep the building's shell sealed to lower the infiltration rate and heat gains. The building code requires an airtightness value of 4 ACH, and by applying the rule-of-thumb the infiltration rate would be 0.2 ACH. this value is required for all housing types in all locations.

6.5.2 Infiltration rate model

The infiltration rate model has different limitations due to lack of data in the field. Most of the infiltration rate models were performed during heating season to predict the distribution of infiltration rates and total heat gain of buildings. This is the first study that predicts the infiltration rate during the cooling season to predict the distribution of infiltration rate of the KSA housing stock and total heat gains. This required assumptions of different variables including the air permeability, which was normally distributed, and the flow exponent of 0.651, which was previously developed by Sherman and Dickerhoff (1998) and showed that the value of 0.651 is sufficient.

The infiltration rate model should be measured by actual measurements using Blower door test or Pulse test to predicate real air infiltration rates of the KSA housing stock. This is important for future research concerning buildings energy performance. This would allow calibration and validation of the infiltration model of this study with existing data during the cooling season. this would increase the data-set of the KSA housings and allows international comparisons with different building stocks.

6.6 Summary

This chapter highlighted a summary and analysis of the results obtained from this research study. This chapter summarised descriptive and inferential statistics using linear regressions, correlations and sensitivity analysis to predict three major factors of the KSA housing stock; the energy performance, the achievable housing energy, carbon emissions and cost reductions and the infiltration rate. The housing energy baselines showed great uncertainty when infiltration rate and ground temperature are not concisely set up in the energy models and alter the models' outputs. The application of alternative energy retrofitting measures were applied on the housing energy baselines and achieved energy demands, carbon emissions and cost reductions. The applied energy retrofitting measures are thermal insulation, external shading, PV system application, LED systems and energy star equipment. The application of the external shading system resulted in the greatest energy savings. This is because the shading effectively lowers excessive solar radiation from reaching the exterior surfaces of the building envelope, leading to significant reductions in energy consumption.

The infiltration rate of the KSA housing stock was predicted using DOMVENT3D_KSA airflow model and found that the KSA housings are more tight than the values set in recent studies in the field. Researchers assume a value of 0.8 ACH while this research's predicted airflow rate never exceeds 0.78 ACH. This conflict is due to lack of the data which may lead to assumptions. The predict airflow rate of the villas is much higher than the apartments due to the exterior surface area that is exposed to weather variations.

Chapter 7

Discussion

This chapter discusses the information sources and the housing archetypes introduced in chapters 3 and 4, the energy model and the infiltration rate model inputs described in Chapter 5 and the predicted results in Chapter 6.

7.1 The energy model inputs

This section investigates the restrictions associated with the determination and application of models' data input and their implications for the results. EnergyPlus is a simulation tool for modelling the energy performance of buildings based on deterministic engineering models, meaning the selected data inputs have a direct impact on the outcomes (Kim et al., 2013). If the inputs have a broad range of potential values, a stochastic method is required to account for the input's probabilistic nature. This allows continuously altering the input within defined boundaries and by myriad computations to investigate the uncertainty in the model's outputs, such as the sensitivity of the infiltration rate value to the model prediction. See Section 6.1.5.3. It is also important to know input uncertainty; due to a lack of data, assumptions had to be made.

7.1.1 The modeling tool

Section 5.1 (p. 119) demonstrates that EnergyPlus is an integrative and simultaneous approach for thermal zone settings and HVAC system performance. EnergyPlus does not presume the HVAC system is capable of meeting zone demands or can predict un-air-conditioned and under-air-conditioned rooms. Using this integrated approach enables solving the most significant flaws of the BLAST and DOE–2 sequential simulations (Spencer, 2010). Space temperature forecasts are inaccurate owing to the absence of input from the HVAC module to the load's calculations. This is important for energy modelling tools because energy modelling systems require accurate predictions of space temperatures due to their sensitivity and influence on the system's size, plant size, occupant comfort and health. This integrated simulation tool enables developers to assess a wide range of procedures that neither BLAST nor DOE–2 can simulate well. This includes accurate system controls, moisture absorption and desorption in various building components, radiant cooling and heating systems, as well as inter-zone airflow. In addition, EnergyPlus applies time step intervals determined by the user to track interactions between zones and their environments and between a zone's air mass and the HVAC system. This is also aided by the ability to modify the code without recompiling to provide standard reports. However, an acknowledged limitation is recognised in the assessment of the ground heat transfer of the temperature foundation calculation and the airflow estimation because EnergyPlus is a thermal load modelling tool and cannot precisely predict airflow rates.

EnergyPlus offers several modelling skills that substantially surpass the capabilities of DOE-2. EnergyPlus can calculate surface temperatures and perform radiation heat balancing. This enables a more accurate heat transfer prediction, particularly in conditions when there is a wider disparity between the temperatures of various surfaces, when radiant heating systems are used or when a surface has high thermal conductivity. EnergyPlus simultaneously executes simulations of the plant loops, systems and envelope, which enable it to simulate the complicated influences of varied pieces of equipment and the environment. It includes a complete documentation of possibilities not available in other simulation tools such as DOE-2, Blast, ESP-r and TAS. The features include calculations for thermal comfort, walls made of phase-changing materials, walls that absorb moisture and more complex HVAC systems (Spencer, 2010).

7.1.2 Weather data and local environment

The weather is an additional key data input. As with the input data and output data files, we employ a basic text-based format rather than a binary file generated by a separate weather processor. Even though meteorological data are only available in few locations of the KSA, simulations were performed using the weather data of each region's capital city, where most people live. This simplicity, however, may make it more difficult to accurately describe various environmental conditions for any location. This demands a broader climate setting to account for the KSA's weather variations by performing more simulations to satisfy the convergence criterion. This mandates a broader climatic setting to run more simulations until the convergence requirement is reached, which is a time-consuming process that demands more advanced computers.

There are significant assumptions made on the nature and local surroundings of the houses. This includes the dwellings' local environment shielding conditions and topography characteristics. Although the terrain type and values have been previously defined by ASHRAE (2009), they must be evaluated by verifiable evidence, especially in the KSA. The wind pressure was calculated by Bernoulli's equation, which assumes no height variation or pressure losses. See Equation 5.2.2 on page 125. The wind pressure characteristics for each wall of a residence were defined by applying the normalised surface pressure coefficient values to the models developed by Swami and Chandra (1988) to account for the wind pressure coefficients. This study assumed all housing archetypes are in the capital cities of the five determined regions. This demands the wind speed profile coefficient value to be 0.33 with a boundary layer thickness of 460 m, and this is more than double the coefficient value supplied for dwellings situated on the countryside, which has a coefficient value of 0.14 and a boundary layer thickness of 270 m.

In addition, all the resources do not offer a detailed explanation of the diverse types of terrain that might be used while designating site locations. This can be established in subsequent research by providing a narrative terrain demonstration that may be verified and associated with physical measurements, such as the geometric building shape or height. These assumptions ought to be verified with data since the experimental sensitivity analysis reveals that wind speed is a major input component that directly influences heat loss, ventilation rate, energy performance and pollutant consternation. This demands a physical measurement to decrease the quantity of uncertainty present in the input variables and their outputs.

The Intergovernmental Panel on Climate Change has investigated climate change employing a variety of potential future emission situations. This can be used to forecast future climate changes that directly influence housing energy demands. This may predict the uncertainties of future weather data for use to evaluate future housing energy demands and carbon emissions rather than relying only on TMY data, which was generated relying on historical data.

7.1.3 Internal air temperatures

The most relevant environmental factor in the physical measurements' studies for energy, thermal comfort and IEQ is air temperature (Auliciems and Szokolay, 2007). There is a lack of data about the internal air temperature of the KSA's dwellings. Only one study found in the literature physically measured the IAT of the KSA's homes, but the study sample was limited. The study sample was limited to only $(N = 19)$ homes, all in a geographic coastline city in the eastern region. This geographical scope is confined to the Dammam coastline, and the results may not be relevant to other communities in the eastern region or to any other dry city in the KSA, which is the majority. This illustrates an opportunity for future work involving a larger sample size to offer a more realistic reflection of the existing conditions of the dwellings over the whole region.

The dynamic calculation of the IAT of homes found that, regardless of the location, the apartment building is always hotter than the villa due to the differences of the thermal mass proportion embodied in the geometry of each archetype. The proportion of the thermal mass influences the heat loss prediction, airflow rate, IAT and energy performance. According to the sensitivity analysis shown in Figures 6.21 and 6.22 on page 177, the dwellings' IAT is linearly related to the increases in the envelope thermal mass of buildings, meaning that increasing the walls' ratio to the building results in hotter interiors. It is also shown in Figure 6.23 on Page 178 that the ability for the concrete to store heat increases over time when interior walls are added.

7.1.4 Floor areas

There are no physical or modelling studies in the KSA about the flooring areas of a considerable number of homes in the literature, the building code or national surveys. This data scarcity is important for the archetypes, as it affects the heat loss calculation and the energy performance of buildings.

Only a few studies in the KSA have explicitly stated the housing flooring areas and dimensions. Krarti et al. (2020) relied on the literature and found a 54-house prototype to develop three housing archetypes that is representative of the KSA's housing stock. However, this representation was not developed by a known stochastic technique; it only relied on the 54 prototypes and disaggregation of the supplied data. Krarti et al. (2020) classify the overall floor area distribution for all dwellings in the KSA according to vintage and dwelling type. It is estimated that the housing stock has about 950 million m2 of floor space, with apartments accounting for 38%, villas for 32% and traditional houses for 15%. The proportion of living floor space that is cooled is much more than that which is heated. This finding is predicted, given that most of the KSA's cities are dominated by hot temperatures that need air conditioning but little or no space heating.

In this research, the flooring areas were assessed by analysing a sample of 182,923 homes, including villas (45%) and apartments (51%). See Section 4.3.3. The mean flooring areas of the villa and the apartments are $\mu = 311\,\mathrm{m}^2$ $(\sigma = 61)$ and $\mu = 120\,\mathrm{m}^2$ $(\sigma = 57)$, respectively, with a total mean of $\mu = 261\,\mathrm{m}^2$ $(\sigma = 84)$. This total average floor space is one of the greatest in the world, exceeding that of the USA and being more than twice that of the UK. This high mean floor area accounts for 5.4 people per house, which is also more than double that of the USA and the UK. The larger housing sizes in the KSA might be due to gender segregation. Figure 4.18 on Page 94 shows the most frequent flooring area for the KSA's dwellings. It demonstrated that most KSA dwellings' flooring areas fall between 250–300 m^2, which was applied to the housing archetypes and to the energy models. See Section 4.4.1.

7.2 Energy model results

This section discusses the energy model's results and indicates where data are missing or incomparable.

7.2.1 Surface solar radiation rate

This section discusses the solar radiation rates impacting the exterior surfaces and windows based on a building's type and elevation. This identifies the quantities of solar heat contributed by each surface and window to the thermal zone and allows the discussion of external heat gain sources. The analysis was conducted for two extremely different days for each location and housing type and provides an evaluation of the clarity and other parameter results.

According to Figures 6.3 and 6.4 on pages 162 and 163, the KSA's direct sunlight radiation rate is a significant contributor to higher cooling energy loads. Disregarding the previously observed heterogeneity difficulties of the housing type and its associated data inputs, physical reasons explain why the quantitative variables of solar radiation vary across climatic zones (Prieto and García, 2021). The variances should be similar for every scenario for dwellings in the same climatic zone unless substantial influential factors have been incorporated. The results are similar for every surface and window in each location. See Table 6.1 (p. 161) and Figures A.1, A.2, A.3 and A.4 in Appendix A. Apartment buildings in the hot season absorb much more heat from the sun, which accelerates the process of reaching peak rate values for the thermal envelope. Apartment buildings possess a greater sun-exposed surface area, have larger volume and comprise more thermal mass, and therefore, they absorb and store more heat from the sun than the villa. Apartment buildings encompass six units considered a single building type, and the data compiled for this property represent the overall mean of all apartments in a specifically oriented facade. This solar rate calculation method has been determined for both buildings. The winter-day findings indicated that Makkah and Dhahran have the lowest amounts of solar radiation rates over other regions. Makkah is situated in a valley. Hence, it has a lower elevation (Youssef et al., 2015), whereas Dhahran is a coastal city with greater humidity levels than the average, and the association between humidity and temperature is inverse monotonic (Rehman and Ahmad, 2004). Even though the surfaces' solar radiation influence on the urban local sun's irradiance is beyond the focus of this study, it is significant to note that solar radiation from surfaces increases the outdoor local simulated sun irradiance by 133% (Heidarinejad et al., 2016).

Moreover, solar energy penetrates more windows than solid surfaces. The windows of the baseline's models were developed according to the minimum requirements of the KSABC with aluminium-frame double-pane windows, with a much lower total mean U-value than the existing conditions found in the literature. The baseline windows' total mean U-value is 2.67 (W/m^2.K), while the glazing SHGC is 0.25 for all locations. The residential stock energy model developed by Krarti et al. (2020) has a single-clear with wood frames, having higher U-value. This implies a clear differentiation in the comparisons between model predictions in the literature. This is also depicted in the thermal envelope insulation application described in Section 7.3.1 (p. 221).

This is the reason for high external heat gain energy from the sun that directly strikes a building's surfaces and windows. A proportion of this energy reflects, while another proportion gets absorbed and transmitted to the inner surface and contributes to more heat gain. The greatest total mean of surfaces' solar radiation rate for the villa archetype is $\mu = 139\,(W/m^2)$ ($\sigma = 46$), while it is much higher for the apartments' building archetype, accounting for $\mu = 165\,(W/m^2)$ ($\sigma = 91$). Despite having the finest indoor conditions among other locations, Abha receives a great deal of sunlight. Abha is situated on mountains in the southern region of the KSA at a height of 2,270 m above sea level.

7.2.2 Archetypes heat gains

Figures6.5, 6.6 and 6.7 revealed the disparity in heat gains' quantity; it increases between the morning and evening hours of the day when the sun is at a lower latitude. The surrounding structures or sun blockers may have a great influence on buildings' heat gains and solar radiation rates. Nonetheless, this research did not consider it due to a lack of data about adjacent buildings in the KSA, so an assumption about the terrain of a city coefficient factor was made. It is clear from the

Figures that the highest external heat gain source is windows, even though windows were used following the KSABC's minimum requirements, being more efficient by implementing a lower U-value and SHGC. A low U-value shows the capacity of a physical element to transfer heat from a warm to a cold region, whereas the SHGC indicates how much solar heat is absorbed and transmitted through the window glazing. This implies a strong positive relationship between U-value, SHGC and IAT, which means lowering the U-value or the SHGC reduces the amount of heat absorbed and transmitted to the indoors. Window glazing allows heat to penetrate to the indoors more than the surfaces, which increases the IAT.

The external heat sources behaved similarly for both seasons and both archetypes, with higher heat gains for the apartment building due to the larger area exposed to the direct sun's radiation, size and volume. See Figures A.5 and A.6 in Appendix A. Significantly, the surface heat gains during a winter's day are three times more than the gains during a summer's day due to the sun angel.

Conversely, internal heat gains may vary according to the systems applied to the energy baselines. This shows a clear contradiction of the studies found in the field. According to Figure 6.8, the interior equipment radiates the most heat, but this does not align with several studies, including Krarti et al. (2020), Aldubyan and Krarti (2021), Algarni and Nutter (2013a), Aldossary et al. (2014b), and Aldossary et al. (2014c). A possible explanation for this conflict is the lack of adequate system power density studies in the KSA. Most building energy performance research conducted in the KSA assumes electrical and lighting power densities, unlike this thesis. This thesis applied the first-order approximation approach to calculate and reflect the existing conditions of the KSA's dwelling system. See Section 5.2.9 (p.137). This probabilistic approach was adopted since most building energy performance research in the KSA assumes power densities for buildings' equipment, appliances and lighting systems. There is no study in the KSA that calculated the power densities of the building systems, either modelling techniques or actual measurements. Figure 5.6 (p. 139) demonstrates a clear data variance among studies. Since the 1980s, the system's power density has decreased due to improvements in their energy efficiency.

Even though the KSABC requires WWR to be less than 25% of a wall, it has a detrimental influence on IAT. Although surfaces have a greater area exposed to the sunlight, surfaces' heat gains are far less than the windows. This is attributable to the KSABC's compulsory installation of envelope thermal insulation. Infiltration heat gains are the lowest due to the KSABC's mandatory airtightness requirements.

7.2.3 Air temperature

This section discusses the temperature of various building components relevant to energy performance involving the OAT, IAT, surface temperature and OPT.

There is a direct linear relationship between OAT and IAT, described in Figure 6.11 (p. 169), which makes the internal conditions of the dwellings extremely uncomfortable. Hence, an HVAC system must run to meet the conditional IAT setpoint of 20°C (Saudi Building Code, 2018). HVAC energy loads are summarised in Figure 6.20 (p. 175). This indicates that the villa requires cooling and heating energy for the summer and winter, respectively, but this is not the scenario with the apartment complex, since it only demands cooling energy most of the year without any heating energy. This result may be explained by the fact that the apartment building stores more heat than the villa due to a more proportional thermal mass. The thermal mass is linearly related to the IAT and to cooling energy demands. See Section 6.1.5.1 on page 176. This has a direct effect on dwellings' internal conditions by reflecting a proportion of the sun's heat rays while absorbing and transmitting other proportions indoors. This initially raises exterior surfaces' temperature, and heat begins to transfer through the wall's layers to the inner surface. The heat transfer might be rapid or delayed depending on various variables involving the weather conditions, thermal mass materials' resistance to heat and others. Thicker walls transmit heat much slower than thinner walls due to the wall's sectional area. This emphasises a clear knowledge gap in the KSA dwellings' surfaces temperature. Only one study in the KSA has examined the interior surface temperatures of buildings; it is based on real data measurements for three schools in three regions. However, this study neglected the outer surface temperature of one educational building. This is important due to the heterogeneity of buildings' energy performance, including the number of occupants, behaviour, activities and

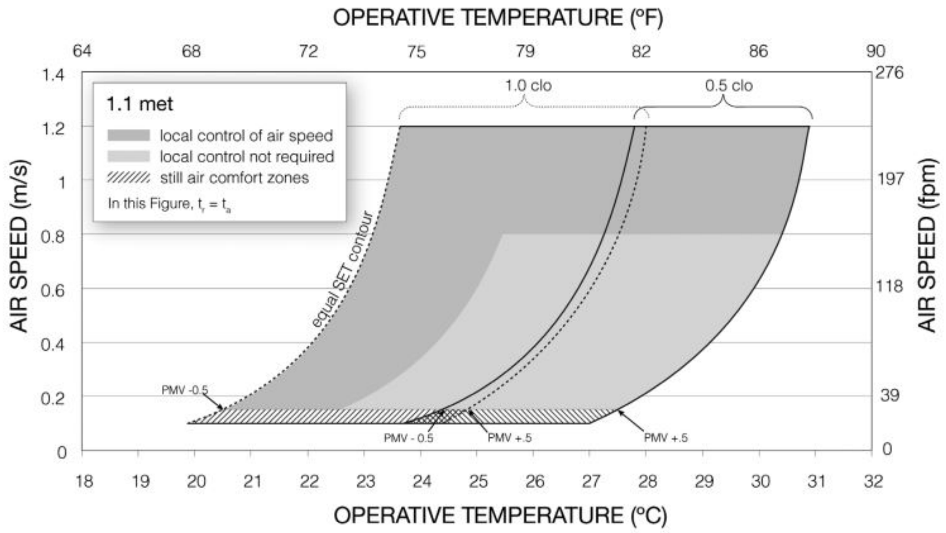

FIGURE 7.1: Acceptable range of operative temperature and air speeds for the comfort zones (ASHRAE, 2010).

scheduling, the applied equipment and systems in the building. All of this has a direct impact on the energy demands of a building, which makes data incomparable.

Once the temperature of internal surfaces is heated by the arrival of eveningdue to the time lag, its radiation begins by releasing this heat to the indoor space. This accelerates the process of rising IAT and, consequently, the OPT. See Section 6.1.3.2. The OPT is critical for evaluating occupants' thermal comfort. Occupants' thermal comfort has diverse modelling approaches. This makes thermal comfort evaluation in the KSA's dwellings challenging due to its heterogeneity. Most human thermal comfort models fail in analysing occupants' comfort and sensation in the KSA because ASHRAE Standard 55-2020 typically relies on a small range of ATs to successfully predict the levels of thermal comfort. See Figure 7.1. The KSA is situated in an exceptionally hot and dry climate that exceeds the AT boundaries of the ASHRAE thermal comfort model (ASHRAE, 2009). The KSA has much wider ranges of OAT, IAT and airspeed. Although the KSA's weather is extremely hot, Saudi citizens tend to wear much heavier clothing, resulting in greater clothing values than other nations (Al-Ajmi et al., 2008). See Section 5.2.10 of page 141.

This present study raises the possibility that acceptable human thermal comfort varies due to heterogeneity in culture, clothing and human behaviour. In fact, the KSA citizens may be able to adopt hotter IAT than others.

7.3 Sensitivity analysis

The sensitivity analysis was used to determine the associations amongst the input and its corresponding outcome.

7.3.1 Envelope

Despite researchers' attempts to limit envelope heat transmission using innovative insulation block modules, substantial heat gain is evident due to the presence of thermal bridges, interrupted insulation and fractures or gaps found in the envelope. None of the varieties of insulated blocks used in the KSA's housing studies has met the KSABC's requirements (Alayed et al., 2021).

The findings presented in Figure 6.21 (p. 177) revealed a strong association between concrete thickness with and without interior walls and IAT. This implies that increasing the proportion of the concrete in the KSA's context results in storing more heat and, therefore, raises the IAT. A similar correlation was detected by increasing only the concrete of the exterior wall's thickness and resulted in raising the IAT. See Figure 6.22 (p. 177). Increasing the exterior or interior concrete of the KSA's buildings raises the ability of surface heat storage to store more heat. See Figure 6.23 (p. 178). In summary, there is a strong positive relationship between increasing the concrete's proportion to the building or its thickness and IAT.

In contrast, Figure 6.31 (p. 184) revealed an inverse association between the baseline's U-value and thermal insulation's thickness. This implies that applying the envelope's thermal insulation reduces the heat transfer to the indoors. This is because the baseline meets the KSABC's minimum requirement, which is applying a 0.75 mm board thermal insulation to the exterior surfaces of the walls. This is also suggested by the regressions displayed in Figure 6.32 (p. 184). The regressions indicated how the IAT reduces from a 0.75 to 200 mm wall thickness. It was determined that the IAT of the thicker wall is lower in the summer, but higher in the winter. This maintains a more desirable IAT in dwellings all year by shielding them from extreme cold in the winter and excessive heat in the summer. This makes the space more comfortable in both seasons, though both seasons require cooling or heating energy to meet the building code regulations of maintaining a setpoint of 20°C for both seasons to achieve occupants' thermal comfort. The findings of thermal envelope associations are consistent with Alayed et al. (2021), who considered envelope insulation and cooling energy requirements for a villa in Riyadh.

Furthermore, the location of the thermal insulation revealed that installing the insulation on the outer surfaces of the exterior walls is more effective than placing it on the inner surfaces. See Figure 6.30 (p. 183), which compares thermal insulation application on the inner and outer surfaces. One of the practical solutions addressed by Alayed et al. (2021) to reduce excessive heat loss without significantly altering the construction assembly process is installing 55-mm thermal insulation on the exterior surfaces of the envelope. Even though placing the insulation on the exterior walls' surface reduces IAT, it must be continuous and without gaps. The interrupted thermal insulation creates areas of the building envelope with greater thermal conductivity, such as windows, doors, skylights and thermal bridges. Thermal bridges are identified as areas of buildings' facades that have extremely high thermal conductivity, resulting from gaps or cracks found in the building's insulating layers (Al-Tamimi, 2021). This allows the heat to rapidly flow from warmer (outside) to colder (inside) regions. Generally, placing the thermal insulation on the exterior surface of the envelope is more efficient because it lowers the chance of having gaps and cracks on the solid walls to obtain continuous insulation. This shields the dwelling's thermal mass by ensuring that the masonry is enclosed within the insulating layer and that this membrane is airtight. This is an effective precautionary measure against condensation and dampness destroying a home. Additionally, exterior insulation does not decrease the interior floor area.

7.3.2 Ground temperature

EnergyPlus and DOE-2 provide a variety of ground models that are fundamentally distinct. DOE-2 implies the perimeter conduction approach with a hypothetical resistance of foundation calculations. The foundation conductance is determined using precalculated findings generated by the Lawrence Berkeley National Laboratory that cover most fundamental foundation types. On the contrary, EnergyPlus utilises a separate foundation simulation tool that employs a three-dimensional tool, which employs a three-dimensional finite element solution, to estimate the monthly subsurface thermal performance. This foundation tool is not directly linked to its space when executing the simulation to decrease the run time. The approximate length of the run time needed to perform the simulation is 10 minutes. Consequently, the user must determine the indoor temperature, which might fluctuate monthly.

Surface temperatures vary substantially on the projected temperature of the space. A decent outcome requires an iterative procedure, which would require an additional modelling duration than can realistically be permitted in an optimisation process. This problem is also explored in Section 5.2.6.1 of Chapter 5. While the EnergyPlus model is more precise, if there is sufficient time to run the foundation simulation, this is impractical for optimisations. Therefore, the DOE-2 model is better suited for residential optimisation at this point. There is a noticeable lack of data regarding GT in the KSA and worldwide; this may be due to the complications of ground floor heat transfer and soil modelling approaches. This encouraged the application of the NRS described in Section 5.2.6.1 (p. 130). This was applied to explore the interaction effects of a random range of GT values. It was found that the GT is effective and directly impacts the energy model's results, but this is not evident in the literature. Figure 6.24 (p. 178) illustrates a positive linear relationship between GT and the predicted IAT. Raising the model's GT would correspondingly increase the total mean IAT.

Most buildings' energy research in the KSA does not identify or involve GT in the analytic process (Bahel et al., 1985; Bahel et al., 1989; Kinsara et al., 1996; Budaiwi and Al-Homoud, 2001; Almutairi et al., 2015). This becomes more critical when using the EnergyPlus tool because it assumes the GT value is a constantly undistributed 18°C (DoE, 2020). This can be seen in studies, such as Matar et al. (2013) and Krarti et al. (2020). However, the mean values of GT of the KSA's cities show that the peak GT for the entire year is in July, while the lowest GT is in January due to weather conditions. See Figure 6.25. The GT used values that directly affect the model's outputs, which is also seen in the infiltration rate.

7.3.3 Infiltration rate

Predicting the infiltration rate and duct leakage is certainly the top priority for housing energy performance model upgrades. See Section 6.1.5.3 (p. 179). EnergyPlus lacks a straightforward model for dwelling duct leakage, unlike other modelling tools, including DOE-2. There is an airflow network modelling approach that can calculate the imbalanced airflow between zones and the outdoors to quantify interconnections between duct leakage, exhaust, wind and infiltration. The only approach to estimate duct leakage in previous versions of EnergyPlus was to manually perform a size run and apply a known duct leakage proportion to predict the airflow. However, Energy Performance of Buildings Group employees at LBNL previously established the basic data-driven duct leakage model that is currently integrated into EnergyPlus and documented in the California Energy Commission's High Performance Commercial Buildings programme (Wray and Sherman, 2010).

Regardless of the existing simulation techniques, it is difficult to effectively model infiltration dynamics. According to ASHRAE HOF (2005), the aggregation technique should be employed to involve various flows in quadrature, following the principles of the Sherman–Grimsrud (LBL) model (Sherman, 1980). Infiltration is fundamentally driven by wind pressure and temperature differentials across the building envelope, causing air to flow through openings or cracks in the envelope.

There is a clear data deficiency in the infiltration rate of the KSA's housing. There is only one study that considered evaluating a range of 0.5, 0.75, 1 and 1.2 (h^{-1}) infiltration rates in the KSA. However, it is outdated and does not reflect the current condition of the stock (Said and Al-Hammad, 1993). Recently, most building energy research in the KSA has assumed the infiltration rate. Krarti et al. (2020) and Aldubyan et al. (2021) assumed an infiltration rate of 0.8 (h^{-1}) for all housing types in the KSA, but they published a following study and increased the rate for all housing types to 1 (h^{-1}) (Aldubyan and Krarti, 2021). None of the reported airflow rates complies with the building code, and it states an airtightness value of 4 ACH instead of the infiltration rate (Saudi Building Code, 2018). Both values, the airtightness and the infiltration rate, can be estimated from one another (Sherman, 1980), as described in Section 5.2.6.2. Here, the infiltration rate was assumed from the airtightness value provided from the building code to be 0.2 (h^{-1}).

The infiltration rate predictions of the free-running building, described in Figure 6.26 (p. 132), display an inverse relationship between the infiltration rate and the IAT. This means that raising the infiltration rate will correspondingly reduce the IAT, which is interesting because of the harsh climatic conditions of the KSA. This might be because the internal environmental state of houses is not air-conditioned or optimised and envelope thermal insulation is absent. By performing the same analysis after applying the required thermal insulation on the exterior building surfaces, the results were divergent. See Figure 6.27 (p. 180). This is because thermal conductivity is non-linearly associated with the ΔT, and this causes a thermal mass lag. This thermal mass lag of a substance is the rate at which it radiates accumulated energy in the form of heat. This directly impacts the IAT and requires cooling energy systems to provide thermally comfortable indoor living spaces. The time lag is caused by thermal inertia, and the greater the thickness and resistance of the material, the greater the time lag. This time delay represents the period that elapses between the emergence of the wave of the highest OAT and the emergence of the wave of the maximum interior surface temperature of the wall exposed to the zones.

7.4 Energy retrofitting measures

This section discusses the energy performance of the applied EERMs to the energy models of the KSA's housing stock. See Section 6.2, as well as Section 7.4.1 for thermal insulation, Section 7.4.2 for exterior shading, Section 7.4.3 for the PV application and Section 7.4.4 for LED system discussions.

7.4.1 Thermal insulation

The five most prevalent envelope thermal insulations found in the Saudi local market were applied to the energy baselines with a varied thickness range. See Section 6.2.1. This application conserved variable energy quantities. See Figure 6.33 (p. 186). It was predicted that the most efficient thermal insulation is ID25, which is a 200 mm polystyrene. This insulation has achieved the highest energy reduction when applied to the outer surface of the envelope. This is better because it reduces the gaps from the inner decoration, which makes the building tighter and reduces infiltration.

The thermal insulation was predicted, but without considering local shielding. The local shielding may impact the building's solar radiation rate, wind speed, wind direction, temperature and others. Most studies do not consider this issue, which demonstrates an additional opportunity for future research.

7.4.2 Exterior shading

The heat gains from the sun are the major cause for increasing the air temperature of the KSA's dwellings. Preventing the sun's rays from impacting the exterior surfaces of the envelope reduces energy demands, CO_2 emissions and cost, which achieves the primary research aim. The eight sun-blocking shading systems applied on the exterior surfaces of the envelope are described in Section 6.2.2.

This evaluation began by blocking the sun from accessing the building through window openings, but this was ineffective due to the small window-to-wall ratio. Even though blocking the entire building from receiving the sun's rays reduced the IAT, the IAT's differences between the models and the locations were observed. Using the egg-crate shading style and covering the roof lowered Tabouk's IAT for both archetypes by a mean of 1.2°C, while it lowered Tabouk's summer's day IAT of the apartment building by 1.5°C. See Table 7.1. This is a considerable amount of IAT reduction because it reduces energy demands by meeting the cooling setpoint in a shorter period. The lowest amount of IAT reduction overall was evident on the winter's day in the villa at Dhahran by 0.35°C, followed by the apartment building on the summer's day by 0.48°C. This is due to high levels of solar radiation and humidity. See Tables 6.1 and 6.2 (p. 161). However, the external shading has a clear drawback as it increases the use of artificial lighting and may have undesired shapes if not designed well. The shading system is effective for various factors involving the building terrain, but this was neglected in this study due to a data shortage regarding neighbouring and adjacent buildings.

TABLE 7.1: The egg-crate shading style effects on IAT in the five regions.

	Villa		Apartment	
ΔT	Winter-day	Summer-day	Winter-day	Summer-day
Riyadh	0.65	0.85	1.14	1.25
Dhahran	0.35	0.76	0.48	1.21
Makkah	0.79	0.83	1.04	1.00
Abha	0.68	0.92	1.15	1.15
Tabouk	1.21	1.23	1.54	1.21

7.4.3 PV

The application of PV systems to shading devices may produce various amounts of electrical energy that can be fed back to a residential building's energy or transferred to the electricity provider for credits. The energy efficiency of PV cells is one of the most effective variables and may reach 45%, though this is often tested under STC. Testing the PV in a controlled environment may not be accurate due to the cells' sensitivity to factors involving dust, humidity and temperature. The energy efficiency of cells has a reverse association with temperature, meaning that increasing cells' temperature results in lowering their energy efficiency (Tyagi et al., 2013). The PV systems should be evaluated through physical applications to account for weather variations and, then, can be applied to energy models to mimic existing conditions. However, this research applied a modest PV energy efficiency of 18% because it was physically implemented and tested in the KSA context. This generated low energy quantities. See Table 6.38 (p. 191). This is because the energy efficiency of the cells is low and its cells' temperature becomes hotter with the KSA's solar radiation. The roofs produced more energy than all elevations due to more exposure with the sun's movement.

7.4.4 First order approximation

Several reports have assumed various power density values for the equipment and systems applied in the KSA's housing energy models. See Figure 5.6 (p. 139). No study in the literature attempts to average these values rather than assume them. Correspondingly, the first-order approximation becomes handy for contributing to the formation of representative mean values that can be applied to describe the realistic power density of the available equipment and systems in the KSA's homes.

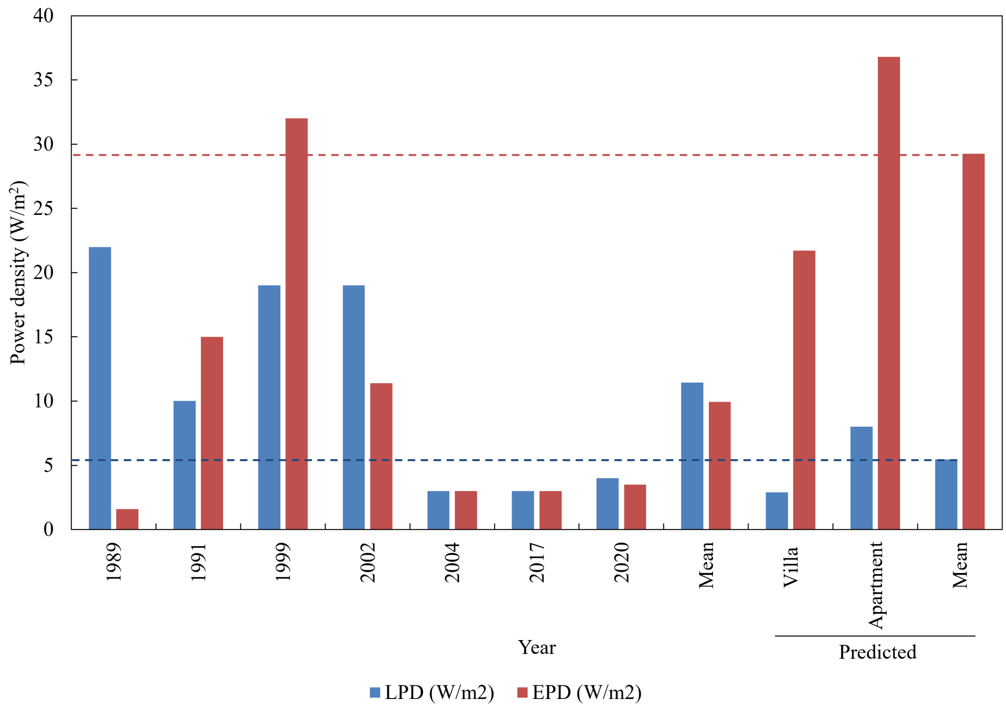

FIGURE 7.2: The literature and predicted models power density comparisons.

See Section 5.2.9. This was done to mimic the existing conditions of the stock by calculating systems' power density based on the energy usage of the identical system, as reported by the national electricity company.

The mean LPD and EPD values found in the literature are 11.4 and 9.9 (W/m2), respectively, and they are different to the predicted mean values of this study. The predicted mean LPD and EPD values are 5.4 and 29.2 (W/m2). See Figures 6.39 and 7.2. The horizontal dashed lines in Figure 7.2 represent the predicted mean values for the LPD (blue) and EPD (red). The literature's mean LPD is more than double the predicted mean, and the literature's mean EPD is almost three times less than the predicted mean value. This inconsistency may be explained by the assumptions found in the literature that are made without considering the real systems applied in the housing stock. This dispersed in values is critical because it affects total energy demands and creates issues in which data become incomparable. In fact, this might produce misleading results that cannot be applicable in practice. Additionally, this fluctuates the payback period conducted by building codes and, thus, affects national energy demands.

7.5 Infiltration rate model

The DOMVENT3D_KSA model was developed in this research to predict the infiltration rate distribution of the KSA's housing stock, which answers the fourth research question. There are three important mechanisms for predicting the infiltration rate distribution involving wind, temperature and mechanical air flow. The mechanism can be calculated using advanced models by determining the pressure throughout every location on the envelope and thereafter accounting for the flow by adjusting the internal pressure. This method is compelling, but its input and processing needs may render it impractical. This encouraged the use of simplified techniques for several situations, despite being less precise. In most basic one-zone models, calculating the pressure flow for a single driving force is a reasonably straightforward task. Each of these three mechanisms induces pressure throughout the enclosure to direct the flow, although Sherman (1992) argued that the spatial distribution of these pressures varies across mechanisms.

7.5.1 Infiltration rate comparison

The infiltration rate distribution of the KSA's housing stock has been predicted and compared in this study using the DOMVENT3D_KSA model described in Section 5.3, which answers the fourth research question. The KSA's infiltration rate predictions are discussed and compared with the UK housing stock rates developed by Jones et al. (2015). The UK context is compared because the DOMVENT3D_KSA model was developed by adapting the DOMVENT3D model of the UK. The apartment airflow rates of the KSA and the UK have been compared, but the villa unit was compared with the detached housing unit of the UK. This is due to two factors: The infiltration rate of the KSA's literature is four times higher than the KSABC and considered extremely high as well as the similarity between the villa and the detached dwellings. They are both single-family detached dwellings with individual land plots.

The KSA's dwellings are large, with a heavy and thick thermal mass and concrete structure. This may make the KSA's dwellings more airtight than other countries, including the UK's dwellings. The KSA's dwelling airflow rates are far less than the

TABLE 7.2: Statistical summary of mean heating and cooling seasons infiltration rates (h^{-1}) by dwelling type and stock.

Country	UK						KSA		
Type	Apartments	Detached	Mean	L=20	SAP	BREDEM	Apartments	Villa	Mean
Minimum	0	0.01	0.005	0.01	0.01	0.01	0.00	0.01	0.00
2%	0.02	0.045	0.0325	0.06	0.06	0.05	0.00	0.07	0.00
25%	0.12	0.195	0.1575	0.3	0.26	0.23	0.01	0.15	0.01
50%	0.23	0.36	0.295	0.5	0.43	0.37	0.01	0.22	0.03
75%	0.37	0.58	0.475	0.7	0.59	0.52	0.02	0.32	0.20
98%	0.9	1.13	1.015	1.23	0.97	0.87	0.04	0.54	0.48
Maximum	1.925	2.505	2.215	2.45	1.54	1.56	0.08	0.78	0.78
Means	0.28	0.42	0.35	0.52	0.44	0.39	0.01	0.24	0.12
SD.	0.225	0.29	0.2575	0.29	0.24	0.21	0.01	0.12	0.14
Sample	3616	4088	7704	19200	19200	19200	765	650	1415

rates used by researchers. Section 7.3.3 clarified that the infiltration rate of the KSA's dwellings is often assumed, not driven by physical measurements or from modelling techniques. Table 7.2 reveals the infiltration rate in a KSA dwelling is predicted to be $0 \leq \overline{N}_I \leq 0.78\,(h^{-1})$, regardless of the building type, with a mean of $\mu = 0.12\,(h^{-1})$ $(\sigma = 0.14)$, while the rates for the UK dwellings are $0.02 \leq \overline{N}_I \leq 1.24\,(h^{-1})$, with a mean of $\mu = 0.35\,(h^{-1})$ $(\sigma = 0.25)$. This demonstrates how infiltration rate ranges are wide between both stocks.

Figure 7.3 conveys a great contradiction in the KSA dwellings' airflow rates that is linearly related to energy demands and carbon emissions. The mean predicted airflow rate of this thesis is closer to the KSABC's required rate than the literature's. The villa unit, for example has a higher infiltration rate than the apartments in the KSA, but both archetypes are much tighter than the UK's dwellings. However, this illustrates a great uncertainty in the KSA's building energy performance studies, as they often rely on an assumed airflow rate of $0.8\,(h^{-1})$, and Section 6.1.5.3 demonstrated how sensitive the airflow rate is to overall energy and carbon emission predictions. Moreover, this signifies the importance of better evaluation schemes that represent the existing conditions of the housing stock rather than assuming rates that are extremely effective and sensitive to energy demands. This assumption clearly changes the model's predictions and indicates inaccuracy in the payback period and the national evaluation schemes. This is important, as it affects national energy demand schemes and decision making.

Table 7.3 shows that the villa has a lower airflow rate of $\mu = 0.24\,(h^{-1})$ $(\sigma = 0.12)$ than the detached dwelling in the UK, with a mean airflow of $\mu = 0.42\,(h^{-1})$

TABLE 7.3: Mean values of key descriptive variables of sampled dwellings.

	UK			KSA		
Type	Apartments	Detached	Mean	Apartments	Villa	Mean
Permeability , Q_{50} ($m^3/h/m^2$)	9.1	9	9.05	9.87	10.72	10.26
Volume, V (m^3)	307.1	191.3	249.2	633	1601.30	1117.2
Envelope Area	256	55.4	155.7	120	1578.00	849
A:V (m^{-1})	1	1.3	1.15	0.19	0.99	0.59
H_I	2.4	3.675	3.0375	1.24	7.66	0.71
N_I	0.28	0.42	0.35	0.01	0.24	0.12

($\sigma = 0.29$). The KSA's apartments have a much tighter mean airflow rate of $\mu = 0.01\,(h^{-1})$ ($\sigma = 0.01$) than the UK's apartments with $\mu = 0.28\,(h^{-1})$ ($\sigma = 0.22$). This may be attributable to various factors, including a larger envelope area exposed to weather variations, the building size and volume, and the location of the KSA's dwellings. Figure 7.3 compares the housing models for both countries and building codes. It reveals that the KSABC requires dwellings to have an infiltration rate of 0.2 (h^{-1}), and this is lower than the SAP, BREDEM and L=20. Although this may tighten the KSA's residential units and reduce energy demands, it can be revised to require airtightness values for housing types to account for variability and uncertainties. The uncertainties involve the buildings' volumes and their exposed area to various weather variations. Figure 7.4 conveys the differences between infiltration rate models applied by researchers and building codes. It revealed significant variations between apartments in both countries, perhaps due to the double volume of the KSA's apartments with an envelope area that is less exposed to the harsh climatic conditions.

The findings indicated that the variation in buildings' physical and environmental characteristics affects energy demands and carbon emission predictions. Consequently, it is essential to recognise how much these outcomes vary depending on these criteria. This will assist in establishing or updating effective national standards and recommendations for housing energy demand assessment and reduction schemes to prevent nationwide energy waste and limit the potential for global warming. The finding suggested that the infiltration rate of the KSA's housing stock should be physically measured using the blower door test or Pulse test, described in Section 3.3.1. This can be connected to the building type with its exact location to build a foundation for a future dataset, such as those of the USA

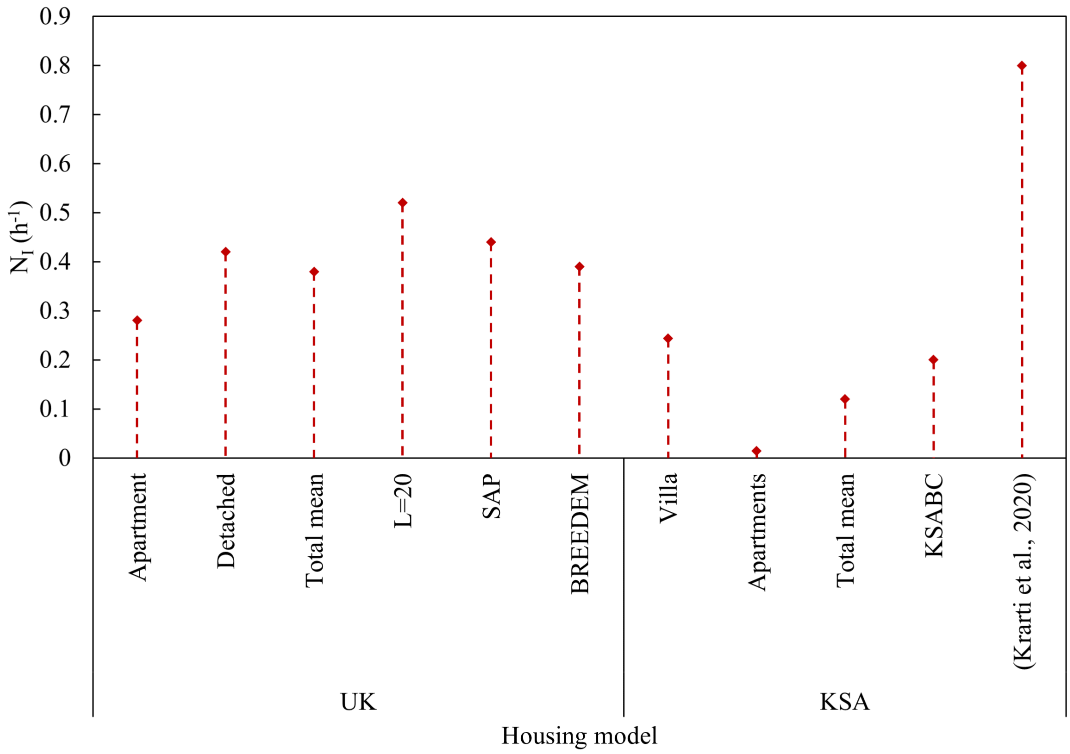

FIGURE 7.3: Infiltration rate comparison between the UK and the KSA.

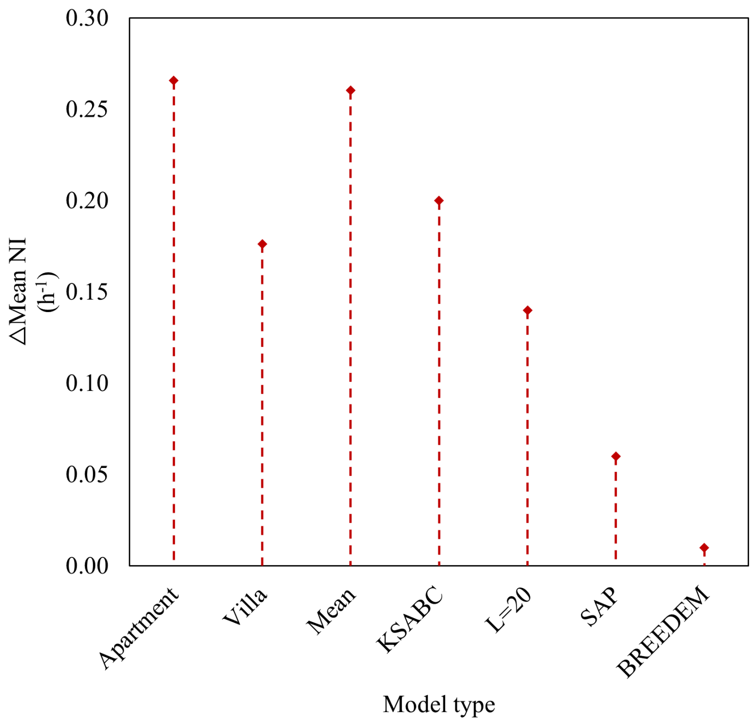

FIGURE 7.4: Infiltration rate differences of between the KSA and the UK dwellings, and building codes.

and the UK. The airflow measurements should clarify the worst areas of leakage in the building envelope and thermal bridges. This contributes in building a more realistic and reflective dataset for airflow rate and heat loss calculations of the KSA housing stock that can be easily compared with international housing stocks.

7.6 Archetypes energy, carbon emissions and cost

The energy demands of the KSA's housing stock have been predicted and reduced using the EnergyPlus building simulation tool. See Chapter 6. This research developed an eligible tool to evaluate the KSA's housing energy demands for benchmarking and improvements. This section initially discusses the results from the identified five regions and then extends the discussions to include the total housing stock in Section 7.6.1.

Applying EERM sequentially for parametric analyses showed clear energy reductions. However, integrating all EERMs does not necessarily save more energy. The integration may convert the indoor radiated heat from the installed systems and, therefore, affect energy loads. The quantity of this radiated heat may add to the space heat and increase cooling energy loads. This heat, if recognised in early design phases, can be used for heating purposes in cold climates. Each of the five KSA regions assessed in this study has a climate that is dominated by cooling energy; thus, it is crucial to enhance the performance of the building envelope to lessen cooling thermal loads. This may be accomplished via the use of envelope thermal insulation, exterior shadings, Energy Star appliances and equipment or by generating on-site electrical energy using PV panels. However, detailed thermal energy assessments are required to determine the optimal selection of building envelope components. This is performed to ensure that optimal design requirements are feasible for a large-scale application in the KSA's context. This highlights the need to identify the most influential design parameters for the KSA's housing stock. This also requires conducting a thorough and systematic simulation analysis that considers the effects of energy retrofitting measures to select optimal design parameters.

The results of the highest impact on energy savings were achieved in the villa in the Abha region from 2.45 to 1.19 (TWh), which is 51.5% of Abha's total housing energy demands. This has a profound influence on yearly electricity bills and lowered them from 135.17 to 56.91 (million USD), about 58% of yearly electricity bills. See Table 6.8 (p. 203). This is due to the higher altitudes (see Table 7.4, p. 235) and the low mean GT. See Figure 6.25 (p. 179). The Abha region is situated on the southern mountains, which positions the villa at an elevation of 2,100 m above sea level. This makes the villa absorb more solar radiation than other locations, but energy savings can be achieved by blocking this solar radiation. This presents a great contradiction to Krarti et al. (2020), who stated that the most energy savings are found in the hottest climates, such as Riyadh or Makkah, but not Abha. A possible explanation for this contradiction may be the lack of adequate thermal insulation of the baselines' envelope found in the literature. This is clearly shown in Alaidroos and Krarti (2016), Krarti et al. (2020), and Aldalbahi (2020), which makes the thermal insulation extremely effective in the hot climate. Moreover, the energy baselines developed in this research applied a minimum of 75 mm thermal insulation on the exterior surfaces of the baselines' envelope to meet the KSABC's requirements.

This research's baselines resulted in a mean 16% higher EUI than the total mean of the literature. See Figure 7.5. The red bar and dashed line in the figure represent the mean EUI (kWh/m^2/year) of the developed energy baselines. The orange bar and dashed line express the mean EUI of previous studies concerning the housing energy demands of the KSA. The dark blue bar and dashed line present the mean EUI of the optimal housing energy model. The mean baseline EUI of this study is 10% higher than the mean of the literature, and this is due to the application of higher power density to the installed systems in the dwellings. See Figure 7.2. The mean lighting power density in the literature is 11.4 (W/m^2), and this is twice the applied value of 5.45 (W/m^2) for this research's energy baselines. In contrast, the mean equipment power density of the literature is 9.9 (W/m^2), which is almost three times lower than the baseline value of 29.2 (W/m^2). This is due to the first-order approximation approach, explained in Section 5.2.9 (p. 194), to disaggregate real power density values and assign them to specific equipment rather than assumptions. This high-power intensity radiates heat, which reduces heating demands in the wintertime, especially in Abha. The predicted EUI of the total housing stock model was separately compared with the recent study by Krarti et al. (2020) and the Saudi Central Bank (SAMA) for four regions. See Figure 7.6. It illustrates clear differences between the reported models and the predicted models, and this may be due to the predicted model's compliance with the KSABC. Additionally, Krarti et al. (2020) included the traditional houses of the KSA in the calculation process. They employed the same row materials of this research to desegregate regions' flooring areas by comparing the total cooling and heating spaces of the residential stock and associated them with their total electrical energy demands. They normalised the data to predict energy use intensity by region.

TABLE 7.4: Summary of the location of the KSA most populated regions.

Weather station	Latitude (°N)	Longitude (°E)	Altitude (m)
Guriat	31.4	37.28	504
Al-Jouf	29.78	40.1	670
Tabuk	28.37	36.6	770
Hail	27.44	41.69	1000
Gassim	26.3	43.77	648
Madina	24.54	39.7	630
Dhahran	26.26	50.16	22
Riyadh New	24.92	46.72	612
Makkah	21.43	39.79	273
Al-Baha	20.29	41.64	1655
Abha	18.23	42.66	2100
Najran	17.61	44.41	1213
Gizan	16.9	42.58	4

The apartments achieved lower energy saving than the villa due to the smaller size with less area exposed to solar radiation, which minimises the effects of the exterior shading system. Apartment buildings possess more proportional thermal mass than the villa and, thus, stores more heat to release it by evening. The highest achievable energy savings of the apartments was in Tabouk, with $\mu = 40\%$ ($\sigma = 5\%$). These results may be due to the cold climate of Tabouk, with higher rates of solar radiation than all regions, except Abha. In fact, Tabouk is the only apartment building that requires heating in the winter. See Figure 6.20 (p. 175). Tabouk's apartments absorb, transfer and radiate heat from the direct sunlight to the internal space by evening due to the time lag, which raises the IAT. This reduces the heating usage and lowers the operational time for the HVAC system to meet the setpoint of 20°C. Makkah has the lowest energy saving in the apartments building due to low altitude, $\mu = 33\%$ ($\sigma = 3\%$). Makkah is a district that is located in the west of the

KSA and situated in a valley resulting in a low elevation of 237 m (Youssef et al., 2015). This is explained by the lower level of solar radiation rate of Makkah than average, see Table 6.2.

Notably, Tabouk, for example achieved the lowest energy savings with higher cost savings than Abha due to the marginal associated cost with the villa's energy use. The energy use of the villa in Tabouk exceeds 6,000 (kWh) and, therefore, applies a higher marginal tariff for load calculations for every extra kWh. The dwelling's electricity tariff is 0.048 (USD) for every 1 (kWh), and it increases when the dwelling's energy use exceeds 6,000 (kWh/month) to reach 0.08 (USD/kWh). In other words, the interval cost of every kWh is higher when dwellings consume more than 6,000 (kWh/month), which changes the calculation cost equation from Equation 7.1 to Equation 7.2, a tariff explained in Section 3.1 (p. 29). Figure 7.7 compares the energy savings of this research with Krarti et al. (2020). Figure 7.8 shows the energy use, carbon emissions and cost differences between the predicted baselines and optimal models in the KSA's five regions and demonstrates that Abha conserves the most amount of energy yearly.

$$\sum_{cost=i}^{cost=\infty} (Dwelling\, cost) = 0.048 * Energy\, use\, (kWh) \tag{7.1}$$

$$\sum_{cost=i}^{cost=\infty} (Dwelling\, cost) = 0.08 * Energy\, use\, (kWh) \tag{7.2}$$

7.6.1 The KSA's housing stock model

The KSA's housing stock energy models have been predicted and evaluated separately to calculate the energy demands, associated carbon emissions and electricity bills of each housing type and region. The housing stock model was developed in Chapter 5 and validated in Section 5.2.11 (p. 144). This resulted in seven energy models that represent one villa and an apartment building consisting of six units. The energy models were preliminary in the five most-populated regions of the KSA for energy demands, carbon emissions and electricity bill assessments. This was extended to the rest of the administrative areas to account for overall

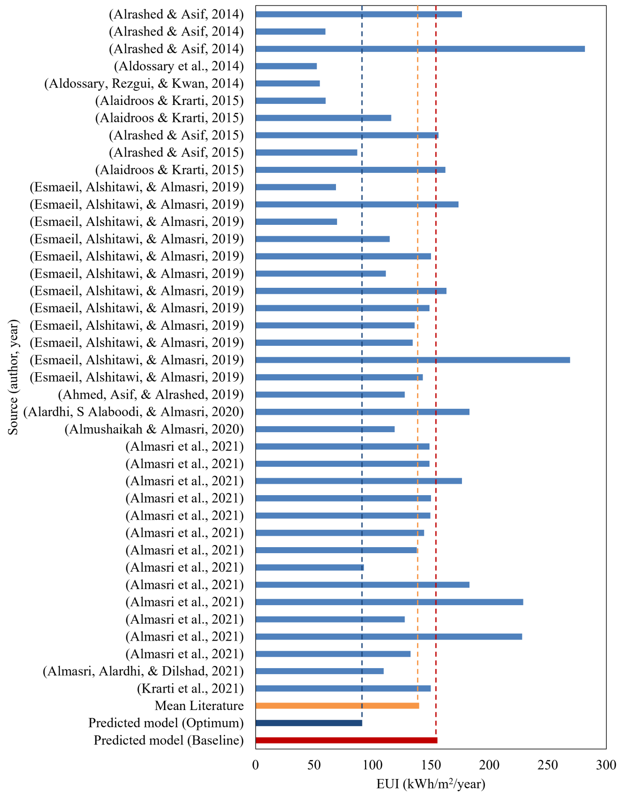

FIGURE 7.5: Energy use Intensity of the KSA dwellings and the predicted model.

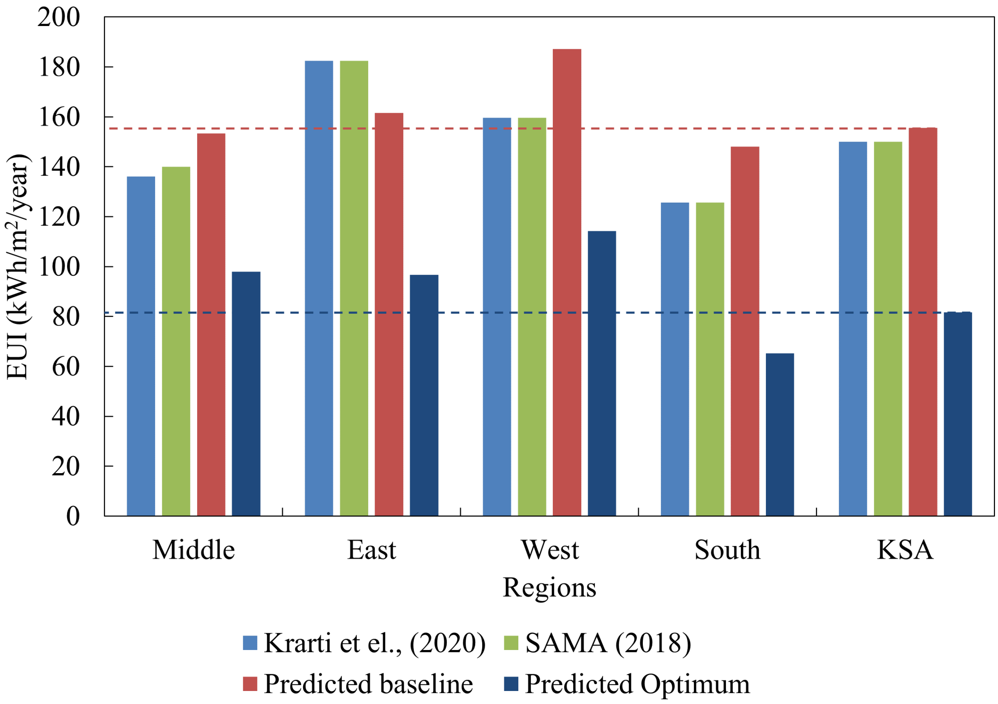

FIGURE 7.6: Housing energy use comparisons.

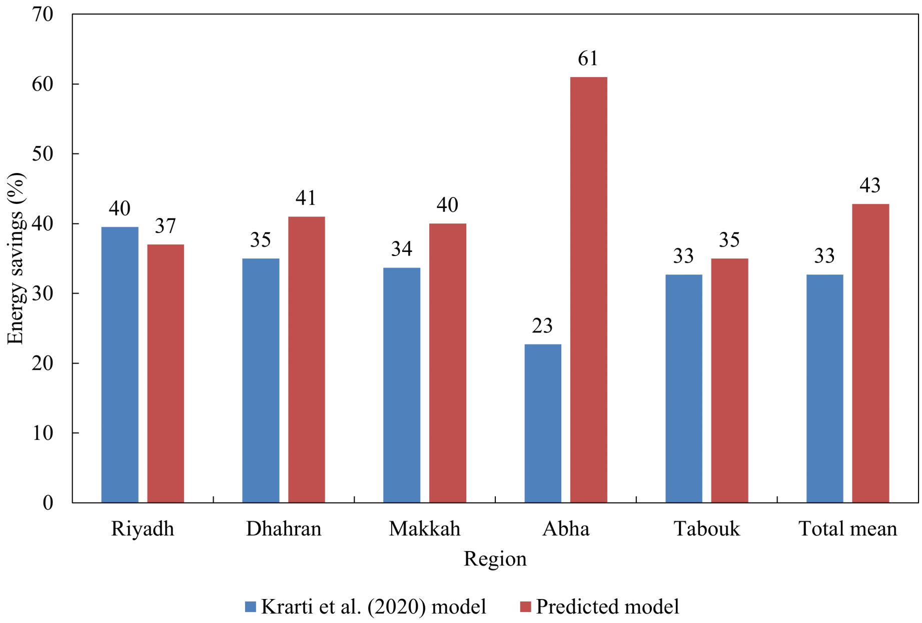

FIGURE 7.7: Energy savings comparisons.

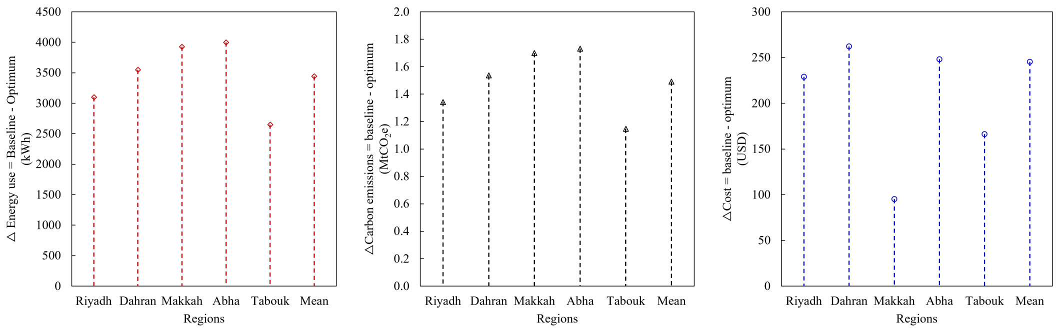

FIGURE 7.8: Predicted energy use (red), carbon emissions (black), and cost (blue) difference for the KSA housing baselines and optimum models of the KSA five regions.

reductions in the KSA. This research contortions to knowledge are summarised in Figure 7.9.

The findings of the current study do not support the previous research conducted by Krarti et al. (2020), Krarti and Howarth (2020), Alaidroos and Krarti (2016), and Aldubyan et al. (2021) stated that the energy demands of the KSA's housing stock can be reduced by 61%, which is not consistent with the 39% energy reduction of this research. There are three possible explanations for this conflict, including the lack of envelope thermal insulation in the baseline of Krarti et al. (2020) and the uniform assumption of 18°C for GT for the entire year. They have not mentioned GT in their papers, they stated that they used EnergyPlus simulation tool for the analysis, and

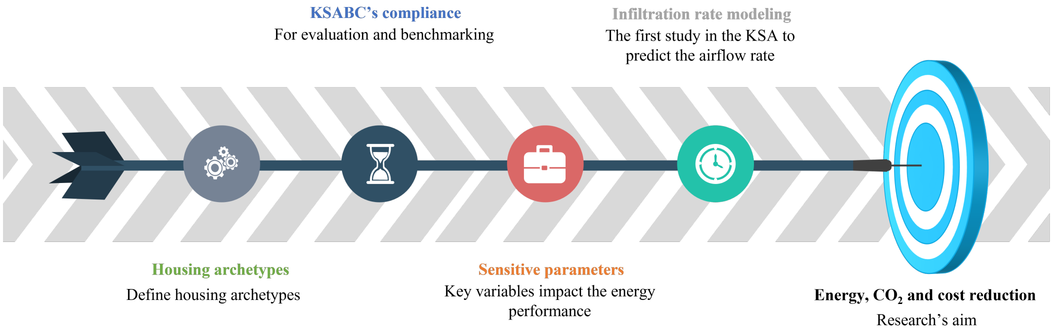

FIGURE 7.9: This research contributions to knowledge.

this tool assumes 18°C for GTs all year long to perform the calculations, even if not manually inputted, see Section 5.2.6.1 (page 130). Additionally, Krarti et al. (2020) assumed infiltration rate to be 0.8 (h^{-1}) to meet the regulations for ventilation for all the housing prototypes and occupants (ASHRAE, 2016; Mendon et al., 2015). The predicted energy use differences between the baselines and the optimum models for all regions, Δ energy use, are presented in Figure 7.10.

This contributes to lower total GHGs emissions and associated air pollutants. It also minimises utility costs, creates jobs and helps stabilise power pricing and unpredictability from an economic perspective. This often has associated long-term benefits involving decreasing overall electrical energy demands, CO_2 emissions and cost, which meets the overall aim of this research. The housing energy efficiency helps diversify utility resource portfolios and may serve as a hedge against the volatility of fuel prices. This has a strong association with the growth of the Kingdom to meet international regulations, including 130 ($MtCO_2e$) of carbon emissions reduction by 2030.

7.7 Limitation

The research limitation is defined as a study's boundaries or deficiencies that may impact the scope, reliability, or adaptability of its conclusions and offer insights to the study approach and results. This highlights areas where the investigation may have proved limited or in which further research is required to improve knowledge of the subject.

This research has identified two types of limitations that can be recognised as the limitations of the housing energy model and the infiltration rate model. A major limitation of both models is the use of only simulation techniques and no actual measurements were performed and this was due to COVID-19.

7.7.1 Energy model limitation

The first detected limitation is the sample size of the research. Even though this research developed housing archetypes in Chapter 4, the research should be vast and versatile to capture various data variation. The sample size was limited due to lack of data in different areas involving housing flooring areas, buildings dimensions, aggregation of information, ground temperature, infiltration rate, thermal insulation locations. External factors like the use of a historical weather data may not be able to reflect future changes in buildings energy behavior. This may lead to moderate generalizability and does not allow to capture accurate outputs.

7.7.2 Infiltration rate model limitation

The infiltration rate model is a simplified modeling approach and it is not able to detect housing dynamics. The simplified approach was applied over other simulation tools like CONTAM due to lack of data in different areas. For instance, CONTAM airflow simulation tool requires data that is not available in the KSA context to be able to run the simulation. This data include air leakage location, height, width and areas. Additionally, it needs relative leakage area RLA to process the simulation which is a ratio of buildings air leakage to the exterior surface area. Even though the simplified approach was applied, it distinguishes valuable information and estimates infiltration rate of the housing stock for the first time in the KSA. Further investigations are required and discussed in the following section.

7.8 Implementation of findings and future work

Table 6.8 (page 203) shows the total reduction amounts of the housing energy demands and its associated carbon emissions, and cost by each region and the overall mean. Figure 7.11 compares the energy use between the baselines and the optimum models in all KSA regions. It shows the energy reduction of Riyadh from 7.3 to 4.6 TWh (37%), Makkah from 9.24 to 5.67 TWh (38.6%), and Dhahran from 4.96 to 2.81 TWh (40%).

In 2016, the KSA's government announced Vision 2030 to introduce large-scale developments in sectors including alternative energy and buildings to obtain a diversified economy and growth. This is being accomplished through the government's long-term plans for current and future renewable energy projects to meet international regulations. One of the earliest phases of the vision is to produce 9.5 GW from alternative energy by 2023. See Chapter 2. This is important, but it requires collaboration among governmental agencies and the private sector to increases competitiveness. This research attempted to reduce housing energy demands because it is responsible for about 52% of the total energy production of the country, resulting in a higher-than-the-world's average per-capita energy use and associated carbon emissions. Therefore, this research quantified housing energy performance to reduce total energy demands, the associated carbon emissions and cost. See Chapter 5. Table 6.8 (p. 203) displays the total reduction amounts of the housing energy demands and its associated carbon emissions, cost by each region and the overall mean. Figure 7.11 compares the energy use between the baselines and the optimal models in all KSA regions. It reveals the energy reduction of Riyadh from 7.3 to 4.6 TWh (37%), Makkah from 9.24 to 5.67 Twh (38.6%) and Dhahran from 4.96 to 2.81 TWh (40%).

There are still many unanswered questions about the housing energy demands in the KSA involving the application of energy-efficiency retrofitting measures, such as employing reflective coatings on roofs, natural ventilation, passive cooling energy strategies and direct or indirect evaporative cooling systems. Moreover, the IEQ of the KSA housing is a critical factor that affects human health. Only six studies considered it, so a further study about IEQ is suggested. Occupants' thermal comfort is still not studied well in the KSA, and this indicates the need to develop a full picture of the housing stock model that considers the trade-off between energy performance, IEQ and thermal comfort. Furthermore, the infiltration rate of the KSA's housing should be physically measured using the blower door test or Pulse test to estimate dynamic and realistic outcomes that can be coupled with energy performance studies. This may be assessed by defining the areas of the housing envelope with most leakage to be sealed or treated, which may include the airflow from windows and doors frames, thermal bridges and skylights. This research used statistical analyses to develop housing archetypes that represent a proportion of the housing stock, but this may result in inaccurate generalisations as much as real measurements due to missing or incomparable data. It will be necessary to conduct more research using these characteristics to build a dataset for the housing stock. The dataset should be in a disaggregated form; it should be versatile and account for all housing types. It should also involve housing flooring areas, IAPs' concentration and thermal comfort conditions. Flooring area is an extremely important parameter that should be clearly stated in the housing or energy censuses in disaggregated forms rather than aggregated. This is important because it allows data comparisons with international housing stocks and energy performance.

The KSA's governmental agencies, academic institutions and private sector should cooperate to promote this field of research. Academics are required to address research challenges using multidisciplinary methodology and a holistic design approach that incorporates the medical sector, physics, chemistry, sociology, anthropology, architecture and engineering insights. To increase competitiveness, government entities such as the Ministry of Housing and Rural Affairs, Ministry of Energy and others should collaborate with the private sector. The public sector should provide the activities necessary to attain policies that are beneficial to citizens. The improvement of energy efficiency and the use of alternative energy sources are examples of critical policy issues to solve. To optimise housing energy performance, the industry must be urged to apply the methods indicated in this document when planning and building dwellings. Efforts should initially be made to apply the EERMs to reduce the energy demands and to meet the international energy and carbon emissions regulations. It is anticipated that this research's outcomes, which have been independently acquired from the application of various EERMs, will have a great influence on the following:

- Categorizing the KSA housing stock to develop a set of archetypal dwellings to represent it (see Chapters 3 and4);

- Supplying a housing energy model for evaluating and reducing the KSA's housing stock energy demands (see Chapters 5);
- Providing a housing infiltration rate model for evaluating the airflow rate and associated heat loss (see Chapters 5);
- Assessing the sensitivities in the KSA's housing energy and infiltration rate models (see Chapter 6);
- Elaborating the most influential variables that alter the models' outcomes (see Chapter 6);
- Defining and inferring the findings (see Chapter 7);
- Describing how the results of the energy and infiltration rate models may be used to educate and analyse the implications of new legislation and to improve the energy efficiency and environmental performance of dwellings (see Chapter 7), hence improving performance;
- Describing how the results of the energy and infiltration rate models can be used to educate and analyse the implications of new legislation and to improve the energy efficiency and environmental performance of dwellings (see Chapter 7), hence improving their performance;
- Determining the requirements for future monitoring, inspecting, and data collection activities (see Chapter 7).

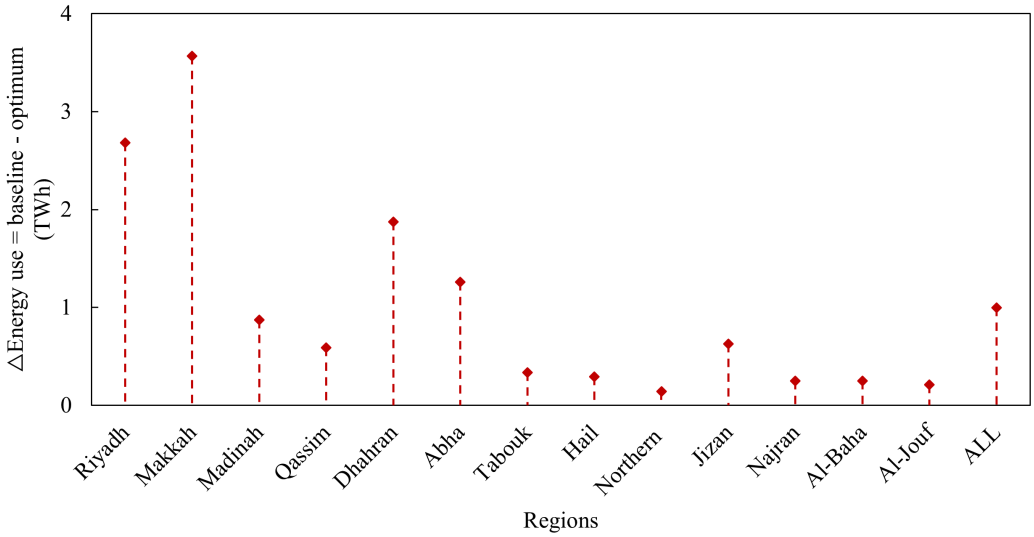

FIGURE 7.10: Predicted energy difference for the baselines and optimum models.

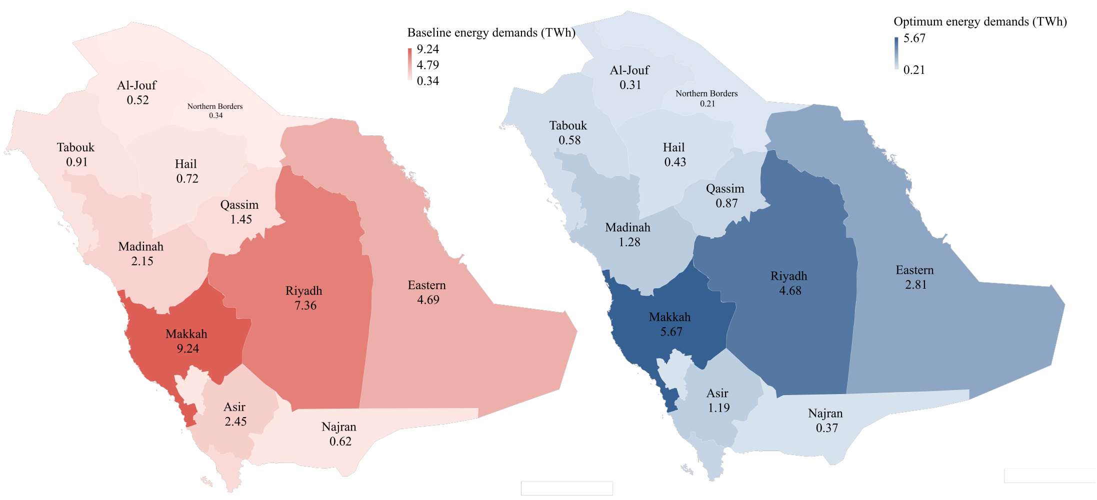

FIGURE 7.11: Housing energy use comparisons.

Chapter 8

Conclusion

This thesis provides an investigative and quantitative analysis of the KSA's housing stock energy demands, carbon emissions and cost. It highlights an estimate of the sensitivities of the energy modelling techniques that influence the overall energy performance, ventilation rates and heat gains. This new knowledge serves as a foundation for assessing and developing laws for the KSA's houses.

These findings are obtained by comparing the relevant results to the thesis's major aim and objectives. See Chapter 1. The first objective was to develop a set of representative dwellings for the KSA's housing stock. This was performed by constructing a collection of archetypal homes classified based on important features with predetermined values. See Section 4. The results accounted for 450 housing archetypes that may represent the totality of the KSA's housing stock; 18 archetypes represent 21%, 134 archetypes represent 74%, and 192 archetypes represent 85% of the total housing stock, which correspond to small, medium or strong effect sizes, respectively.

The first seven housing archetypes represent 10% of the total housing stock and account for a single-family villa unit of two floors and six apartments in a building block of three floors, consisting of two units on each floor. These archetypes have been defined according to relevant parameters, which are vintage, housing type, number of rooms, number of bedrooms, number of storeys and flooring areas. The most influential parameter is housing age, because it increases the total number of archetypes, while the common factors include building materials, cooking fuels and socio-economic status. The data processing of the archetypes considered severe flaws involving managing large volumes of data, enhancing data quality and addressing the complexity of data integration and preparation. Different crucial components are absent from public censuses, or their precision falls below expectations. This includes housing flooring areas, occupancy patterns, internal air temperature, illumination and equipment and lighting power densities. The models' capability is restricted by the number of details given by the governmental surveys. An observed lack of tenant patterns prohibits the model from measuring their influence on energy performance. This is critical because it allows the consideration of the effects of each housing type on its occupants. Moreover, this allows better thermal comfort modelling techniques and provides tenants' activities and metabolic rates. It also assists in IEQ evaluations of the dwelling's indoor pollutant concentrations. This has clear effects on occupants' health, though only a few studies have considered IAQ in the KSA's homes due to a lack of data.

The second objective was to evaluate the internal conditions of the KSA's housing stock by identifying variables including IAT, relative humidity, solar radiation rates, surface temperature and external and internal heat gains according to each housing type and location. This has been conducted using the EnergyPlus simulation tool to assess the housing's energy demands. It reveals that the internal conditions of the KSA's dwellings are not thermally comfortable, and they must rely on air-conditioning systems to achieve occupants' thermal comfort. The major key parameter for thermal comfort is IAT, and the KSA's building code states that the internal air temperature should have a cooling setpoint of 20 °C. This should be updated to include local psychometric charts and reflective thermal comfort models derived from the KSA's context with higher air temperature boundaries rather than relying on international models with lower temperature limits that are not applicable to the KSA's context. This can be updated and included in the new versions of the KSA's building codes.

The third objective was to develop an accurate predictive model that can quantify the energy performance of any given location that complies with the minimum requirements of the building code. This model clarified the needs for various sensitivity analyses that have strong associations with energy performance predictions. It is critical to show that the models' ground temperature is extremely sensitive to energy performance predictions; a strong relationship was discerned.

Likewise, researchers mostly assume the infiltration rate, and most KSA building energy performance research neglects it or assumes 0.8 (h^{-1}) as a sufficient value. This is not necessarily true, as it has never been measured or studied. Indeed, the ground temperature is critically sensitive and can alter the total energy prediction. It is also high compared to other building stocks, such as the UK's. It was also determined that there is a direct positive relationship between the infiltration rate, heat gains and the energy performance. Increasing the infiltration rate may result in inaccurate outcomes, and this may mislead the decision-making process, change the payback period and affect local economic targets. Therefore, an infiltration rate model was developed to predict the airflow rate of the KSA's housing stock.

The fourth objective was to establish an infiltration rate model that predicts the infiltration rate and associated heat loss of the KSA's housing stock. This is done through MATLAB software to develop the DOMVENT3D_KSA model. This model expected airflow rate values that are more similar to the KSA's building code, 0.2 (h^{-1}), than the values used in the literature, 0.8 (h^{-1}), for both housing archetypes, and showed that the KSA's housing heat loss may reach 37.3MWh with a median of 1.97MWh. Additionally, the KSA's building code states one value of infiltration rate should be used regardless of the location or the housing type, but the infiltration rate model developed determined airflow rates for every housing unit, each region and the total mean. This is important due to the extensive impact of climate conditions on airflow rates and heat loss calculations. This should be incorporated into the KSA's building code to draw up a set of airflow rates according to building type and location.

The fifth objective was to reduce the KSA's housing energy demands by applying various energy-efficiency retrofitting measures, which lowers the associated carbon emissions and the monthly electricity bills of the dwellings. The major reason for excessive housing energy demands is the heat absorbed from solar radiation, and this rises the temperature of the surfaces and eventually increases the IAT. Thus, the first energy retrofitting measure applied to the energy model was envelope thermal insulation. This was done by applying five thermal insulation types on the exterior or interior envelope surfaces with a range of five thicknesses for each type. This showed that the insulation is an effective measure that would be beneficial in reducing the KSA's housing energy demands, but it should be applied on the exterior surface of the envelope. Blocking direct solar radiation was considered by implementing exterior shading systems on the envelope, not just the windows. This is done because blocking solar radiation from windows would not result in a clear effect on energy prediction because of the low window-to-wall area. The third-applied EERM was to replace the equipment and lightning systems with LED appliances to reduce the power density, which resulted in great energy reduction, regardless of the location. The application of PV systems to exterior shading produced a small amount of electrical energy. The energy demands of the KSA's housing was reduced by a total mean of 0.97 TWh (39%), which lowered carbon emissions by 0.42 million $MtCO_2e$ (39%) and lowered cost by about $72.39 million (49.5%).

This research concludes by highlighting a set of recommendations and future research opportunities for the KSA housing stock;

- A national data-set development in disaggregated forms;
- More versatile and divers housing data to capture different building characteristics;
- More investigations about critical aims involving IEQ, IAP, occupants thermal comfort, airflow rates;
- Realistic measurements of housing airflow rates;

The results of this research show the need and urgency to undertake measures to reduce total housing energy demands and to decrease local carbon emissions to meet the international targets set by the Paris Agreement to limit the global warming potential. This work endeavours to achieve more energy-efficient dwellings and safeguard natural resources, which is supported by the KSA government's Vision 2030 policy.

Appendix A

AppendixA

TABLE A.1: Statistical test data of actual and simulated model.

X Actual	Y Simulated	Predicted P	Confidance Min	Max	Prediction Min	Max
4199	3205	3460	2924	3996	2220	4700
4885	3509	4288	3840	4737	3084	5493
5368	5151	4880	4485	5275	3694	6065
5690	5912	5235	4866	5603	4058	6412
7911	8275	7838	7464	8212	6660	9017
9125	9139	9258	8753	9764	8031	10485
9122	9282	9258	8753	9764	8031	10485
9201	9447	9376	8858	9895	8144	10609
9089	8445	9258	8753	9764	8031	10485
7010	7424	6773	6448	7098	5609	7937
5315	4640	4762	4357	5166	3573	5950
4287	3535	3578	3055	4101	2344	4812

TABLE A.2: Regression descriptive statistics.

Slope	1.18
Seslope	0.07
RSQ	0.96
F	249.87
SS regr	62877956.41
intercept	-1509.90
SEinterc	526.83
SEy	501.64
d.f.	10.00
SSres	2516419.11
n	12.00
Xmean	6766.67
SSxx	44906666.67
T.95	2.23
SE	501.64
Pearsons r	0.98
p-valuer	<0.001

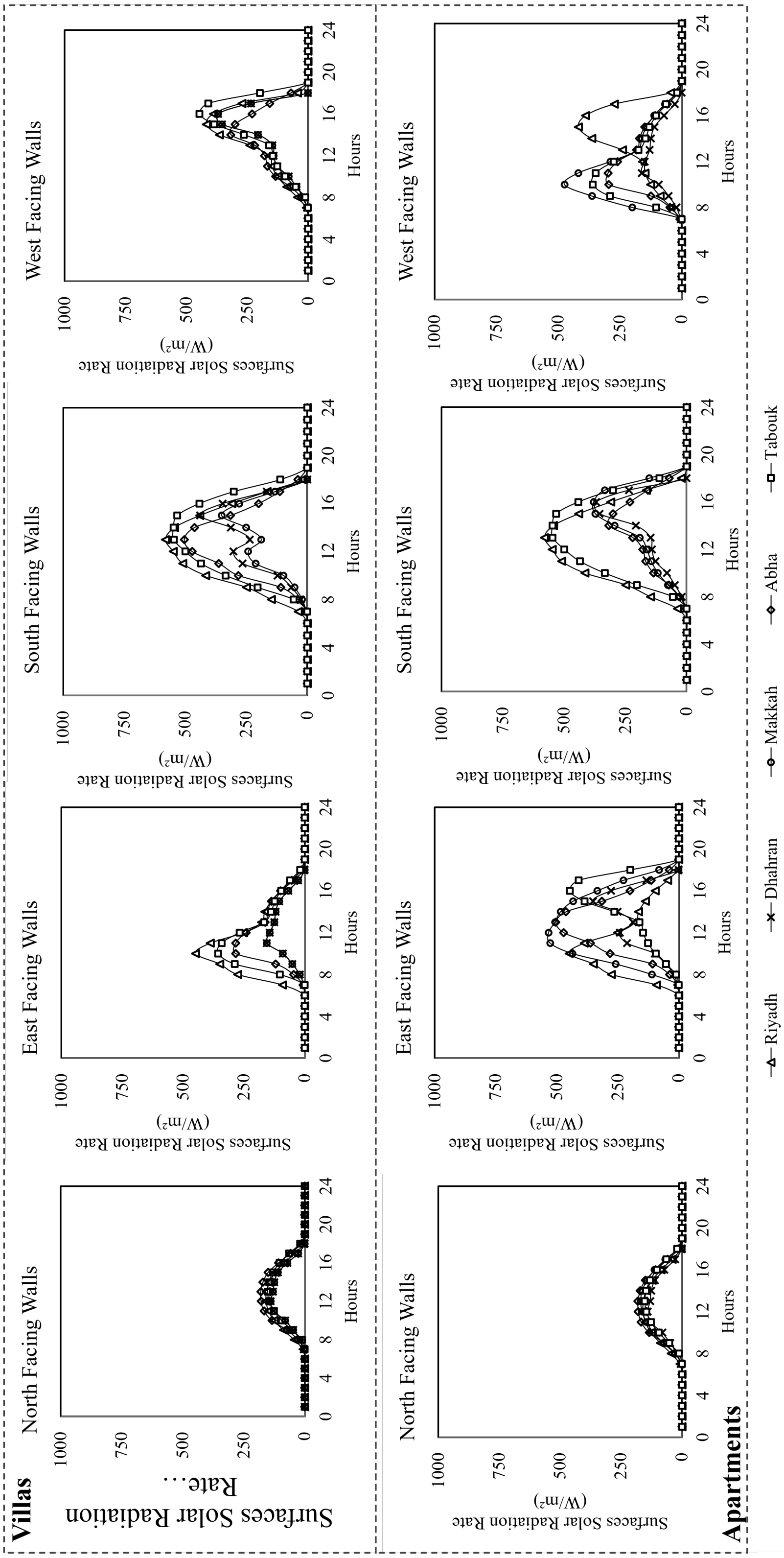

FIGURE A.1: Surfaces solar radiation rate for the archetypes in January.

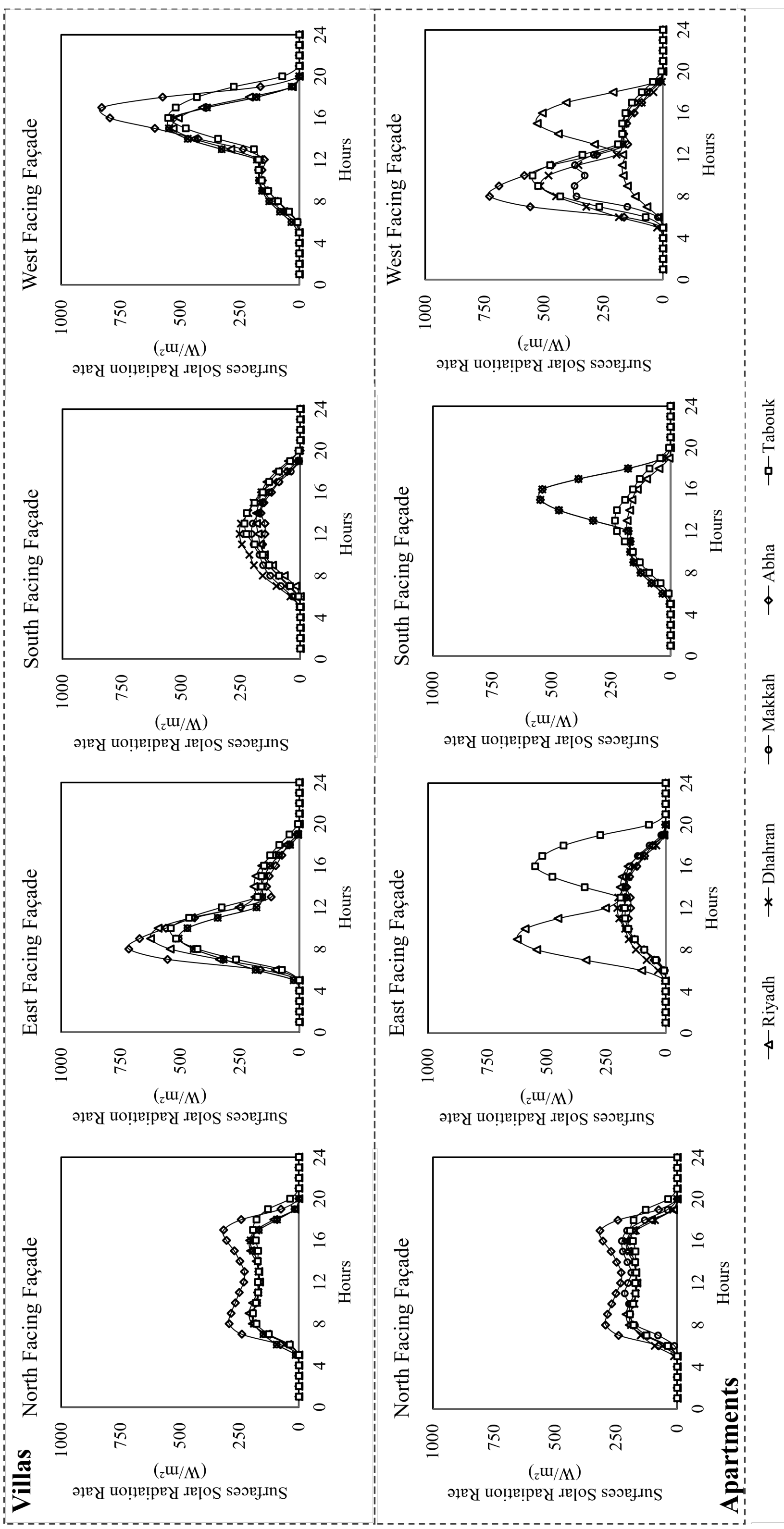

FIGURE A.2: Surfaces solar radiation rate for the archetypes in July.

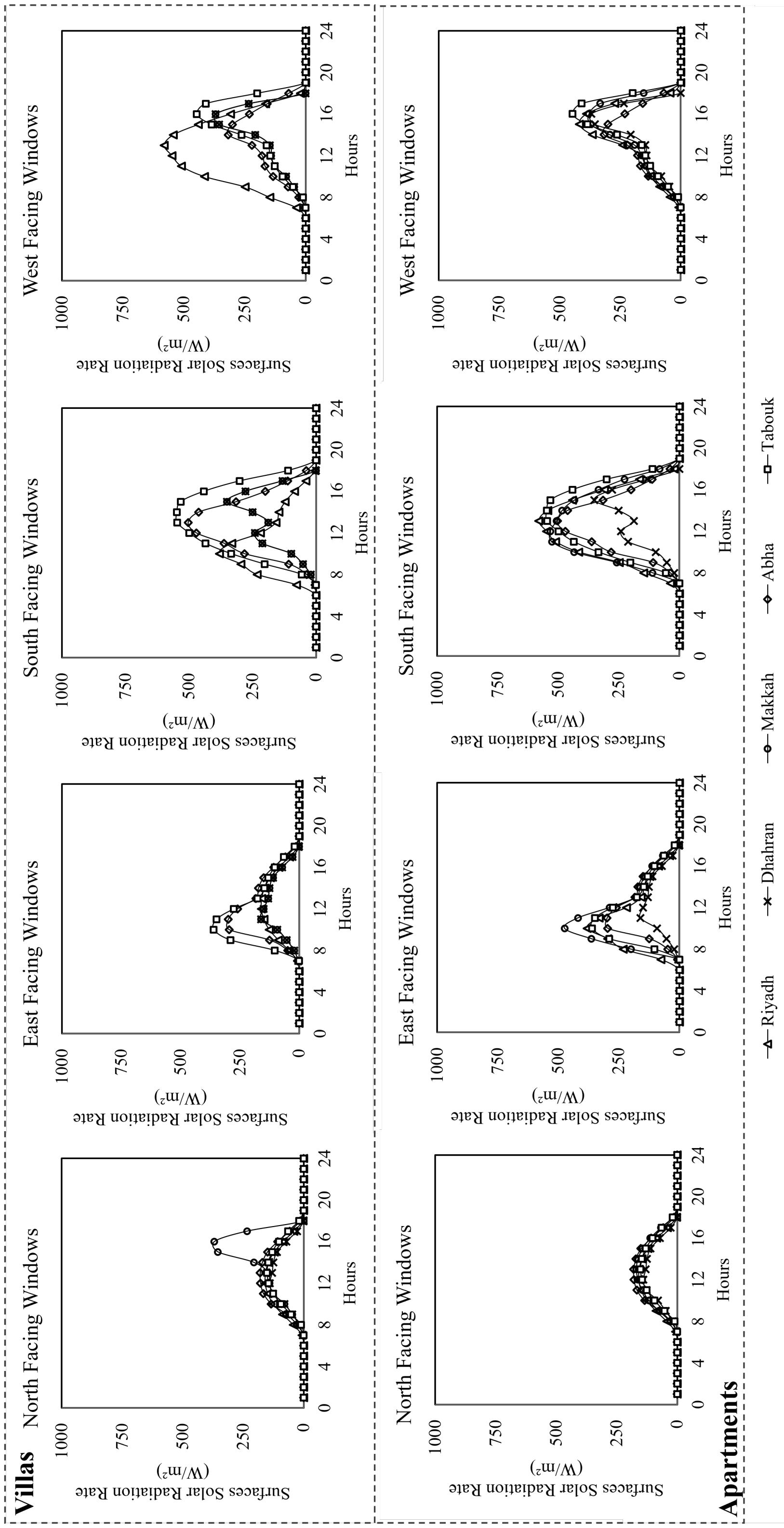

FIGURE A.3: Windows solar radiation rate for the archetypes in January.

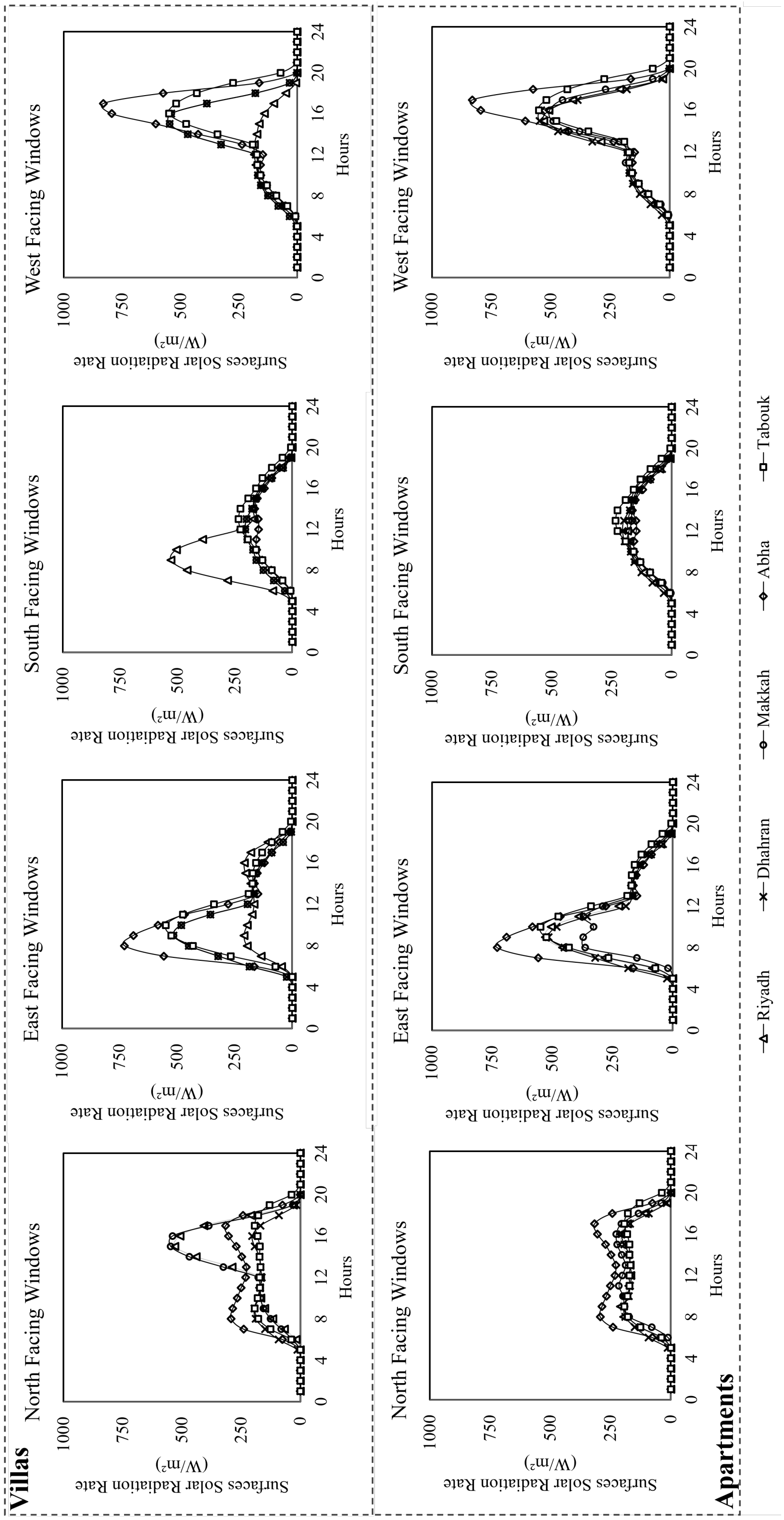

FIGURE A.4: Windows solar radiation rate for the archetypes in July.

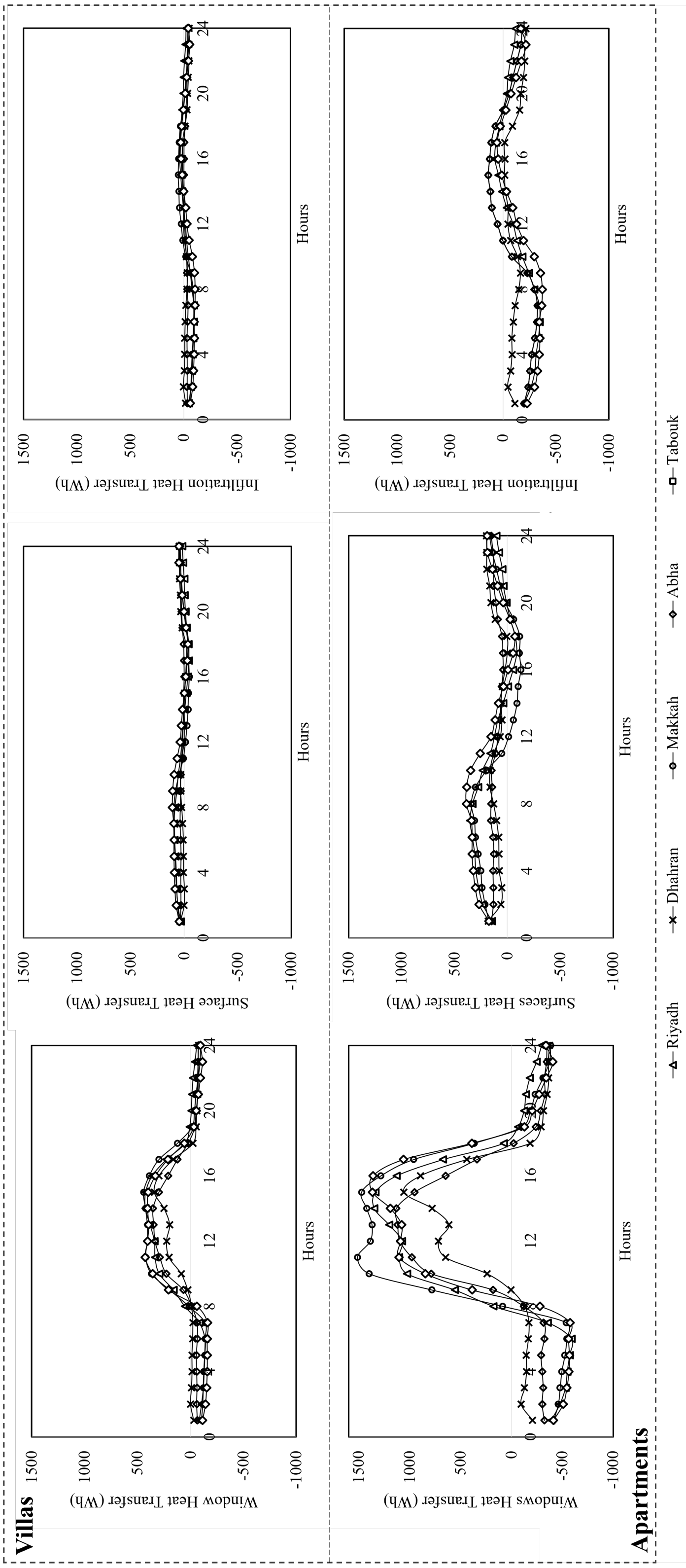

FIGURE A.5: External heat gains sources for the archetypes in January.

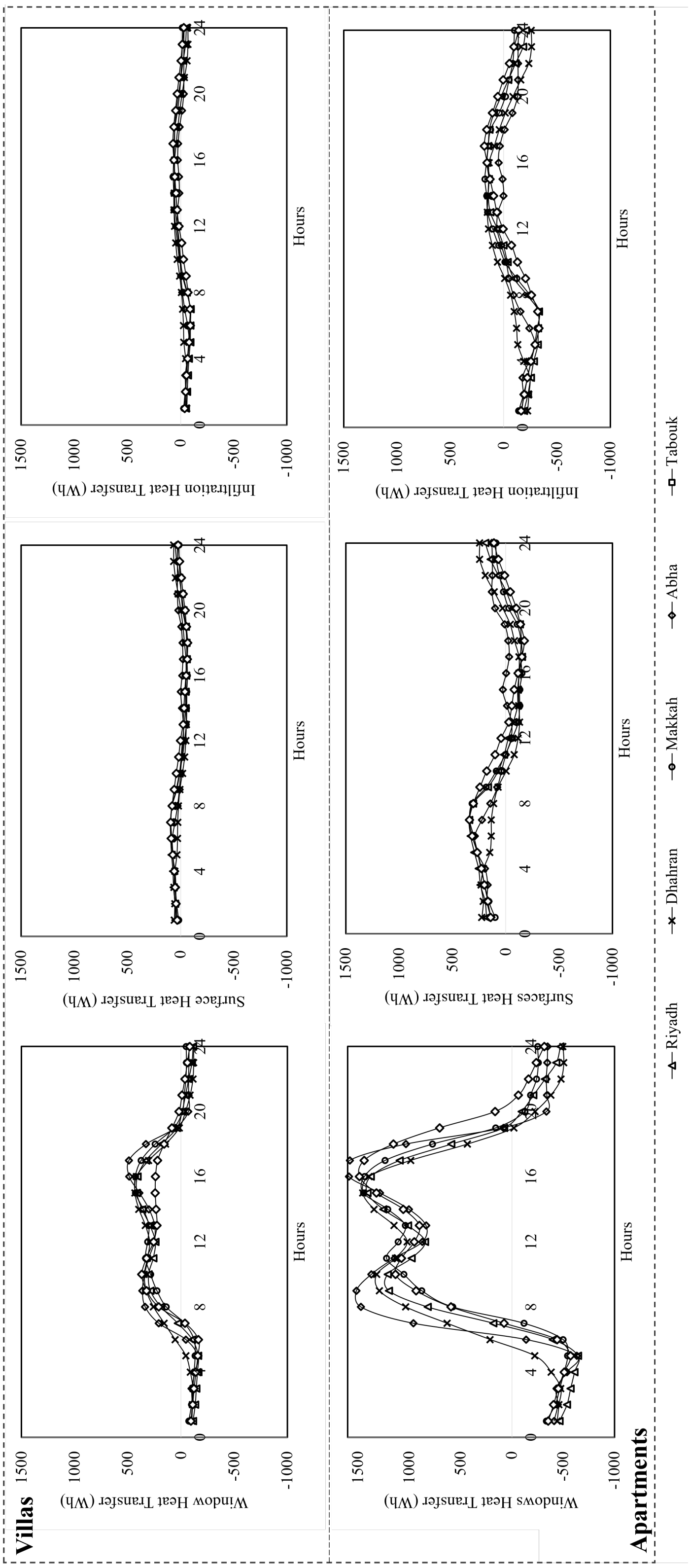

FIGURE A.6: External heat gains sources for the archetypes in July.

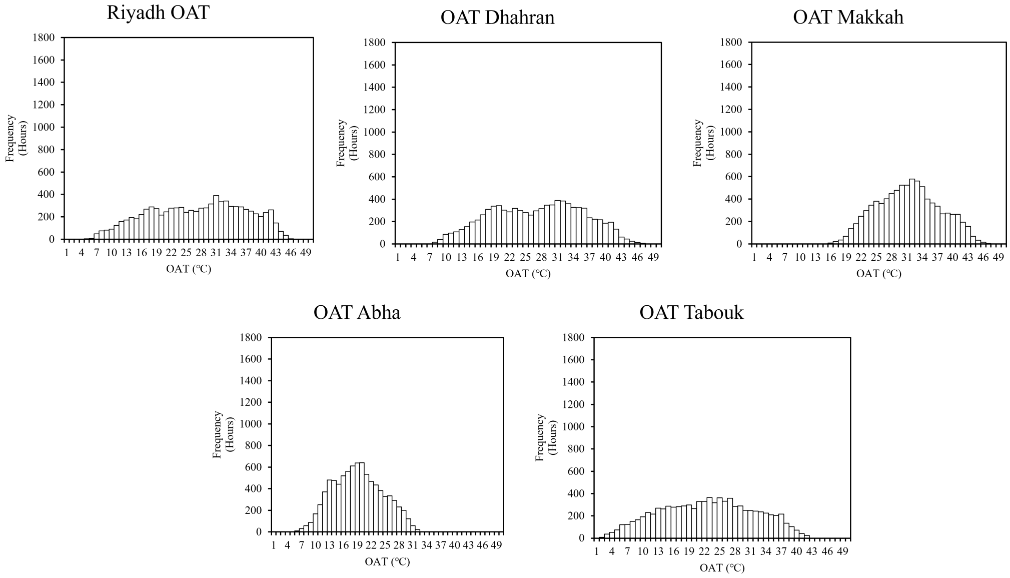

FIGURE A.7: OAT histograms for the five regions of the KSA.

TABLE A.3: Predicted total mean energy reduction of the KSA housing stock.

Region	Parameter	Housing Archetype (%)		Total	
		Villa	Apartments	Mean	SD
Riyadh	EERM1	2.7	6.3	4.5	2.5
	EERM2	9.2	16.0	12.6	4.8
	EERM3	17.4	39.2	28.3	15.4
	EERM4	26.0	40.8	33.4	10.5
	Total	35.7	37.6	36.7	1.3
Dhahran	EERM1	10.0	6.4	8.2	2.6
	EERM2	15.2	15.6	15.4	0.3
	EERM3	23.6	39.1	31.3	11.0
	EERM4	31.7	40.8	36.2	6.4
	Total	40.4	39.3	39.8	0.7
Makkah	EERM1	8.8	6.1	7.5	1.9
	EERM2	17.2	17.3	17.3	0.1
	EERM3	18.8	35.7	27.3	11.9
	EERM4	25.9	37.2	31.5	8.0
	Total	39.3	37.3	38.3	1.5
Abha	EERM1	38.1	-9.5	14.3	33.6
	EERM2	34.8	-1.7	16.5	25.8
	EERM3	50.3	34.7	42.5	11.0
	EERM4	58.5	37.1	47.8	15.2
	Total	60.8	29.1	45.0	22.4
Tabouk	EERM1	8.0	7.5	7.7	0.3
	EERM2	3.9	15.2	9.6	8.0
	EERM3	19.7	43.0	31.3	16.4
	EERM4	29.5	44.8	37.2	10.8
	Total	35.1	39.1	37.1	2.8
Total mean	EERM1	14.9	4.1	9.5	7.6
	EERM2	16.1	13.4	14.7	1.9
	EERM3	26.7	38.4	32.5	8.3
	EERM4	35.1	40.2	37.6	3.6
	Total	42.6	36.9	39.8	4.1
	SD	9.5	18.0	13.6	3.1

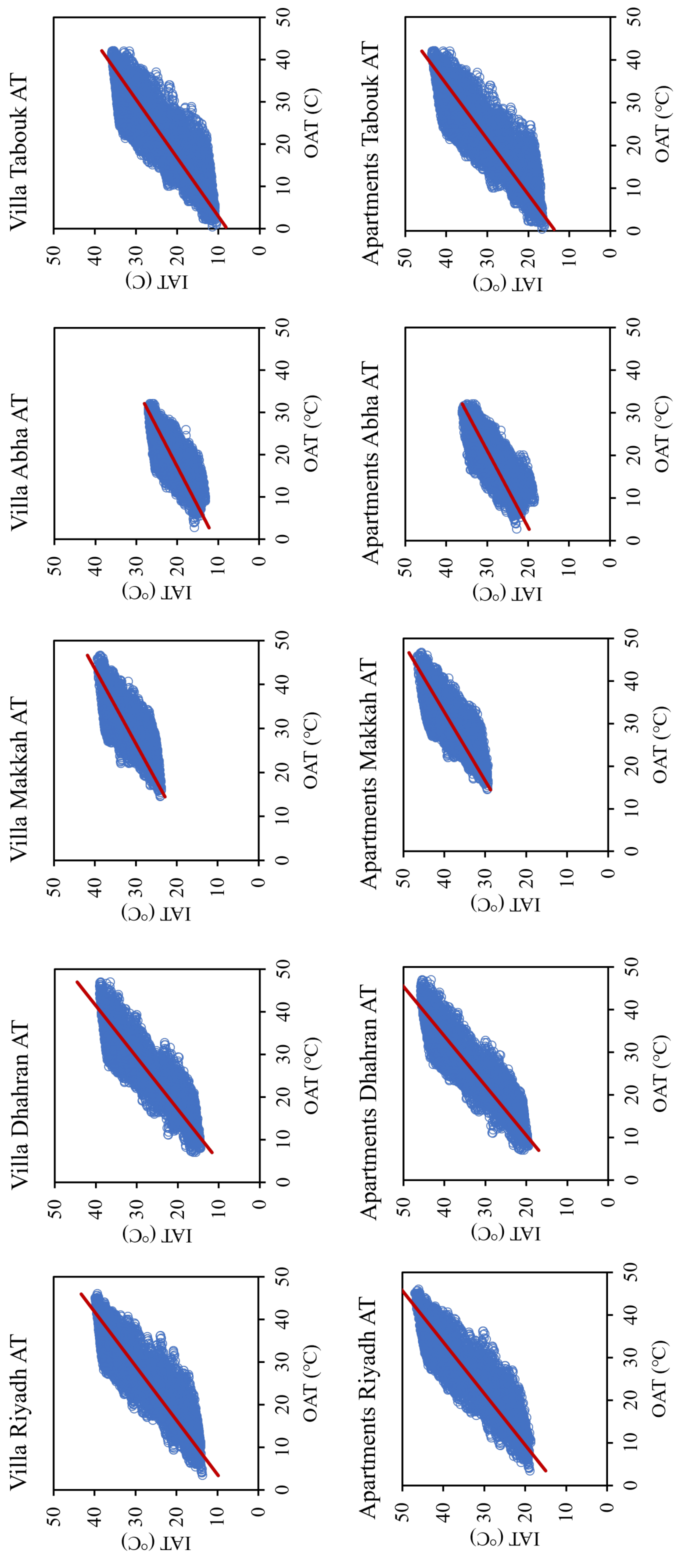

FIGURE A.8: Linear relationships between IAT and OAT for the villa and the apartments located in five regions of the KSA.

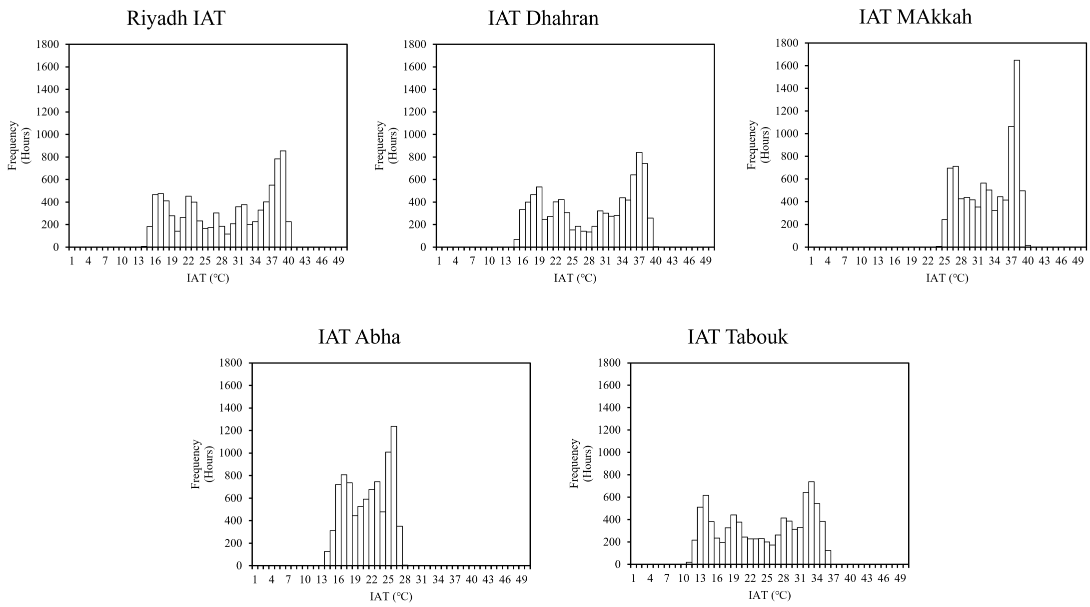

FIGURE A.9: Predicted IAT frequency for the villa located in the KSA five regions.

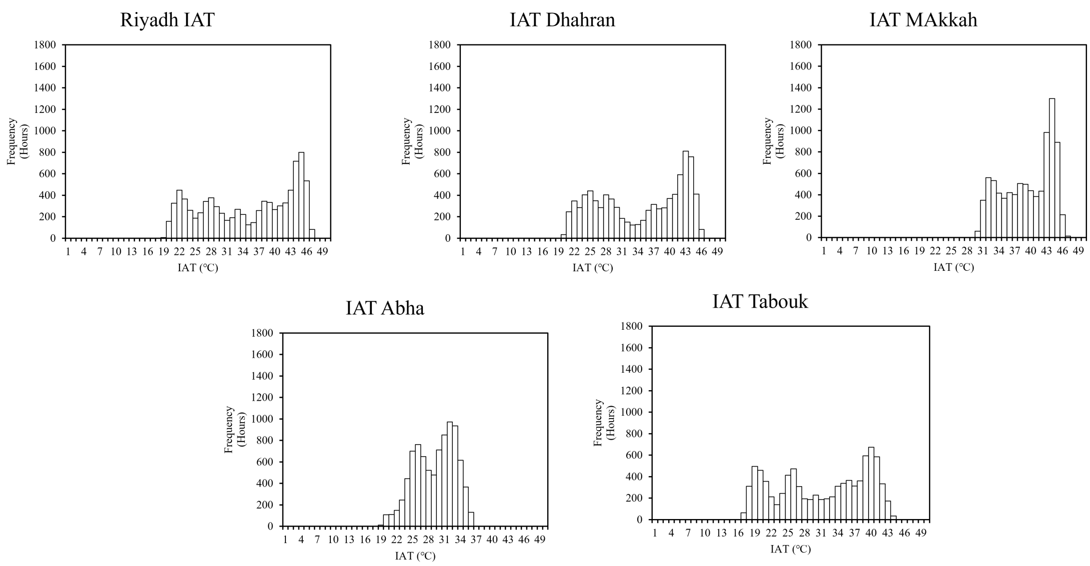

FIGURE A.10: Predicted IAT frequency for the apartments located in the KSA five regions.

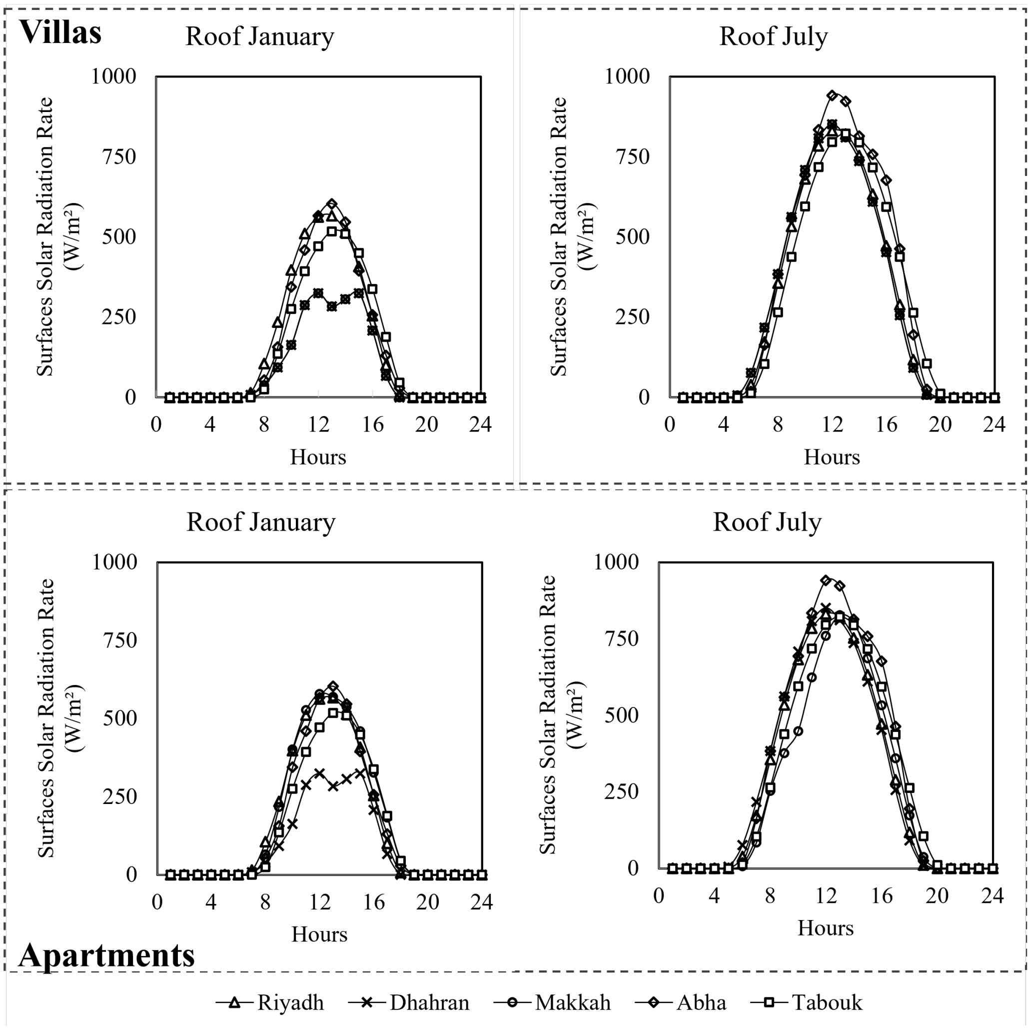

FIGURE A.11: Surfaces solar radiation rate for the archetypes roofs.

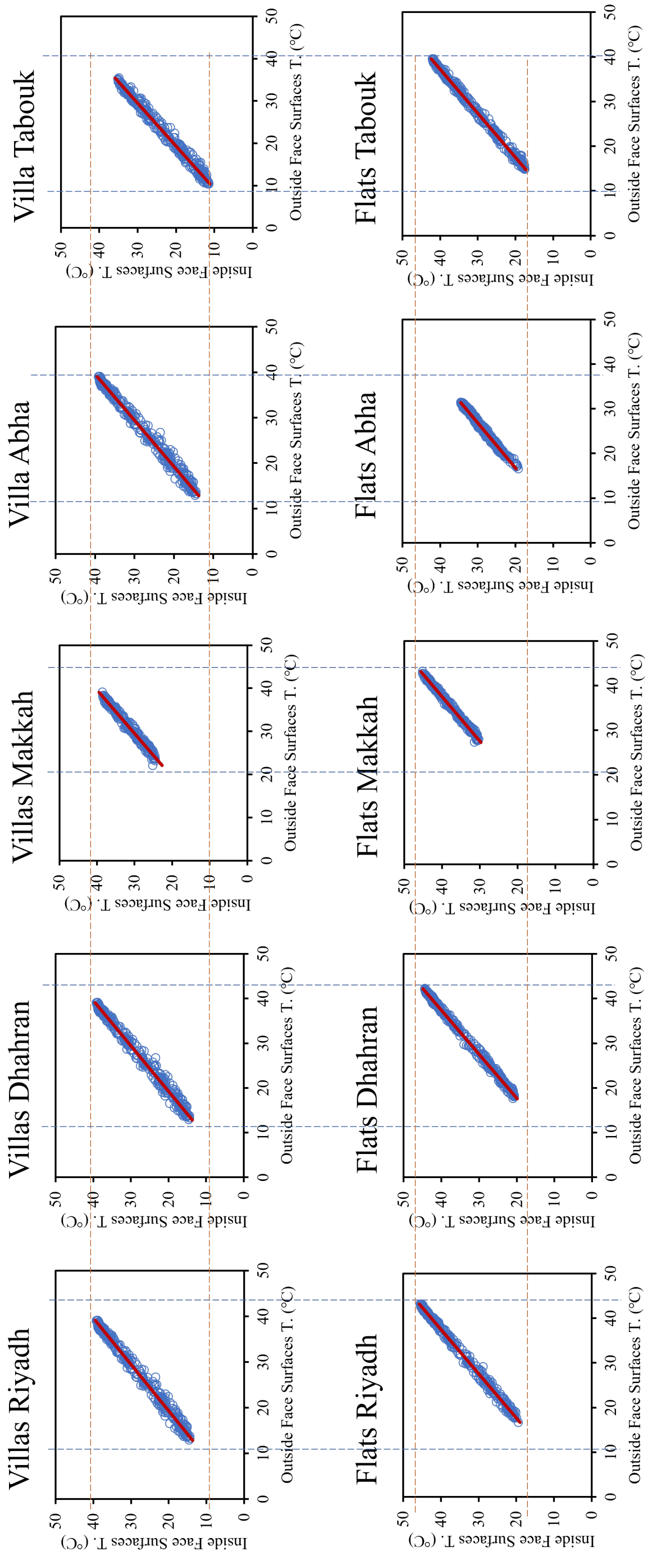

FIGURE A.12: Linear relationships between surfaces faces temperature for the archetypes.

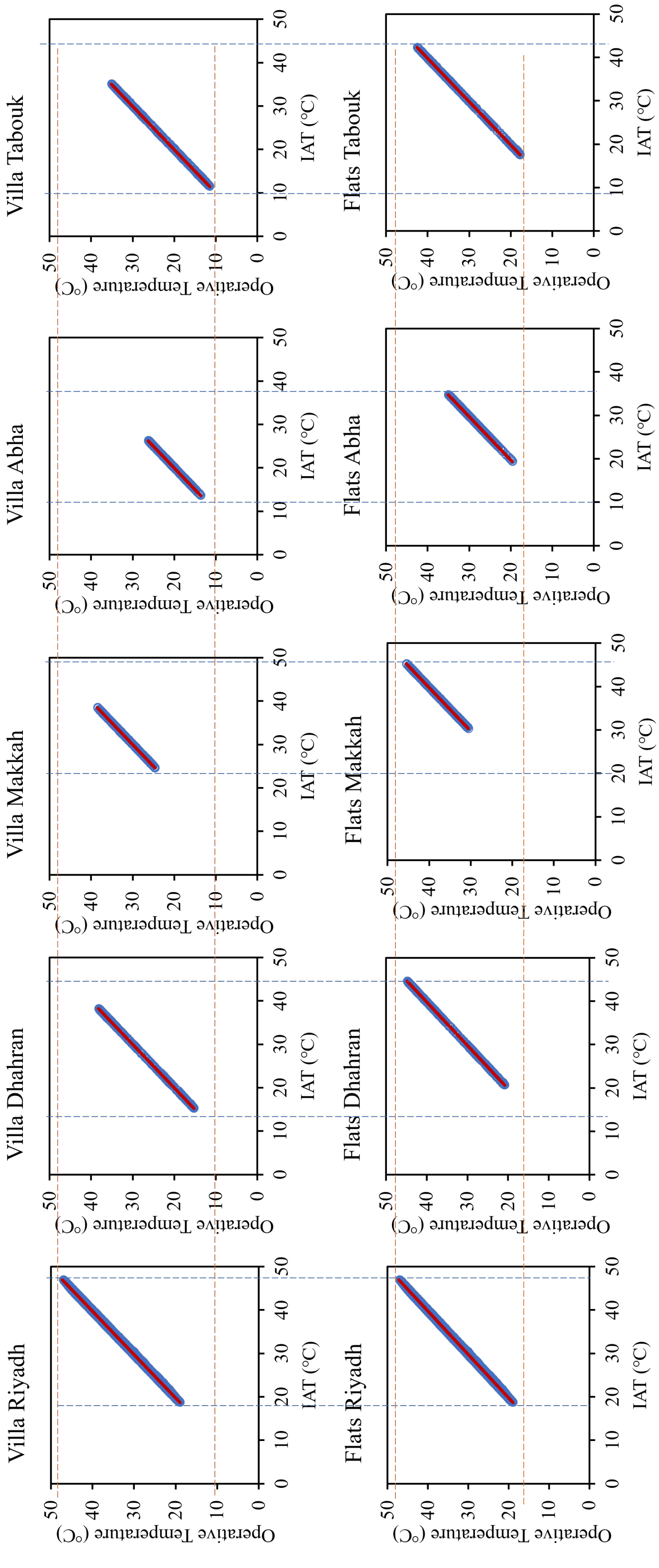

FIGURE A.13: Linear relationships between IAT and OPT for the archetypes.

TABLE A.4: Predicted energy use, cost and associated carbon emissions reduction.

	Total Villa Energy and Cost, and CO_2 Reductions (%)														
	Months	1	2	3	4	5	6	7	8	9	10	11	12	Mean	SD
Riyadh	Energy	39	39	39	36	34	33	33	32	34	38	40	45	37	4
	Cost	39	39	47	47	42	39	39	38	42	48	49	47	43	4
	CO_2	39	39	39	36	34	33	33	32	34	38	40	45	27	4
Dhahran	Energy	40	43	43	40	38	36	38	41	41	43	44	43	41	2
	Cost	42	47	59	71	76	74	77	78	75	76	67	54	66	13
	CO_2	40	43	43	40	38	36	38	41	41	43	44	43	37	2
Makkah	Energy	41	41	40	38	37	37	36	39	40	41	42	42	40	2
	Cost	54	52	50	47	44	44	43	46	48	50	52	54	48	4
	CO_2	41	41	40	38	37	37	36	39	40	41	42	42	32	2
Anha	Energy	63	64	63	62	61	57	58	58	58	62	64	64	61	3
	Cost	69	70	71	71	70	69	69	69	69	71	71	71	70	1
	CO_2	63	64	63	62	61	57	58	58	58	62	64	64	46	3
Tabouk	Energy	30	33	39	38	35	34	34	34	35	37	38	31	35	3
	Cost	30	33	38	46	49	50	51	51	50	47	36	26	42	9
	CO_2	30	33	39	38	35	34	34	34	35	37	38	31	34	3
Total	Energy	43	44	45	43	41	40	40	41	42	44	46	45	43	2
	Cost	47	48	53	56	56	55	56	56	57	58	55	50	54	4
	CO_2	45	46	46	43	41	39	40	41	42	44	46	46	34	3
	Total Apartments Energy and Cost, and CO_2 Reductions (%)														
	Months	1	2	3	4	5	6	7	8	9	10	11	12	Mean	SD
Riyadh	Energy	44	43	40	35	31	31	30	30	32	35	39	43	36	6
	Cost	48	47	43	37	33	32	31	31	34	37	42	48	39	7
	CO_2	39	40	39	37	37	37	36	36	37	38	39	39	32	1
Dhahran	Energy	44	44	40	35	32	31	30	30	32	35	39	42	36	5
	Cost	48	48	43	38	34	33	32	32	34	37	42	45	39	6
	CO_2	42	42	41	39	38	38	38	38	39	39	40	40	33	1
Makkah	Energy	37	37	36	33	31	30	30	30	31	33	34	36	33	3
	Cost	40	40	38	35	32	32	32	31	33	35	36	39	35	3
	CO_2	38	39	38	37	36	37	36	36	37	38	38	38	31	1
Anha	Energy	37	36	33	31	30	28	28	28	29	33	36	37	32	3
	Cost	41	40	37	34	33	30	30	31	32	36	39	41	35	4
	CO_2	30	30	29	29	29	29	29	29	29	29	30	30	25	1
Tabouk	Energy	46	47	45	40	36	35	33	33	35	39	43	45	40	5
	Cost	51	52	48	43	38	37	35	35	38	41	46	50	43	6
	CO_2	40	42	41	39	38	38	38	38	39	39	40	39	34	1
Total	Energy	42	41	39	35	32	31	30	30	32	35	38	41	35	4
	Cost	46	46	42	37	34	33	32	32	34	37	41	44	38	5
	CO_2	38	39	38	37	36	36	36	36	37	37	38	37	32	1

TABLE A.5: Predicted energy reduction and generation for the villa archetype.

	Villa Archetype Energy Reduction (kWh)														
	Months	1	2	3	4	5	6	7	8	9	10	11	12	Mean	SD.
Riyadh	Baseline	5560	5646	7735	10433	13614	14384	15519	15266	13328	11734	8008	6337	10630	3827
	EERM1	5410	5517	7518	10107	13303	14252	15387	15304	13060	11083	7620	5528	10341	3911
	EERM2	5948	5964	7679	9525	11898	12528	13403	13352	11666	10317	7661	5916	9655	2934
	EERM3	3170	3878	5869	8675	11883	13014	14088	14032	11862	9803	5978	3074	8777	4245
	EERM4	2343	3058	4915	7748	10925	12086	13129	13073	10935	8846	5055	2296	7867	4195
	Total	3384	3447	4713	6640	8937	9673	10460	10390	8765	7292	4798	3486	6832	2788
	PV	13	15	17	18	19	21	21	20	19	17	14	12	17	3
Dhahran	Baseline	5642	5797	8023	10851	14309	14890	16710	17063	14642	13106	8575	6652	11355	4275
	EERM1	5345	5306	7287	9976	13158	13963	15061	14781	12835	11224	7615	6031	10215	3761
	EERM2	5856	5832	7541	9456	11875	12381	13270	13048	11583	10486	7699	6537	9630	2836
	EERM3	2971	3619	5625	8537	11834	12740	13841	13538	11684	9916	5951	3873	8678	4105
	EERM4	2150	2799	4671	7611	10876	11812	12882	12579	10757	8959	5028	2985	7759	4067
	Total	3368	3303	4567	6561	8891	9503	10285	10050	8645	7441	4832	3816	6772	2697
	PV	12	14	16	18	21	21	21	20	19	16	14	12	17	3
Makkah	Baseline	9926	9269	11615	12991	15080	15395	15784	16369	15768	14552	12528	10575	13321	2512
	EERM1	9070	8505	10694	12025	14142	14369	14862	14752	13969	12799	11037	9510	12145	2333
	EERM2	8828	8231	10067	10913	12516	12605	13019	12957	12341	11598	10208	9122	11034	1715
	EERM3	7511	7255	9436	10741	12784	13168	13517	13371	12764	11649	9697	7870	10814	2396
	EERM4	6555	6391	8478	9814	11825	12239	12558	12412	11836	10690	8770	6914	9874	2386
	Total	5823	5492	7024	8020	9545	9717	10051	9975	9413	8520	7268	6135	8082	1696
	PV	14	16	18	19	19	20	20	19	19	17	15	13	17	2
Abha	Baseline	8758	8524	10375	10858	12094	12919	13346	13193	11999	10979	9467	9106	10968	1750
	EERM1	5118	4891	6110	6625	7563	8556	8720	8588	7864	6735	5461	5218	6787	1445
	EERM2	5713	5633	6745	7015	7772	8413	8592	8483	7927	7264	6271	5982	7151	1093
	EERM3	2971	3631	4753	5308	6274	7458	7483	7228	6747	5735	4339	3514	5453	1616
	EERM4	2188	2819	3823	4388	5319	6532	6527	6271	5822	4783	3453	2643	4547	1568
	Total	3257	3076	3818	4154	4774	5491	5588	5489	5000	4213	3401	3284	4295	948
	PV	16	20	21	22	22	23	22	21	23	22	20	17	21	2
Tabouk	Baseline	5079	4723	5958	8057	10496	11683	13173	12843	11316	9089	6072	5061	8629	3209
	EERM1	5261	4838	5914	7471	9382	10452	11476	11243	9962	8171	5862	5241	7939	2498
	EERM2	5355	5168	6507	7953	9783	10589	11732	11474	10308	8753	6503	5396	8293	2468
	EERM3	2293	2712	4243	6650	9021	10462	11928	11552	10076	7607	4289	2305	6928	3674
	EERM4	1780	2068	3332	5725	8064	9535	10969	10594	9149	6652	3387	1766	6085	3542
	Total	3532	3154	3656	5034	6789	7662	8702	8444	7337	5711	3737	3491	5604	2104
	PV	12	15	17	20	20	22	21	21	19	16	13	11	17	4
Total mean	Baseline	6993	6792	8741	10638	13119	13854	14906	14947	13411	11892	8930	7546	10981	3115
	EERM1	6041	5811	7505	9241	11510	12318	13101	12934	11538	10002	7519	6306	9485	2790
	EERM2	6340	6166	7708	8972	10769	11303	12003	11863	10765	9684	7668	6590	9153	2209
	EERM3	3783	4219	5985	7982	10359	11368	12171	11944	10627	8942	6051	4127	8130	3207
	EERM4	3003	3427	5044	7057	9402	10441	11213	10986	9700	7986	5139	3321	7227	3152
	Total	3873	3694	4756	6082	7787	8409	9017	8870	7832	6635	4807	4042	6317	2047
	PV	13	16	18	19	20	21	21	20	20	18	15	13	18	3

TABLE A.6: Predicted energy reduction and generation for the apartments archetypes.

		Apartments Archetype Energy Reduction (kWh)													
	Months	1	2	3	4	5	6	7	8	9	10	11	12	Mean	SD.
Riyadh	Baseline	28056	27690	33647	37987	44436	45890	48398	48216	43689	40841	32980	27657	38291	8045
	EERM1	25640	25252	31114	35652	42240	43782	46214	45887	41075	37852	30396	25445	35879	8092
	EERM2	25329	24334	29097	31928	36601	37229	39180	39063	35632	33806	28519	25204	32160	5528
	EERM3	12778	13897	18382	23201	29152	31097	33110	32928	28898	25562	18214	12370	23299	7915
	EERM4	12115	13307	17732	22577	28510	30476	32469	32287	28276	24918	17581	11700	22662	7919
	Total	16980	16668	20629	23744	28202	29121	30809	30661	27415	25203	20269	16928	23886	5444
	PV	18	21	24	27	29	31	31	30	28	25	19	16	25	5
Dhahran	Baseline	27617	27209	33291	37778	44726	45572	48310	47427	43589	41383	33199	29828	38327	7836
	EERM1	25303	24801	30730	35429	42409	43388	46006	44943	40883	38383	30628	27538	35870	7825
	EERM2	25164	24099	28955	31855	36865	37160	39274	38617	35702	34545	28897	27012	32345	5383
	EERM3	12341	13429	18029	22995	29445	30782	33024	32143	28799	26106	18434	14574	23342	7686
	EERM4	11678	12835	17378	22370	28802	30161	32383	31501	28177	25461	17800	13914	22705	7688
	Total	16081	15730	19668	22889	27630	28240	30038	29341	26648	25104	19876	17854	23258	5254
	PV	17	20	23	26	31	31	31	29	27	24	19	16	25	6
Makkah	Baseline	36473	33954	40235	41682	46014	46032	47242	46864	45080	44009	39670	37001	42021	4532
	EERM1	33645	31313	37386	39320	43812	43831	45046	44580	42483	40931	36830	34324	39458	4715
	EERM2	31145	28633	33435	34355	37652	37289	38461	38347	36746	36026	33068	31635	34733	3191
	EERM3	21197	20155	24952	26888	30724	31232	31950	31573	30281	28720	24880	21725	27023	4348
	EERM4	20551	19572	24309	26268	30084	30614	31311	30933	29662	28079	24258	21079	26393	4344
	Total	22532	20841	24842	26169	29240	29128	30058	29912	28485	27349	24700	23066	26360	3145
	PV	20	23	26	28	29	30	30	29	27	24	21	18	25	4
Abha	Baseline	23129	22449	26473	27004	29318	30653	31374	31045	29337	27958	24828	24066	27303	3145
	EERM1	24842	24471	29053	29814	32484	33976	34631	33957	32075	30544	26910	25893	29887	3669
	EERM2	24777	23680	27358	27457	29400	30105	30875	30602	29131	28464	25915	25570	27778	2380
	EERM3	12643	13941	16754	17441	19586	21613	21770	21046	20077	18793	15954	14185	17817	3153
	EERM4	11978	13349	16102	16809	18935	20988	21121	20398	19450	18142	15321	13527	17177	3153
	Total	16253	15786	18787	19283	20943	21882	22406	22160	20875	19730	17343	16853	19358	2365
	PV	17	20	23	26	31	31	31	29	27	24	19	16	25	6
Tabouk	Baseline	25319	25107	30742	34651	39573	41630	44896	44083	40732	36947	29865	25312	34905	7458
	EERM1	22940	22516	27941	31993	37140	39135	42308	41349	37786	33881	27299	23151	32287	7360
	EERM2	23313	22282	26736	29224	32972	33948	36419	35913	33362	31077	26282	23485	29584	5070
	EERM3	9988	11262	15479	19872	24296	26841	29611	28799	25944	21677	15097	9990	19905	7351
	EERM4	9298	10661	14826	19245	23651	26219	28970	28157	25321	21029	14464	9295	19261	7362
	Total	15112	14656	18224	20968	24503	25697	27894	27369	25004	22426	18066	15334	21271	4889
	PV	17	21	25	29	29	32	32	30	28	23	18	15	25	6
Total mean	Baseline	28119	27282	32877	35820	40813	41955	44044	43527	40485	38228	32108	28773	36169	6203
	EERM1	26474	25670	31245	34441	39617	40822	42841	42143	38860	36318	30413	27270	34676	6332
	EERM2	25946	24606	29116	30964	34698	35146	36842	36508	34115	32784	28536	26581	31320	4310
	EERM3	13789	14537	18719	22079	26641	28313	29893	29298	26800	24172	18516	14569	22277	6091
	EERM4	13124	13945	18069	21454	25996	27691	29251	28655	26177	23526	17885	13903	21640	6093
	Total	17392	16736	20430	22611	26104	26814	28241	27889	25685	23962	20051	18007	22827	4219
	PV	18	21	24	27	30	31	31	30	28	24	19	16	25	5

TABLE A.7: Monthly villa energy reductions by percentages.

		Villas Energy Reductionas (%)													
	Months	1	2	3	4	5	6	7	8	9	10	11	12	Mean	SD.
Riyadh	EERM1	2.7	2.3	2.8	3.1	2.3	0.9	0.8	-0.3	2.0	5.5	4.8	12.8	2.7	-2.2
	EERM2	-7.0	-5.6	0.7	8.7	12.6	12.9	13.6	12.5	12.5	12.1	4.3	6.6	9.2	23.3
	EERM3	43.0	31.3	24.1	16.9	12.7	9.5	9.2	8.1	11.0	16.5	25.3	51.5	17.4	-10.9
	EERM4	57.9	45.8	36.5	25.7	19.8	16.0	15.4	14.4	18.0	24.6	36.9	63.8	26.0	-9.6
	Total	39.1	38.9	39.1	36.4	34.4	32.7	32.6	31.9	34.2	37.9	40.1	45.0	35.7	27.2
	PV	0.23	0.26	0.21	0.17	0.14	0.15	0.13	0.13	0.14	0.15	0.17	0.19	0.16	0.08
Dhahran	EERM1	5.3	8.5	9.2	8.1	8.0	6.2	9.9	13.4	12.3	14.4	11.2	9.3	10.0	12.0
	EERM2	-3.8	-0.6	6.0	12.9	17.0	16.9	20.6	23.5	20.9	20.0	10.2	1.7	15.2	33.7
	EERM3	47.3	37.6	29.9	21.3	17.3	14.4	17.2	20.7	20.2	24.3	30.6	41.8	23.6	4.0
	EERM4	61.9	51.7	41.8	29.9	24.0	20.7	22.9	26.3	26.5	31.6	41.4	55.1	31.7	4.9
	Total	40.3	43.0	43.1	39.5	37.9	36.2	38.4	41.1	41.0	43.2	43.7	42.6	40.4	36.9
	PV	0.22	0.25	0.20	0.16	0.14	0.14	0.13	0.12	0.13	0.13	0.16	0.17	0.15	0.08
Makkah	EERM1	8.6	8.2	7.9	7.4	6.2	6.7	5.8	9.9	11.4	12.0	11.9	10.1	8.8	7.1
	EERM2	11.1	11.2	13.3	16.0	17.0	18.1	17.5	20.8	21.7	20.3	18.5	13.7	17.2	31.7
	EERM3	24.3	21.7	18.8	17.3	15.2	14.5	14.4	18.3	19.1	20.0	22.6	25.6	18.8	4.6
	EERM4	34.0	31.0	27.0	24.5	21.6	20.5	20.4	24.2	24.9	26.5	30.0	34.6	25.9	5.0
	Total	41.3	40.8	39.5	38.3	36.7	36.9	36.3	39.1	40.3	41.5	42.0	42.0	39.3	32.5
	PV	0.14	0.17	0.16	0.15	0.13	0.13	0.12	0.12	0.12	0.12	0.12	0.12	0.13	0.10
Abha	EERM1	41.6	42.6	41.1	39.0	37.5	33.8	34.7	34.9	34.5	38.7	42.3	42.7	38.1	17.4
	EERM2	34.8	33.9	35.0	35.4	35.7	34.9	35.6	35.7	33.9	33.8	33.8	34.3	34.8	37.5
	EERM3	66.1	57.4	54.2	51.1	48.1	42.3	43.9	45.2	43.8	47.8	54.2	61.4	50.3	7.7
	EERM4	75.0	66.9	63.2	59.6	56.0	49.4	51.1	52.5	51.5	56.4	63.5	71.0	58.5	10.4
	Total	62.8	63.9	63.2	61.7	60.5	57.5	58.1	58.4	58.3	61.6	64.1	63.9	60.8	45.8
	PV	0.18	0.23	0.20	0.20	0.18	0.17	0.16	0.16	0.19	0.20	0.21	0.18	0.19	0.13
Tabouk	EERM1	-3.6	-2.4	0.7	7.3	10.6	10.5	12.9	12.5	12.0	10.1	3.5	-3.6	8.0	22.1
	EERM2	-5.4	-9.4	-9.2	1.3	6.8	9.4	10.9	10.7	8.9	3.7	-7.1	-6.6	3.9	23.1
	EERM3	54.8	42.6	28.8	17.5	14.0	10.4	9.5	10.1	11.0	16.3	29.4	54.4	19.7	-14.5
	EERM4	65.0	56.2	44.1	28.9	23.2	18.4	16.7	17.5	19.1	26.8	44.2	65.1	29.5	-10.4
	Total	30.5	33.2	38.6	37.5	35.3	34.4	33.9	34.3	35.2	37.2	38.5	31.0	35.1	34.4
	PV	0.24	0.32	0.29	0.24	0.19	0.19	0.16	0.16	0.17	0.18	0.22	0.22	0.20	0.11
Total mean	EERM1	12.8	14.1	14.3	14.3	14.2	13.2	14.7	16.2	16.1	17.1	16.1	14.3	14.9	16.2
	EERM2	9.8	9.1	10.9	14.8	17.2	18.0	19.2	20.6	19.3	17.5	12.9	11.0	16.1	29.3
	EERM3	47.7	39.7	32.5	25.4	21.7	18.4	18.7	20.8	21.1	25.2	33.1	45.5	26.7	-3.4
	EERM4	58.1	51.1	43.6	34.5	29.3	25.4	25.3	27.5	28.2	33.6	43.8	55.9	35.1	-1.0
	Total	43.4	45.0	45.8	43.3	41.1	39.9	40.0	41.4	42.0	44.4	46.2	44.5	42.6	36.1
	PV	0.19	0.24	0.20	0.18	0.15	0.15	0.14	0.14	0.15	0.15	0.17	0.17	0.16	0.10

TABLE A.8: Monthly apartments energy reduction by percentages.

		Apartments Energy Reductions (%)													
	Months	1	2	3	4	5	6	7	8	9	10	11	12	Mean	SD.
Riyadh	EERM1	8.6	8.8	7.5	6.1	4.9	4.6	4.5	4.8	6.0	7.3	7.8	8.0	6.3	-0.6
	EERM2	9.7	12.1	13.5	16.0	17.6	18.9	19.0	19.0	18.4	17.2	13.5	8.9	16.0	31.3
	EERM3	54.5	49.8	45.4	38.9	34.4	32.2	31.6	31.7	33.9	37.4	44.8	55.3	39.2	1.6
	EERM4	56.8	51.9	47.3	40.6	35.8	33.6	32.9	33.0	35.3	39.0	46.7	57.7	40.8	1.6
	Total	39.5	39.8	38.7	37.5	36.5	36.5	36.3	36.4	37.2	38.3	38.5	38.8	37.6	32.3
	PV	0.06	0.08	0.07	0.07	0.06	0.07	0.06	0.06	0.06	0.06	0.06	0.06	0.07	0.06
Dhahran	EERM1	8.4	8.9	7.7	6.2	5.2	4.8	4.8	5.2	6.2	7.2	7.7	7.7	6.4	0.1
	EERM2	8.9	11.4	13.0	15.7	17.6	18.5	18.7	18.6	18.1	16.5	13.0	9.4	15.6	31.3
	EERM3	55.3	50.6	45.8	39.1	34.2	32.5	31.6	32.2	33.9	36.9	44.5	51.1	39.1	1.9
	EERM4	57.7	52.8	47.8	40.8	35.6	33.8	33.0	33.6	35.4	38.5	46.4	53.4	40.8	1.9
	Total	41.8	42.2	40.9	39.4	38.2	38.0	37.8	38.1	38.9	39.3	40.1	40.1	39.3	33.0
	PV	0.06	0.07	0.07	0.07	0.07	0.07	0.06	0.06	0.06	0.06	0.06	0.05	0.06	0.07
Makkah	EERM1	7.8	7.8	7.1	5.7	4.8	4.8	4.6	4.9	5.8	7.0	7.2	7.2	6.1	-4.0
	EERM2	14.6	15.7	16.9	17.6	18.2	19.0	18.6	18.2	18.5	18.1	16.6	14.5	17.3	29.6
	EERM3	41.9	40.6	38.0	35.5	33.2	32.2	32.4	32.6	32.8	34.7	37.3	41.3	35.7	4.1
	EERM4	43.7	42.4	39.6	37.0	34.6	33.5	33.7	34.0	34.2	36.2	38.9	43.0	37.2	4.1
	Total	38.2	38.6	38.3	37.2	36.5	36.7	36.4	36.2	36.8	37.9	37.7	37.7	37.3	30.6
	PV	0.05	0.07	0.06	0.07	0.06	0.07	0.06	0.06	0.06	0.06	0.05	0.05	0.06	0.09
Abha	EERM1	-7.4	-9.0	-9.7	-10.4	-10.8	-10.8	-10.4	-9.4	-9.3	-9.2	-8.4	-7.6	-9.5	-16.7
	EERM2	-7.1	-5.5	-3.3	-1.7	-0.3	1.8	1.6	1.4	0.7	-1.8	-4.4	-6.3	-1.7	24.3
	EERM3	45.3	37.9	36.7	35.4	33.2	29.5	30.6	32.2	31.6	32.8	35.7	41.1	34.7	-0.3
	EERM4	48.2	40.5	39.2	37.8	35.4	31.5	32.7	34.3	33.7	35.1	38.3	43.8	37.1	-0.3
	Total	29.7	29.7	29.0	28.6	28.6	28.6	28.6	28.6	28.8	29.4	30.1	30.0	29.1	24.8
	PV	0.07	0.09	0.09	0.10	0.10	0.10	0.10	0.09	0.09	0.08	0.08	0.07	0.09	0.18
Tabouk	EERM1	9.4	10.3	9.1	7.7	6.1	6.0	5.8	6.2	7.2	8.3	8.6	8.5	7.5	1.3
	EERM2	7.9	11.3	13.0	15.7	16.7	18.5	18.9	18.5	18.1	15.9	12.0	7.2	15.2	32.0
	EERM3	60.6	55.1	49.6	42.7	38.6	35.5	34.0	34.7	36.3	41.3	49.4	60.5	43.0	1.4
	EERM4	63.3	57.5	51.8	44.5	40.2	37.0	35.5	36.1	37.8	43.1	51.6	63.3	44.8	1.3
	Total	40.3	41.6	40.7	39.5	38.1	38.3	37.9	37.9	38.6	39.3	39.5	39.4	39.1	34.4
	PV	0.07	0.08	0.08	0.08	0.07	0.08	0.07	0.07	0.07	0.06	0.06	0.06	0.07	0.08
Total mean	EERM1	5.8	5.9	5.0	3.8	2.9	2.7	2.7	3.2	4.0	5.0	5.3	5.2	4.1	-2.1
	EERM2	7.7	9.8	11.4	13.6	15.0	16.2	16.4	16.1	15.7	14.2	11.1	7.6	13.4	30.5
	EERM3	51.0	46.7	43.1	38.4	34.7	32.5	32.1	32.7	33.8	36.8	42.3	49.4	38.4	1.8
	EERM4	53.3	48.9	45.0	40.1	36.3	34.0	33.6	34.2	35.3	38.5	44.3	51.7	40.2	1.8
	Total	38.1	38.7	37.9	36.9	36.0	36.1	35.9	35.9	36.6	37.3	37.6	37.4	36.9	32.0
	PV	0.06	0.08	0.07	0.08	0.07	0.07	0.07	0.07	0.07	0.06	0.06	0.06	0.07	0.08

Bibliography

Abdelrahman, MA, SAM Said, and A Ahmad (1993). "A comparison of energy consumption and cost-effectiveness of four masonry materials in Saudi Arabia". In: *Energy* 18.11, pp. 1181–1186.

Abdelrahman, MA et al. (1990). "Thermal conductivity of some major building materials in Saudi Arabia". In: *Journal of Thermal Insulation* 13.4, pp. 294–300.

Abdelrahman, Mohamed Ali and Aftab Ahmad (1991). "Cost-effective use of thermal insulation in hot climates". In: *Building and Environment* 26.2, pp. 189–194.

Abdmouleh, Zeineb, Rashid AM Alammari, and Adel Gastli (2015). "Recommendations on renewable energy policies for the GCC countries". In: *Renewable and Sustainable Energy Reviews* 50, pp. 1181–1191.

Abdou, Adel A and Ismail M Budaiwi (2005). "Comparison of thermal conductivity measurements of building insulation materials under various operating temperatures". In: *Journal of building physics* 29.2, pp. 171–184.

Aboneama, Wael A (2018). "Creating a unique sustainable rating system for Saudi Arabia to achieve environmental assessment and 2030 vision". In: *European Journal of Sustainable Development* 7.4, pp. 269–269.

Abuhussain, Mohammed Awad, David Hou Chi Chow, and Steve Sharples (2018). "Assessing the Adaptability of the Saudi Residential Building's Energy Code for Future Climate Change Scenarios". In: *SMART AND HEALTHY WITHIN THE TWO-DEGREE LIMIT (PLEA 2018), VOL 1*, pp. 74–79.

Adolfsson, Andreas, Margareta Ackerman, and Naomi C Brownstein (2019). "To cluster, or not to cluster: An analysis of clusterability methods". In: *Pattern Recognition* 88, pp. 13–26. ISSN: 0031-3203.

Agency, United States Environmental Protection (2016). *Climate Change Indicators: Atmospheric Concentrations of Greenhouse Gases*.

— (2018). *Conducting effective baseline energy assessments*. URL: `https://www.nqa.com/en-gb/resources/blog/february-2018/effective-baseline-energy-assessment`.

Ahmad, Aftab (2004). "ENERGY SIMULATION FOR A TYPICAL HOUSE BUILT WITH DIFFERENT TYPES OF MASONRY BUILDING MATERIALS." In: *Arabian Journal for Science & Engineering (Springer Science & Business Media BV)* 29.

Ahmad, Eball H (2002). "Cost analysis and thickness optimization of thermal insulation materials used in residential buildings in Saudi Arabia". In: *Proceedings of the 6th Saudi Engineering Conference, Dhahran, Saudi Arabia*, pp. 14–17.

Ahmed, Hadeel Noman Saied (1991). "Thermal insulation economics for Saudi residential buildings". PhD thesis. King Fahd University of Petroleum and Minerals (Saudi Arabia).

Al-Ajlan, Saleh A (2006). "Measurements of thermal properties of insulation materials by using transient plane source technique". In: *Applied thermal engineering* 26.17-18, pp. 2184–2191.

Al-Ajmi, Farraj F et al. (2008). "Thermal insulation and clothing area factors of typical Arabian Gulf clothing ensembles for males and females: measurements using thermal manikins". In: *Applied ergonomics* 39.3, pp. 407–414.

Al-Hadhrami, Luai M and A Ahmad (2009). "Assessment of thermal performance of different types of masonry bricks used in Saudi Arabia". In: *Applied thermal engineering* 29.5-6, pp. 1123–1130.

Al-Hathloul, Saleh Ali (1981). "Tradition, continuity and change in the physical environment: The Arab-Muslim city". Thesis. Massachusetts Institute of Technology.

Al-Hazmy, Majed M (2006a). "Analysis of coupled natural convection–conduction effects on the heat transport through hollow building blocks". In: *Energy and Buildings* 38.5, pp. 515–521.

— (2006b). "Analysis of coupled natural convection–conduction effects on the heat transport through hollow building blocks". In: *Energy and Buildings* 38.5, pp. 515–521. ISSN: 0378-7788.

Al-Homoud, Mohammad S (1997a). "Optimum thermal design of air-conditioned residential buildings". In: *Building and Environment* 32.3, pp. 203–210.

Al-Homoud, Mohammad S (1997b). "Optimum thermal design of office buildings". In: *International Journal of Energy Research* 21.10, pp. 941–957.

— (2004). "The effectiveness of thermal insulation in different types of buildings in hot climates". In: *Journal of Thermal Envelope and Building Science* 27.3, pp. 235–247. ISSN: 1097-1963.

— (2005a). "A systematic approach for the thermal design optimization of building envelopes". In: *Journal of building physics* 29.2, pp. 95–119. ISSN: 1744-2591.

— (2005b). "Performance characteristics and practical applications of common building thermal insulation materials". In: *Building and environment* 40.3, pp. 353–366.

— (2009). "Envelope thermal design optimization of buildings with intermittent occupancy". In: *Journal of Building Physics* 33.1, pp. 65–82.

Al-Homoud, Mohammad S and Moncef Krarti (2021). "Energy efficiency of residential buildings in the kingdom of Saudi Arabia: review of status and future roadmap". In: *Journal of Building Engineering*, p. 102143.

Al-Homoud, Mohammad Saad (2001). "Computer-aided building energy analysis techniques". In: *Building and Environment* 36.4, pp. 421–433. ISSN: 0360-1323.

Al-Jarallah, MI (2005). "Anomalous indoor radon concentration in a dwelling in Qatif city, Saudi Arabia". In: *Radiation protection dosimetry* 117.4, pp. 408–413. ISSN: 1742-3406.

Al-Khateeb, HM et al. (2017). "Seasonal variation of indoor radon concentration in a desert climate". In: *Applied Radiation and Isotopes* 130, pp. 49–53.

Al-Maghlouth, AA (2007). *The Development of Real Estate Investment in Saudi Arabia*.

Al-Mayouf, Abdualelah and Abdallah Al-Khayyal (2011). "Provision of public housing in Saudi Arabia: Past, current and future trends". In: *Population* 2004, p. 2007.

Al-Mofeez, I (2010). "Predicted vs. actual energy savings of retrofitted house". In.

Al-Mofeez, Ibraheem A (2007). "Electrical energy consumption pre and post energy conservation measures: a case study of one-story house in Dhahran, Saudi Arabia". In: *J King Saud Univ* 19.2, pp. 1–12.

Al-Naimi, Ibrahim Mubarak (1989a). "The potential for energy conservation in residential buildings in Dammam region, Saudi Arabia". Thesis. Newcastle University.

— (1989b). "The potential for energy conservation in residential buildings in Dammam region, Saudi Arabia". PhD thesis. University of Newcastle upon Tyne.

Al-Rehaili, A (1999). "Outdoor-indoor air quality in Riyadh: Particulate Matter, Pb and CO". In: *WIT Transactions on The Built Environment* 44. ISSN: 1853126950.

Al-Rehaili, AM (2002). "Outdoor-indoor air quality in Riyadh: SO 2, NH 3, and HCHO". In: *Environmental monitoring and assessment* 79.3, pp. 287–300. ISSN: 0167-6369.

Al-Saadi, S and I Budaiwi (2007). "Performance-based envelope design for residential buildings in hot climates". In: *Proceedings of building simulation*, pp. 1726–1733.

Al-Saleh, Ferdoas S (2007). "Measurements of indoor gamma radiation and radon concentrations in dwellings of Riyadh city, Saudi Arabia". In: *Applied Radiation and Isotopes* 65.7, pp. 843–848. ISSN: 0969-8043.

Al-Sanea, SA and MF Zedan (2001). "Effect of insulation location on thermal performance of building walls under steady periodic conditions". In: *International journal of ambient energy* 22.2, pp. 59–72.

Al-Sanea, Sami A, MF Zedan, and SN Al-Hussain (2012a). "Effect of thermal mass on performance of insulated building walls and the concept of energy savings potential". In: *Applied Energy* 89.1, pp. 430–442. ISSN: 0306-2619.

— (2012b). "Effect of thermal mass on performance of insulated building walls and the concept of energy savings potential". In: *Applied Energy* 89.1, pp. 430–442.

Al-Shaalan, Abdullah, Wakeel Ahmed, Abdulhameed Alohaly, et al. (2014). "Design guidelines for buildings in Saudi Arabia considering energy conservation requirements". In: *Applied Mechanics and Materials*. Vol. 548. Trans Tech Publ, pp. 1601–1606.

Al-Shaalan, Abdullah M (2012). "EER improvement for room air-conditioners in Saudi Arabia". In.

Al-Shaalan, Abdullah M, Ahmed Wakeel, and Abdulhameed Alohaly (n.d.). "Appropriate electric energy conservation measures for big mosques in Riyadh

City". In: *Applied Mechanics and Materials*. Vol. 492. Trans Tech Publ, pp. 24–30. ISBN: 3037859911.

Al-Tamimi, Nedhal (2017). "A state-of-the-art review of the sustainability and energy efficiency of buildings in Saudi Arabia". In: *Energy Efficiency* 10.5, pp. 1129–1141.

— (2021). "An Optimum Thermal Insulation Type and Thickness for Residential Buildings in Three Different Climatic Regions of Saudi Arabia". In: *Civ. Eng. Archit* 9, pp. 317–327.

Alaidroos, Alaa and Moncef Krarti (2015). "Optimal design of residential building envelope systems in the Kingdom of Saudi Arabia". In: *Energy and Buildings* 86, pp. 104–117. ISSN: 0378-7788.

— (2016). "Evaluation of passive cooling systems for residential buildings in the Kingdom of Saudi Arabia". In: *Journal of Solar Energy Engineering* 138.3, p. 031011.

Alayed, Essam, Richard O'hegarty, and Oliver Kinnane (2021). "Thermal envelope analysis for new code compliance of Saudi Arabian dwellings". In: *Energy and Buildings* 243, p. 110997.

Aldalbahi, Salman (2020). "The structure of the current housing provision in Saudi Arabia: an institutional perspective". PhD thesis. University of Sheffield.

Aldawoud, Abdelsalam (2013). "Conventional fixed shading devices in comparison to an electrochromic glazing system in hot, dry climate". In: *Energy and Buildings* 59, pp. 104–110. ISSN: 0378-7788.

Aldossary, Naief A, Yacine Rezgui, and Alan Kwan (2014a). "Domestic energy consumption patterns in a hot and humid climate: A multiple-case study analysis". In: *Applied Energy* 114, pp. 353–365.

— (2014b). "Domestic energy consumption patterns in a hot and humid climate: A multiple-case study analysis". In: *Applied Energy* 114, pp. 353–365. ISSN: 0306-2619.

— (2014c). "Domestic energy consumption patterns in a hot and humid climate: A multiple-case study analysis". In: *Applied Energy* 114, pp. 353–365. ISSN: 0306-2619.

Aldubyan, Mohammad and Moncef Krarti (2021). "Impact of Stay Home Living on Energy Demand of Residential Buildings: Saudi Arabian Case Study". In: *Energy*, p. 121637.

Aldubyan, Mohammad, Moncef Krarti, Eric Williams, et al. (2021). *Residential Energy Model for Evaluating Energy Demand and Energy Efficiency Programs in Saudi Residential Buildings*. Tech. rep. King Abdullah Petroleum Studies and Research Center.

Algarni, S and D Nutter (2013a). "Geospatial representation of the residential energy use in Saudi Arabia". In: *Proceedings of the 2013 ASME Early Career Technical Conference (ECTC), April*, pp. 4–6.

— (2013b). "Geospatial representation of the residential energy use in Saudi Arabia". In: *Proceedings of the 2013 ASME Early Career Technical Conference (ECTC), April*, pp. 4–6.

Alghamdi, Abdulrahman S and Khalid A Aleissa (2014). "Influences on indoor radon concentrations in Riyadh, Saudi Arabia". In: *Radiation Measurements* 62, pp. 35–40. ISSN: 1350-4487.

AlGhamdi, Abeer et al. (2020). *Saudi Arabia Energy Report*. Tech. rep.

Alhozaimy, Abdulrahman M (2008). "Chemical composition of cements produced in Saudi Arabia and its influence on concrete strength". In: *Journal of King Saud University-Engineering Sciences* 20.2, pp. 69–75.

Alkhathlan, Khalid A (2013). "The nexus between remittance outflows and growth: A study of Saudi Arabia". In: *Economic Modelling* 33, pp. 695–700.

Almasoud, AH and Hatim M Gandayh (2015). "Future of solar energy in Saudi Arabia". In: *Journal of King Saud University-Engineering Sciences* 27.2, pp. 153–157.

Almazroui, Mansour (2020). "Changes in temperature trends and extremes over Saudi Arabia for the period 1978–2019". In: *Advances in Meteorology* 2020.

Almazroui, Mansour et al. (2012). "Recent climate change in the Arabian Peninsula: annual rainfall and temperature analysis of Saudi Arabia for 1978–2009". In: *International Journal of Climatology* 32.6, pp. 953–966.

Almehrej, Majid Ibrahim (2015). "A design guide for contemporary Saudi Arabian homes in Riyadh". Thesis. Northumbria University.

Almutairi, Kamel et al. (2015). “Life cycle assessment and economic analysis of residential air conditioning in Saudi Arabia”. In: *Energy and Buildings* 102, pp. 370–379. ISSN: 0378-7788.

Alnowaiser, Mohammed A (1996a). “Toward a residential zoning regulation approach for Saudi Arabia”. In: *Journal of Architectural and Planning Research*, pp. 91–106. ISSN: 0738-0895.

— (1996b). “Toward a residential zoning regulation approach for Saudi Arabia”. In: *Journal of Architectural and Planning Research*, pp. 91–106. ISSN: 0738-0895.

Alrashed, Farajallah and Muhammad Asif (2015). “Climatic classifications of Saudi Arabia for building energy modelling”. In: *Energy Procedia* 75, pp. 1425–1430. ISSN: 1876-6102.

Alrashed, Frajallah and M Asif (2012). “Prospects of renewable energy to promote zero-energy residential buildings in the KSA”. In: *Energy Procedia* 18, pp. 1096–1105.

Alwetaishi, M, Mohamed Gadi, and UH Issa (2017). “Reliance of building energy in various climatic regions using multi criteria”. In: *International Journal of Sustainable Built Environment* 6.2, pp. 555–564.

Alyousef, Yousef and Paul Stevens (2011). “The cost of domestic energy prices to Saudi Arabia”. In: *Energy Policy* 39.11, pp. 6900–6905.

Amoatey, Patrick et al. (2018a). “Indoor air pollution and exposure assessment of the gulf cooperation council countries: A critical review”. In: *Environment international* 121, pp. 491–506. ISSN: 0160-4120.

— (2018b). “Indoor air pollution and exposure assessment of the gulf cooperation council countries: a critical review”. In: *Environment international* 121, pp. 491–506.

Amran, YH Ahssein et al. (2020). “Renewable and sustainable energy production in Saudi Arabia according to Saudi Vision 2030; Current status and future prospects”. In: *Journal of Cleaner Production* 247, p. 119602.

Andersson, Fredrik O, Magnus Åberg, and Sven P Jacobsson (2000). “Algorithmic approaches for studies of variable influence, contribution and selection in neural networks”. In: *Chemometrics and intelligent laboratory systems* 51.1, pp. 61–72.

Anis, Wagdy AY (2001). "The impact of airtightness on system design". In: *ASHRAE journal* 43.12, p. 31.

Antar, Mohamed A (2010a). "Thermal radiation role in conjugate heat transfer across a multiple-cavity building block". In: *Energy* 35.8, pp. 3508–3516. ISSN: 0360-5442.

— (2010b). "Thermal radiation role in conjugate heat transfer across a multiple-cavity building block". In: *Energy* 35.8, pp. 3508–3516.

Antar, Mohamed A and Hasan Baig (2009a). "Conjugate conduction-natural convection heat transfer in a hollow building block". In: *Applied Thermal Engineering* 29.17-18, pp. 3716–3720. ISSN: 1359-4311.

— (2009b). "Conjugate conduction-natural convection heat transfer in a hollow building block". In: *Applied Thermal Engineering* 29.17-18, pp. 3716–3720.

Arabia, Saudi (2020). "Ministry of Economy and Planning". In: *Saudi Arabia Population Census*.

Argiriou, A et al. (1999). "Comparison of methodologies for TMY generation using 20 years data for Athens, Greece". In: *Solar Energy* 66.1, pp. 33–45.

ASHRAE, ANSI (2010). "Standard 55-2010:"Thermal Environmental Conditions for Human Occupancy"". In: *ASHRAE, Atlanta USA*.

— (2016). "ASHRAE standard 62.2-ventilation and acceptable indoor air quality in residential buildings". In: *Report, The American Society of Heating, Refrigerating and Air-Conditioning Engineers*.

ASHRAE, US (2009). "ASHRAE handbook fundamentals. Atlanta, Georgia: US". In: *American Society of heating refrigerating and air-conditioning engineers*.

Ashwan M. Abdul Salam A., & Mouselhy M. (2012). "Population growth, structure and distribution in Saudi Arabia". In: *King Faisal and the Modernisation of Saudi Arabia*, pp. 33–46.

ASTM, E (1999). "Standard test method for determining air leakage rate by fan pressurization". In: *West Conshohocken, PA*, pp. 19428–2959.

Attia, Shady et al. (2012). "Selection criteria for building performance simulation tools: contrasting architects' and engineers' needs". In: *Journal of Building Performance Simulation* 5.3, pp. 155–169.

Attia, Shady et al. (2013). “Assessing gaps and needs for integrating building performance optimization tools in net zero energy buildings design”. In: *Energy and Buildings* 60, pp. 110–124. ISSN: 0378-7788.

Auliciems, A and SV Szokolay (2007). “PLEA Note 3: Thermal Comfort”. In: *Brisbane: PLEA in association with Department of Architecture University of Queensland*.

Auliciems, Andris (1981). “Towards a psycho-physiological model of thermal perception”. In: *International Journal of Biometeorology* 25.2, pp. 109–122. ISSN: 0020-7128.

Avci, Mesut et al. (2013a). “Model predictive HVAC load control in buildings using real-time electricity pricing”. In: *Energy and Buildings* 60, pp. 199–209. ISSN: 0378-7788.

— (2013b). “Model predictive HVAC load control in buildings using real-time electricity pricing”. In: *Energy and Buildings* 60, pp. 199–209.

Averchenkova, Alina and Samuela Bassi (2016). *Beyond the targets: assessing the political credibility of pledges for the Paris Agreement*. Tech. rep. Some institution.

Bagneid, Amr A (2007). “TOWARDS THE REVIVAL OF THE SUSTAINABLE COURTYARD ARCHETYPE: AN EVALUATION OF COURTYARD VERSUS PAVILION ARCHETYPES COMPARATIVE ASSESSMENTS”. In: *Conference: International Conference on Sustainable Urbanism, Squaring off: A New Paradigm for Urban ChangeAt: Texas A&M University*.

Bahaidarah, Haitham et al. (2015). “Performance evaluation of a PV module under climatic conditions of Dhahran, Saudi Arabia”. In: *Energy exploration & exploitation* 33.6, pp. 909–929.

Bahammam, Ali (1998). “Factors which influence the size of the contemporary dwelling: Riyadh, Saudi Arabia”. In: *Habitat International* 22.4, pp. 557–570. ISSN: 0197-3975.

Bahel, V, H Bakhsh, and R Srinivasan (1985). “Seasonal performance of a central air conditioner in Dhahran, Saudi Arabia. A computer simulation study”. In: *International journal of refrigeration* 8.5, pp. 305–310. ISSN: 0140-7007.

Bahel, V, S Said, and MA Abdelrahmen (1989). “Validation of DOE-2.1 A and a microcomputer based hourly energy analysis computer program for a residential building”. In: *Energy* 14.4, pp. 215–221. ISSN: 0360-5442.

Baig, H and MA Antar (2008). "Conduction/Natural convection analysis of heat transfer across multi-layer building blocks". In: *Euro. Therm. Sci* 5.

Baik, Ahmad (2017). "From point cloud to jeddah heritage BIM nasif historical house–case study". In: *Digital Applications in Archaeology and Cultural Heritage* 4, pp. 1–18.

Baker, Scott, David Ponniah, and Simon Smith (1999). "Survey of risk management in major UK companies". In: *Journal of Professional Issues in Engineering Education and Practice* 125.3, pp. 94–102.

Baker, Scott R, Nicholas Bloom, and Steven J Davis (2016). "Measuring economic policy uncertainty". In: *The quarterly journal of economics* 131.4, pp. 1593–1636.

Ball, Jeffrey (2015). "Why the Saudis are going solar". In: *The Atlantic*.

Batterman, S and H Burge (1995). *HVAC systems as emission sources affecting indoor air quality: A critical review. Final report, September 1993-June 1994*. Report. Michigan Univ., Ann Arbor, MI (United States). Dept. of Environmental and ...

Bayar, Yilmaz and Marius Dan Gavriletea (2019). "Energy efficiency, renewable energy, economic growth: evidence from emerging market economies". In: *Quality & Quantity* 53.4, pp. 2221–2234.

Bolin, Bert and Bo R Doos (1989). "Greenhouse effect". In.

Brinkworth, BJ et al. (1997). "Thermal regulation of photovoltaic cladding". In: *Solar energy* 61.3, pp. 169–178.

Brøgger, Morten and Kim Bjarne Wittchen (2018). "Estimating the energy-saving potential in national building stocks–A methodology review". In: *Renewable and Sustainable Energy Reviews* 82, pp. 1489–1496.

Brown, Steve K et al. (1994). "Concentrations of volatile organic compounds in indoor air–a review". In: *Indoor air* 4.2, pp. 123–134.

Brun, Roland, Peter Reichert, and Hans R Künsch (2001). "Practical identifiability analysis of large environmental simulation models". In: *Water Resources Research* 37.4, pp. 1015–1030.

BS, BSI (1991). "5925. Code of Practice for Ventilation Principles and Designing for Natural Ventilation". In: *British Standard Institution*.

Budaiwi, I and A Abdou (2013). “HVAC system operational strategies for reduced energy consumption in buildings with intermittent occupancy: The case of mosques”. In: *Energy conversion and management* 73, pp. 37–50.

Budaiwi, I and Mohammad S Al-Homoud (2001). “Effect of ventilation strategies on air contaminant concentrations and energy consumption in buildings”. In: *International journal of energy research* 25.12, pp. 1073–1089. ISSN: 0363-907X.

Budaiwi, IM (2011). “Envelope thermal design for energy savings in mosques in hot-humid climate”. In: *Journal of Building Performance Simulation* 4.1, pp. 49–61.

Budaiwi, Ismail M (2003). “Air conditioning system operation strategies for intermittent occupancy buildings in a hot-humid climate”. In: *Proceedings of the 8th IBPSA conference. Eindhoven, Netherlands*. Citeseer, pp. 11–14.

Budaiwi, Ismail M and Mohammad S Al-Homoud (2001). “Effect of ventilation strategies on air contaminant concentrations and energy consumption in buildings”. In: *International journal of energy research* 25.12, pp. 1073–1089.

Building Energy Modeling with IESVE (n.d.). URL: `https://www.iesve.com/software/building-energy-modeling`.

Bulut, Hüsamettin (2003). “Generation of typical solar radiation data for Istanbul, Turkey”. In: *International journal of energy research* 27.9, pp. 847–855.

— (2004). “Typical solar radiation year for southeastern Anatolia”. In: *Renewable Energy* 29.9, pp. 1477–1488.

C168, ASTM (2014). *Standard Terminology Relating to Thermal Insulation*.

Calaqutit, John Kaiser, Ben Richard Hughes, and Polytimi Sofotasiou (2015). “Design and Optimisation of a Novel Passive Cooling Wind Tower”. In: *Conference: The 14th International Conference on Sustainable Energy Technologies (SET)At: Nottingham, UK*.

Cao, Xiaodong, Xilei Dai, and Junjie Liu (2016). “Building energy-consumption status worldwide and the state-of-the-art technologies for zero-energy buildings during the past decade”. In: *Energy and buildings* 128, pp. 198–213.

Carratt, Anneleise, Georgios Kokogiannakis, and D Daly (2020). “A critical review of methods for the performance evaluation of passive thermal retrofits in residential buildings”. In: *Journal of Cleaner Production* 263, p. 121408.

Carrié, FR, R Jobert, and V Leprince (2012). "Methods and techniques for airtight buildings". In: *AIVC, Contributed Report* 14.

Casset, A and JJ Braun (2010). "Relationships between indoor allergens, sensitization, and allergic asthma and rhinitis symptoms". In: *Revue des maladies respiratoires* 27.8, pp. 913–920. ISSN: 0761-8425.

center, national climatic data (n.d.). *World Data Center for Meteorology, Asheville*. URL: `https://www.ncdc.noaa.gov/wdcmet`.

Chai, Tianfeng and Roland R Draxler (2014). "Root mean square error (RMSE) or mean absolute error (MAE)?–Arguments against avoiding RMSE in the literature". In: *Geoscientific model development* 7.3, pp. 1247–1250.

Christopher Frey, H and Sumeet R Patil (2002). "Identification and review of sensitivity analysis methods". In: *Risk analysis* 22.3, pp. 553–578.

Cohen, Jacob (2013). *Statistical power analysis for the behavioral sciences*. Routledge.

Company, Saudi Electricity (2018). *Energy tariff*.

Cooke, TF (1991). "Indoor air pollutants: a literature review". In: *Reviews on environmental Health* 9.3, pp. 137–160.

Costa, Vanessa Aparecida Caieiro da, Victor Figueiredo Roriz, and Karin Maria Soares Chvatal (2017). "Modeling of slab-on-grade heat transfer in EnergyPlus simulation program". In: *Ambiente Construído* 17.3, pp. 117–135.

Council, WE (2017). "Average electricity consumption per electrified household". In: *Energy Efficiency Indicators*.

Crawley, Drury B et al. (2004). "EnergyPlus: new, capable, and linked". In: *Journal of Architectural and Planning Research*, pp. 292–302.

Creswell, John W and Vicki L Plano Clark (2017). *Designing and conducting mixed methods research*. Sage publications.

Cullen, Alison C, H Christopher Frey, and Christopher H Frey (1999). *Probabilistic techniques in exposure assessment: a handbook for dealing with variability and uncertainty in models and inputs*. Springer Science & Business Media.

Das, Payel et al. (2014). "Using probabilistic sampling-based sensitivity analyses for indoor air quality modelling". In: *Building and environment* 78, pp. 171–182.

De Dear, Richard and Gail Schiller Brager (1998a). "Developing an adaptive model of thermal comfort and preference". In.

De Dear, Richard and Gail Schiller Brager (1998b). "Developing an adaptive model of thermal comfort and preference". In.

DECC (2013). *United Kingdom housing energy fact file*.

Deru, M and P Burns (2003). *Infiltration and natural ventilation model for whole-building energy simulation of residential buildings*. Tech. rep. National Renewable Energy Lab.(NREL), Golden, CO (United States).

Desai, Bharat H (2018). "14. United Nations Environment Program (UNEP)". In: *Yearbook of International Environmental Law* 29, pp. 441–448.

Destaillats, Hugo et al. (2008). "Indoor pollutants emitted by office equipment: A review of reported data and information needs". In: *Atmospheric Environment* 42.7, pp. 1371–1388. ISSN: 1352-2310.

DoE, Department of Energy (2022). *climate.onebuilding.org*. URL: `https://climate.onebuilding.org/default.html`.

DoE, USA (2020). *EnergyPlus*. URL: `https://www.energy.gov/eere/buildings/downloads/energyplus-0`. (accessed: 01.11.2020).

Dols, W Stuart, Brian Polidoro, et al. (2015). "CONTAM user guide and program documentation: Version 3.2". In.

Drury, CB et al. (1999). "EnergyPlus: a new generation building energy simulation program". In: *Proc. Renewable and Advanced Energy Systems for the 21st Century, Maui, Hawaii, April 1999. New York: ASME*.

Eben Saleh, MA (1990). "Thermal insulation of buildings in a newly built environment of a hot dry climate: the Saudi Arabian experience". In: *International journal of ambient energy* 11.3, pp. 157–168.

Edmonds, James A, MA Wise, and CN MacCracken (1994). *Advanced energy technologies and climate change: An analysis using the global change assessment model (GCAM)*. Tech. rep. Pacific Northwest National Lab.(PNNL), Richland, WA (United States).

El-Desoky, Gaber E et al. (2014). "Seasonal concentrations of lead in outdoor and indoor dust and blood of children in Riyadh, Saudi Arabia". In: *Environmental geochemistry and health* 36.3, pp. 583–593. ISSN: 0269-4042.

El-Sharkawy, Mahmoud F and Mohamed EH Noweir (2014). "Indoor air quality levels in a University Hospital in the Eastern Province of Saudi Arabia". In: *Journal of family & community medicine* 21.1, p. 39.

El-Sharkawy, Mahmoud Fathy and Wasim Javed (2018). "Study of indoor air quality level in various restaurants in Saudi Arabia". In: *Environmental Progress & Sustainable Energy* 37.5, pp. 1713–1721.

El-Sharkawy, Mahmoud Fathy Mohamed (2014). "Study the indoor air quality level inside governmental elementary schools of Dammam City in Saudi Arabia". In: *International Journal of Environmental Health Engineering* 3.1, p. 22. ISSN: 2277-9183.

Elmahdy, AH (2003). "Quantification of air leakage effects on the condensation resistance of windows". In: *ASHRAE Transactions* 109.1, pp. 600–606.

Emmerich, Steven J et al. (2001). "Validation of multizone IAQ modeling of residential-scale buildings: a review". In: *Transactions-American Society of Heating Refrigerating and Air Conditioning Engineers* 107.2, pp. 619–628.

Energy Systems Research UNITESP-R, University of Strathclyde (n.d.). URL: `https://www.strath.ac.uk/research/energysystemsresearchunit/applications/esp-r/`.

England, Public Health (Jan. 1992). *National Radiological Protection Board (NRPB): Publications*. URL: `https://www.gov.uk/government/collections/national-radiological-protection-board-nrpb-report-series`.

Etheridge, David (2011). *Natural ventilation of buildings: theory, measurement and design*. John Wiley & Sons.

Eurostat statistics database (2012). URL: `http://ec.europa.eu/eurostat`.

Evins, Ralph (2013). "A review of computational optimisation methods applied to sustainable building design". In: *Renewable and sustainable energy reviews* 22, pp. 230–245. ISSN: 1364-0321.

Fadaak, Tarek Ali (1984). *Urban housing policy evaluation in the Kingdom of Saudi Arabia*. Portland State University. School of Urban and Public Affairs.

Fadan, Y. M (1983). "The development of contemporary housing in Saudi Arabia (1950-1983): a study in cross-cultural". Thesis. octoral dissertation, Massachusetts Institute of Technology.

Fanger, P Ole (2006). "What is IAQ?" In: *Indoor air* 16.5, pp. 328–334. ISSN: 1600-0668.

Faruqui, Ahmad et al. (2011). "Bringing demand-side management to the kingdom of Saudi Arabia". In: *The Brattle Group*.

Fasiuddin, M and I Budaiwi (2011). "HVAC system strategies for energy conservation in commercial buildings in Saudi Arabia". In: *Energy and Buildings* 43.12, pp. 3457–3466.

Felimban, Ahmed et al. (2019). "Assessment of current energy consumption in residential buildings in Jeddah, Saudi Arabia". In: *Buildings* 9.7, p. 163.

Ferguson, Christopher J (2016). "An effect size primer: a guide for clinicians and researchers." In: *Professional Psychology: Research and Practice*.

Field, Andy, Jeremy Miles, and Zoë Field (2012). *Discovering Statistics Using R*.

Fisher, Ronald A (1956). "Statistical methods and scientific inference." In.

Fisk, William J (2015). "Review of some effects of climate change on indoor environmental quality and health and associated no-regrets mitigation measures". In: *Building and environment* 86, pp. 70–80. ISSN: 0360-1323.

Fisk, William J and Anibal T De Almeida (1998). "Sensor-based demand-controlled ventilation: a review". In: *Energy and buildings* 29.1, pp. 35–45. ISSN: 0378-7788.

Fraedrich, Doug and A Goldberg (2000). "A methodological framework for the validation of predictive simulations". In: *European Journal of Operational Research* 124.1, pp. 55–62.

Frick, Robert W (1996). "The appropriate use of null hypothesis testing." In: *Psychological Methods* 1.4, p. 379.

Fugler, D (2001). "Air infiltration from attached garages in Canadian houses". In.

Fung, Pak L et al. (2021). "Evaluation of white-box versus black-box machine learning models in estimating ambient black carbon concentration". In: *Journal of aerosol science* 152, p. 105694.

Gale, Robert W et al. (2009). "Semivolatile organic compounds in residential air along the Arizona- Mexico border". In: *Environmental science & technology* 43.9, pp. 3054–3060. ISSN: 0013-936X.

GAS (2019). *General Authority for Statistics*. URL: `https://www.stats.gov.sa/en/897` (visited on 08/03/2020).

Generating power (n.d.). URL: `https://www.un.org/en/climatechange/climate-solutions/cities-pollution`.

Geyer, Philipp, Arno Schlüter, and Sasha Cisar (2017). “Application of clustering for the development of retrofit strategies for large building stocks”. In: *Advanced Engineering Informatics* 31, pp. 32–47.

Ghiassi, Neda and Ardeshir Mahdavi (2017). “Reductive bottom-up urban energy computing supported by multivariate cluster analysis”. In: *Energy and Buildings* 144, pp. 372–386.

Grandjean, Arnaud, Jérôme Adnot, and Guillaume Binet (2012). “A review and an analysis of the residential electric load curve models”. In: *Renewable and Sustainable energy reviews* 16.9, pp. 6539–6565. ISSN: 1364-0321.

Grondzik, W, A Al-Hammad, and N Harm (1989). “Thermal and Economic Performance of Insulation for Saudi Buildings”. In: *Third Progress Report, King Abdul Aziz City for Science and Technology, PN AR-8* 49.

Gueye, Soguy Mak-Karé et al. (2014). “Coordinating self-sizing and self-repair managers for multi-tier systems”. In: *Future Generation Computer Systems* 35, pp. 14–26.

Guideline, ASHRAE et al. (2014). “Measurement of energy, demand, and water savings”. In: *ASHRAE guidel* 4, pp. 1–150.

Hamdan, Amani K (2015). “Reforming higher education in Saudi Arabia: Reasons for optimism”. In: *Higher Education Revolutions in the Gulf*. Routledge, pp. 153–178.

Hamid, M Abd-el et al. (1990). “Energy conservation and its implication for architectural design and town planning in the hot-arid areas of Saudi Arabia and the Gulf states”. In: *Solar & wind technology* 7.2-3, pp. 131–138.

Handbook, ASHRAE (2001). “Fundamentals, 2001, ASHRAE, Atlanta”. In.

Harding, Kevin Graham (2018). “Heat transfer introduction”. In: *University of the Witwatersrand: Johannesburg, South Africa*, pp. 1–62.

Hashim, HM et al. (2018). “Cooling load calculations”. In: *IOP Conference Series: Materials Science and Engineering*. Vol. 463. 3. IOP Publishing, p. 032030.

Heidarinejad, Mohammad et al. (2016). “Influence of building surface solar irradiance on environmental temperatures in urban neighborhoods”. In: *Sustainable Cities and Society* 26, pp. 186–202.

Hirsch, J (2018). *DOE2. 2 Whole Building Energy Simulation Analysis Using eQUEST Version 3.65*.

Hopfe, Christina Johanna (2009). "Uncertainty and sensitivity analysis in building performance simulation for decision support and design optimization". In: *PhD diss., Eindhoven University*.

Housing, Ministry of (2020). *Saudi Arabia*. URL: `https://www.housing.gov.sa/en/node` (visited on 2020).

Humphreys, MA, HB Rijal, and JF Nicol (2013). "Updating the adaptive relation between climate and comfort indoors; new insights and an extended database". In: *Building and environment* 63, pp. 40–55. ISSN: 0360-1323.

Husman, Tuula (1996). "Health effects of indoor-air microorganisms". In: *Scandinavian journal of work, environment & health*, pp. 5–13. ISSN: 0355-3140.

ICRP Protection, Radiological (2007). "ICRP publication 103". In: *Ann ICRP* 37.2.4, p. 2.

INE (2014). *Auditoría técnica a la base de datos del levantamiento censal año 2012*.

Institution, British Standards (2015). *Thermal Performance of Buildings: Determination of Air Permeability of Buildings: Fan Pressurization Method*. British Standards Institution.

Iqbal, Imran and Mohammad S Al-Homoud (2007). "Parametric analysis of alternative energy conservation measures in an office building in hot and humid climate". In: *Building and environment* 42.5, pp. 2166–2177. ISSN: 0360-1323.

Irena (2017). *Planning for the renewable future: Long-term modelling and tools to expand variable renewable power in emerging economies*.

Jokisalo, Juha et al. (2009). "Building leakage, infiltration, and energy performance analyses for Finnish detached houses". In: *Building and Environment* 44.2, pp. 377–387.

Jones, Andy P (1999). "Indoor air quality and health". In: *Atmospheric environment* 33.28, pp. 4535–4564. ISSN: 1352-2310.

Jones, B and C Molina (2017). "Indoor air quality". In.

Jones, Benjamin, Andrew Persily, and Max Sherman (2016). "The origin and application of leakage-infiltration ratios". In: *ASHRAE AIVC IAQ 2016, Defining Indoor Air Quality: Policy, standards and Best Practices*.

Jones, Benjamin et al. (2013a). “A stochastic approach to predict the relationship between dwelling permeability and infiltration in English apartments”. In.

Jones, Benjamin et al. (2013b). “The effect of party wall permeability on estimations of infiltration from air leakage”. In: *International Journal of Ventilation* 12.1, pp. 17–30.

Jones, Benjamin et al. (2015). “Assessing uncertainty in housing stock infiltration rates and associated heat loss: English and UK case studies”. In: *Building and environment* 92, pp. 644–656.

Jones, BM et al. (2014). “Modelling uniformly porous facades to predict dwelling infiltration rates”. In: *Building Services Engineering Research and Technology* 35.4, pp. 408–416.

Jones, Roger N (2000). “Analysing the risk of climate change using an irrigation demand model”. In: *Climate research* 14.2, pp. 89–100.

Judson, Richard S et al. (2012). “Aggregating data for computational toxicology applications: the US Environmental Protection Agency (EPA) aggregated computational toxicology resource (ACToR) system”. In: *International journal of molecular sciences* 13.2, pp. 1805–1831.

Kalamees, Targo (2007). “Air tightness and air leakages of new lightweight single-family detached houses in Estonia”. In: *Building and environment* 42.6, pp. 2369–2377.

Kalogirou, Soteris A and Yiannis Tripanagnostopoulos (2006). “Hybrid PV/T solar systems for domestic hot water and electricity production”. In: *Energy conversion and management* 47.18-19, pp. 3368–3382.

KAPSARC (2021). *The King Abdullah Petroleum Studies and Research Center*. URL: `http://apps.kapsarc.org/kbeat/` (visited on 06/10/2021).

Karjalainen, Sami and Olavi Koistinen (2007). “User problems with individual temperature control in offices”. In: *Building and Environment* 42.8, pp. 2880–2887. ISSN: 0360-1323.

Kaschuba-Holtgrave, Andreas et al. (2020). “Individual unit and guard-zone airtightness tests of apartment buildings”. In: *Journal of Building Physics* 43.4, pp. 301–337.

Kavgic, Miroslava et al. (2010). “A review of bottom-up building stock models for energy consumption in the residential sector”. In: *Building and environment* 45.7, pp. 1683–1697. ISSN: 0360-1323.

Kayyal, Abdullah A (2004). *Property Rights, Transaction Costs, and Neighbourhood Governance: A Case Study of Arriyadh, Saudi Arabia*.

Keefe, David (2010). “Blower door testing”. In: *Journal of Light Construction*, pp. 1–7.

Kim, Hae-Young (2017). “Statistical notes for clinical researchers: Chi-squared test and Fisher’s exact test”. In: *Restorative dentistry & endodontics* 42.2, p. 152.

Kim, Young-Jin, Seong-Hwan Yoon, and Cheol-Soo Park (2013). “Stochastic comparison between simplified energy calculation and dynamic simulation”. In: *Energy and Buildings* 64, pp. 332–342.

Kinsara, Adnan A, Moustafa M Elsayed, and Omar M Al-Rabghi (1996). “Proposed energy-efficient air-conditioning system using liquid desiccant”. In: *Applied Thermal Engineering* 16.10, pp. 791–806. ISSN: 1359-4311.

Kleijnen, Jack PC (1995). “Verification and validation of simulation models”. In: *European journal of operational research* 82.1, pp. 145–162.

Kleijnen, Jack PC and Jon C Helton (1999). “Statistical analyses of scatterplots to identify important factors in large-scale simulations, 1: Review and comparison of techniques”. In: *Reliability Engineering & System Safety* 65.2, pp. 147–185.

Kleijnen, Jack PC and Robert G Sargent (2000). “A methodology for fitting and validating metamodels in simulation”. In: *European Journal of Operational Research* 120.1, pp. 14–29.

Krane, Jim (2017). “Beyond 12.5: The implications of an increase in Saudi crude oil production capacity”. In: *Energy Policy* 110, pp. 542–547.

Krarti, M and Nicholas Howarth (2020). “Transitioning to high efficiency air conditioning in Saudi Arabia: A benefit cost analysis for residential buildings”. In: *Journal of Building Engineering* 31, p. 101457.

Krarti, Moncef, Mohammad Aldubyan, and Eric Williams (2020). “Residential building stock model for evaluating energy retrofit programs in Saudi Arabia”. In: *Energy* 195, p. 116980.

Krauter, Stefan et al. (1999). “Combined photovoltaic and solar thermal systems for facade integration and building insulation”. In: *Solar Energy* 67.4-6, pp. 239–248.

Kuehn, Bridget M (2014). "WHO: More than 7 million air pollution deaths each year". In: *Jama* 311.15, pp. 1486–1486.

Kumar, Prashant et al. (2016). "Real-time sensors for indoor air monitoring and challenges ahead in deploying them to urban buildings". In: *Science of the Total Environment* 560, pp. 150–159. ISSN: 0048-9697.

Lan, Li, Pawel Wargocki, and Zhiwei Lian (2011). "Quantitative measurement of productivity loss due to thermal discomfort". In: *Energy and Buildings* 43.5, pp. 1057–1062.

Leblanc, Richard (1991). "Air tightness tests on components used to join different or similar materials of the building envelope". In.

Lee, Kyoung Ok, Mario A Medina, and Xiaoqin Sun (2016). "Development and verification of an EnergyPlus-based algorithm to predict heat transfer through building walls integrated with phase change materials". In: *Journal of Building Physics* 40.1, pp. 77–95.

Lee, Timothy and Runming Yao (2013). "Incorporating technology buying behaviour into UK-based long term domestic stock energy models to provide improved policy analysis". In: *Energy Policy* 52, pp. 363–372.

Li, Feng and Jianlei Niu (2007). "Application of a whole room indoor air quality (IAQ) model". In: *Building Simulation 2007, BS 2007*, pp. 849–853.

Li, Wai-Ming, Shun Cheng Lee, and Lo Yin Chan (2001). "Indoor air quality at nine shopping malls in Hong Kong". In: *Science of the Total Environment* 273.1-3, pp. 27–40.

Li, Yan-Fu et al. (2010). "A systematic comparison of metamodeling techniques for simulation optimization in decision support systems". In: *Applied Soft Computing* 10.4, pp. 1257–1273. ISSN: 1568-4946.

Liebana, EA and AH Calleja (1998). "El aire en interiores: metodos de control y depuracion". In: *Enciclopedia de Salud y Seguridad en el Trabajo* 45.7-11.

Lima, Raoni Venâncio dos Santos (2007). "A influência de decisões arquitetônicas na eficiência energética do Campus vol. 1/UFRN". MA thesis. Universidade Federal do Rio Grande do Norte.

Limat, S et al. (2000). "Cost-effectiveness of CD34+ dose in peripheral blood progenitor cell transplantation for non-Hodgkin's lymphoma patients: a single centre study". In: *Bone marrow transplantation* 25.9, pp. 997–1002.

Loga, Tobias, Britta Stein, and Nikolaus Diefenbach (2016). "TABULA building typologies in 20 European countries—Making energy-related features of residential building stocks comparable". In: *Energy and Buildings* 132, pp. 4–12.

Lowe, RJ (2000). "Ventilation strategy, energy use and CO2 emissions in dwellings-a theoretical approach". In: *Building Services Engineering Research and Technology* 21.3, pp. 179–185.

Luengas, Angela et al. (2015). "A review of indoor air treatment technologies". In: *Reviews in Environmental Science and Bio/Technology* 14.3, pp. 499–522. ISSN: 1569-1705.

Lyberg, Mats D (1997). "Basic air infiltration". In: *Building and Environment* 32.2, pp. 95–100.

Machairas, Vasileios, Aris Tsangrassoulis, and Kleo Axarli (2014). "Algorithms for optimization of building design: A review". In: *Renewable and sustainable energy reviews* 31, pp. 101–112. ISSN: 1364-0321.

MacPhaul, D and C Etter (2010). *HVAC System Design for Humid Climates*.

Mahdi, Wael and Marc Roca (2012). "Saudi Arabia plans $109 billion boost for solar power". In: *Bloomberg*.

Maklad, Yasser (2014). "Generation of an Annual Typical Meteorological Solar Radiation for Armidale NSW, Australia". In: *IOSR Journal of Engineering (IOSRJEN)* 4.4, p. 2014.

Mallawaarachchi, Harshini and Lalith De Silva (2013). "Green framework to improve indoor air quality in buildings: reducing the impact of sick building syndrome on office workers in Sri Lanka: a literature review". In.

Marasini, Donata, Piero Quatto, and Enrico Ripamonti (2016). "The use of p-values in applied research: Interpretation and new trends". In: *Statistica* 76.4, pp. 315–325.

Mashat, Bassam (2015). "Indoor and outdoor microbial aerosols at the holy mosque: a case study". In: *Atmospheric Pollution Research* 6.6, pp. 990–996.

Mata, Érika, A Sasic Kalagasidis, and Filip Johnsson (2014). “Building-stock aggregation through archetype buildings: France, Germany, Spain and the UK”. In: *Building and Environment* 81, pp. 270–282.

Matar, Walid (2015). *Modeling residential electricity consumption and efficiency within an economic framework: Insights gained by using an engineering-based approach*.

— (2017). “A look at the response of households to time-of-use electricity pricing in Saudi Arabia and its impact on the wider economy”. In: *Energy strategy reviews* 16, pp. 13–23. ISSN: 2211-467X.

Matar, Walid, Rodrigo Echeverri, and Axel Pierru (2016). “The prospects for coal-fired power generation in Saudi Arabia”. In: *Energy Strategy Reviews* 13, pp. 181–190. ISSN: 2211-467X.

Matar, Walid and Amro M Elshurafa (2018). “Electricity transmission formulations in multi-sector national planning models: An illustration using the KAPSARC energy model”. In: *Energy Reports* 4, pp. 328–340.

Matar, Walid et al. (2013). “Modeling the Saudi energy economy and its administered components: The KAPSARC energy model”. In.

MATLAB (2010). *version 7.10.0 (R2010a)*. Natick, Massachusetts: The MathWorks Inc.

Maziad, Faris A al (1999). *The influence of Envelope Design Parameters on the Building Energy Performance for Housing Applications in Saudi Arabia, Eastern Province*. King Faisal Univ.

McMullan, Randall (2017). *Environmental science in building*. Palgrave Macmillan Education.

Mees, C and X Loncourt (2015). “L’étanchéité à l’air des bâtiments”. In: *Technical Information Note*.

Meiss, Alberto and Jesús Feijó-Muñoz (2015). “The energy impact of infiltration: A study on buildings located in north central Spain”. In: *Energy Efficiency* 8.1, pp. 51–64.

Melikov, Arsen Krikor (2016). “Advanced air distribution: improving health and comfort while reducing energy use”. In: *Indoor air* 26.1, pp. 112–124. ISSN: 0905-6947.

Mendell, Mark J and Garvin A Heath (2005). "Do indoor pollutants and thermal conditions in schools influence student performance? A critical review of the literature". In: *Indoor air* 15.1, pp. 27–52.

Mendon, VV et al. (2015). *2015 IECC: Energy Savings Analysis*. Tech. rep. Pacific Northwest National Lab.(PNNL), Richland, WA (United States).

Merwe, Deon van der, Ronette Gehring, and Jennifer L Buur (2018). "Toxicokinetics in veterinary toxicology". In: *Veterinary Toxicology*. Elsevier, pp. 133–143.

Mohamed, RI, ZZ Alfull, and ND Dawood (2014). "Measurements of radon gas concentrations in dwellings of Al-Madinah Al-Munawarah province in Saudi Arabia". In: *Radiation protection dosimetry* 158.2, pp. 156–161.

Molina, Constanza et al. (2020). "A data analysis of the Chilean housing stock and the development of modelling archetypes". In: *Energy and Buildings* 206, p. 109568.

Monawar, Abdulghani Hassan (2001). "A study of energy conservation in the existing apartment buildings in Makkah Region, Saudi Arabia". Thesis. Newcastle University.

Monn, Christian (2001). "Exposure assessment of air pollutants: a review on spatial heterogeneity and indoor/outdoor/personal exposure to suspended particulate matter, nitrogen dioxide and ozone". In: *Atmospheric environment* 35.1, pp. 1–32. ISSN: 1352-2310.

Moran, Michael J et al. (2010). *Fundamentals of engineering thermodynamics*. John Wiley & Sons.

Moura, Maria Cecilia P, Steven J Smith, and David B Belzer (2015). "120 years of US residential housing stock and floor space". In: *PloS one* 10.8, e0134135.

Moustapha, AF, Frank J Costa, and Allen G Noble (1985). "Urban development in Saudi Arabia: Building and subdivision codes". In: *Cities* 2.2, pp. 140–148. ISSN: 0264-2751.

Mubarak, Faisal A (1999). "Cultural adaptation to housing needs: a case study, Riyadh, Saudi Arabia". In: *IAHS Conference Proceedings*. Citeseer, pp. 1–7.

— (2004). "Urban growth boundary policy and residential suburbanization: Riyadh, Saudi Arabia". In: *Habitat international* 28.4, pp. 567–591. ISSN: 0197-3975.

Mujeebu, Muhammad Abdul and Othman Subhi Alshamrani (2016). "Prospects of energy conservation and management in buildings–The Saudi Arabian scenario versus global trends". In: *Renewable and Sustainable Energy Reviews* 58, pp. 1647–1663. ISSN: 1364-0321.

Municipality, Riyadh (2018). *Saudi Arabia: Riyadh Municipality*. Website.

Nagel, Rolf (2016). "A holistic approach for energy flow simulations in early design". In: *Transportation Research Procedia* 14, pp. 1601–1610.

Najid, Mohammed Abdul (2010). "The impact of HVAC system operation and selection on energy efficiency in office buildings in hot climates". Thesis.

Nguyen, Anh-Tuan, Sigrid Reiter, and Philippe Rigo (2014). "A review on simulation-based optimization methods applied to building performance analysis". In: *Applied Energy* 113, pp. 1043–1058. ISSN: 0306-2619.

Nicol, Fergus and Michael Humphreys (2010). "Derivation of the adaptive equations for thermal comfort in free-running buildings in European standard EN15251". In: *Building and Environment* 45.1, pp. 11–17. ISSN: 0360-1323.

Nicol, J Fergus and Michael A Humphreys (1973). "Thermal comfort as part of a self-regulating system". In: ISSN: 0306-9931.

— (2002). "Adaptive thermal comfort and sustainable thermal standards for buildings". In: *Energy and buildings* 34.6, pp. 563–572. ISSN: 0378-7788.

Nilashi, Mehrbakhsh et al. (2015). "A knowledge-based expert system for assessing the performance level of green buildings". In: *Knowledge-Based Systems* 86, pp. 194–209.

Nottingham Technology, University of (2019). *Pulse, proposed as new alternative test in UK government consultation for construction industry*. URL: `https://blogs.nottingham.ac.uk/newsroom/2019/10/25/nottingham-technology-pulse-proposed-as-new-alternative-test-in-uk-government-consultation-for-construction-industry/` (visited on 12/08/2020).

Numan, MY, FA Almaziad, and WA Al-Khaja (1999). "Architectural and urban design potentials for residential building energy saving in the Gulf region". In: *Applied Energy* 64.1-4, pp. 401–410. ISSN: 0306-2619.

Nurunnabi, Mohammad (2017). “Transformation from an oil-based economy to a knowledge-based economy in Saudi Arabia: the direction of Saudi vision 2030”. In: *Journal of the Knowledge Economy* 8.2, pp. 536–564.

Nyrop, Richard F (1984). *Saudi Arabia, a country study*. Vol. 550. Foreign Area Studies, American University.

Oladokun, Michael G and Isaac A Odesola (2015). “Household energy consumption and carbon emissions for sustainable cities–A critical review of modelling approaches”. In: *International Journal of Sustainable Built Environment* 4.2, pp. 231–247.

Omran, Mahamed GH, Andries P Engelbrecht, and Ayed Salman (2007). “An overview of clustering methods”. In: *Intelligent Data Analysis* 11.6, pp. 583–605. ISSN: 1088-467X.

Orme, Malcolm, Martin W Liddament, and Andrew Wilson (1994). *An analysis and data summary of the AIVC's numerical database*. Oscar Faber.

— (1998). *Numerical data for air infiltration and natural ventilation calculations*. Air Infiltration and Ventilation Centre Coventry, UK.

Ortiz, Marco, Laure Itard, and Philomena M Bluyssen (2020). “Indoor environmental quality related risk factors with energy-efficient retrofitting of housing: A literature review”. In: *Energy and Buildings* 221, p. 110102.

Öst, HA and R Paldanius (2017). “Optimization of power system with engine based hybrid solutions for the Saudi Arabia Smart Grid 2017”. In: *2017 Saudi Arabia Smart Grid (SASG)*. IEEE, pp. 1–7.

Österbring, Magnus et al. (2016). “A differentiated description of building-stocks for a georeferenced urban bottom-up building-stock model”. In: *Energy and Buildings* 120, pp. 78–84.

Papst, Ana Lígia et al. (1999). “Uso de Inercia Termica no Clima Subtropical-estudo de caso em Florianopolis-SC”. In: *Civil Engineering. Florianópolis _ Brazil, Federal University of Santa Catarina, Thesis (in Portuguese)*.

Parsons, KC (2000). “Environmental ergonomics: a review of principles, methods and models”. In: *Applied ergonomics* 31.6, pp. 581–594. ISSN: 0003-6870.

Pasos, Alan Vega et al. (2019). “Comparison between infiltration rate predictions using the divide-by-20 rule of thumb and real measurements”. In: *40th AIVC Conference, 8th TightVent Conference, 6th Venticool Conference, October*, pp. 420–429.

Pasos, Alan Vega et al. (2020). “Estimation of the infiltration rate of UK homes with the divide-by-20 rule and its comparison with site measurements”. In: *Building and Environment* 185, p. 107275.

Peretti, Clara and Stefano Schiavon (2011). “Indoor environmental quality surveys. A brief literature review.” In.

Persily, Andrew, Amy Musser, and Steven J Emmerich (2010). “Modeled infiltration rate distributions for US housing”. In: *Indoor air* 20.6, pp. 473–485.

Persily, Andrew, Amy Musser, and Dennis D Leber (2006). *A collection of homes to represent the US housing stock*. US Department of Commerce, Technology Administration, National Institute of . . .

Persily, Andrew Keith (1982). *Understanding air infiltration in homes*. Princeton University.

Petrie, Thomas W et al. (2002). “How Insulating Concrete Form vs. Conventional Construction of Exterior Walls Affects Whole Building Energy Consumption: Results from a Field Study and Simulation of Side-by-Side Houses”. In: *Proceedings*, pp. 1235–1246.

Phillips, Aloysius, Daniel Janies, and Ward Wheeler (2000). “Multiple sequence alignment in phylogenetic analysis”. In: *Molecular phylogenetics and evolution* 16.3, pp. 317–330.

Pittomvils, J, H Hens, and F Van Bael (1996). “Evaluation of ventilation system in very low energy houses.” In: *Proceedings: Optimum Ventilation and Airflow Control in Buildings, 17th Air Infiltration and Ventilation Centre Conference*.

Praprost, Marlena, Katherine A Fleming, and Matthew Dahlhausen (2020). *ENERGY STAR for tenants: An online energy estimation tool for commercial office building tenants*. Tech. rep. National Renewable Energy Lab.(NREL), Golden, CO (United States).

Prieto, Jesús-Ignacio and David García (2021). “Global solar radiation models: A critical review from the point of view of homogeneity and case study”. In: *Renewable and Sustainable Energy Reviews*, p. 111856.

Prignon, Martin and Geoffrey Van Moeseke (2017). “Factors influencing airtightness and airtightness predictive models: A literature review”. In: *Energy and Buildings* 146, pp. 87–97.

Public Works, Riyadh: Ministry of and Housing Ministry (1990). “Deputy Ministry for Housing (DMH). Housing in Saudi Arabia, Objectives and Policies”. In.

Qin, Ruqiong and Chunyi Duan (2017). “The principle and applications of Bernoulli equation”. In: *Journal of Physics: Conference Series*. Vol. 916. 1. IOP Publishing, p. 012038.

Rehman, Heidy (2012). “Saudi petrochemicals: the end of the magic porridge pot”. In: *Citi Research: Equities* 2.

Rehman, Shafiqur (1998). “Solar radiation over Saudi Arabia and comparisons with empirical models”. In: *Energy* 23.12, pp. 1077–1082.

Rehman, Shafiqur and Aftab Ahmad (2004). “Assessment of wind energy potential for coastal locations of the Kingdom of Saudi Arabia”. In: *Energy* 29.8, pp. 1105–1115.

Reinhart, Christoph F and Carlos Cerezo Davila (2016). “Urban building energy modeling–A review of a nascent field”. In: *Building and Environment* 97, pp. 196–202.

Robert, Wójcik and Kosiński Piotr (2015). “Seeming air tightness of construction partitions”. In: *Energy Procedia* 78, pp. 1519–1524.

Roser, Max, Hannah Ritchie, and Esteban Ortiz-Ospina (2013). “World population growth”. In: *Our world in data*.

Ryan, Emily M and Thomas F Sanquist (2012). “Validation of building energy modeling tools under idealized and realistic conditions”. In: *Energy and buildings* 47, pp. 375–382.

SAID, SA M and MA Abdelrahman (1989). “Energy efficiency of a building in the eastern province of Saudi Arabia: parametric analysis with DOE2. 1A”. In: *ASHRAE transactions* 95, pp. 147–152.

Said, SAM and A Al-Hammad (1993). “Energy conservation measures on residential buildings in Saudi Arabia”. In: *International journal of energy research* 17.4, pp. 327–338.

Said, SAM, MA Habib, and MO Iqbal (2003). "Database for building energy prediction in Saudi Arabia". In: *Energy conversion and management* 44.1, pp. 191–201. ISSN: 0196-8904.

Said, Syed-Ahmed M, Hamid M Kadry, and Basil I Ismail (1996). *Climatic conditions for Saudi Arabia*. Report 0001-2505. American Society of Heating, Refrigerating and Air-Conditioning Engineers . . .

Salam, Mohammad Asif and Sami A Khan (2018). "Transition towards sustainable energy production–A review of the progress for solar energy in Saudi Arabia". In: *Energy Exploration & Exploitation* 36.1, pp. 3–27.

Salama, Khaled Fikry and Mahmoud Mohammed Berekaa (2016). "Assessment of air quality in Dammam slaughter houses, Saudi Arabia". In: *Int. J. Med. Sci. Public Health* 5, p. 287.

Saleh, Mohammed Abdullah Eben (1998). "The integration of tradition and modernity: A search for an urban and architectural identity in Arriyadh, the capital of Saudi Arabia". In: *Habitat International* 22.4, pp. 571–589. ISSN: 0197-3975.

— (2001a). "The evolution of planning & urban theory from the perspective of vernacular design: MOMRA initiatives in improving Saudi Arabian neighbourhoods". In: *Land Use Policy* 18.2, pp. 179–190. ISSN: 0264-8377.

— (2001b). "The evolution of planning & urban theory from the perspective of vernacular design: MOMRA initiatives in improving Saudi Arabian neighbourhoods". In: *Land Use Policy* 18.2, pp. 179–190.

Saltelli, Andrea (1999). "Sensitivity analysis: Could better methods be used?" In: *Journal of Geophysical Research: Atmospheres* 104.D3, pp. 3789–3793.

Saltelli, Andrea and Paola Annoni (2010). "How to avoid a perfunctory sensitivity analysis". In: *Environmental Modelling & Software* 25.12, pp. 1508–1517. ISSN: 1364-8152.

Samet, Jonathan M (1993). "Indoor air pollution: a public health perspective". In: *Indoor Air* 3.4, pp. 219–226. ISSN: 0905-6947.

Samet, Jonathan M, Marian C Marbury, and John D Spengler (1987). "Health effects and sources of indoor air pollution. Part I". In: *American Review of Respiratory Disease* 136.6, pp. 1486–1508. ISSN: 0003-0805.

Samet, Jonathan M, Marian C Marbury, and John D Spengler (1988). "Health effects and sources of indoor air pollution. Part II". In: *American Review of Respiratory Disease* 137.1, pp. 221–242. ISSN: 0003-0805.

Saudi Arabia, Ministry of ousing (2020). *Housing Program | Saudi Vision 2030*. URL: https://vision2030.gov.sa/en/programs/Housing.

Saudi Building Code, the National Committee of (2018). *Saudi Building Code*. URL: https://www.sbc.gov.sa/En/Pages/default.aspx (visited on 08/03/2020).

Sawford, Michael (Mar. 2019). *Abouttas*. URL: https://www.edsltas.com/about-tas/.

Saxena, Amit et al. (2017). "A review of clustering techniques and developments". In: *Neurocomputing* 267, pp. 664–681. ISSN: 0925-2312.

Scott, Daniel, C Michael Hall, and Stefan Gössling (2016). "A report on the Paris Climate Change Agreement and its implications for tourism: Why we will always have Paris". In: *Journal of Sustainable Tourism* 24.7, pp. 933–948.

SEC (2018). *Energy tariff*. URL: https://www.se.com.sa/en-us/Pages/home.aspx.

Sharif, Salem M, Muhammad Fauzi Mohd Zain, and Mastor Surat (2010). "Concurrence of thermal comfort of courtyard housing and privacy in the traditional arab house in Middle East". In: *Australian Journal of Basic and Applied Sciences* 4.8, pp. 4029–4037. ISSN: 1991-8178.

Sherman, Max H (1987). "Estimation of infiltration from leakage and climate indicators". In: *Energy and buildings* 10.1, pp. 81–86. ISSN: 0378-7788.

— (1992). "Superposition in infiltration modeling". In: *Indoor Air* 2.2, pp. 101–114.

Sherman, Max H and Wanyu R Chan (2006). "Building air tightness: research and practice". In: *Building Ventilation: the state of the Art* 1, pp. 137–162.

Sherman, Max H and Darryl J Dickerhoff (1998). "Air-tightness of US dwellings". In: *Transactions-American Society of Heating Refrigerating and Air Conditioning Engineers* 104, pp. 1359–1367.

Sherman, Max H and Mark P Modera (1986). "Comparison of measured and predicted infiltration using the LBL infiltration model". In: *Proceedings Measured Air Leakage of Buildings, ASTM STP* 904, pp. 325–347.

Sherman, Max H and Max H Sherman (1986). *Infiltration degree-days: a statistic for quantifying infiltration-related climate*. Applied Science Division, Lawrence Berkeley Laboratory, University of California.

Sherman, Max Howard (1980). “Air infiltration in buildings”. PhD thesis. University of California, Berkeley.

Shi, Liang et al. (2021). “Impact of soil model complexity on the long-term thermal performance prediction of a new shallow bore ground heat exchanger”. In: *Science and Technology for the Built Environment*, pp. 1–12.

Shi, Shanshan, Chen Chen, and Bin Zhao (2015). “Air infiltration rate distributions of residences in Beijing”. In: *Building and Environment* 92, pp. 528–537.

Shin, Hyun Kook and Jae Hun Jo (2013). “Air leakage characteristics and leakage distribution of dwellings in high-rise residential buildings in Korea”. In: *Journal of Asian Architecture and Building Engineering* 12.1, pp. 87–92.

Shipworth, Michelle et al. (2010). “Central heating thermostat settings and timing: building demographics”. In: *Building Research & Information* 38.1, pp. 50–69.

Smargiassi, Audrey et al. (2008). “Prediction of the indoor temperatures of an urban area with an in-time regression mapping approach”. In: *Journal of exposure science & environmental epidemiology* 18.3, pp. 282–288.

Soiferman, L Karen (2010). “Compare and Contrast Inductive and Deductive Research Approaches.” In: *Online Submission*.

Solar heat-gain coefficient ratings for Windows (n.d.). URL: `https://www.nachi.org/shgc-ratings-windows.htm`.

Solmaz, Aslihan Senel (2019). “A critical review on building performance simulation tools”. In: *Alam cipta* 12.2, pp. 7–21.

Sousa Gustavo & Jones, Benjamin M, Parham A Mirzaei, and Darren Robinson (2018). “An open-source simulation platform to support the formulation of housing stock decarbonisation strategies”. In: *Energy and Buildings* 172, pp. 459–477.

Sousa, Gustavo et al. (2017). “A review and critique of UK housing stock energy models, modelling approaches and data sources”. In: *Energy and Buildings* 151, pp. 66–80.

Spencer, J (2010). "Analysis of EnergyPlus for use in residential building energy optimization". In: *Master's thesis, University of Colorado, Boulder, CO*.

statistics, U.S. Energy Information Administration EIA independent and analysis (2019). *Saudi Arabia*. URL: `https://www.eia.gov/outlooks/aeo/nems/2020/buildings/` (visited on 08/03/2020).

Stephen, RK (1998). *Airtightness in UK dwellings: BRE's test results and their significance*. CRC.

Stevanović, Sanja (2013). "Optimization of passive solar design strategies: A review". In: *Renewable and Sustainable Energy Reviews* 25, pp. 177–196. ISSN: 1364-0321.

Stevens, Paul and Glada Lahn (2011). "Burning oil to keep cool: The hidden energy crisis in Saudi Arabia". In: *Chatham House, London*.

Strohmeier, Brian R et al. (2010). "What is asbestos and why is it important? Challenges of defining and characterizing asbestos". In: *International Geology Review* 52.7-8, pp. 801–872.

Sundell, Jan (2004). "On the history of indoor air quality and health". In: *Indoor air* 14.s 7, pp. 51–58. ISSN: 0905-6947.

Swami, Muthusamy V and Subrato Chandra (1987). "Procedures for calculating natural ventilation airflow rates in buildings". In: *ASHRAE final report FSEC-CR-163-86, ASHRAE research project*.

Swami, MV and S Chandra (1988). "Correlations for pressure distribution on buildings and calculation of natural-ventilation airflow". In: *ASHRAE transactions* 94.1, pp. 243–266.

Swan, Lukas, V Ismet Ugursal, and I Beausoleil-Morrison (2008). "A new hybrid end-use energy and emissions model of the Canadian housing stock". In: *3rd Canadian Solar Buildings Conference*. Citeseer.

Swan, Lukas G and V Ismet Ugursal (2009). "Modeling of end-use energy consumption in the residential sector: A review of modeling techniques". In: *Renewable and sustainable energy reviews* 13.8, pp. 1819–1835. ISSN: 1364-0321.

Swecon, Scan Plan and Action Master Plan Abha (2020). "The Ministry of Municipal and Rural Affairs". In: *Saudi Arabia*.

Taleb, Hanan M and Steve Sharples (2011). "Developing sustainable residential buildings in Saudi Arabia: A case study". In: *Applied Energy* 88.1, pp. 383–391. ISSN: 0306-2619.

Talib, K (1984a). *Shelter in Saudi Arabia. 1984: St.*

Talib, Rothengatter (1984b). "A behavioural approach to improving traffic behaviour of young children". In: *Ergonomics* 27.2, pp. 147–160. ISSN: 0014-0139.

Tham, Kwok Wai (2016). "Indoor air quality and its effects on humans—A review of challenges and developments in the last 30 years". In: *Energy and buildings* 130, pp. 637–650.

Thébault, S and R Bouchié (2015). "Estimating infiltration losses for in-situ measurements of the building envelope thermal performance". In: *Energy Procedia* 78, pp. 1756–1761.

Tian, Wei (2013). "A review of sensitivity analysis methods in building energy analysis". In: *Renewable and sustainable energy reviews* 20, pp. 411–419. ISSN: 1364-0321.

Tinker, John A and K Buijan (1998). "Thermal performance of fenestration systems in the hot climate of Saudi Arabia". In: *Proceedings of the Thermal Performance of the Exterior Envelopes of Buildings VII, ASHRAE, Florida, USA*, pp. 311–319.

Trochim, William MK and James P Donnelly (2001). *Research methods knowledge base*. Vol. 2. Atomic Dog Pub. Macmillan Publishing Company, New York.

Tyagi, VV et al. (2013). "Progress in solar PV technology: Research and achievement". In: *Renewable and sustainable energy reviews* 20, pp. 443–461.

UK, GOV (2013). *Standard Assessment Procedure*.

UNI, ENISO (2008). "Energy performance of buildings—calculation of energy use for space heating and cooling". In: *Standard UNI EN ISO* 13790, p. 2008.

Union, European (2002). "Directive 2002/91/EC of the European Parliament and of the Council of 16 December 2002 on the energy performance of buildings". In: *Official Journal*.

Vakiloroaya, Vahid et al. (2014). "A review of different strategies for HVAC energy saving". In: *Energy conversion and management* 77, pp. 738–754.

Van Dijk, H, M Spiekman, and P De Wilde (2005). “A monthly method for calculating energy performance in the context of European building regulations”. In: *Building Simulation*, pp. 255–262.

Vohra, Muhammad Saeed (2011). “Personal formaldehyde exposure level in the gross anatomy dissecting room at College of Medicine King Saud University Riyadh”. In: *International journal of occupational medicine and environmental health* 24.1, pp. 108–113. ISSN: 1232-1087.

Waheeb, Sahl Abdullah (2005). “Impact of shading devices on indoor sunlight distribution and building energy performance, with reference to Saudi Arabia”. PhD thesis. University of Nottingham.

Wahl, Emma (2017). *Buildings in Arid Desert Climate: Improving Energy Efficiency with Measures on the Building Envelope*.

Waisman, Henri et al. (2019). “A pathway design framework for national low greenhouse gas emission development strategies”. In: *Nature Climate Change* 9.4, pp. 261–268.

Walton, George and William S Dols (2006). *CONTAM 2.4 user guide and program documentation*. Tech. rep.

Wang, Gang and Li Song (2012). “Air handling unit supply air temperature optimal control during economizer cycles”. In: *Energy and Buildings* 49, pp. 310–316.

Ward, MP and TE Carpenter (1996). “Simulation modeling of the effect of climatic factors on bluetongue virus infection in Australian cattle herds. I. model formulation, verification and validation”. In: *Preventive Veterinary Medicine* 27.1-2, pp. 1–12.

Weschler, Charles J (2009). “Changes in indoor pollutants since the 1950s”. In: *Atmospheric Environment* 43.1, pp. 153–169. ISSN: 1352-2310.

WHO (2010). *WHO guidelines for indoor air quality: selected pollutants*. World Health Organization. Regional Office for Europe.

Wiesmann, Daniel et al. (2011). “Residential electricity consumption in Portugal: Findings from top-down and bottom-up models”. In: *Energy Policy* 39.5, pp. 2772–2779.

Wigo, Hans (2008). "Effects of intermittent air velocity on thermal and draught perception during transient temperature conditions". In: *International Journal of Ventilation* 7.1, pp. 59–66.

— (2013). "Effects of intermittent air velocity on thermal and draught perception–a field study in a school environment". In: *International Journal of Ventilation* 12.3, pp. 249–256.

Wilcox, Bruce A and Theresa A Weston (2001). "Measured Infiltration Reduction in California Production Houses Using Housewrap". In: *Thermal Performance of the Exterior Envelopes of Buildings VIII*.

Wong, Johnny Kwok-Wai et al. (2014). "The effects of the indoor environment of residential care homes on dementia suffers in Hong Kong: A critical incident technique approach". In: *Building and environment* 73, pp. 32–39.

World Health Organization (2001). *The world health report 2001 - Mental Health: New Understanding, New Hope*. Tech. rep. Genf, Schweiz. URL: `http://www.who.int/whr/2001/en/index.html` (visited on 03/07/2012).

Wray, Craig and Max Sherman (2010). *Duct Leakage Modeling in EnergyPlus and Analysis of Energy Savings from Implementing SAV with InCITeTM*. Tech. rep. Lawrence Berkeley National Lab.(LBNL), Berkeley, CA (United States).

Wu, Fu-Chun and Hsieh Wen Shen (1999). "First-order estimation of stochastic parameters of a sediment transport model". In: *Journal of Hydraulic Research* 37.2, pp. 213–227.

Yang, Wei et al. (2014). "Thermal comfort requirements in the summer season in subtropical urban spaces". In: *Intelligent Buildings International* 6.4, pp. 224–238.

Yao, Runming and Koen Steemers (2005). "A method of formulating energy load profile for domestic buildings in the UK". In: *Energy and buildings* 37.6, pp. 663–671.

Yousef, AMM and K Zimami (2019). "Indoor radon levels, influencing factors and annual effective doses in dwellings of Al-Kharj City, Saudi Arabia". In: *Journal of Radiation Research and Applied Sciences* 12.1, pp. 460–467.

Youssef, Ahmed M et al. (2015). "Assessment of rockfall hazard at Al-Noor Mountain, Makkah city (Saudi Arabia) using spatio-temporal remote sensing data and field investigation". In: *Journal of African Earth Sciences* 101, pp. 309–321.

Yu, Shenwei et al. (2022). "Optimization of Wall Thickness Based on a Comprehensive Evaluation Index of Thermal Mass and Insulation". In: *Sustainability* 14.3, p. 1143.

Zaatari, Marwa et al. (2014). "Ventilation and indoor air quality in retail stores: A critical review (RP-1596)". In: *HVAC & Research* 20.2, pp. 276–294. ISSN: 1078-9669.

Zhang, Bo-Ming, Shu-Yuan Zhao, and Xiao-Dong He (2008). "Experimental and theoretical studies on high-temperature thermal properties of fibrous insulation". In: *Journal of Quantitative Spectroscopy and Radiative Transfer* 109.7, pp. 1309–1324.

Zhang, Xing-Ping and Xiao-Mei Cheng (2009). "Energy consumption, carbon emissions, and economic growth in China". In: *Ecological economics* 68.10, pp. 2706–2712.

Zhang, Xingxing et al. (2012). "Review of R&D progress and practical application of the solar photovoltaic/thermal (PV/T) technologies". In: *Renewable and Sustainable Energy Reviews* 16.1, pp. 599–617.

Zhang, Y. and D. Yeung (2012). "Overlapping Community Detection via Bounded Nonnegative Matrix Tri-Factorization". In: *In Proc. ACM SIGKDD Conf.* Pp. 606–614.

Zheng, Xiaofeng et al. (2020). "A practical review of alternatives to the steady pressurisation method for determining building airtightness". In: *Renewable and Sustainable Energy Reviews* 132, p. 110049.

Østergård, Torben, Rasmus L Jensen, and Steffen E Maagaard (2016). "Building simulations supporting decision making in early design–A review". In: *Renewable and Sustainable Energy Reviews* 61, pp. 187–201. ISSN: 1364-0321.